Nutrient dynamics in shallow tidally-dominated estuaries

A thesis submitted in fulfilment

of the requirements for the degree of

Doctor of Philosophy

in

Earth Sciences

at

The University of Waikato

by

Hui Woon Tay

2011

THE UNIVERSITY OF
WAIKATO
Te Whare Wānanga o Waikato

Abstract

Te Puna and Waikareao estuaries are shallow tidally-dominated estuaries in Tauranga Harbour located on the Bay of Plenty Coast, New Zealand. Tauranga Harbour is the site of a large commercial port surrounded by urban development. The primary aim of this thesis was to determine the variations of dissolved inorganic nitrogen concentrations and fluxes in both Te Puna and Waikareao estuaries over short time-scales in different seasons through field experiments and a dynamically coupled three-dimensional (3D) hydrodynamic-biogeochemical model.

To gain insight in the short temporal variability in nutrient concentrations, 24-hourly measurements of dissolved nutrients were conducted over four periods (winter, summer, start of spring, and end of spring) within one year in Te Puna and Waikareao estuaries. The nitrate and ammonium concentrations showed distinctive tidal patterns with rising values during ebb flow. This tidal asymmetry caused a flux of DIN seaward with net fluxes ranging from 34 to 358 kg/tidal cycle of nitrate and 22 to 93 kg/tidal cycle of ammonium. The variations in concentrations observed within tidal cycles were of a similar magnitude to the variations measured over 19-years at comparable times of the year.

To further understand the sources and sinks that may control the variations measured during these short-time scale experiments, the hydrodynamic-biogeochemical model, ELCOM-CAEDYM, was set-up for both Te Puna and Waikareao estuaries. Tidal exchange of water within the harbour and its sub-estuaries was shown to have an impact on the circulation patterns in various parts of Tauranga Harbour. Hence, a hydrodynamic modelling exercise of the southern basin of Tauranga Harbour was undertaken. The model results established that the salinity profiles are tidally-driven while the temperature profiles are sensitive to wind. Residence times varied across the harbour with increasing residence times in the upper reaches of the estuary and also in sub-estuaries with constricted mouths. Model simulations of Te Puna and Waikareao estuaries also showed the sensitivity of water temperature to wind. Spatial variations in DIN, DO and residence times across both the sub-estuaries were observed from model simulations.

Twenty-two scenarios were simulated in both Te Puna and Waikareao estuaries by altering the forcing conditions in the model as from analysis of field measurements from the 24-hourly sampling, showed that it was difficult to differentiate between competing sources (freshwater inflows, wind mixing and sediment fluxes) of DIN input into Te Puna and Waikareao estuaries. From the scenarios, it was found that the inter-annual variation in concentration of nitrate is primarily driven by freshwater inflows, while ammonium is primarily influenced by sediment fluxes. Ammonium is sensitive to seasonal variation in temperature with higher simulated ammonium concentrations in summer. The impacts of stream discharges on estuary DIN concentrations were mostly localised to the inflow locations with minimal impact on estuary-wide concentrations due to strong tidal flushing. The modelling scenarios also demonstrated the heterogeneities in DIN concentrations from upper to lower estuary, highlighting the difficulty of monitoring estuary health using point measurements.

From the modelling scenarios, groundwater was identified as a significant contributor of DIN into the estuaries, with contribution ranging from 2% to 37%. The seasonal variation in pore-water nitrate and ammonium concentrations in a tidal flat margin at Waikareao Estuary was determined. Vertical profiles of sediment pore-water were sampled in wells that were dug into the intertidal sand flat to provide snapshots of nitrate and ammonium concentrations at different times of the year. Pore-water recycling processes were an important DIN source to the estuaries during ebb tide with greatest concentration observed in mid-winter and summer. Pore-water profiles showed ammonium as the dominant form of DIN in the wells. Nitrate concentration was higher in surface sediment and ammonium dominated the mid-depth regions (25-50 cm). Long-term monitoring of Kopurereroa Stream which discharges into Waikareao Estuary, showed higher nitrate concentration than the tidal flat wells and other monitored sites. This further highlights that the primary source of nitrate into estuaries is through freshwater discharge and ammonium is dominated by sediment recycling processes.

From both field experiments and modelling scenarios, it is found that dissolved nutrient concentrations were highly variable in both estuaries with distinctive tidal patterns and also seasonal variations.

Acknowledgements

First and foremost, I would like to thank my supervisors, Dr Karin Bryan, Dr Conrad Pilditch and Dr Willem de Lange, for their guidance, support and motivation. Thank you for your belief in my capabilities, flexibility to pursue interesting developments in my work, and for sharing your views with me. I would also like to thank Prof. David Hamilton for his inputs and guidance.

I would also like to thank the New Zealand Coastal Society for the Student Scholarship and the travel grants, and Broad Memorial Fund.

I would also like to thank the Bay of Plenty Regional Council staff especially Glenn Ellery, Craig Putt, and Stephen Park for sharing data and answering all my queries.

I sincerely appreciate all the help of the technical staff from Department Earth and Ocean Sciences, Biological Sciences and Chemistry. Special thanks go to Chris McKinnon for his endless help with field work planning and trips and also to Jacinta Parenzee for letting me use the soils lab. Thanks to Dirk Immenga and Craig Hosking for assistance with oceanographic equipments. A long list of field assistants braved the sun and cold on one or more occasions. Unfortunately I could not name them all here, however their willingness to take time out of their own busy schedules was enormously appreciated.

Thanks to Sydney Wright and Vicki Smith for all your patience and helping me with my enquiries. I would also like to thank all the lecturers and technical staffs from the Department of EOS, Biology and Chemistry that I have bothered with questions throughout the last couple of years.

I would like to thank my fellow students over the years for their friendship, good humour and support through both high and low times – Gegar Prasetya, Renee Schicker, Bryna Flaim (et al.).

Most importantly thank you to my family and friends; firstly my family for their constant encouragements, and support and secondly my friends who made me laugh when I needed it most. Last, but certainly not least, I would like to thank Daniel James who was there for me from day one.

Table of Contents

List of Figures

List of Tables

Chapter One: Introduction

1.1 Overview

The coastal zone plays a key role in biogeochemical cycles and estuaries often act as efficient filters for land-derived material. Inputs of dissolved and particulate constituents from catchments have increased as a result of human growth (Valiela et al. 1992). This has resulted in deterioration of water quality that leads to loss of biodiversity and concerns about the potential for dramatic changes in ecosystem structure and function (Cederwall and Elmgren 1990; Howarth et al. 2000). However, without a detailed knowledge of ecological dynamics, natural variations in the ecosystem may be mistaken for the effect of a pollutant.

This thesis concentrates largely on the variation of dissolved inorganic nitrogen in the coastal environment. Nitrogen (N) is often the limiting nutrient in many coastal and estuarine ecosystems for primary production (Howarth 1988; Howarth and Marino 2006). Human activities have more than increased the rate of nitrogen entering the aquatic systems (Rabouille et al. 2001; Galloway et al. 2004). More specifically, increased urban development in coastal areas and intensification of agriculture are both considered substantial contributors of nutrients to estuaries. Depending on environmental conditions, a number of biogeochemical processes may contribute to the nitrogen species in the aquatic environment. The key biogeochemical processes in the nitrogen cycle are summarized briefly in Figure 1.1. These are inputs from run-off, atmospheric deposition, groundwater and oceanic exchange, and also the cycling of nutrients in the water column and sediments through the processes of nitrification, denitrification and mineralisation.

Estuaries receive their primary freshwater input through fluvial discharges but there is direct evidence that groundwater inflow may contribute nutrients into the water column (Slomp and Van Cappellen 2004; Kroeger and Charette 2008). Continued urbanization and agricultural development in catchments can lead to increased inputs of nitrogen from fertilizer and wastewater to groundwater and part of these nutrients are released to estuaries. The magnitude of land-derived nutrient transport by groundwater is set by the concentrations of nutrients near-shore, attenuation processes along flowpaths and by groundwater flow rates (Bowen et al. 2007). Examples of the ecological impact of groundwater flow into

coastal zones have been given by Valiela et al. (1978, 1992, 2002), who showed that groundwater inputs of nitrogen are critical to the overall nutrient economy of salt marshes. Corbett et al. (1999, 2000) estimated that groundwater nutrient inputs are approximately equal to nutrient inputs provided by surface freshwater runoff in Florida Bay. In shallow estuaries with extensive tidal flats, the permeability of the sediments facilitates pore-water seepage and groundwater seepage that can lead to rapid exchange with the overlying water. This rapid exchange can enhance remineralisation rates and nutrient cycling in the estuaries.

The largest reservoir of N is N_2 gas (78%) of the atmosphere that must be fixed by microorganisms before it is readily useable by other organisms (Francis et al. 2007). Along this flowpath, microorganisms directly catalyze the processes of nitrification and denitrification. The N_2 gas is reduced to ammonium by N-fixing microbes. Decomposition of organic nitrogen through ammonification in oxic conditions can also releases ammonium (1) (Herbert 1999). Dissolved inorganic nitrogen (DIN) also becomes available to organisms when organic nitrogen in living tissue degrades (2) (Brock 2001). Ammonium can be oxidized to nitrite and nitrate through the aerobic process of nitrification (3) (Berounsky and Nixon 1993). DIN may be removed from the environment by denitrification and anammox. Denitrification is the dissimilatory reduction of nitrate to N_2 by bacteria (4) (Dong et al. 2006). Anaerobic ammonium oxidation (anammox) where NH_4^+ combined with NO_2^- to form N_2 gas is another alternative pathway of removal of N (5) (Santoro 2010). Ammonium may also be transformed from nitrate under anaerobic condition through dissimilatory nitrate reduction to ammonia (6) (DNRA) (Gardner et al. 2006). In shallow coastal marine ecosystems the major factors controlling nitrate and ammonium concentrations are inputs arising from fluvial discharges, groundwater inputs and from exchange across the sediment-water interface. Coastal sediments provide a matrix for transformations and cycling of N (Simon 1988). For example, microbial denitrification in estuarine sediment has been found to remove excess nitrate from terrestrial nitrogen loading (Wang et al. 2003; Tuerk and Aelion 2005). While at low tide when the water table drops and oxygen diffuses from the surface layer, the ammonium produced by DRNA may be converted back to nitrate via nitrification (Korom 1992).

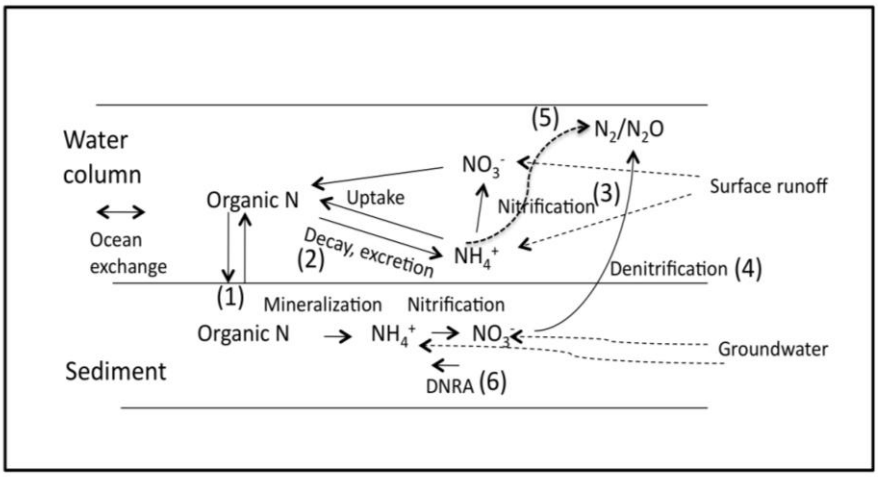

Figure 1.1 A simplified version of the nitrogen cycle in an estuarine environment (adapted from Herbert 1999).

Nutrient processes in estuaries are subjected to physical forcings that can influence the rate of vertical mixing, horizontal transport or production rate (DiLorenzo et al. 2004; Caffrey et al. 2007). These nutrient processes are dynamic, depending on nutrient loading rates, water residence time, tidal exchange and biological uptake (Caffrey et al. 2007). Each of the physical forcings has a characteristic timescale variability such as the tidal periods (12 hour to 14 days), storm events of enhanced stream flow and wind stress (2 to 5 days), seasonal cycles of irradiance and temperature, and the interannual variability of river flow (Magnien et al. 1992; Grelowski et al. 2000; DiLorenzo et al. 2004).

In shallow, tidally dominated estuaries, tidal exchange has dominant influence on nutrient concentrations (Figure 1.2). However variations in nutrient concentrations is not only caused by tides but by wind-induced currents (Sigleo et al. 2005). During inundation, the effect of tidal currents along with wind-induced currents can reworked the sediments leading to resuspension of particulates. Other than generating surface flows, the effects of tides lead to diffusive and advective exchange of water through the sediment-water interface. Diffusion from pore-water is an important pathway for export of dissolved nutrients in tidal flat (Billerbeck et al. 2006). Horizontal drainage of porewaters can export substantial qualities of dissolved nutrients (Jordan and Correll 1985). Vertical exchange of solute resulting from groundwater flow can also contributed towards fluxes of nutrients into the estuaries (Giblin and Gaines 1990; Harvey and Nuttle 1995).

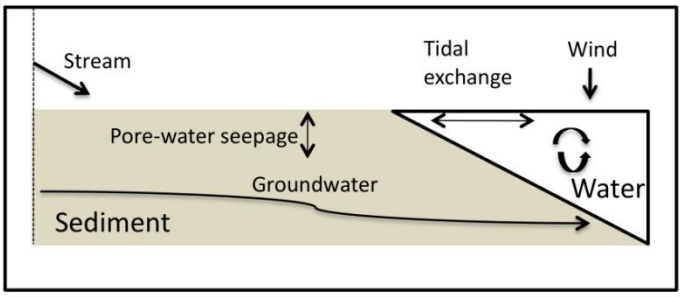

Figure 1.2 Schematic of the main hydrodynamic drivers in shallow estuaries.

Modelling of estuarine water bodies has played a useful role in advancing the understanding of transport of water and material in conjunction with management of water resources in estuarine environments. Process-based numerical models can provide important information on the fate of nutrients within the system. In recent decades, coupled physical-biological models have been widely applied to the marine environment to simulate the physical and biogeochemical processes and study the interactions between them (e.g. Xu and Hood 2006; Lacroix et al. 2007). The dynamics of nutrients in shallow estuaries are particularly difficult to understand, and thus a numerical model can be used as a tool to study the circulation patterns and nutrient dynamics. The nutrient dynamics depend on the interplay between the water chemistry and the complex bathymetry that drives spatially variable residual currents and mixing regimes.

1.2 Objective and aims

The overriding hypothesis of this thesis is to understand nutrient dynamics in two shallow estuaries, and how these are influenced by variations of physical, biogeochemical and biological factors. The primary objective of this thesis is to determine the seasonal, tidal and diel variations in influencing dissolved inorganic nitrogen dynamics in shallow tidally dominated sub-estuaries. These concentration variations cause fluxes of dissolved inorganic nitrogen to and from the coastal zone. The source and variability of dissolved inorganic nitrogen was studied with the help of two field experiments and a coupled three-dimensional hydrodynamic-ecologic model. The studies were conducted in Te Puna Estuary and Waikareao Estuary located in the southern basin of Tauranga Harbour. There are three main components to this study: firstly, a study of the short-time scale changes in physical and biogeochemical processes, secondly, coupling of a

hydrodynamic and ecological model to explore nutrient feedbacks, and finally the role of the porewater contribution to nutrient fluxes of a tidal flat margin. The main aims of each chapter are summarized as follows:

- In Chapter 2, the tidal variability in nutrient concentrations and fluxes over tidal timescales in shallow tidally-dominated estuaries are described. These nutrient concentrations and fluxes variations are addressed using field measurements from two shallow intertidal estuaries of similar size but with varying distance from the harbour mouth. Historical data from previous studies were used to analyse and quantify the long-term spatial variations in nutrients. Although these previous studies were conducted at different sites in Tauranga Harbour, and at different temporal and spatial scales, the results of all studies will be combined to give an overview of the harbour nutrient variations. Field experiments from Waikareao and Te Puna will give insight into the tidal variations in the harbour which is needed to interpret the historical data.
- Currents within Waikareao and Te Puna estuaries are largely tidal driven, and controlled by the water properties at the entrance of these estuaries, which are in turn controlled by the hydrodynamics in the Tauranga Harbour as a whole. In Chapter 3, the results of the application of a large-scale 3D model of interactions of hydrodynamics, salinity and temperature in the circulation of the southern basin of Tauranga Harbour are presented. A secondary objective of this chapter was also to provide temperature and salinity output that is used as forcing conditions in the hydrodynamic model for both Waikareao and Te Puna estuaries.
- In Chapter 4, the hydrodynamic and biogeochemical model results of Waikareao and Te Puna Estuaries using a 3D hydrodynamic ecologic model are described. The simulated results were calibrated with in situ hydrodynamic measurements, and temperature, salinity and nutrient data taken over a tidal time-scale during the field experiments described in Chapter 2. The influence of short-term circulation patterns on the DIN patterns in the two estuaries was also investigated.
- In Chapter 5, a series of model scenarios were developed to explore the contribution of wind, freshwater pulses, groundwater and sediment porewater and climatic variations in shelf DIN to the DIN concentrations

and patterns in the two estuaries (such as might be induced by upwelling). Specifically, 22 scenarios were developed to determine the potential sources of nitrate and ammonium in the two estuaries. Scenarios included varying streams discharge and nutrient loading to the two estuaries, and excluding groundwater and sediment pore-water fluxes in turn.

- In Chapter 6, a study to ascertain the contribution of shallow tidal flat porewater towards the seasonal concentrations of dissolved inorganic nitrogen is presented. Vertical profiles of sediment porewater composition were sampled to provide snapshots of DIN concentrations at seven different times of the year.

Chapter Two: Dissolved nutrient variations in shallow tidally-dominated estuaries

2.1 Introduction

Nutrient inputs to estuaries have increased globally as a result of human population growth, intensification of agriculture and changing catchment land-use (e.g. Sin et al. 1999; Lillebø et al. 2005; van der Struijk and Kroeze 2010). Increased nutrient inputs generally stimulate primary production in surface waters, which increases rates of sedimentation to, and decomposition of organic matter in bottom waters, which may potentially become hypoxic (Rosenberg et al. 1990). Other symptoms of estuarine eutrophication include phytoplankton blooms, loss of seagrasses and decreases in biocomplexity (Cederwall and Elmgren 1990; Michel et al. 2000). Most estuarine eutrophication studies have been focused on large estuaries with long residence times (Boynton et al. 1995; Soetaert et al. 2006). Much less is known about the timescale and variability of nutrient concentrations and fluxes in small, well-flushed estuaries (Caffrey et al. 2007).

Variability in estuarine nutrient fluxes can be driven by fluctuations in the nutrient inputs, but also by changes to the internal nutrient cycling with the estuary. Considering that nutrient inputs to estuaries can be from a variety of sources such as surface discharges, atmospheric deposition, groundwater discharge and exchanges with the coastal shelf (Correll et al. 1992; Paerl 1997; Lampman et al. 1999), these inputs can vary both temporally and spatially with climate-driven patterns. For example, in some estuaries, nutrients may be readily transported through the system in winter in association with peak rainfall and discharge (Sigleo and Frick 2007). Internal regeneration of nutrients can, however be a significant proportion of terrestrial inputs (Nixon et al. 1976) and in shallow water systems can be seasonally modulated as the decomposition of organic matter in the sediments drives regeneration processes (D'Andrea et al. 2002; Eyre and Ferguson 2005). In cases where the euphotic zone extends to the bed, benthic primary producers play an important role in controlling nutrient fluxes to and from the water column (Dalsgaard 2003). These benthic-pelagic nutrient exchanges can be particularly important when accompanied by high water velocities, which create sediment resuspension via wind-wave action (Le Hir et al. 2000) or induce large tidal excursions.

Shallow, well-flushed estuaries often have intertidal flats, which can represent a large proportion of the estuary area. The term ‘shallow’ used in this thesis context was to define an estuary with large proportion of intertidal flat areas. On a daily basis, these tidal flats are dewatered by evaporation and ebb tide drainage and they are re-hydrated by infiltration of tidal waters during flood tides, terrestrial discharges and precipitation. The oscillatory pattern of tidal dewatering and infiltration influences solute transport through sediment porewaters while waves and wind-driven currents lead to sediment resuspension (Werner et al. 2006; Beck et al. 2008). The dewatering and resuspension effects can also ultimately control the movement of nutrients into and out of the bed, and thus the morphology of these flats can play a major role in determining nutrient pathways (Billerbeck et al. 2006b).

Estuarine water quality studies typically assess nutrient concentrations by using monthly sampling regimes to detect seasonal and inter-annual changes (Sigleo and Frick 2007; Falco et al. 2010). Most studies have been confined to estuaries with long residence times (e.g. Neuse River Estuary (Christian et al. 1991) and Elbe Estuary (Dähnke et al. 2008)), and with reduced confounding effects from tidal advection processes. Nevertheless, such sampling regimes can miss episodic changes that arise, for example from intense rainfall-runoff events (Whiting et al. 1987). Short-term nutrient pulses following rainfall events can enhance primary production at time scales ranging from hours to weeks (Valiela et al. 1978; Whiting et al. 1987; Hubertz and Cahoon 1999; Pereira-Filho et al. 2001; Caffrey et al. 2007). In estuaries with large tidal prisms, logistical constraints can limit the effectiveness and representativeness of sampling strategies. For example, accessibility at low tide, lack of exact knowledge of the tidal wave propagation throughout a large estuary, and the necessity of sampling multiple sites in one excursion can result in spatio-temporal time series data that are difficult to interpret and relate to environmental variables.

Here seasonal, tidal and diel variations in dissolved inorganic nutrient concentrations and fluxes to and from surrounding coastal regions, in two small, sandy, well-flushed estuaries were quantified. This study provides a contrast to those that have been undertaken in larger estuarine systems with smaller tidal

exchanges (e.g. Chesapeake Bay (Dauer et al. 2000), Albermarle-Pamlico Estuarine System (Burkholder et al. 2006) and Oder Estuary (Grelowski et al. 2000). The estuaries studied here are similar in size and geometry, but vary somewhat in their degree of urbanization, but also in the distance of their entrances to the open shelf. Although there are a number of studies that model nutrient loads to New Zealand estuaries (e.g. Parfitt et al. 2006; Partfitt et al. 2008; Heggie and Savage 2009), and many New Zealand governmental organizations routinely monitor estuarine nutrient concentrations, very few studies exist where measurements are collected at timescales that allow estimates of actual fluxes and how these might vary through time. Moreover, although many studies have measured nutrient fluxes into estuaries, relatively few have measured the exchanges across the lower (seaward) boundaries (e.g. Boynton et al. 1995). The objectives of this chapter were therefore to (1) determine the relative differences in inorganic nutrient mass fluxes at tidal time scales versus seasonal and interannual time scales, and (2) to assess whether these small estuaries acted as net sources or sinks of dissolved inorganic nutrients for the adjoining coastal zone.

2.2 Methods

The two estuarine study sites were the Waikareao and Te Puna Estuaries, which are sub-estuaries located in Tauranga Harbour in the Bay of Plenty region, on the east coast of North Island, New Zealand (Figure 2.1). The harbour catchment has an area of 200 km^2 with a variety of land uses including horticulture, agriculture, urban and industry. The Wairoa River is the largest freshwater input into the harbour (Park 2004), contributing on average 17.6 $m^3 s^{-1}$. Tides in the harbour are semi-diurnal (springs ~ 1.9 m and neaps ~ 1.2 m) and the water column is vertically well mixed (Heath 1985). Waikareao Estuary is located 4.5 km south and Te Puna Estuary is 12 km southwest of the harbour mouth (Figure 2.1). Both estuaries have single constricted mouths and extensive intertidal areas (~75%). The Kopurereroa Stream flows into Waikareao Estuary while at Te Puna Estuary there is little freshwater discharge. Table 2.1 summarizes the physical characteristics of the Waikareao and Te Puna estuaries. The region experiences a temperate climate with average daily maximum summer temperature ranging from 22 to 25° C over the months of December to March. Average daily maximum

winter temperature ranges from 14-15°C and daily minimum is from 5-6°C. Mean rainfall for Tauranga area is 1200 mm per year (Stokes et al. 2010).

Long-term monitoring data (nitrate, phosphate, ammonium and salinity) have been collected by Bay of Plenty Regional Council since 1991 and are presented as part of this study. Data were collected every two to four months, generally between the period of mid and peak flood tide at six sites surrounding the Te Puna and Waikareao estuaries but within the main Tauranga Harbour (Figure 2.1).

Sampling was conducted during winter (24-26 June 2008), start of spring (4-6 September 2008), end of spring (13-15 November 2007) and late summer (14-16 March 2008) from jetties, which protruded into the main entrance channel of each estuary and also at the Kopurereroa Stream where it flows into Waikareao Estuary (Figure 2.1A and B). The winter and start of spring sampling occasions were characterized by rain events during sampling (Table 2.2). The rainfall data were measured at Tauranga Airport. On each of the four sampling periods, samples were taken hourly at each estuary over two semi-diurnal tidal cycles (one day-time and one night-time cycle) and Kopurereroa Stream was sampled every 2 hours. Vertical profiles of conductivity-temperature-depth were taken hourly at each jetty (marked on Figure 2.1) with a Seabird Electronics Conductivty-Temperature-Depth sensor (CTD) (Washington, USA). There were no vertical variations in salinity or temperature. The water depth at Waikareao was measured with the CTD (adding an offset to account for the distance between the pressure sensor and the bottom of the instrument) and at Te Puna it was obtained from a tide gauge attached to a jetty that is operated by the Bay of Plenty Regional Council.

Water samples were pumped from the surface and just above the bottom at the main jetty sampling sites (Figure 2.1) and immediately filtered through 0.45 µm Advantec glass fiber filters into acid-washed vials. Two water samples each from surface and bottom were collected. Samples were frozen before analysis for ammonium, phosphate, nitrate and nitrite using a Lachat Instruments flow injection analyzer (FIA, Zellweger Analytics, 2000) (APHA 1992). The surface and bottom nutrient concentrations were later averaged (T-statistic was conducted and it was found that the bottom and surface nutrient concentrations were

insignificantly different). The filters were placed in dark containers, frozen and later analyzed for chlorophyll a (chl.-*a*) using the fluorometric method of Arar and Collins (1997) with correction of phaeophytin following extraction in 90% acetone.

For each sampling period, the dissolved inorganic nitrogen (DIN, defined as ammonium plus nitrate) fluxes was calculated for water entering and leaving at the estuary mouth and the DIN budget was estimated, based on the LOICZ (Land-Ocean Interactions in the Coastal Zone) biogeochemical model (Gordon et al. 1996). DIN inputs were from flood tide water and the stream in the case of Waikareao and the outputs were from ebb tides. DIN contributions from precipitation were disregarded, as they were negligible compared to other sources as atmospheric deposition has been estimated to be only 1-2 kg N/ha/yr in New Zealand (Parfitt et al. 2006; Heggie and Savage 2009). Nitrate and ammonium fluxes for each tidal cycle were approximated as averages for concentrations taken during the 3 hr of peak-ebb and peak-flood flow, respectively. Peak ebb and flood times were estimated from the mid-tide water levels. Flow and water level measurements from an Acoustic Doppler Current Profiler (ADCP, Sontek, USA) collected in the channel directly offshore of the jetty in Te Puna in June 2010 over two tidal cycles indicate that the peak ebb and flood were symmetric and occurred at mid-tide (data not shown). Estuarine water surface areas at mid-tide were calculated from bathymetry created by combining LiDAR and single beam echo sounding measurements. The Bay of Plenty Regional Council provided the LiDAR data and single beam echo sounder (Knudsen, Canada) measurements were conducted by the University of Waikato. The volume of water was estimated by multiplying the mid-tide area of estuary by the tidal range. The DIN fluxes from each estuary into Tauranga Harbour were then estimated by multiplying these averages by the total volume of water entering and leaving each estuary over a tidal cycle. Since sampling dates were chosen so that high tide occurred near midnight and midday, flux calculations could be done separately for day and night sampling. The meteorological data (precipitation and evaporation) used in this study were from measurements at Tauranga Airport meteorological station. These data, precipitation (Table 2.2) and evaporation, for the 24-hour sampling periods were downloaded from the National Institute of Water and Atmospheric Research

(NIWA) Cliflo database to account for additions/losses of freshwater in the estuaries.

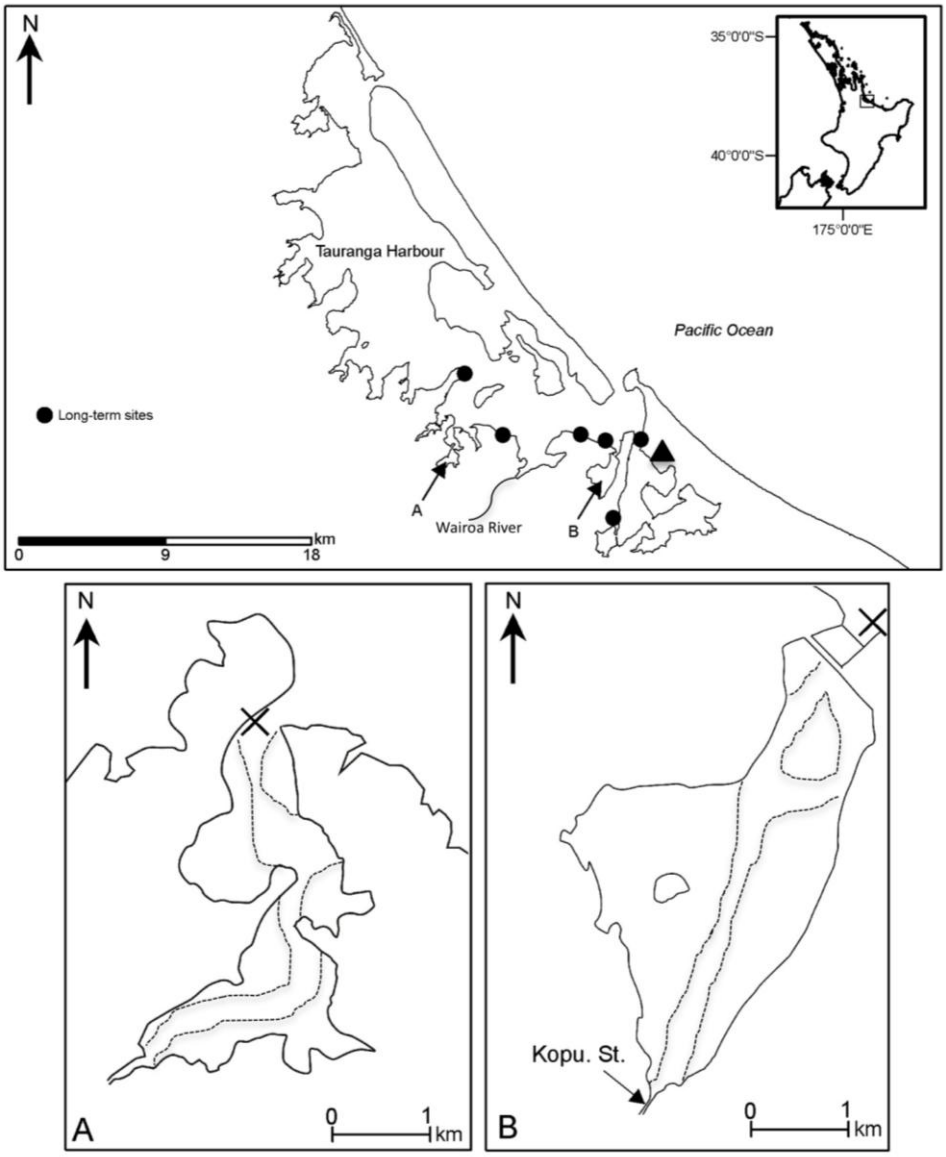

Figure 2.1 Map of Tauranga Harbour (North Island, New Zealand) showing the location of the study estuaries (A) Te Puna and (B) Waikareao and sites monitored by the Bay of Plenty Regional Council (black points). The filled triangle marked the location of Tauranga Aiport where the meteorological station is situated. In Te Puna and Waikareao 'X' marks the location where 24-hour sampling was undertaken. Kopu. St. = Kopurereroa Stream.

Table 2.1 Physical characteristics of Waikareao and Te Puna estuaries.

Physical characteristics	Waikareao	Te Puna
Mid tide estuary area (km^2)	2	1.4
Catchment area (km^2)	75	22.2
Average channel depth (m)	2.2	2.1
Distance from harbour entrance (km)	4.5	12
Intertidal area (%)	55	61
Main catchment land use (%)	54% agriculture	83% agriculture
	8% urban	16% forest (native)

Table 2.2 Rainfall for Te Puna and Waikareao estuaries on the day of field sampling. Rainfall data was from National Institute of Water and Atmospheric Research (NIWA) CliFlo database.

Season	Rainfall (mm)	
	Te Puna	Waikareao
Winter	0.8	9
Start of spring	0.6	0
End of spring	0	0.6
Summer	4.6	0

2.3 Results

2.3.1 Tidal and seasonal variations in water properties and nutrient concentrations

Seasonal measurements of nitrate, phosphate and ammonium concentrations made at six sites since 1991 spanned a similar concentration range to those measured in the Waikareao and Te Puna estuaries during the four intensive 24 h sampling periods (Figure 2.2). When considering only the long-term (19-yr) data collected in the same month as the sampling dates (March, June, September and November) in this study, the pattern in the data is observed to be similar to the four intensive 24 h sampling measurements (Figure 2.3). Both the long-term measurements and the data from the current study indicate that mean DIN concentrations were generally higher in winter and at the start of spring than in the other two seasons (Figure 2.3). Maximum concentrations occurred in winter and spring, with minimum concentrations in summer (Figure 2.3). Phosphate did not appear to follow a temporal pattern, and concentrations were generally five times lower than DIN concentrations, consistent with other estuarine studies (e.g. Boynton et al. 1995).

The long-term data were partitioned into three timescales: interannual (by year), seasonal (by month- January to December) and sub-seasonal. These were extracted by averaging the data by month (seasonal averages) and by year (annual averages) while the remaining variance was considered to be sub-seasonal. Nine percent of the variance in nitrate was explained by the seasonal pattern, and 7% by the interannual, so that the remaining 84% was unaccounted for, or sub-seasonal; for ammonium the breakdown was 1%, 16% and 83% for seasonal, interannual and subseasonal respectively; and for phosphate was 4%, 6%, 90% respectively. The nitrate levels were correlated with salinity ($r=-0.53$, $p<0.001$), which strengthened when considering only seasonal ($r= -0.8$, $p<0.001$) or interannual variations ($r= -0.85$, $p<0.001$). Conversely, ammonium and phosphate were not well correlated with salinity ($r= -0.29$ $p<0.001$ for ammonium; $r =-0.12$, $p<0.001$ for phosphate). However, phosphate concentrations were well correlated with ammonium concentrations at a seasonal time scale ($r = 0.75$, $p<0.001$). The monthly mean salinities for the 19-year dataset were higher than those observed during the four 24-hour sampling periods in the corresponding month, whereas the monthly mean nitrate and ammonium concentrations were lower. The long-term measurements were made consistently closer to high tide. Interestingly, the variance in long-term nutrient concentrations for samples taken in the months corresponding to each of the four 24-hour measurements was nearly identical (Figure 2.3). The greatest monthly variances in the long-term data were observed between June and September (winter to early spring). Mean values and the coeffiecient of variation were calculated for the long-term data and the 24-hour measurements data (Appendix 1).

In addition to the bias toward high-tide sampling in the long-term data, there was a systematic spatial bias towards sampling at similar stages of the tide across sites. Extracting only samples collected between 4 and 5 h after/before high tide allowed better comparison between sites (see sampling locations in Figure 2.1), and showed that the difference in the mean nitrate concentrations (averaged over 19 years) between the site nearest Te Puna and the site nearest Waikareao was 0.013 mg/L and ammonium was 0.0004 mg/L (difference of means test, $p<0.05$). Average salinity was ~ 1 lower near Te Puna. The variance in salinity, nitrate and ammonium experienced over the 19-years was also greater near Te Puna. However, the magnitude of these site differences is much smaller than the

differences between sampling periods, indicating that long-term variations are greater than those measured at Te Puna and Waikareao (shorter term tidal variations are controlled for by only considering the same stage of the tide). This tidal restriction limits the resolution of the dataset to only 8 (near Waikareao) and 18 (near Te Puna) points respectively.

The 24-hour experiments allowed a detailed examination of the intertidal and daily variations in nutrient concentrations along with salinity and temperature. In three of the four sampling periods, the outgoing water measured at the jetty was warmer at the end of the day (by ~ 4 ^{o}C) than at the beginning of the day and colder in the morning low tide than the evening low tide of the previous day (Figure 2.4). In winter, however, tidal variations in temperature (differences between low and high tide) exceeded diurnal variations (differences between morning and evening low tide). Salinity of the incoming water was always higher than the outgoing water, and there was no discernible day-night variation. Both the incoming and outgoing water for Te Puna Estuary was fresher than for Waikareao Estuary. There were insignificant differences between both Te Puna and Waikareao Estuaries salinity.

There were subtle changes in salinity and temperature between sampling dates, with both variables increasing from winter to summer (Figure 2.4). The largest increase in salinity occurred between the start of spring and the end of spring, whereas the temperature increased consistently from winter through to summer. The salinity decrease was greatest during low tide of winter and early spring, with Te Puna lower than Waikareao by 1.5 and 9.7, respectively. In late spring and summer, the differences were smaller. In the winter and start of spring samplings there were rain events preceding and during the sampling period which were evident as lower salinity for Te Puna in particular (Figure 2.4). Temperatures in both estuaries were generally comparable except for the end of spring sampling period when Te Puna was nearly 4^{o}C warmer than Waikareao.

In both estuaries, DIN concentrations tended to be higher at low tide than at high tide (Figure 2.5). Phosphate levels (not shown) did not vary appreciably with the tide or seasonally (Figure 2.3). In winter and start of spring samplings, tidal variations were more evident than at the end of spring and summer when DIN concentrations were consistently lower (Figure 2.5). The tidal variations in nitrate

concentration were greater than in for ammonium in both estuaries. DIN was strongly negatively correlated with salinity in both estuaries with r=-0.84, p <0.05, at Waikareao and r=-0.89, p<0.05, at Te Puna. Concentrations of DIN decreased consistently from winter to summer, whereas phosphate levels were highest in late spring. There were some anomalies in the spring period, when DIN concentrations in incoming tides were greater in early spring than late spring. The largest of these anomalies was the very high average nitrate concentration (~0.5 mg L^{-1}) coming into Te Puna Estuary during the day on the incoming tide. This was not accompanied by elevated ammonium concentrations. Seasonal changes occurred in molar ratios of dissolved inorganic nitrogen to phosphate at the different temporal scales (Figure 2.3). Ratios of DIN: PO_4^{3-} was higher in winter than in summer, but ratios varied throughout tidal cycles due mostly to the highly dynamic nature of nitrate concentrations (Figure 2.3).

The dissolved oxygen (in % saturation) varied diurnally with higher concentrations in the late afternoon and lower concentrations during the period from night to morning period (Figure 2.6). This pattern was most pronounced at the start and end of spring. The dissolved oxygen (% saturation) was highest at the start of spring and lowest in winter. Chlorophyll *a* also generally followed a diurnal pattern with maxima in mid to late afternoon (Figure 2.7). This pattern was more pronounced at the start and end of spring. Relatively low concentrations of chl-*a* values occurred in winter and summer.

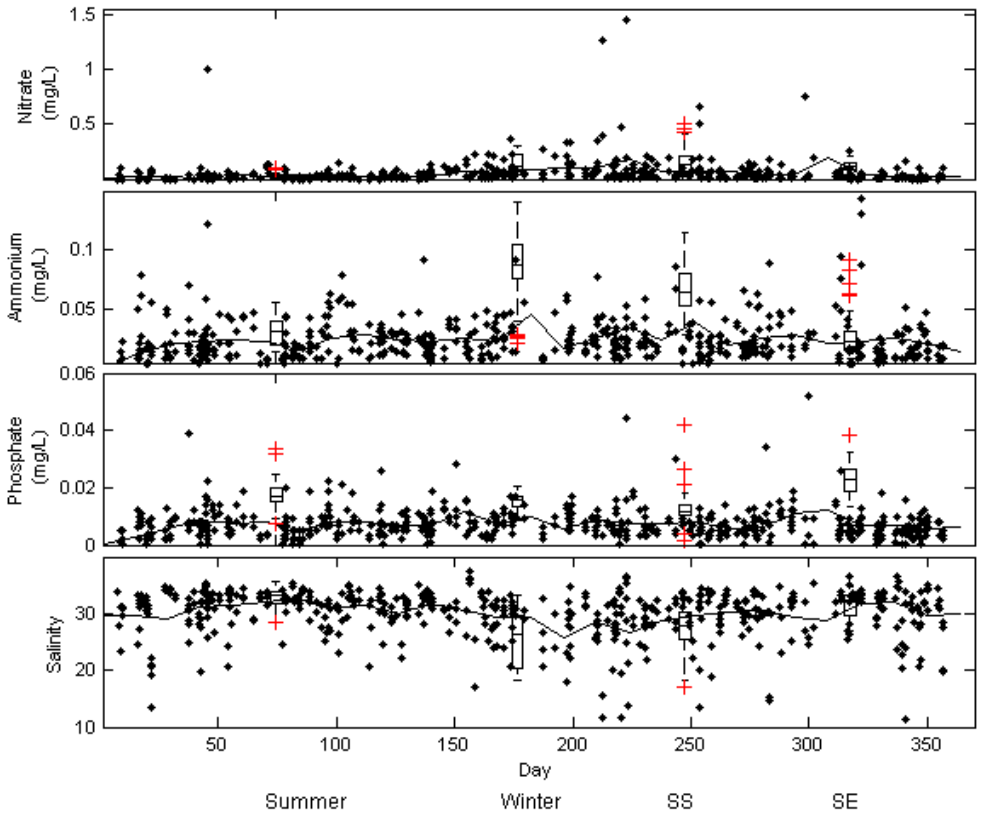

Figure 2.2 Comparison of intra-annual variations in nitrate, ammonium and phosphate concentrations and salinity from a long-term data set (1991-2009) with those measured during this study. Long-term data (black dots) comprise of quarterly measurements made at six sites and the solid line represents the median value. Data from the current study have been summarized in box plots (with data from both estuaries combined into one box). The horizontal line in the box plot shows the median, the boxes the inter-quartile range and the crosses represent the outliers. The seasons are under the x-axis with SS denoting start of spring and SE end of spring.

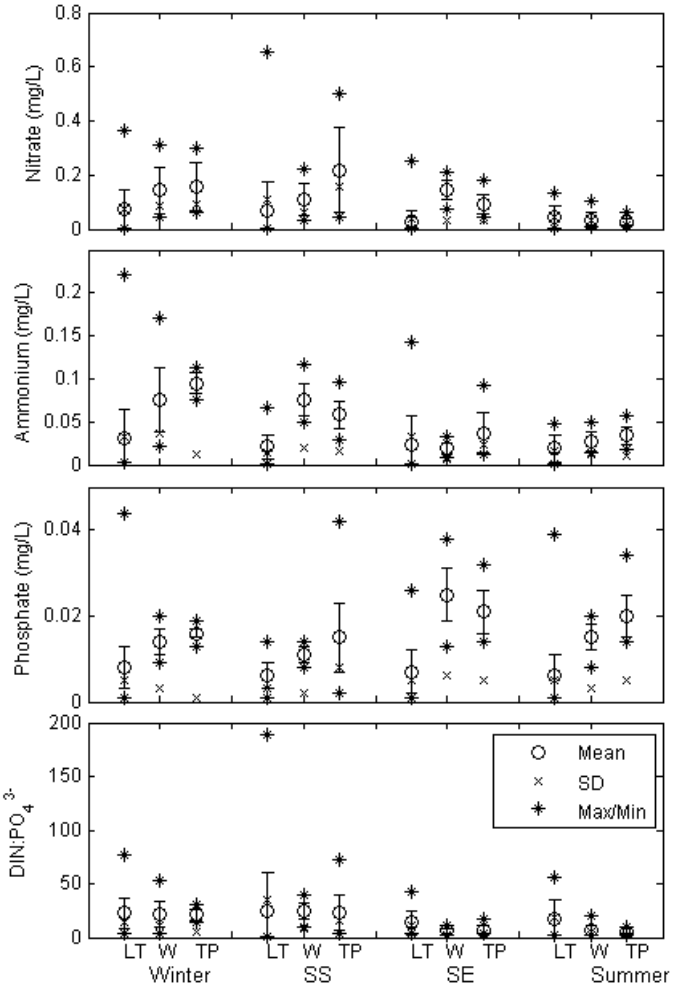

Figure 2.3 Mean (M), standard deviation (SD) and range of nitrate, ammonium and phosphate concentrations, and DIN:PO_4^{3-} molar ratios from a long-term dataset (1991-2009) and from the Waikareao and Te Puna Estuaries measured in this study. For the mean of long-term dataset, data were averaged in the month of when sampling occurred in Waikareao and Te Puna. For Waikareao and Te Puna estuaries, the statistics were calculated using all data collected in the 24 h sampling period after first averaging surface and bottom water concentrations. LT: Long-term; W: Waikareao Estuary; TP: Te Puna Estuary; W: Waikareao Estuary; SS: start of spring; SE: end of spring.

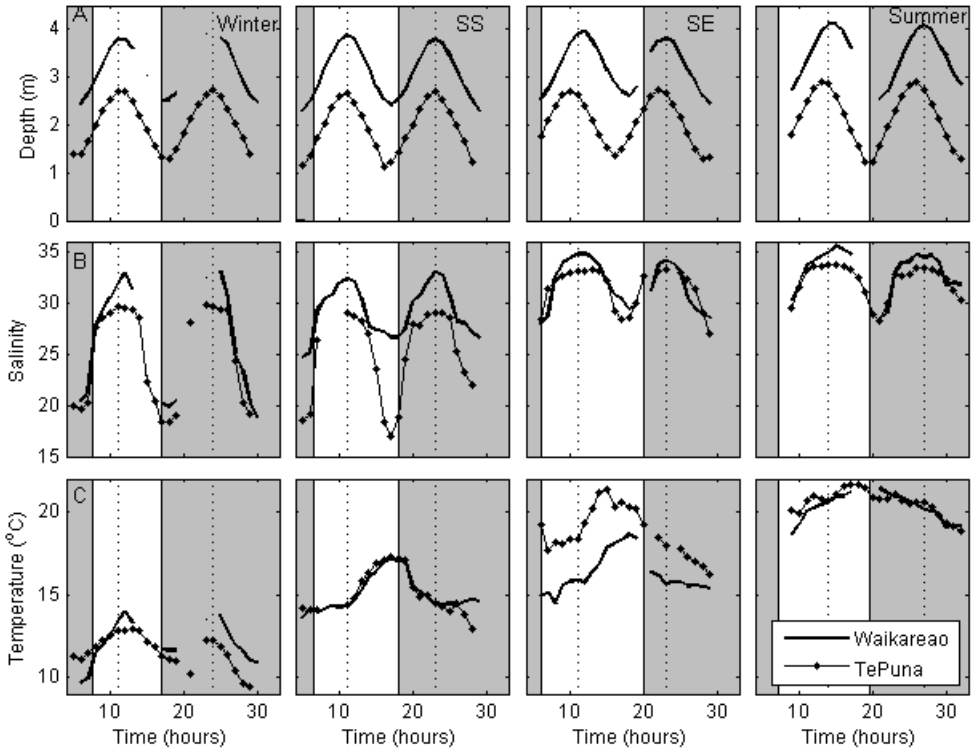

Figure 2.4 Changes in (A) water depth, (B) salinity and (C) temperature during a 24 h period at Waikareao and Te Puna Estuary on four sampling occasions. The CTD data were depth-averaged. The grey panels represent early morning and night, and the white panels represent daylight hours. Vertical dashed lines indicate high tide. SS = start of spring; SE = end of spring. For end of spring at Waikareao Estuary, the night sampling was done first, however in the plot the early morning to evening data is presented first to standardize the plot. Missing points indicated missing CTD casts.

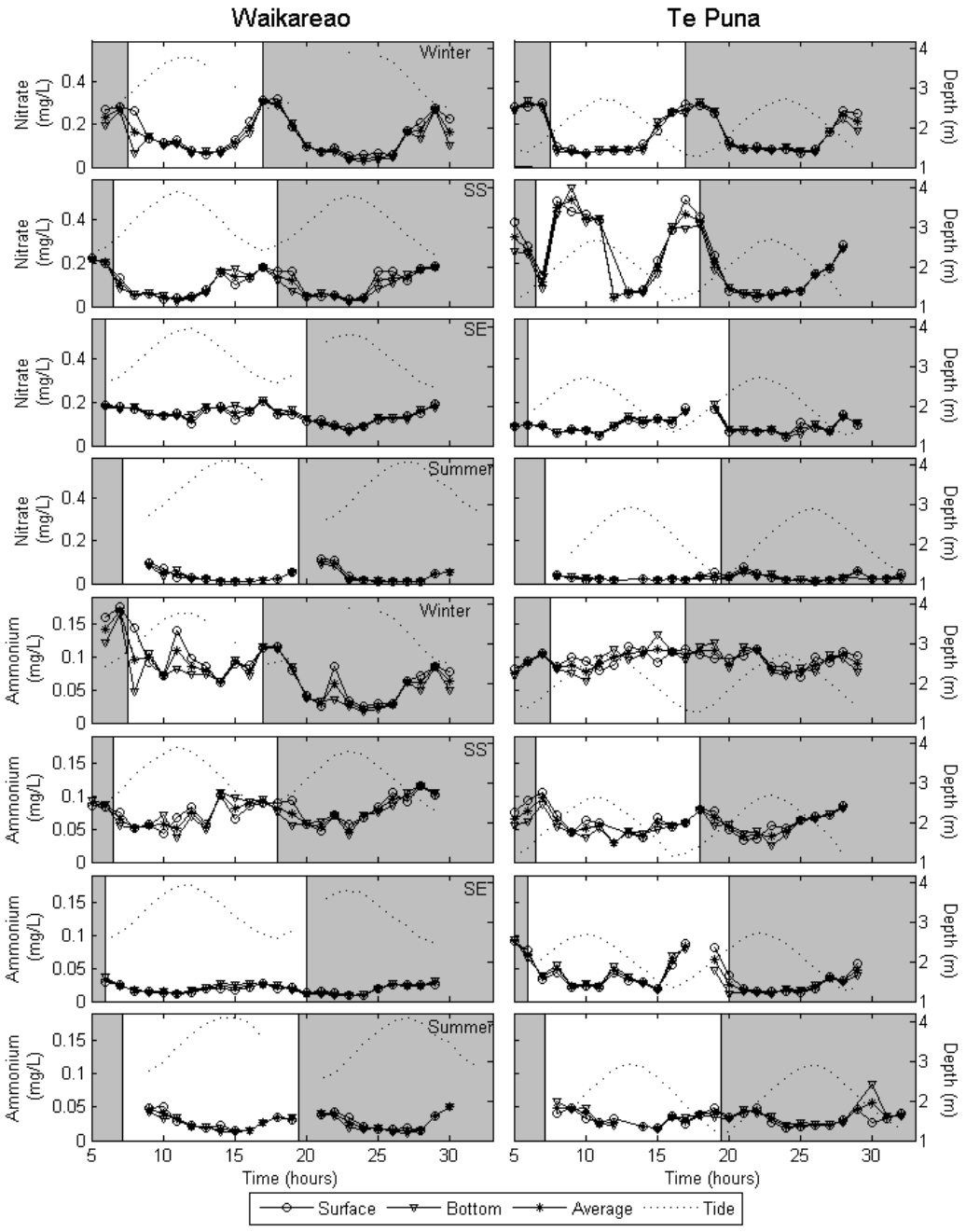

Figure 2.5 Changes in nitrate and ammonium concentrations during a 24 hour period on four sampling occasions. The grey panels represent early morning and night, and the white panels represent daylight hours and, the dotted black line represents the tidal cycle. SS = start of spring; SE = end of spring. For end of spring at Waikareao Estuary, the night sampling was done first, however in the plot the early morning period to evening data is presented first to standardize the plot. Each data point represents two samples.

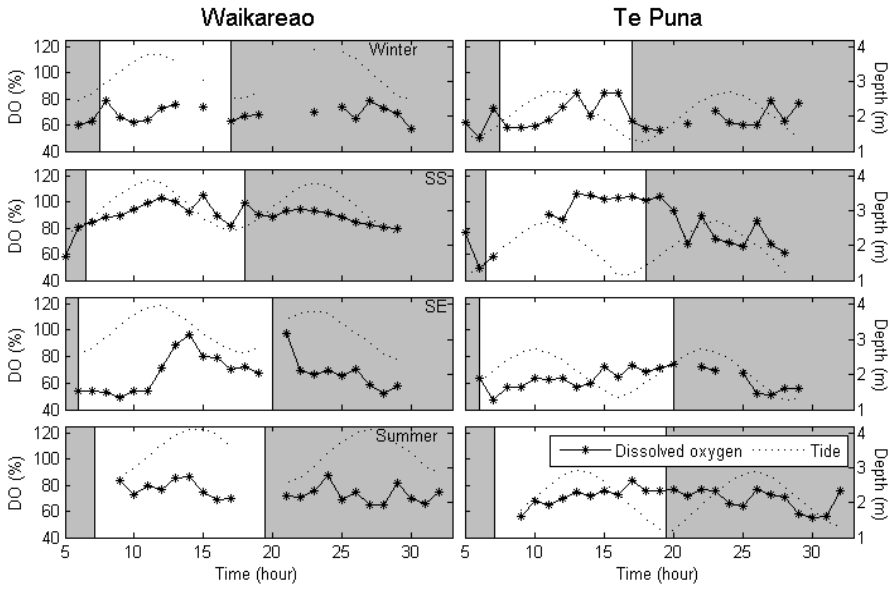

Figure 2.6 Changes in depth-integrated dissolved oxygen (% saturation) during a 24 hour period on four sampling occasions. The grey panels represent the early morning and night, the while panels represent daylight hours and the dashed lines represented the tidal cycle. SS = start of spring; SE = end of spring. For end of spring at Waikareao Estuary, the night sampling was done first, however in the plot the early morning period to evening data is presented first to standardize the plot.

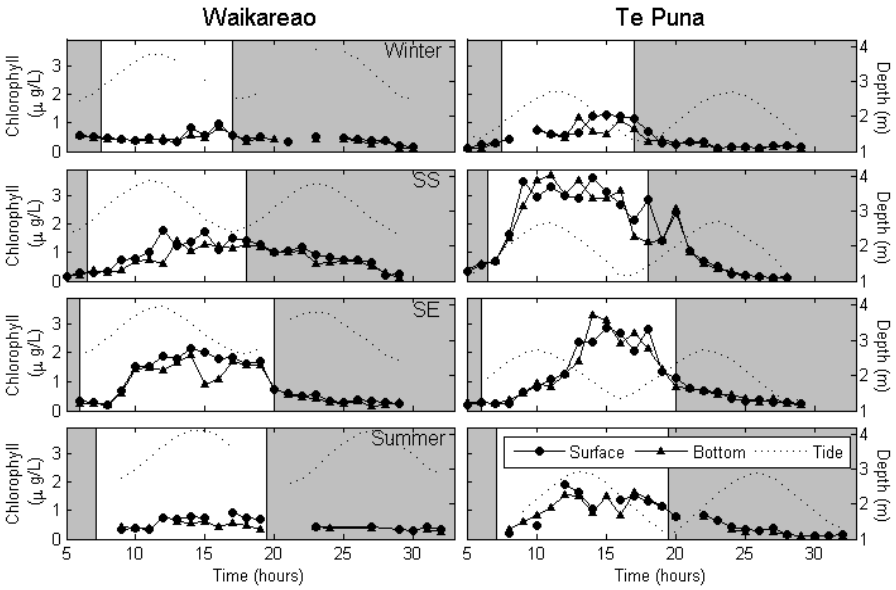

Figure 2.7 Changes in chlorophyll *a* concentration during a 24 hour period on four sampling occasions. The grey panels represent early morning and night, the while panels represent daylight hours, and the dashed lines represented the tidal cycle. SS = start of spring; SE = end of spring. For end of spring at Waikareao Estuary, the night sampling was done first, however in the plot the early morning period to evening data is presented first to standardize the plot.

2.3.2 Nutrient fluxes

Both estuaries were net exporters of DIN to the main harbour: between 34 and 358 kg per tidal cycle of nitrate and 22 and 93 kg per tidal cycle of ammonium (Table 2.3). The nutrient fluxes were normalized to catchment area in the last column of Table 2.3 to compare with literature values (see Discussion). Net nitrate fluxes decreased in both estuaries from winter to summer. For ammonium a similar seasonal pattern was not observed. In Te Puna the net ammonium flux was highest at the end of spring whereas in Waikareao it was highest in winter and the start of spring. Nitrate fluxes were generally three times higher than ammonium in both Waikareao and Te Puna. The winter increase in net nitrate export rates (which was the main driver of variations in DIN concentrations) was caused mostly by an increase in nitrate concentrations on the ebb tide rather than a reduction of concentrations on the flood tide (Figure 2.8). Conversely ammonium fluxes were mostly small because differences in concentrations between flood and ebb tide were small. DIN measured at Kopurereroa Stream (not shown) gave net fluxes from this source between 13-33% for nitrate and 2-23% for ammonium relative to total net fluxes for each of the respective nutrients.

There were diurnal patterns in net DIN fluxes with both estuaries, with greater export of ammonium and to a lesser extent nitrate at night than during the day (Figure 2.8). For ammonium, the net flux during the night exceeded that during the day by three to five times. The difference was greatest in winter while for nitrate it was 1 to 2 times at both Waikareao and Te Puna estuaries. One exception to both estuaries acting as net exporters of DIN was in Te Puna Estuary at the start of spring, where there was a net import of DIN. Generally, however, the large magnitude of gross fluxes of DIN relative to net fluxes indicates the dominance of tidal transport in these estuaries.

Net ecosystem metabolism (*NEM*) was also calculated for each season at both estuaries. Both Waikareao and Te Puna were autotrophic, in that NEM was always positive (Appendix 2).

Table 2.3 Seasonal variations in net fluxes of nitrate and ammonium averaged over two tidal cycles at Waikareao and Te Puna Estuaries. SS= start of spring; SE = end of spring. The first three columns are normalized by estuary size, and the fourth column is normalized by catchment size.

Estuary	Nitrate (kg /tidal cycle)	Ammonium (kg /tidal cycle)	Nitrate (kg /tidal cycle/km^2)	Ammonium (kg /tidal cycle/km^2)	DIN (kg N/tidal cycle/km^2)	DIN (kg N/yr/ha)
Waikareao						
Winter	-357.7	-85.1	-178.8	-42.6	-221.4	-40.9
SS	-295.3	-92.6	-147.6	-46.3	-193.9	-35.8
SE	-136.3	-30.0	-68.1	-15.0	-83.1	-15.4
Summer	-82.3	-49.9	-41.2	-25.0	-66.1	-12.2
Te Puna						
Winter	-310.6	-22.1	-221.9	-15.8	-237.7	-86.8
SS	-102.5	-43.7	-73.2	-31.2	-104.4	-38.1
SE	-90.8	-64.2	-64.8	-45.9	-110.7	-40.4
Summer	-33.5	-34.9	-23.9	-24.9	-48.9	-17.8

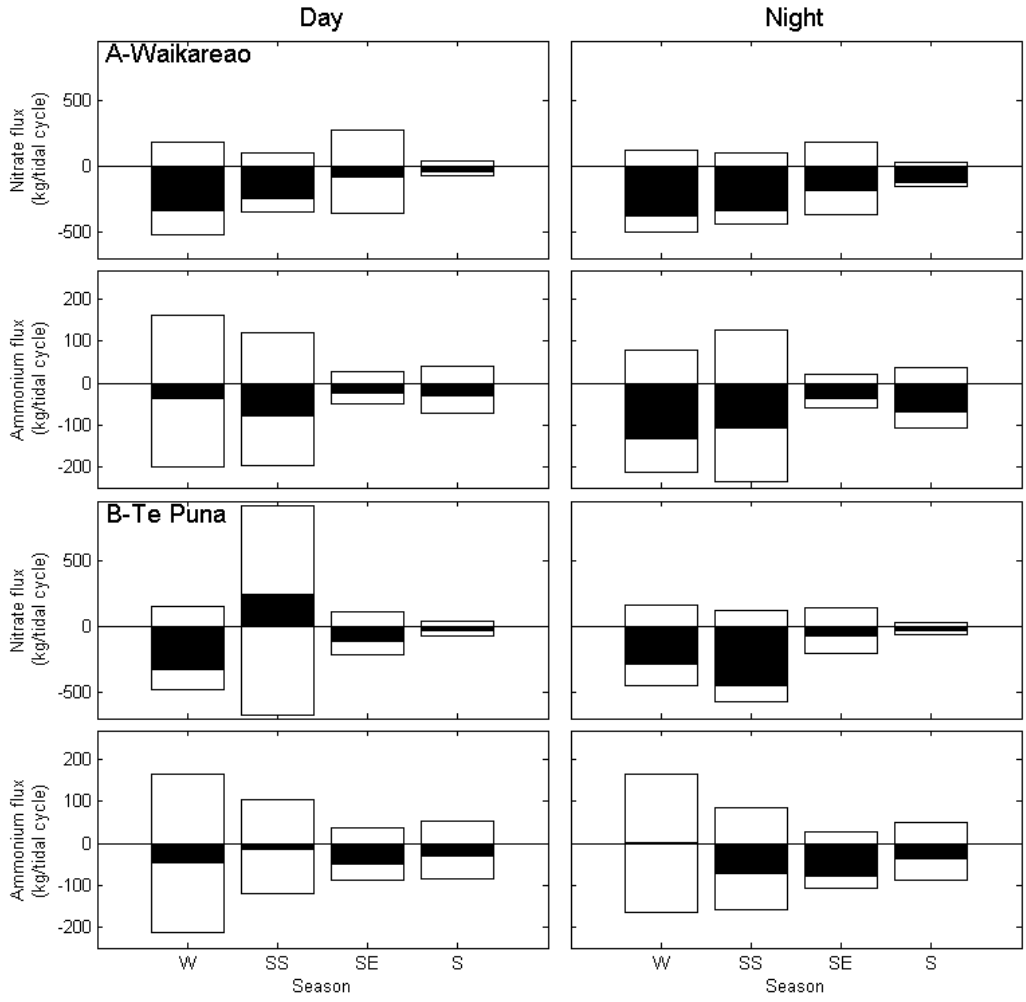

Figure 2.8 Day-night differences in nitrate and ammonium fluxes at Waikareao (A) and Te Puna (B) estuaries for the four sampling periods. Positive values represent flood tide fluxes and negative values ebb tide fluxes. The black bar indicates net flux. W: Winter; SS: start of spring; SE: end of spring; S: summer.

2.4 Discussion

The average nutrient concentrations in Waikareao and Te Puna Estuaries were low relative to levels considered to be associated with the risk of nuisance algal blooms, eutrophication and hypoxia. More impacted estuaries can have concentrations an order of magnitude or more, higher. For example, nitrate concentrations in the Elbe Estuary can be as high as 20.5 mg L^{-1} (Dähnke et al. 2008), while nitrate concentrations in Ebro Estuary ranged seasonally from 0.1 to 12 mg L^{-1} (Falco et al. 2010). This study's seasonal ranges were comparable to those measured in other shallow estuaries, for example nitrate concentrations ranged from 0.45 to 1.08 mg L^{-1} in Biscayne Bay corresponding mostly to dry and wet periods (Caccia and Boyer 2005).

Whether elevated concentrations pose a risk of eutrophication depends on the timescale over which the nutrient levels persist, which largely depend on the hydrodynamic regime (Christian et al. 1991). Both Te Puna and Waikareao estuaries are well-flushed and well-mixed so that over each tidal cycle some 48-75% of the water is exchanged with water from the main harbour, which in turn is also rapidly exchanged with the shelf, giving nutrients little time to accumulate. The highly flushed environment limits the capacity for phytoplankton to adapt and grow in response to the prevailing nutrient concentrations. Conversely, benthic algae and macrophytes may respond to nutrient concentrations that vary on such short time scales (Valiela et al. 1997). It is also important to note that the variability in DIN drives mostly shifts in the ratio of DIN to phosphate both over tidal cycles and during the year, complicating an understanding of which nutrient (N versus P) might be ultimately limit phytoplankton growth. Though in winter growth is more likely to be limited by light whilst in summer it is DIN.

Sampling at four discrete time scales from hourly through to routine bi-monthly over 19-years of monitoring allowed for determination of the relative importance of interannual, seasonal, tidal and episodic components. The majority of the variation in nutrient concentrations was attributed to tidal variations and episodic events. The long-term monitoring was biased towards high tide (lower-DIN, higher salinity). Variations observed within tidal cycles were of a similar magnitude to the variations measured over all 19 years at comparable times of the year. The average DIN concentrations were generally higher for the estuaries in comparison to long-term monitoring. The estuaries sampling regime covers concentration from different stages of the tide, and the large differences between low and high tide concentration leads to higher average DIN concentration. However, the long-term sampling was generally conducted at high tide and this only give a representative concentration of the particular stage of the tide. Moreover, in order for a long-term sampling programme to be able to control for variability from tidal fluctuations, there would need to be sampling consistently at the same stage of the tide, with high-tide measurements indicative of nutrients contributed from the shelf, and low-tide measurements indicative of contributions from the catchment. Sampling at low tide is more likely to allow for identification of land-derived nutrient sources as well as internal (intra-estuarine) fluxes.

Conversely, coordinating a sampling regime with tidal excursions is less critical in micro-tidal estuaries.

The high correlation between nitrate and salinity (and lack of correlation of ammonium and phosphate with salinity) in the 19-year dataset indicates that the nitrate variations are controlled by changes to the freshwater input to the estuary whereas the ammonium and phosphate concentrations are more likely to be related to nutrient cycling processes within the estuary. Increases in freshwater input occur with elevated precipitation and reduced evapo-transpiration in winter, and the 24-hour sampling indicated that the salinity difference between incoming and outgoing water was greatest in winter. Nutrient concentrations generally increase with rainfall, as nutrients are washed off the catchments, however, responses vary depending on the flushing of the estuary, and nutrient (specifically ammonium and phosphate) levels in poorly flushed estuaries can increase during drought periods often in response to bottom-water anoxia (Boynton et al. 1995; Hamilton et al. 2006; Møhlenberg et al. 2007, Caffrey et al. 2007) and decrease during flooding events as nutrients are flushed from the estuary (Burkholder et al. 2006). From long-term rainfall records (not shown), the rainfall pattern observed during the high-frequency sampling was typical of the winter period. The long-term nutrient data spanned similar concentrations range as the estuaries in winter suggesting rainfall events contribution towards nutrient concentrations. The distance from nutrient sources, the nutrient species and the steepness of the catchment also determine the loss of nutrients between sources in the catchment and the estuary. Te Puna and Waikareao estuaries have short, steep catchments that are largely devoted to dairy farming relying on intensive fertilizer use (Table 2.1). Te Puna is further from the harbour mouth, and thus would be more influenced by catchment processes (which might account for the slightly elevated and more variable DIN and lower salinity).

The higher average ammonium concentration observed in both estuaries during winter and spring in comparison to long-term data is related to the sampling regime. The estuaries sampling regime covers different stages of the tide, and the large differences between low and high tide concentration leads to higher average ammonium concentration, while the long-term data was collected once at high tide. The rapid flushing in winter and active vertical mixing in the estuaries lead

to ammonium regenerated from sediment and from shallow upper estuary regions to be transported into surface water. This frequent mixing coupled with high flushing rate is also a likely explanation for the higher concentration of ammonium in winter.

Both estuaries were net exporters of DIN to Tauranga Harbour. Incoming water was consistently lower in DIN than outgoing water, suggesting that recycling processes within the estuary and inputs from surface runoff and groundwater seepage exceeded the estuaries' nutrient demand. By comparison other studies have shown a strongly seasonal cycle of net import and export (Gardner and Kjerfve 2006; Sigleo and Frick 2007). There are very few measurements of DIN fluxes into estuaries in New Zealand. Heggie and Savage (2009) gave total nitrogen (TN) loading rates of approximately 0.6-17.0 kg yr^{-1} ha^{-1} of catchment for Otago (South Island, NZ) catchments, with the rate depending linearly (r^2=0.99) on the percentage of agriculture in the catchment. Waikareao and Te Puna values of 5-29 kg yr^{-1} ha^{-1} of N are high relative to those of Heggie and Savage (2009), especially as DIN/TN ratios are commonly on the order of 50% (Boynton et al. 1995). The differences in nutrient fluxes between the Te Puna and Waikareao estuaries are broadly consistent with the differences that Heggie and Savage predict will occur because of the relative difference in the percentage of the catchment in agricultural land use. Their simple regression model that relates nutrient loading to percentage of agricultural land use predicts a 66% difference, while this study finds an average of 47% difference. Processes occurring in the fringing areas of the estuary can modify this balance (both Te Puna and Waikareao are fringed by large mangrove areas). Parfitt et al. (2006) model the nitrogen loading and output from New Zealand, broken down by region, and show that the loading to the Bay of Plenty region (wherein Tauranga Harbour lies) is around 37 kg yr^{-1} ha^{-1}, and given an nationally-averaged output rate of 30% of input (calculated from their Table 1 and 2), gives 11 kg yr^{-1} ha^{-1}. Again Waikareao and Te Puna average values are larger than the predicted levels for the region. Waikareao and Te Puna have short steep catchments, which are characteristic of many New Zealand catchments suggesting limited attenuation (e.g. denitrification) from source (catchment) to estuary. The phosphorus loading to the catchment was smaller than nitrogen, 10 kg yr^{-1} ha^{-1} (Parfitt et al. 2008) and the phosphate concentrations were low and variable at both estuaries (usually < 0.04 mg/L)

which may be related in part to sediment characteristics, the highly reactive chemistry of this species, and adsorption of phosphate to sediment particles (Sundby et al. 1992; Page et al. 1995; Spiteri et al. 2008).

Although the fluxes reported here are low on the international scale (e.g. Zhang 1996; Grelowski et al. 2000), the catchment landscape alterations surrounding both Waikareao and Te Puna are relatively recent with intensive horticulture and agriculture occurring only in the last 50 years compared to the catchment land use in some northern hemisphere estuaries which have anthropogenic influences that date back thousands of years (Correll et al. 1992; Dauer et al. 2000). Catchment changes can take many years to substantially alter nutrient inputs into estuaries, as nutrients can be stored in groundwater reservoirs and sediments (Howarth et al. 1996).

It is difficult to differentiate between sediment processes, catchment and groundwater input and direct atmospheric inputs as sources of the observed DIN exports. Freshwater inputs of nutrients were estimated using the tidal prism method and the mean salinity relative to high water salinity (see Equation 2.1 below):

$$V_r = V_t\left(\frac{S_{HT}}{S_{LT}} - 1\right)$$

$$R = V_r/T$$

(Equation 2.1)

Where V_t is the volume of water entering the estuary between low and high tide (m^3), and V_r is the volume of freshwater entering the estuary over a tidal cycle (m^3), R is the freshwater discharge (m^3/s), and T is the tidal period (taken as 12.4 × 3600 s), and S_{HT} and S_{LT} are the high and average tide salinity. The concentration of DIN in the freshwater inputs is then the net nitrate flux divided by the discharge. Equation (2.1) demonstrates that if all the nitrate/ammonium were coming from the freshwater input with no alteration (i.e. no transformations between species), then the freshwater would have a concentration of nitrate of ~0.45/0.24 mg/L (Waikareao/Te Puna) and ~0.14/0.11 mg/L of ammonium in start of spring. In winter and spring, this is consistent with measurements of DIN in the Kopurereroa Stream, but in summer the estimates of nutrient concentrations

using this method are 3-4 times larger. Given that there is no particular reason for the freshwater DIN contribution to be much higher in summer, it is likely that sediment processes play a more important role in summer. Incubation experiments with water collected from Chesapeake Bay by Shiah and Ducklow (1994), showed that bacterial production increased along with substrate enrichment at high temperature, > 20 ºC. This showed the sensitivity of bacteria to temperature, which in turn can influence nutrient recycling processes as many of the processes are microbially-mediated. Rocha and Cabral (1998) found that nitrate dynamics in intertidal sediments of the Sado Estuary are strongly influenced by tidal action as periodic immersion and exposure influence oxygen supply to the sediment. This oxygen supply has an impact on the nitrification/denitrification zone, which can lead to high rates of nutrient cycling and transformations of nitrate in porewater (Caffrey et al. 2003).

This study provides surprisingly similar values (average 2 times higher) to those observed by Sandwell et al. (2009) using benthic chambers at a mid-tidal sandflat in Tauranga Harbour. They found effluxes of ammonium from sediments ranged from 4.25-26.6 kg km^{-2} tidal $cycle^{-1}$, which they attributed primarily to bivalve excretion and respiration. The similarity is surprising because the fluxes calculated here represent an integration of the fluxes over the whole estuary whereas benthic chambers will be specific to the chamber area. At Waikareao and Te Puna, field sampling was done at the constricted estuarine mouths where water exported from the estuary is likely to be homogenized.

The exchange of nutrients across the sediment-water interface can supply a significant fraction of nutrient requirements for primary production in the overlying water of estuaries (Billen 1978; Callender and Hammond 1992). The relative importance of this source compared to external loadings has been found to vary substantially and can account for a large percentage of nitrogen demand in the water column as shown in previous studies such as in Chesapeake Bay (Boynton and Kemp 1985), and three North Carolina estuaries (Fisher et al. 1982). In shallow-water where a large portion of the benthos is within the photic zone, the effects from activities of benthic microalgae are superimposed on mineralization processes mobilizing in surficial sediments.

2.5 Conclusions

Measurements of nitrate, ammonium and phosphate are presented along with key environmental conditions collected over tidal, seasonal and interannual timescales. Variations on sub-seasonal scales constitute the largest source of variability, likely balanced between episodic and tidally-driven processes. The nitrate variations were largely associated with increased freshwater inputs, where as ammonium and phosphate were more likely to be related to cycling and regeneration within the sediments. The tidal prism calculations suggest that sediment fluxes dominate over freshwater fluxes at least for a summer month. Although concentrations were on average low, low-tide/high-tide differences resulted in a high flux of DIN from the catchment, relative to predictions based on nitrogen loading models. Sampling regimes need to be adapted and focused to account for the high temporal variability of nutrient inputs/outputs to better understand nutrient sources/sinks in small estuaries.

Chapter Three: The hydrodynamics of Tauranga Harbour

3.1 Introduction

Chapter 2 showed that there was a general export of DIN from Te Puna and Waikareao Estuaries into Tauranga Harbour as a whole, which changed between seasons. In order to understand the role of physical and biological processes controlling the DIN concentration, a hydrodynamic-biogeochemical model was applied. However circulations in these estuaries are largely controlled by circulation in the larger harbour. Therefore the first stage of this work was to characterize the hydrodynamics of the wider harbour. By providing an understanding of the hydrodynamics will ultimately give insights not only into the overall fate of terrestrial inputs, but also the exchange of sediments, pollutants, nutrients and also larvae between the estuary and the coastal seas. During transport, these can undergo alterations due to settling, chemical alterations, and in the final case growth and decomposition that can change the seabed environment (e.g. morphology, sedimentation rate), and the composition of the overlying water column (e.g. oxygen and acidity). The competing effects of vertical mixing and stratification control the distribution in the water column, and the availability of nutrients and oxygen to the benthic environment.

In New Zealand a wide variety of estuarine environments occur, such as drowned river valleys, barrier-enclosed estuaries, river mouth estuaries, estuaries resulting from tectonic activity and fjords, which may be, classified either by physiography or salinity structure (Healy and Kirk 1992). Recently Hume et al. (2007) provided a controlling factor classification of New Zealand estuaries, based on broad scale physical components (e.g. climate, oceanic and riverine conditions, catchment characteristics). Based on Hume et al. (2007) Level 2 classification on estuary hydrodynamic processes, the north-west coast estuaries are generally Class B and C in which the river volume is greater than the tidal volume entering the estuaries, while on the north east coast, the estuaries are generally Class D, E, and F where there is little river influence and are relatively shallow. In the southeast and west of the North Island, the estuaries are generally Class B.

Tauranga Harbour, a barrier-enclosed estuarine lagoon on the north east coast (Davies-Colley and Healy 1978), or category F estuaries according to Hume et al. (2007), is one of the largest estuaries in New Zealand, and forms a particularly important case for detailed study because it is a zone of conflict from a wide range of catchment and estuarine-based activities. These types of estuaries are generally shallow and contain extensive intertidal flats, and have always been assumed to be vertically well mixed and well flushed (Healy and Kirk 1992), and thus minimising the risks associated with stratification and accumulation of terrestrial wastes. Commercial development is centered around the entrance to the southern basin which is the locale for the country's largest export port, Port of Tauranga. Like most urban waterways, Tauranga Harbour must accommodate the increase in commercial shipping associated with the Port combined with the growing population in the sub-catchments surrounding the harbour, who want marinas and easy-access to the coast. Such multiple uses are not always consistent with the primodial ecology of this otherwise mangrove- and seagrass-lined habitat, which is well known for its shellfish beds. In many of New Zealand estuaries the coastal effects from catchment development and navigation activities has resulted in increased sedimentation, heavy metals, and catchment runoff (Chagué-Goff et al. 2000; Abrahim and Parker 2002; Oldman et al. 2009).

Predicting the impact of these developments requires a sound understanding of the hydrodynamic drivers. To date, the most recent study on the hydrodynamics of Tauranga Harbour has been concentrated on the southeastern entrance channel mouth investigating the dynamics of tidal flow in the tidal channel, which serves as the Port's main navigation channel (Vennell 2006; Spiers et al. 2009). A 1983 study commissioned by Bay of Plenty Harbour Board conducted by Black (1984), Healy (1984) and Barnett (1985), comprised of a major field campaign, a hydrodynamic and sediment transport model, and a morphological study. Another unpublished 3-D numerical modelling study was also undertaken as part of the sedimentation study commissioned by Bay of Plenty Regional Council in 2009. However, despite the number of studies and thesis on the area, there is not one paper that characterizes the circulation, salinity and temperature structure in the southern basin of Tauranga Harbour.

At the basis of a hydrodynamic study is the interaction between freshwater discharge, tidal circulation and atmospheric forcing. Estuarine behaviour adjusts dynamically to changes in river flows and tidal forcings, adjusting the salinity and temperature distribution in estuaries (MacCready 1999). These dynamics are modulated to a lesser extent be variations due to precipitation, evaporation, wind stress and surface heat balance. Key variables needed to manage and maintain the health of an estuarine system are (1) the residual circulation patterns which can be large in shallow, wide estuaries (2) residence times and (3) the vertical structure. Residual circulation controls the pathways that advected material takes, and thus is useful for a variety of applications such as determining likely sources of larval recruits for restoring shellfish beds or determining the areas that are likely affected by point-source contaminants. The residence time is the representative timescale which a particle or constituent stays in the harbour. The residence time in an estuary is controlled mainly by the relative strength of salinity-driven circulation and tidal currents. Large freshwater inflow and strong tides lead to shorter residence times. Furthermore, the residence times are also affected by estuarine bathymetry such as constricted arms and channels. The vertical structure controls the conditions that are experienced by the benthos, in particular the penetration of oxygen to deeper areas, which is needed to fuel a multitude of biological and biogeochemical processes such as bacterial decomposition and shellfish growth.

This chapter describes key features of the tidal and wind-induced circulation within the southern basin of Tauranga Harbour, combining results from both a comprehensive field programme and implementation of a 3-dimensional hydrodynamic model. The role of the field data was to assist in calibration of the hydrodynamic model. The model provided spatial and temporal information on tides and currents and helped to determine the influence of wind on circulation patterns. It also provided information on the influence of Wairoa River discharge on the salinity-temperature patterns in the harbour. A calibrated numerical model of harbour dynamics offers information over greater spatial and temporal scales and resolutions than instrument deployments can provide. The numerical models enable the influences of a variety of forcing functions to be isolated and resolved. Although the results are specific to Tauranga Harbour, its shallow intertidal

morphology, characterized by constricted entrances is typical of many New Zealand estuaries.

3.2 Methods

3.2.1 Field site description

Tauranga Harbour is a mesotidal estuarine lagoon on the northeast coast of New Zealand's north island (Figure 3.1) (Krüger and Healy 2006). The barrier enclosed estuarine lagoon is impounded by two Holocene barrier tombolos, Mt Maunganui in the Tauranga (southern) basin, Bowentown in the Katikati (northern) basin, and a 24-km long sand barrier island (Matakana Island) (Davies-Colley and Healy 1978). The two barriers are connected with a large tidal flat separating them and following past studies on the harbour (Barnett 1985), it is assumed that there is little or no exchange of water between each. Therefore only the southern basin is simulated in this study (area: 110 x 10^6 km^2; volume: 120 x 10^6 m^3). The harbour has large tidal flat regions (208 km^2), which are exposed during periods of low tide and a spring tidal range of 2m (Heath 1976). Wairoa River is the main freshwater input into the harbour with a mean inflow of 17.6 m^3s^{-1} (Park 2004). The harbour catchment is well-developed with extensive horticultural (5%), land-cropping (0.1%), pasture (34%), wetland (2.1%), urban-open spaces (0.3%), urban (3%), mixed scrubs (4%), bare ground (0.1%), coastal sand (0.1%), indigenous forest (44%) and planted forest (9%) (Environment Bay of Plenty Regional Council).

3.2.2 Data collection

An 11-day field campaign was undertaken from February 3, 1999 to February 11, 1999 to obtain data for calibration of the numerical model. C. Pilditch provided this data for use in the numerical modelling in this thesis. Three electromagnetic InterOcean S4 current meters (Figure 3.2), were deployed over four tidal cycles at Omokoroa, Motuhou and Western channel transects (Figure 3.2) to determine tidal elevation, current speed, current direction, water salinity and water temperature. The three electromagnetic S4 current meters were deployed at three transects: Omokoroa (3-5 February 1999), Motuhou (6-8 February 1999) and Western (9-11 February 1999). Conductivity, temperature and depth casts were also taken at each station using Seabird electronics CTD. Table 3.1 summarises the measured water properties at each site.

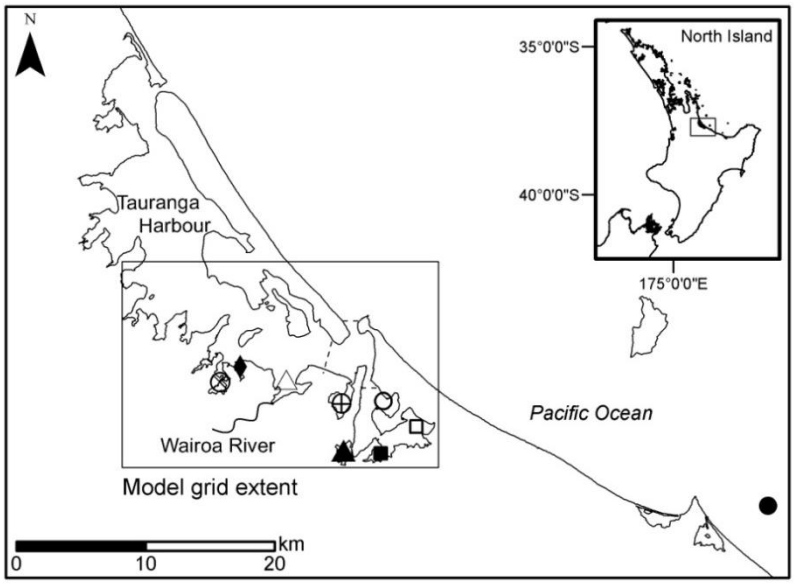

Figure 3.1 Location map of the study area in the southern basin of Tauranga Harbour and outlining the extent of the model grid. The harbour is subdivided into different regions based on Hume et al. (2009) to classify residence times. The location of Pukehina wave buoy is marked with a black-filled circle. Waipu Bay: O; Rangataua Bay: □; Welcome Bay: □ (filled in black); Waimapu Estuary: Δ (filled in black); Waikareao Estuary: ⊕; Waikaraka Estuary: ◊ (filled in black); Te Puna Estuary: ⊗; Dashed line: Deep Channel South (DCS).

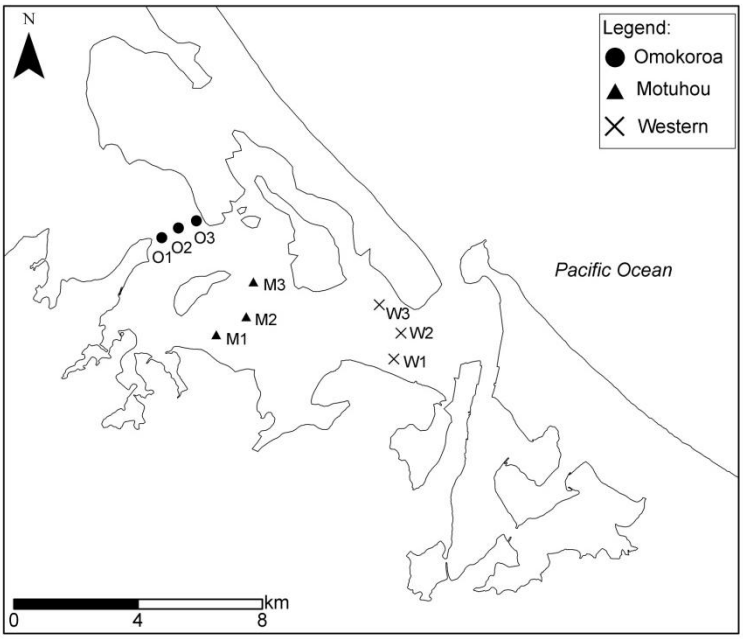

Figure 3.2 Site map of the location of S4 currents meters deployment in Omokoroa, Motuhou and Western, Tauranga Harbour. At each site, three S4 were deployed (O1, O2, O3: Omokoroa; M1, M2, M3: Motuhou; W1, W2, W3- Western).

Table 3.1 Summary of transects (Omokoroa, Motuhou and Western) for InterOcean S4 current meters deployment at the southern basin of Tauranga Harbour. At each transect there are three S4 deployed (O1, O2, O3, M1, M2, M3, W1, W2, W3). The measured variables by each S4 differed at each stations with (S: speed; D: direction; E: elevation; Sal: salinity; T: temperature).

Transect	Station	Position (BOP NZGD 1949)		Sampling date		Measured variables
		N	E	Start date	End date	
Omokoroa	1	714821.09	263540.05	3/02/1999	5/02/1999	S, D, E
	2	714917.41	263727.58	3/02/1999	5/02/1999	S, D, Sal, T
	3	715274.50	263929.66	3/02/1999	5/02/1999	S, T
Motuhou	1	711642.44	265351.01	6/02/1999	8/02/1999	S, D, E
	2	712762.58	267283.91	6/02/1999	8/02/1999	S, D, Sal, T
	3	713401.61	267920.35	6/02/1999	8/02/1999	S, T
Western	1	711225.48	271929.05	9/02/1999	11/02/1999	S, D, E
	2	711717.68	271785.44	9/02/1999	11/02/1999	S, D, Sal, T
	3	712430.61	271790.73	9/02/1999	11/02/1999	S, T

3.2.3 Model description and set-up

The Estuary, Lake and Coastal Ocean Model (ELCOM) is a 3D hydrodynamic model (Hodges et al. 2000; Hodges and Dallimore 2006) used for predicting velocity, salinity and temperature distribution in water bodies. The ELCOM version used in the present study is based on the unsteady Reynolds-averaged, hydrostatic Boussinesq, Navier-Stokes and scalar transport equations (Hodges et al. 2000). In ELCOM, a grid cell is considered dry if the total water depth at the cell centre and at the four sides surrounding the cell does not exceed zero. When the grid cell is dry, no mass flux is permitted to cross the side of the cell. Tidal elevations along the open ocean boundary of the model domain were derived from a time-series of tidal elevation from the National Institute of Water and Atmospheric Research (NIWA) tidal model (http://www.niwa.co.nz/our-services/online-services/tides). The tidal constituents used for the tidal model are the M2, S2, N2 and K2. The tides were reduced to Tauranga chart datum, with a default value set to adjust for MSL in the model. Unfortunately, there are very few measurements of shelf salinity variations. Therefore, open boundary salinity was derived from four offshore transects carried out at the Bay of Plenty shelf between October 2003 and May 2004 (Park 2005). The offshore transects were taken on the eastern site of the Tauranga Harbour mouth. For each transect, sea surface salinity (<20 meters depth) was extracted, averaged and interpolated between the four days of measurements to provide an estimate of seasonal changes in salinity. It was assumed that the offshore salinity in February 1999 was the same as the

offshore transect from February 2004. The period when the offshore transect was collected was neither a La Niña or El Niño event. Bay of Plenty Regional Council maintained a wave buoy located in the Bay of Plenty at 13 km offshore of Pukehina Beach (Figure 3.1). The wave buoy measured wave and temperature conditions every 20 minutes. As the wave buoy was only deployed in April 2002, temperature measured by the wave buoy in February 2008 was used for the model, as it was the only available summer data provided by the council. Both February 1999 and 2008 are La Niña Years, and average air temperature difference of 0.2 °C (the mean February temperature for 2008 was 19.5°C and for 1999 was 19.7 °C). Meteorological data (wind, air temperature, relative humidity, solar radiation, atmospheric pressure and rainfall) collected by the Tauranga Aero Aws climate station, which is located at the Tauranga Airport (-37.673S, 176.196E), was used for this study. These data were obtained from the National Institute of Water and Atmospheric Research (NIWA) CliFlo database.

The freshwater inflow boundaries into the southern basin of the Harbour are Wairoa River, Waipapa River, Waimapu Stream, Kopurereroa Stream, Te Puna Stream, Wainui River and Aongatete River. (Figure 3.3) The inflow rate of rivers and streams that flow into the southern basin of Tauranga Harbour were sourced from Bay of Plenty Regional Council's monitoring data archives. The regional council monitoring provided continuous flow data for Wairoa River, Waipapa River, Waimapu Stream and Kopurereroa Stream. For Wainui and Aongatete rivers, the inflow records were sparse hence a design hydrograph for each river was also created based on the empirical model in the U.S. Soil Conservation Service handbook (SCS 1972; SCS 1975) (Appendix 3). For the ungauged stream, Te Puna Stream, a storm hydrograph was also created to estimate the flow rate of the stream. As the stream drains an ungauged catchment, a modelled design hydrograph was required for freshwater model input. The design hydrograph was estimated from rainfall data using the empirical model outlined in the U.S. Soil Conservation Service handbook (SCS 1972; SCS 1975), which has been adapted to specific catchments in the Auckland region (Beca 1999). Water temperature for the rivers and streams were sourced from the air temperature from Tauranga Airport downloaded from CliFlo website.

Bathymetric data for the model were compiled from a number of sources. The channels were obtained from singlebeam surveys with some additional multibeam data collected by the University of Waikato. Data for the rest of the harbour were obtained from a combination of soundings, digitized charts and digitized Navy fairsheets (provided by C. Pilditch). All data were to New Zealand Map Grid coordinates and reduced Tauranga chart datum. The model grid resolution is 75 x 75 m. Figure 3.4 showed the bathymetric grid of the southern basin of Tauranga Harbour used in the ELCOM modelling. The simulations were performed for the period when the field data were collected (3-11 February 1999), unless stated otherwise in the text. Due to all simulations beginning from a cold start (i.e. flat water, and no currents), a period of 3 days (6 tidal cycles) was allowed for the model to 'warm up' before model results were extracted. The temperature and salinity initial conditions were spatially varying as it takes many days of model time to establish an equilibrium salinity and temperature distribution. The horizontal salinity variations needed for the initial conditions were generated assuming that salinity ranged linearly from the values observed at mid tide at Omokoroa to the open ocean salinity. The model was calibrated by adjustment of the bottom drag coefficient within physically reasonable limits.

Scenarios were developed to address the potential needs of people working in the harbour, as well as to understand the drivers of the physical properties at the mouths of Te Puna and Waikareao Estuaries needed for biogeochemical modelling in later Chapters. The scenarios were simulated for February 2008 unless stated otherwise in the text. February 2008 was chosen as the year for which simulations were undertaken because there were offshore water temperature measurements collected by the wave buoy. The base case (Scenario 0) was simulated with actual wind conditions. In Scenario 1, the wind conditions were 'switched off' in order to examine the effect on circulation patterns in the southern basin. Scenario 1 was developed to look at the circulation patterns in the southern basin when there was no wind in comparison with the base case. For the residence times comparison with the base case, the harbour was sub-divided into various sub-regions based on those defined in the study conducted by NIWA on the harbour sedimentation patterns (Hume et al. 2009). For the division of the regions, refer to Figure 3.1. Scenario 2 was developed to simulate conditions occurring during a high Wairoa River discharge i.e. when the bypass located at

Ruahihi Power Station was open (15 April 2008) and when the bypass was closed (1 April 2008). Wairoa River is the main freshwater inflow into Tauranga Harbour with a mean freshwater inflow of 17.6 m^3s^{-1} (Park 2004). On certain days of the year, the bypass at Ruahihi Power Station, situated 12.5 km away from the river mouth is open to let water through downstream. The opening of the bypass released large amounts of freshwater (~540 m^3 s^{-1}) into the harbour.

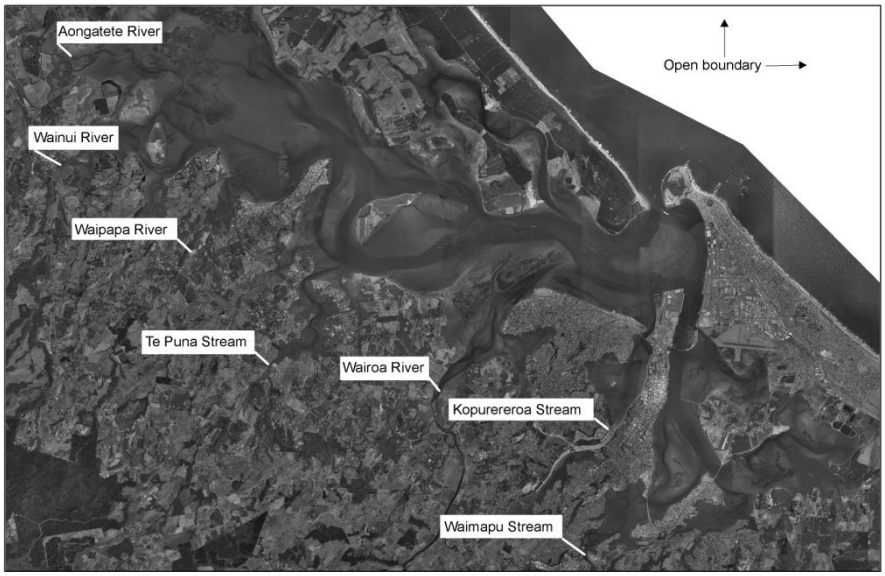

Figure 3.3 Location of inflow boundaries (Wairoa River, Waipapa River, Waimapu Stream, Kopurereroa Stream, Te Puna Stream, Wainui River and Aongatete River) and open boundary for the southern basin of Tauranga Harbour model.

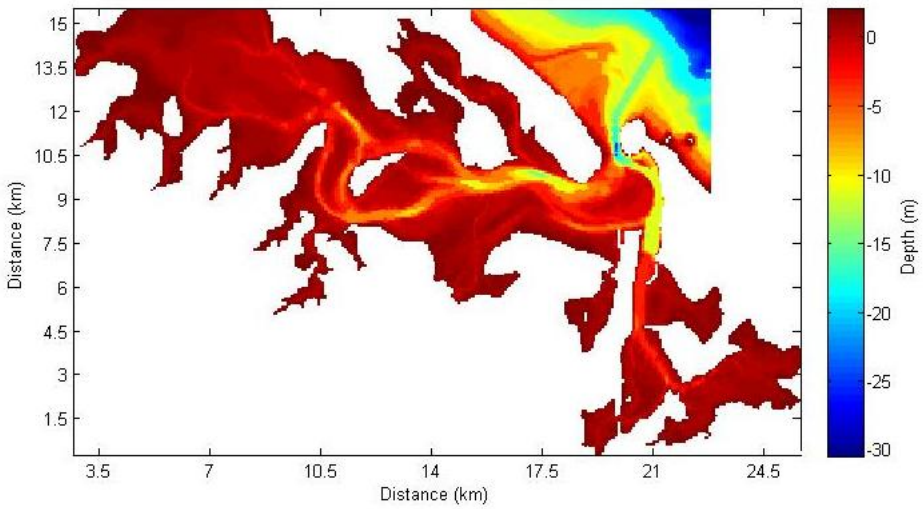

Figure 3.4 Southern basin of Tauranga Harbour bathymetry (75 x 75 m grid) at low tide in NZMG (New Zealand Map Grid) referenced to chart datum.

3.3 Results

3.3.1 Water elevation, current speed and direction

The model was calibrated by adjustment of bottom drag coefficient between 0.001 and 0.02. The best results were achieved using a spatially varying bottom drag coefficient (BDC), BDC = 0.01 in areas deeper than 1m, and BDC = 0.005 in areas less than 1m deep. Figure 3.5 illustrates time-series of measured and modelled data for the sampling period (February 9-11 1999) at the Western channel station 1. Simulation results for the Western channel are in good agreement with the measured data. Tidal elevation was generally consistent (Figure 3.5). Model calibration for current speed and direction (Figure 3.5) was generally good, with the general trend better represented for incoming water (absolute difference of 0.01-0.04 ms^{-1}) compared to the outgoing water (absolute difference of 0.08 to 0.1 ms^{-1}). The model was also calibrated against 8 other stations (Figure 3.2) with S4 data collected from 3-11 February. Simulation results for the other stations at Omokoroa, Motuhou and Western channels are in good agreement with the measured data (Appendix 4 shows a summary of model fits). Tidal elevation was generally consistent. At Omokoroa station 1, the simulated incoming tide was over-predicted by 0.3 ms^{-1} and the direction error during outgoing tide was probably attributed to noise in the data. At Omokoroa station 2, the simulated speeds for the outgoing tide were under-predicted by 0.2-0.3 ms^{-1}. At Motuhou station 2 and 3 and Western station 2, the simulated current speed for the outgoing tide was under-predicted by 0.2 ms^{-1}.

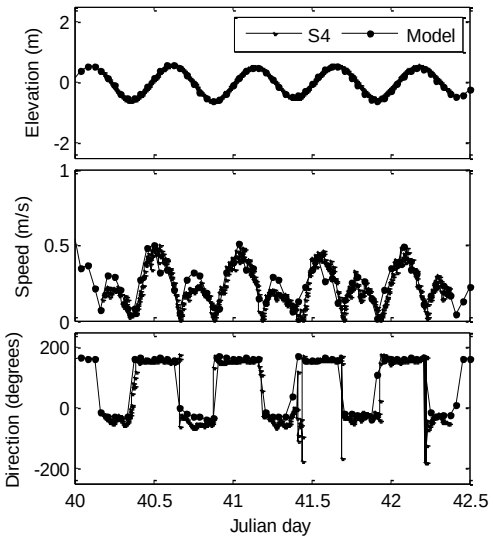

Figure 3.5 Modelled (ELCOM) against measured (S4) water elevation, current speed and direction at Western Station 1.

3.3.2 Salinity and temperature

The modelled temperature and salinity varied spatially across the southern basin of the harbour (Figure 3.6, Appendix 4). The measured salinity (from CTD) suggested that the water column to be relatively well mixed in the vertical but demonstrates a horizontal gradient from the Western stations to the Omokoroa stations (Figure 3.6, Appendix 4). Obviously, the salinity variation is difficult to reproduce without a much better understanding of the open water salinity and also the degree of input from other freshwater sources (groundwater). Measured (S4 and CTD) temperature showed that the water temperature had diurnal signal, which the model found very difficult to reproduce. The degree of mixing and the surface temperature depend on the speed of the wind. The wind speed used for this model was from the airport, which is 14 km away. In comparison to year-long wind data (not shown) from Otumoetai (located on the west of Waikareao Estuary), the airport wind speed is relatively similar. However in summer, the airport wind speed was lower by 3 m/s.

At Western station 2, the modeled temperature showed good comparison with the measured water temperature with modelled temperature between 1 to 2 ^{o}C lower than temperature measured by the S4 and CTD. However at Omokoroa station 2, the temperature profile showed ebb-flow imbalances during the late afternoon where the field temperature showed an increase in temperature during the late afternoon low tide but the modelled temperature did not, which ultimately lead to a difference of temperature of 3 ^{o}C on the outgoing tide.

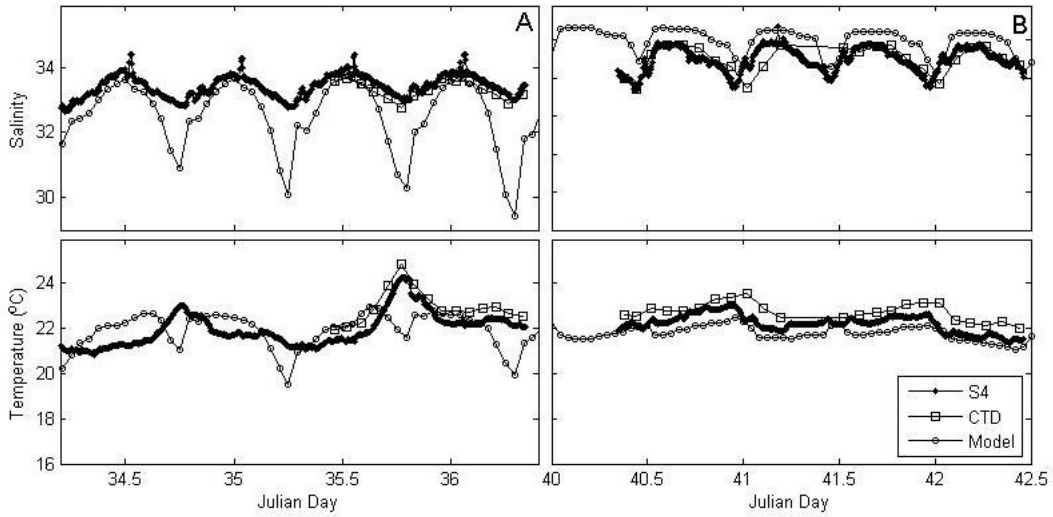

Figure 3.6 Measured CTD (depth-averaged) and S4, and modelled (ELCOM) and salinity and temperature at Omokoroa 2 (A) and Western 2 (B).

3.3.3 Scenarios

3.3.3.1 Characteristics of the M2 tide

The M2 (and S2) amplitude and phase were extracted from a model data-file through a freeware tidal harmonic analysis package (the t-tide code was written by R. Pawlowicz). The phase-lags were relative to the entrance of Tauranga Harbour mouth (Latitude: 37°38'12"S; Longitude: 176°9'47"E). The M2 amplitude attenuates through the main harbour entrance from 0.86 to 0.77 m as the tidal flow is constricted through the narrow entrance (Figure 3.7). The tidal amplitude continues to decline as it moves through the inner harbour channels to reach amplitude of 0.74 m at Motuhou channel. The S2 amplitude (Figure 3.8) also attenuates through the harbour entrance from 0.13 to 0.10 m and declines as it moved inwards into the harbour. The phase lines indicate the timing of the tidal wave, with locations along the same line experiencing high tides at the same time. The gradient of the phase lines indicates the tidal wave speed (e.g. a difference in phase of 30° is a timing difference of $30^{\circ}/360^{\circ}$ x 12.4 hours ~ 1 hours). Phase lines that are closer together indicate the tidal wave propagates slowly and vice versa. The M2 phase lines show that the largest phase difference occurs through the confines of the entrance channel followed by a more slowly varying change within the shallower, wider inner basin (Figure 3.9). The constrictions made by the entrances to Rangataua Bay also slow the tidal wave down by approximately 0.75 hours. With the exception of the main flood tidal delta, the residual currents were relatively low over the tidal flats with greater velocities in the channel

(Figure 3.10). The residual flow was also relatively low in the sub-estuaries. However in the constricted mouth between Rangataua Bay and Waimapu Estuary, the residual currents were stronger and are ebb-directed. In the middle harbour, residual currents are stronger in the channel. In the lower harbour, the residual flow is the greatest due to its constricted morphology. The residual flow is relatively strong immediately seaward of the harbour mouth with backward flow forming to the west of the harbour mouth.

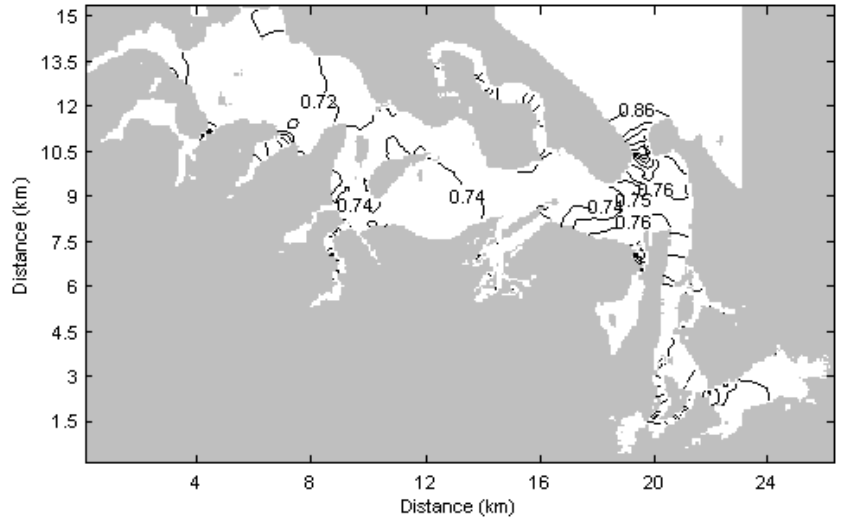

Figure 3.7 Model produced co-amplitudes (m) of the M2 tide.

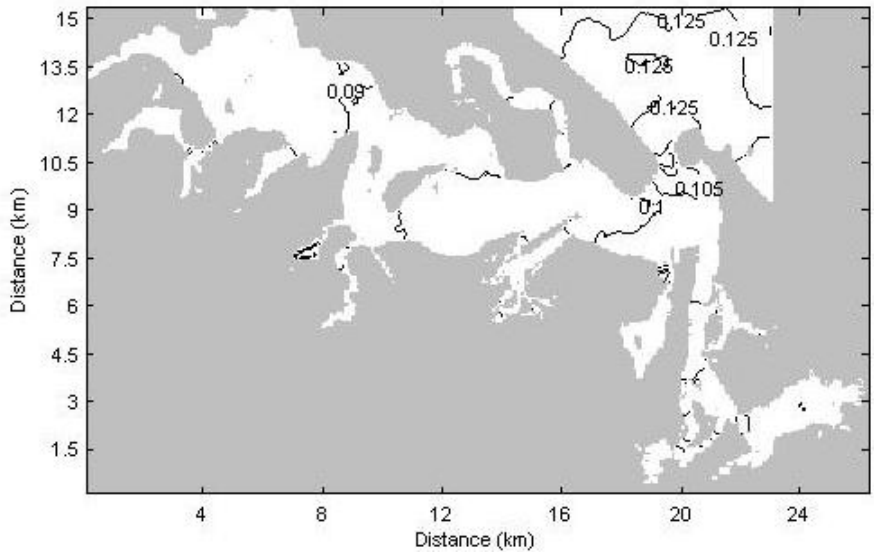

Figure 3.8 Model produced co-amplitude (m) of the S2 tide.

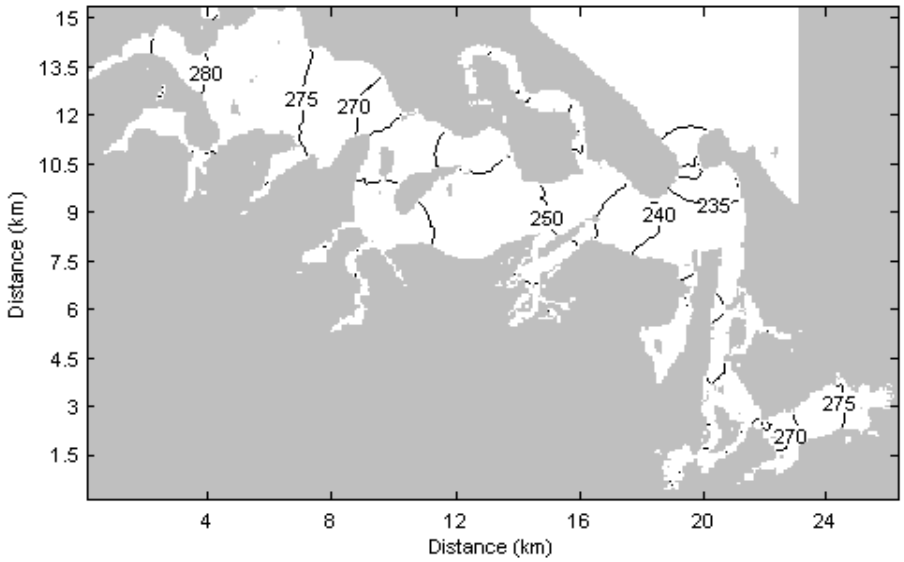

Figure 3.9 Model produced phase (degrees) of the M2 tide.

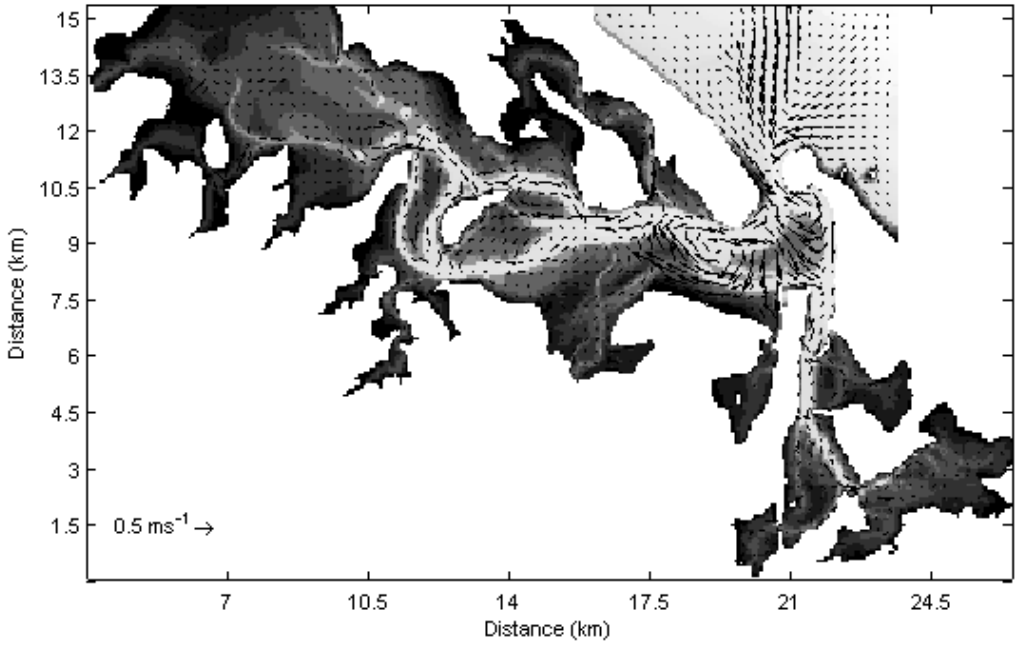

Figure 3.10 Time-averaged residual currents speed and direction. White areas indicate dry land.

3.3.3.2 Salinity, temperature and residence times

Wind and no wind conditions were modelled to determine the impact on these conditions. It is found that temperature is very sensitive to wind mixing as seen in Figure 3.11. No wind (i.e. calm) conditions resulted in warmer temperature throughout the harbour with temperature generally >22 ^{o}C, while adding wind to the model resulted in a decrease in water temperature with a range between 18 to 22 ^{o}C in various parts of the harbour.

The residence time is the average time, which a parcel of water spends in a certain grid cell before it leaves the region of interest. ELCOM calculates the residence time of water in each cell by assigning a water age and the age of water increased till the water of that region is replaced by new water. The harbour was generally well flushed with residence times between 2 to 4 days near the harbour mouth and Western Channel. However, the residence times increased by a factor of two toward the north end of the basin (Figure 3.11 and Table 3.2). Table 3.2 showed the averaged residence times of water in sub-regions of Tauranga Harbour (defined by the Tauranga Harbour Sediment study and shown in Figure 1.1 of the report (Hume et al. 2009)) with wind and without wind. The residence times were also higher in sub-estuaries with constricted entrances such as Rangataua Bay and Welcome Bay (Figure 3.11). The funnel shape of the harbour between Sulphur Point and the wharf (~2 km from the southern basin harbour mouth), and the relatively narrow entrance means that the water inside the sub-estuaries was resident some ~5 days longer than in the main channel outside such as Deep Channel South (DCS on Figure 3.1).

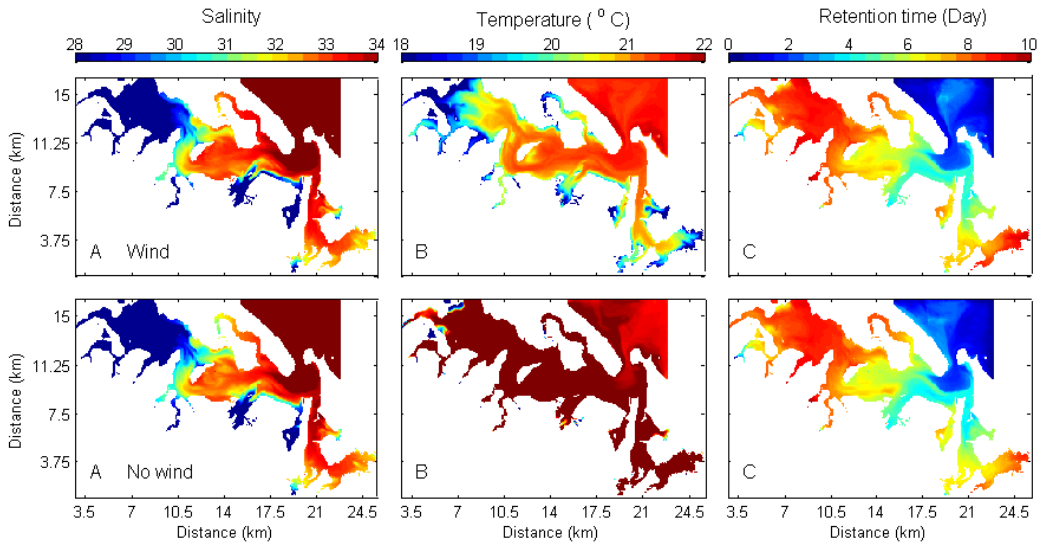

Figure 3.11 Depth-averaged salinity (A), temperature (B) and retention time (C) in the southern basin of Tauranga Harbour with dominant wind condition (top panels) and no wind condition (bottom panels).

Table 3.2 Average residence times of sub-estuaries division in the southern basin of Tauranga Harbour under no wind condition and with dominant wind condition.

Sub-estuaries division	Average residence times (day)	
	Wind simulated	No wind simulated
Waipu Bay	4.8	4.3
Rangataua Bay	7.8	7.1
Welcome Bay	8.2	7.4
Waimapu Estuary	6.4	6.1
Waikareao Estuary	6.3	5.9
Wairoa River mouth	4.7	4.3
Te Puna Estuary	7.4	7.3
Waikaraka Estuary	7.2	7.0
Deep channel south	3.1	2.9

3.3.3.3 Wairoa River discharge

Freshwater inflow from the head of Wairoa River mouth would be expected to decrease the salinity of the water column and thus influence horizontal salinity gradients. A 'curtain' was extracted from the model stretching from the river mouth to the harbour mouth, the location of which is marked in Figure 3.12. The Wairoa river input causes a stratified water column that gradually becomes more and more vertically well mixed with distance from the river mouth (Figure 3.13). The surface horizontal salinity front (defined as the maximum surface salinity gradient) occurs at 3000 m from the point where the river enters the estuary (Figure 3.13). Under low flow conditions, the maximum stratification is 13 between the surface and bottom layer. During high discharge events, (1) the salinity front moves down stream (2) the depth-averaged salinity decreases by a maximum at the river mouth by 5, but the decrease is still apparent near the harbour entrance, and in fact the whole harbour is 3 to 5 fresher (3) the vertical stratification near the harbour mouth increased by 1 between the surface and bottom layer. Between 6000 to 10000 m (harbour mouth), there was minimal variation in salinity. The average temperature dropped 1 ^{o}C when the bypass was open from harbour mouth up to 5000 m away. From the river mouth until 4000m the temperature was lower by 4^{o}C when the bypass was open (Figure 3.13, Panel 2 and 4). The Wairoa River's water temperature was set to measured air temperature (see Methods 3.2.3), hence the simulated water temperature might be under-estimated and the result is only representative of that particular period.

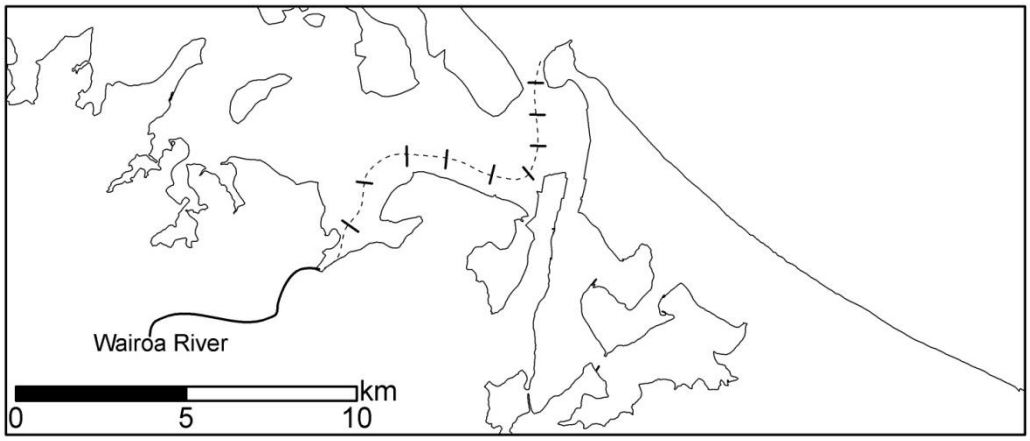

Figure 3.12 Dotted line represented the profile taken from Tauranga Harbour southern basin entrance to Wairoa River mouth. The black lines marked each 1000m.

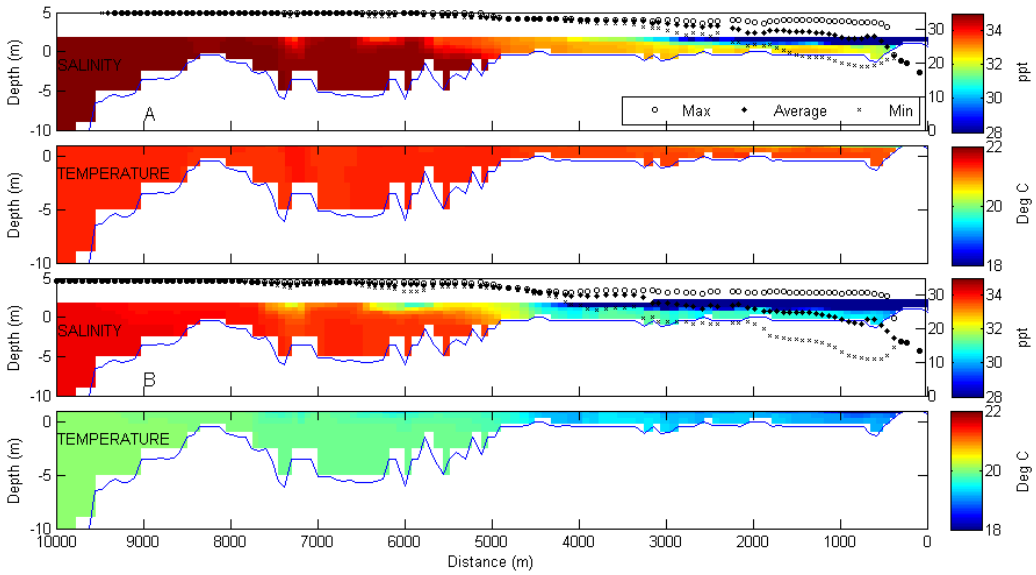

Figure 3.13 Tidal average of salinity and temperature in the harbour from Wairoa River mouth (0 metres) to the harbour mouth (9825 metres at Mount Maunganui entrance) along the main channel, (A) under normal flow condition, 1 April 2008, (B) when the Ruahihi Power station bypass is open on the 15 April 2008. The markers o, ∗, x represented the depth-averaged maximum, average and minimum salinity.

3.4 Discussion

The M2 and S2 tidal amplitude varied surprisingly little throughout the southern Harbour. Tidal ranges are greater at DCS where the channel opening is deeper and wider compared to further inwards of the basin such as in Waikaraka and Te Puna estuaries. The M2 tidal amplitude attenuates by only 0.1 m (and S2 by 0.02 m) through the main harbour entrance as the tidal flow is constricted. Both the amplitude decreased gradually as the tidal wave moved further inwards into the harbour. The constriction at the mouth of the harbour increases current speed. The

geometry and presence of constricted mouth lead to a delay of tide coming into most of the sub-estuaries such as the delay at the entrance of Rangataua Bay of 45 minutes.

In estuaries such as the Tauranga Harbour (a barrier-enclosed lagoon) which has low-lying intertidal flats but incised with relatively deep channels, the circulation is complex with strong tidal currents in constricted channels such as in Omokoroa Point and at the mouth, and low currents in the shallow regions. The time-averaged residual circulation patterns in Tauranga Harbour showed highly channelized residual currents with strongest flow occurring at the harbour mouth and directly out of the harbour mouth. The circulation patterns are likely to affect larval dispersal as in some parts of the harbour such as in the Omokoroa region, the larvae can be retained while in other areas such as Wairoa channel, they are exported into the shelf environment. The area inwards of Motuhou channel has a longer residence time compared to the DCS region and Wairoa River mouth, which enabled retention of food sources for the larvae to be self-sustaining.

Either with or without wind in the model, there is a gradient in salinity between the upper and lower harbour, with three distinct salinity regions, upward of Omokoroa point, the region between Omokoroa Point and Western channel and finally, just inside of the harbour entrance. The higher salinity water was preferentially retained in the deep channels in the lower harbour. This was because the residence time of these channels was less. In the intertidal regions, the tidal flat areas will always be exposed only to saltier high tide water, and the channels will experience the whole tidal range of salinity conditions. Therefore on average the channels will be less salty than the intertidal areas.

In the harbour above Omokoroa Point, the modelled water temperature showed cooler temperatures when wind was included (Figure 3.10) but as shown in the S4 and CTD measurements, the model under-predicted the water temperatures notably during ebb tide. The ebb-flow imbalances observed in the temperature in late afternoon ebb tide at Omokoroa could be due to the heating of the shallow tidal flat area by solar radiation during low tide period in the late afternoon. This heated water is intermixed with flood tide water, and during the next ebb tide the heated water passes by the measuring station at Omokoroa Point. During the later

stages of outgoing tide, the lowered water level causes the water to be confined to the channels which are deeper and do not heat up as much as the shallow regions. This ebb-flow imbalance during low tide in late afternoon was also observed in 24-hour CTD casts taken at the mouth of Te Puna and Waikareao estuaries, which are sub-estuaries in Tauranga Harbour, in summer and spring (See Chapter 2). Moreover, as the meteorological boundary conditions were sourced from Tauranga Airport, the air temperature at Omokoroa might differ considerably 14 km away. The average February 2008 air-temperature measured at Otumoetai weather station, which is situated closed to Waikareao Estuary, was higher by 1.6 °C in comparison to airport air temperature. Strong winds can be effective at extracting heat from shallow areas through evaporation and enhanced mixing.

ELCOM uses a fixed water albedo in calculating the heat exchange between air and water but in estuaries with extensive tidal flats the surface tidal flat albedo has been shown to change as a function of the periodic exposure to solar radiation caused by the tidal cycle (Kim et al. 2007). Heat exchange with the sediment has been shown to be important in rivers where it accounted for 15% of the observed energy exchange in a detailed study of the River Blithe in UK (Evans et al. 1998). That study found that the majority of the measured bed heat flux was caused by short-wave radiation from the river bed which overwhelmed long wave radiation from the river bed. In ELCOM, any excess of short wave energy at the bottom water column is reflected back into the domain. Benthic heat exchanges has been shown to be relatively small compared with surface and horizontal exchanges in the water column (Heath 1977), however the temperature gradient of exposed sediments can undergo a noticeable change as the tide floods over the shore and it has been suggested that rapid heat exchange occurs between the intertidal sediments and incoming tidal water (Harrison and Phizacklea 1987a, b).

Heath (1976) found that the average residence time of water at Tauranga Harbour to be between 0.8 to 1.5 days based on tidal prism method. The tidal prism method gives bulk flushing for a whole estuary or sub-estuary regardless of variation in freshwater inflow, which is an important driving force in estuaries. However, these model simulations suggested the irregular geometry and curved channels create quiescent side embayments, which increase the residence times compared to the simple shapes that the tidal prism method was developed for. In

some areas of the harbour, the Heath averaged residence time underestimated the residence time by a factor of 4 to 6. The DCS has lower residence time in part largely due to the deep channel and its close proximity to the entrance, which makes this region the most well flushed in the harbour. In comparison, Rangataua Bay and Welcome Bay have longer residence time due to their constricted estuary mouths. Wairoa River mouth is not constricted as compared to other sub-estuaries, hence the residence times was lower. It is interesting to note that the residence times was higher in the lower harbour sub-estuaries with constricted mouths such as Waikareao Estuary and Rangataua Bay in response to wind variation. Geyer (1997) also found that shallow estuaries with constricted mouths, can inhibit wind-induced mixing. However, the wind-induced mixing also depends on the direction and speed of wind of stress.

From the simulation of Wairoa River scenario, the model showed that the periodic opening of the Ruahihi bypass caused variation in salinity and temperature in the harbour. The simulated scenario showed that with the opening of the bypass, the horizontal salinity extended downstream. Varieties of macrofauna group have been found distributed in Tauranga Harbour such as bivalves, crustacean, and polychaetes (Roper 1990; Cole et al. 2000). Bivalves species that are dominant in Tauranga Harbour such as *Paphies australis* are sensitive to altered salinity regimes. McLeod and Wing (2008) demonstrated that bivalves (*Austrovenus stutcburyi* and *Paphies australis*) were smaller in river deltas near the outflow of a power station in Doubtful Sound, and with sustained exposure (>30 days) to low salinity (<10) bivalve survivorship significantly decreased, however the bivalves can sustained periods of exposure to freshwater up to at least 20 days if followed by a periods of return to normal seawater salinity. However, the periodic opening of the bypass at Ruahihi Power Station altered the salinity structure more from the river mouth to 6 km away from the river mouth. This salinity environment may restrict bivalves to the deeper water in the channel. McLeod and Wing (2008) examined current salinity environment in Doubtful Sound in light of their laboratory experiments and found that bivalves are restricted to deeper waters (5-6m depth).

3.5 Conclusions

A three-dimensional hydrodynamic model complemented by field data, has produced information of current propagation in southern basin of Tauranga. The model has established that the salinity profiles are tidally driven while the temperature profiles are sensitive to wind. Wind-driven circulation reduces the temperature especially at the tidal flat areas by 2-4 ^{o}C in the upper parts of the harbour. The residence times varied across the harbour with low residence times in the mouth of the harbour and in sub-estuaries that are well exposed (Wairoa River). The residence times were high in sub-estuaries with constricted entrances and further inwards into the harbour. The periodic opening of the bypass at Ruahihi Power Station decreases the salinity and temperature more than 7 km away from the mouth which can affect the ecological condition of the harbour.

Chapter Four: Hydrodynamic-biogeochemical modelling in the shallow tidally-dominated estuaries, Te Puna and Waikareao

4.1 Introduction

Chapter 2 identified that DIN concentrations in the sub-estuaries of the harbour varied over tidal cycles causing export of nutrients into the main Harbour. In general, physical mechanisms that determine the transport of constituents can strongly influence the water quality of the estuarine system. Temporal and spatial changes in mixing, stratification and residual circulation can impact the distribution of nutrients, pollutants and dissolved oxygen (Becker et al. 2009). Ecological processes such as primary production only occur if adequate conditions are found (e.g. light, nutrients, temperature) (Gameiro et al. 2007). Systems with long residence times are particularly susceptible to developing algal blooms when nutrient loads increase (Dauer et al. 2000) whereas estuaries with short residence times are characterized by strong water currents which usually prevent eutrophication by flushing nutrients out of the system (Grall and Chauvaud 2002). Thus, at the core of any study on the nutrient inputs and fluxes in a coastal system is a detailed study of hydrodynamic and ecological conditions of that particular system. Chapter 3 identified the sub-estuaries Te Puna and Waikareao had longer residence times relative to the main harbour.

In coastal transition systems such as estuaries, tightly-coupled geological, hydrodynamic, geochemical and biological processes are modulated by a wide array of forcing mechanisms which include light, temperature, wind stress, waves, tides, freshwater discharge, as well as continental and oceanic nutrient inputs. These forcings operate on very different temporal and spatial scales, and together set strong constraints on the biogeochemical functioning of the estuaries. Varying geomorphology may lead to regions of different nutrient levels within an estuary. The process of urban eutrophication can further increase this water quality heterogeneity where different inflows (streams, rivers, runoff) transport varying nutrient loads into an estuary reflecting the landscape and land use of their individual catchments. The delivery of nutrients depends not only on the sources of nutrients to the estuary but also on the advective and dispersive processes that transport and retain the material (Eyre 1993).

In recent decades, coupled physical-biological models have been widely applied to the marine environment to simulate both physical and biogeochemical processes and study the interactions between them, especially the effect of physical factors on biological communities and chemical conditions. The complexity of the physical models ranges from box (Li et al. 2000) and 1-D models (e.g. Marra and Ho 1993; Doney et al. 1996) to fully 3-D hydrodynamic models (e.g. Lima and Doney 2004). The biological models range from simple nutrient-phytoplankton-zooplankton models (e.g. Doney et al. 1996; Liu and Chai 2009) to multi-nutrient, multi-species and size-structured ecosystem models (e.g. Moore et al. 2002; Lima and Doney 2004). When such models are applied to estuarine and coastal waters they can provide a means of assessing potential impacts of eutrophication and hence provide a tool for management strategies.

The main objective of this chapter was to understand the circulation and biogeochemical patterns in Waikareao and Te Puna Estuaries using a calibrated 3D hydrodynamic –ecological model numerical model. It outlines first calibration of the hydrodynamic driver, then the biogeochemical model. Both Te Puna Estuary and Waikareao Estuary are shallow sub-estuaries located in the southern basin of Tauranga Harbour, and thus rely on the incoming water properties from the main harbour, which were modeled in Chapter 3. Both estuaries experience a wide range of tidal currents both within the estuary's channel networks and on extensive intertidal flat regions, creating complex hydrodynamic flows. The hydrodynamic model, ELCOM, offers the ability to predict the hydrodynamic flows and scalar transports within the estuary (Hodges et al. 2000). By coupling the water quality model, CAEDYM, to the hydrodynamic driver, ELCOM (Hipsey et al. 2006a), it is possible to model aspects of the biogeochemical dynamics in Te Puna Estuary and Waikareao Estuary. CAEDYM is a generic water quality model capable of coupling to a range of hydrodynamic drivers, including 2 and 3-D models of lakes and reservoirs (Romero et al. 2004; Burger et al. 2008), rivers and estuaries (Chan et al. 2002; Robson and Hamilton 2004), and the coastal ocean (Spillman et al. 2007; Rao et al. 2009).

4.2 Methods

4.2.1 Site description and data collection

The two estuarine study sites were the Waikareao and Te Puna Estuaries, which are sub-estuaries located in Tauranga Harbour in the Bay of Plenty region, on the east coast of North Island, New Zealand (Figure 4.1). The harbour catchment has an area of 200 km^2 with a variety of land uses including horticulture, agriculture, urban and industry. The Wairoa River is the largest freshwater input into the harbour (Park 2004), contributing on average 17.6 $m^3 s^{-1}$. Tides in the harbour are semi-diurnal and the water column is vertically well mixed (Heath 1985). Waikareao Estuary is located 4.5 km south and Te Puna Estuary is 12 km southwest of the harbour mouth. Both estuaries have single constricted mouths and extensive intertidal areas.

Hydrodynamic data were collected on the 13-15th November 2007, alongside nitrate and ammonium field sampling (see Chapter 2). To obtain current direction, velocity and water elevation in the estuary, two Falmouth Scientific Inc. (FSI), an Acoustic Doppler Velocimeter (Triton ADV) and RBR pressure sensor (RBR Ltd, Canada) were deployed over four tidal cycles, two at Te Puna and two at Waikareao estuaries (Figure 4.1). The current meters were deployed on weighted frames. On one of the frames, the ADV and an FSI was deployed together (Station A: 1869047.435E, 5826925.050N) and on another frame, another FSI with a pressure sensor were deployed together (Station B: 1868631.043E, 5827465.041N) at Te Puna. At Waikareao, the ADV and an FSI were deployed together (Station A: 1879027.352E, 5825418.265N) and on another frame, another FSI with a pressure sensor were deployed together (Station B: 1879144.362E, 5826223.790N). The measured parameters for the current meters and pressure sensor are listed in Table 4.1, 4.2. Conductivity, Temperature and Depth (CTD) casts were taken hourly during the four sampling occasions previously presented in Chapter 2 (winter, start of spring, end of spring and summer) for dissolved oxygen, salinity and temperature. The salinity, temperature and dissolved oxygen from the CTD casts were depth-averaged because the measurements showed little vertical variation.

Note that all salinities reported here are given in the dimensionless practical salinity units (approximately equivalent to parts per thousand).

Table 4.1 Summary of station (A and B) for ADV and FSI current meters, and RBR pressure sensor deployment at Te Puna Estuary during end of spring field sampling (13-14 November 2007). At each station, two current meters were deployed. The measured variables by each current meters differed with (U, V, W: velocities; S: speed; D: direction; P: pressure; h: elevation; Sal: salinity; T: temperature).

Station	Current meters	Position (NZTM) N	E	Sampling date Start date	End date	Measured variables
A		5826925.05	1869047.44	13/11/2007	14/11/2007	
	ADV					U, V, W, S, D, P, Sal, T
	FSI					U,V,W, P
B		5827465.04	1868631.04	13/11/2007	14/11/2007	
	FSI					U,V,W, P
	RBR					P, h, T

Table 4.2 Summary of station (A and B) for ADV and FSI current meters, and RBR pressure sensor deployment at Waikareao Estuary during end of spring field sampling (14-15 November 2007). At each station, two current meters were deployed. The measured variables by each current meters differed with (U, V, W: velocities; S: speed; D: direction; P: pressure; h: elevation; Sal: salinity; T: temperature).

Station	Current meters	Position (NZTM) N	E	Sampling date Start date	End date	Measured variables
A		5826223.79	1879144.36	14/11/2007	15/11/2007	
	ADV					U, V, W, S, D, P, Sal, T
	FSI					U,V,W, P
B		5825418.26	1879027.35	14/11/2007	15/11/2007	
	FSI					U,V,W, P
	RBR					P, h, T

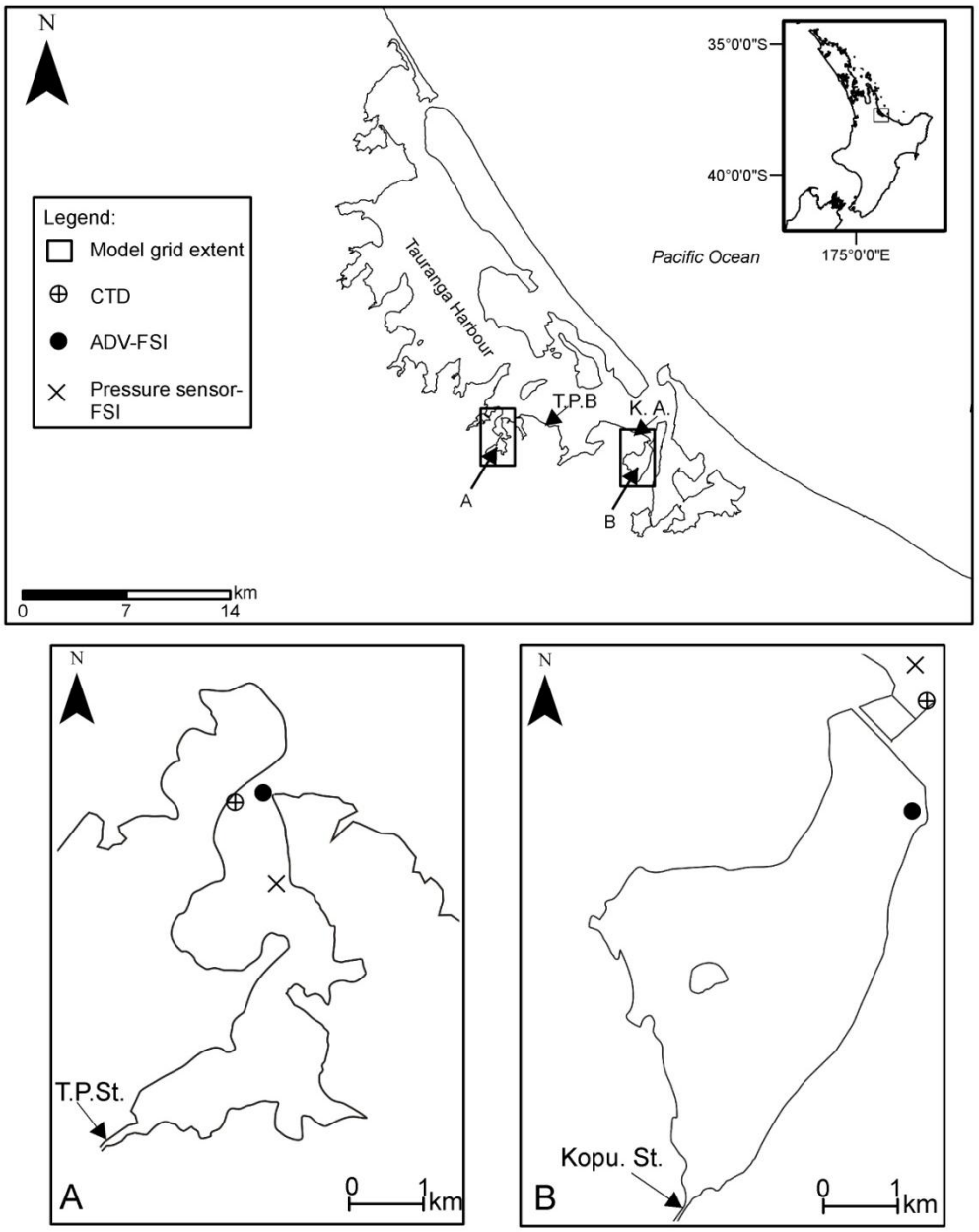

Figure 4.1 Location map of the study areas, Te Puna Estuary (A) and Waikareao Estuary (B) in the southern basin of Tauranga Harbour, North Island, New Zealand, outlining the model grid extent. The markers marked the location of the deployment of current meters in the two estuaries in November 2007 and CTD during the four sampling occasions. T.P.St: Te Puna Stream; Kopu. St.: Kopurereroa Stream; T.P.B: Te Puna Beach; K.A.: Kulim Avenue.

4.2.2 Model description and set-up

A 3-D numerical model is used to provide a range of hydrodynamic conditions in the Te Puna and Waikareao estuaries which are two of the sub-estuaries found along the landward (west) flank of Tauranga Harbour, needed for the application of the coupled hydrodynamic-ecological model, ELCOM-CAEDYM. The estuary and lake computer model (ELCOM) solves the unsteady hydrostatic, Boussinesq, Reynolds-averaged Navier-Stokes equation and the scalar transport equation, and

is described in detail by Hodges et al. (2000). ELCOM can be dynamically-coupled to the computational aquatic ecosystem dynamics model (CAEDYM) to simulate key elemental cycles (C, N, P and Si). CAEDYM consists of a series of partial differential equations to simulate time-varying concentrations of biogeochemical variables, accounting for processes such as nutrient cycling, oxygen dynamics and sediment-water interactions. ELCOM and CAEDYM are coupled such that ELCOM simulated salinity and temperature, passing the values for these parameters to CAEDYM for modification of ecological state variables while CAEDYM passes the water quality variables to ELCOM for advective and dispersive processes (Robson and Hamilton 2003; Romero et al. 2004; Hipsey et al. 2006a).

For chemical and biological simulations, CAEDYM requires the user to specify a number of variables, which are allocated at each boundary in the model as shown in Table 4.3 (refer to Hipsey et al. 2006a for further details). For this study four groups of phytoplankton (marine diatoms, dinoflagellates, freshwater diatoms and cyanobacteria) were simulated including two freshwater, one estuarine and one marine group (Table 4.3). The four groups chosen are common in numerical modelling studies of phytoplankton in estuaries (Robson and Hamilton 2004). CAEDYM itself consists of a series of process-based partial differential equations that dynamically simulate concentrations of biogeochemical variables including nutrients and phytoplankton based on parameterization of processes such as nutrient cycling, oxygen dynamics, and primary production (refer to Hipsey et al. 2006a for further details). Further listing of the required parameters and their descriptions is in Appendix 5.

The estuary mouths are designated as the open boundaries in the model for both Waikareao and Te Puna. For Te Puna Estuary, water level along the open boundary of the model domain was derived from a tide gauge located at the Kotuku Reserve Wharf, Te Puna (Marked on Figure 4.1 as CTD sampling location). The tide gauge measured tidal elevation for every 5 minutes and the datum is Moturiki datum. For Waikareao Estuary, the open boundary was forced with a time-series of tidal elevation measured by the NIWA tide model located at the main harbour mouth. A 0.65 hour delay was added to this value to account for the propagation of the tidal wave between the main entrance and the entrance to

Waikareao. This delay is demonstrated in Figure 3.9 (Chapter 3) where the tidal wave slowed down after entering the harbour. Open boundary salinity and temperature were derived from salinity and temperature from the southern basin model runs (Chapter 3) due to limited salinity and temperature data being available within the harbour. The south basin model was run for the four sampling occasions and data (salinity and temperature) from the locations of Motuhou station 1 and Western station 1 were extracted to provide forcing for the smaller models as these stations have been previously calibrated with measured CTD data for salinity and temperature in Chapter 3 (see Chapter 3 for location of stations). For the open boundary, the nutrient concentrations of the variables were derived from the Bay of Plenty Regional Council archives. The council has previously collected transects of physical, biological and chemical measurements within the harbour at selected sites and over the coastal shelf out to 200 m water depth within the Bay of Plenty (Park 2005). The concentration of the nutrients and DO from Te Puna Beach and Kulim Avenue (Figure 4.1) were used as open boundary conditions. The concentrations of the variables were extracted from the time closest to the sampling period. Note that these measurements were generally collected at high tide but they were used as the boundary condition for all stages of the tide in the modelling. The marine phytoplankton concentrations were extracted from surface transects (<20 m depth) taken at the shelf, averaged and interpolated between the days of measurements to create the phytoplankton concentrations. The phytoplankton concentrations from the shelf showed similar relative abundace to chlorophyll a concentration (unpublished data) measured within Tauranga Harbour.

Climate data (wind, air temperature, relative humidity, solar radiation, atmospheric pressure and rainfall) collected by the Tauranga Aero Aws climate station located at the Tauranga Airport (-37.673S, 176.196E) was used for this study. These data were obtained from the National Institute of Water and Atmospheric Research (NIWA) CliFlo database. Additional rainfall data for Te Puna Estuary were sourced from a rain gauge operated by Bay of Plenty Regional Council, which is located at Omokoroa. Additional air temperature, wind direction and wind speed were obtained from a meteorological station maintained by Bay of Plenty Regional Council at Otumoetai for Waikareao Estuary. Wind data were not used during the model calibration as it was found that the water

temperature was sensitive towards wind-inclusion (see Section 4.3.3 for further discussion).

A number of techniques were used to collect and process bathymetry data for Te Puna Estuary and Waikareao Estuary. Bay of Plenty Regional Council conducted the most recent bathymetry survey of the two estuaries using LiDAR in 2008. The LiDAR data are in NZTM (New Zealand Transverse Mercator) projections and vertical heights to Moturiki Datum. To accurately represent the channel bathymetry, which is not mapped by the LIDAR, a series of depth soundings were taken using a single-beam (echosounder) on 12th February 2009 in Te Puna Estuary and 2nd June 2010 for Waikareao Estuary. For Te Puna Estuary, the single-beam data were referenced to Tauranga Chart Datum. The datum was later adjusted to Moturiki datum so that it was consistent with the LiDAR data. The echosounder data of Waikareao Estuary was already referenced to Moturiki datum and the NZTM projections. The single-beam data were extracted using the HydroPro software and exported in ASCII format to be gridded in Matlab.

Measuring water depth using a single-beam echo sounder relies on accurate representation of the speed of sound in water. The single-beam software comes with a depth and spike filter, which has two filtering options (set ranges and spike detection) (Reeve 2008). However, neither of these methods was efficient in filtering out high frequency noise produced by the single-beam sonar in shallow water in this case. The noise was thought to be a result of sediments in the water column and shallow water reflections. A despiking algorithm was written in Matlab using low-pass filtering techniques to remove the noise. The single-beam was not capable of measuring accurately depths that were less than one meter and so these data-points were removed prior to gridding. Fortunately these areas were included in the LiDAR survey, which was under taken at low tide. After despiking, the echosounder data were gridded and areas where interpolation occurred which was beyond the range of the single-beam survey were removed or ‘blanked’.

The LiDAR data, which were provided by the Council in ArcGIS format, were exported into ASCII format to be gridded in Matlab. A blanking algorithm was written to blank out-of-water or the channel areas that had been surveyed using the single-beam. After that, both LiDAR and single-beam data were combined in

Matlab to create a bathymetry grid (Figure 4.2, 4.3). In areas where the single-beam and LiDAR data overlapped, priority was given to points that had better resolution especially in the channel area. The echo sounder track often crossed the main channel in a diagonal pattern. Interpolation across this diagonal pattern could result in artificial 'waves' along the main axis of the channel. To force the interpolation to interpolate linearly along the axis or thalweg of the channel, the points along the deepest part of the channel were linearly interpolated along the thalweg. This line of data was then added to the main body of the survey data and the whole dataset regridded. This removed the bathymetric waves that occurred along the thalweg. The same procedure was used to insure that channels that were too deep for the LiDAR and too shallow for the boat to survey were still retained in the final bathymetry. In this case, interpolation along the thalweg was performed between the measured channel depth at the seaward end of the thalweg, and the shoreline at the landward edge of the thalweg. There were only 200m of channel at the very highest portions of the estuaries that did not have channel coverage.

A 10 x 10 metre grid resolution was chosen for the model simulation for Te Puna and Waikareao estuaries, which enabled detailed areas such as the channel of the estuary to be studied and observed in detail. The grid size chosen is based on a trade-off between model runtime and spatial resolution. Although smaller resolutions are better, the resolution chosen resulted in an 8-day run time for the biogeochemical modelling, so was considered a minimum. Grid spacing is important as it determines the extent at which processes can be identified. Finer resolution is best in order to identify small-scale processes, but this will increase the model simulation time.

The stream inflow boundaries entering into Waikareao Estuary and Te Puna Estuary are Kopurereroa Stream and Te Puna Stream respectively. The inflow rate of Kopurereroa Stream was sourced from the Bay of Plenty Regional Council's monitoring archives. Te Puna Stream is ungauged and the stream flow was estimated based on the SCS storm runoff hydrograph (SCS 1972; SCS 1975). The design hydrograph was estimated from rainfall data using the empirical model outlined in the U.S. Soil Conservation Service handbook (SCS 1972; SCS 1975), which has been adapted to specific catchments in the Auckland region (Beca

1999). Daily rainfall data were sourced from a rain gauge monitored by the Council located at Omokoroa. Rainfall events of 20, 40, 60 and 100 mm were choosen for the calculation of storm hydrodraphs for the input of freshwater into the model. A minimal rainfall event of 10 mm was required to generate any discernible stream flow from catchment runoff using the SCS rainfall-runoff model. Therefore a minimal rainfall event of 20 mm was chosen though catchment runoff and subsequent stream flow were calculated with rainfall events smaller than 20 mm, a sufficient discharge and flow velocity would be required to flush stream nutrients into the estuary. In order to characterize the influence of freshwater discharge on the transport of nutrient, a range of stream discharges were calculated for model input. For more details of the storm hydrograph design can be found in Appendix 3. Other inputs into both estuaries included groundwater inflows which are estimated as daily discharge. The groundwater seep locations were identified by air photos. The groundwater seeps were incorporated as bottom inflow in the model. The groundwater discharges are located on the sand-banks that flank both the margins at Waikareao and on the upper sand-banks that flank the margins at Te Puna.

The stream inflow nutrient data was also sourced from Bay of Plenty Regional Council's monitoring data archives of river and streams. The council monitored Kopurereroa Stream from 1990 until now. The nutrient concentrations from November 2007 until the end of December 2008 were used as the stream boundary conditions for Waikareao. The groundwater inflow nutrient concentrations in the Waikareao Estuary were set to the same concentration at the Kopurereroa stream boundary condition, as there were no other available data sources. Nutrient concentrations were not monitored at Te Puna Stream (catchment size: 22 km^2), hence the water stream inputs were estimated from the catchment of the nearest monitored inflow, Waipapa River (catchment size 36 km^2). Waipapa River is situated ~4 km away from Te Puna. The main catchment activities in both estuaries are dominated by pasture, orchard and cropland and so the run-off behavior should be similar. No adjustments to the concentration were made for the slight differences in catchment size. The nutrient variables monitored at Waipapa River by the council from end of 2007 until the end of 2008, were used as the Te Puna Stream boundary conditions. The groundwater inflow nutrient concentrations in Te Puna were set to the same concentration at the Te Puna

Stream boundary condition, as there are not other sources of data. The concentration of the two freshwater phytoplankton groups were derived from the Lake Rotorua modelling (Hamilton et al. 2005; Burger 2006). It was assumed that Te Puna and Kopurereroa Streams' phytoplankton concentrations were similar to the stream phytoplankton concentrations coming out of Lake Rotorua. The phytoplankton concentration from Lake Rotorua may lead to over-estimation of the primary production at the estuaries.

The CAEDYM configuration file allows the user to specify sediment nutrient fluxes. Sediment release is affected by the pH and O_2 concentration of the overlying water column. A constant flux rate of NH_4^+, NO_3^- and PO_4^{3-} between the sediment and overlying water was prescribed. The constant flux rate of NH_4^+ (0.02 g/m^2/day (Robson and Hamilton 2004)), NO_3^- (-0.03 g/m^2/day (Hipsey et al. 2006b; Missaghi and Hondzo 2010)) and PO_4^{3-} (0.004 g/m^2/day (Robson and Hamilton 2004)), between the sediment and overlying water was prescribed.

Note that all salinities reported here are given in the dimensionless practical salinity units (approximately equivalent to parts per thousand). DIN referred in this chapter is a combination of ammonium and nitrate.

For calibrating the hydrodynamic and biogeochemical part of the model (ELCOM-CAEDYM), simulations were made over a period where the modelled output could be compared with field data. Due to all simulations beginning from a cold start (i.e. flat water, uniform salinity and temperature, and no currents), a period of 3 days (6 tidal cycles) was allowed for the model to 'warm up' before model results were extracted. The model was simulated for five days in summer, winter, start of spring and end of spring coinciding with when field data was collected (for further details of sampling dates, refer to Chapter 2), unless stated otherwise in the text. The model run-time is eight days to simulate a five day period hydrodynamic-biogeochemical output. Summer is defined as March, winter as June, start of spring as September and end of spring as November.

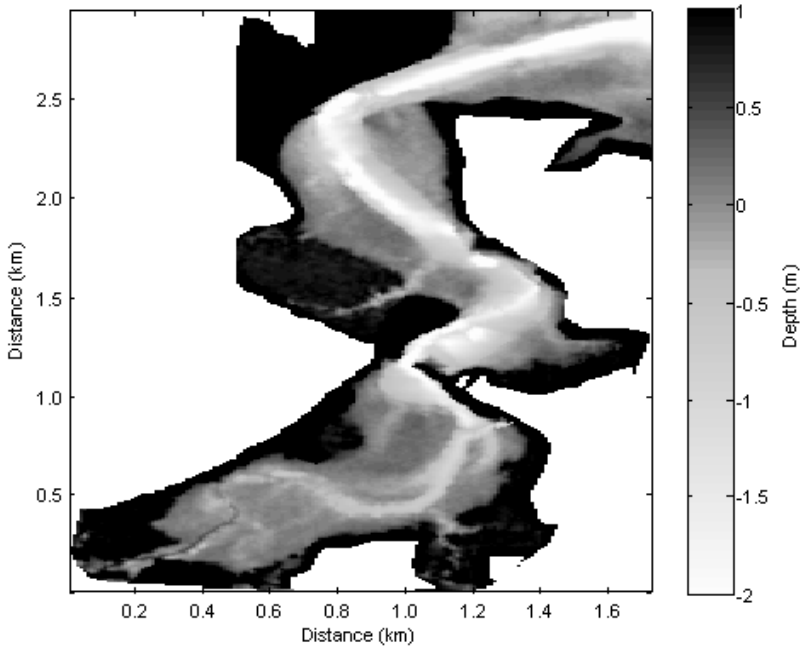

Figure 4.2 ELCOM bathymetric grid of Te Puna Estuary.

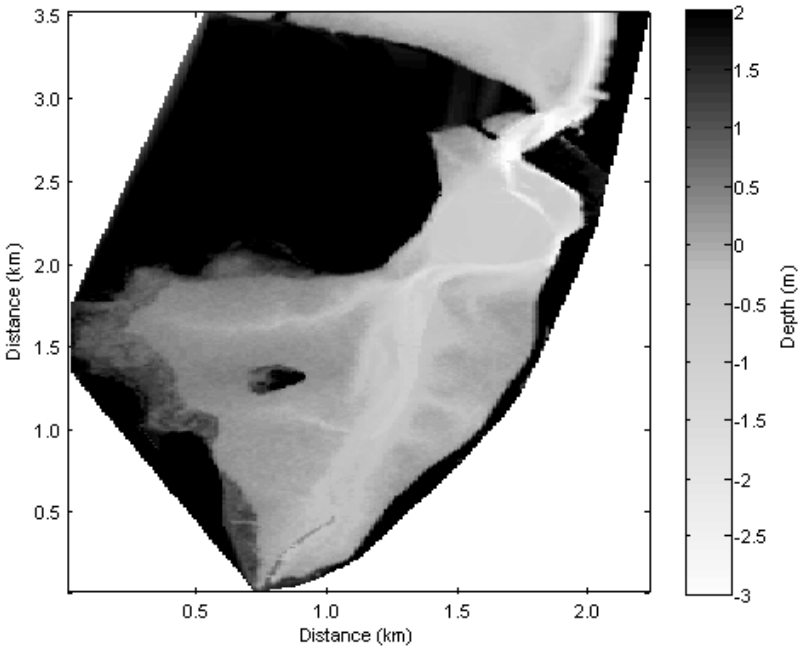

Figure 4.3 ELCOM bathymetric grid of Waikareao Estuary.

Table 4.3 Variables simulated in Te Puna Estuary and Waikareao Estuary using the coupled model ELCOM-CAEDYM.

CAEDYM variable name	Units
DO (DO)	(mg/L)
Ammonium (NH_4^+)	(mg/L)
Nitrate (NO_3^-)	(mg/L)
Labile particulate organic nitrogen (PONL)	(mg/L)
Labile dissolved organic nitrogen (DONL)	(mg/L)
Dissolved reactive phosphorus (PO_4^{3-})	(mg/L)
Labile particulate organic phosphorus (POPL)	(mg/L)
Labile dissolved organic phosphorus (DOPL)	(mg/L)
Labile dissolved organic carbon (DOCL)	(mg/L)
Labile particulate organic carbon (POCL)	(mg/L)
Suspended solids (SSOL1)	(g m^3)
Tracers/colours	(-)
Phytoplankton groups	
Dinoflagellates (DINOF)-estuarine	(µg chl a l^{-1})
Marine diatoms (MDIAT)- marine	(µg chl a l^{-1})
Freshwater diatoms (FDIAT)-freshwater	(µg chl a l^{-1})
Cyanobacteria (CYANO)-freshwater	(µg chl a l^{-1})

4.3 Results

4.3.1 Current speed and direction

4.3.1.1 Te Puna

Modelled (ELCOM) water elevations, current speed and direction from Stations A and B from the corresponding grid cells in the model domain were extracted to compare with data measured by the current meters (Figure 4.4 and 4.5). ELCOM's hydrodynamics (current speed and water elevation) for the estuary domain were calibrated by varying the bottom friction coefficient in the model to find the smallest root-mean square error (RMSE) between modelled and measured data. Simulation results for Station A and B are in good agreement with the measured data. Tidal elevation was generally consistent with RMS of 0.07-0.1 m. Model calibration for current speed and direction was generally good with the general trend better represented for incoming water. During ebbing tide, at station A, the modelled speed was under-predicted by 0.3 m s^{-1} at Station A and by 0.15

m s^{-1} at Station B. The first ebb tide current speed and direction fitted better than the second ebb tide due to biofouling of the sensor acoustic receivers/transmitters by sea lettuce (*Ulva* spp.).

ELCOM's allows users to specify a uniform or varying bottom drag coefficient (BDC). The spatially varying results of the calibration suggested that a spatially varying BDC would be needed to best fit the model result with field data (Table 4.4 and 4.5). A varying bottom drag coefficient was applied across the model domain with areas with a higher (more bottom friction: 0.01) BDC value was set in the channel areas and a lower (reduced bottom friction: 0.005) in the tidal flat areas.

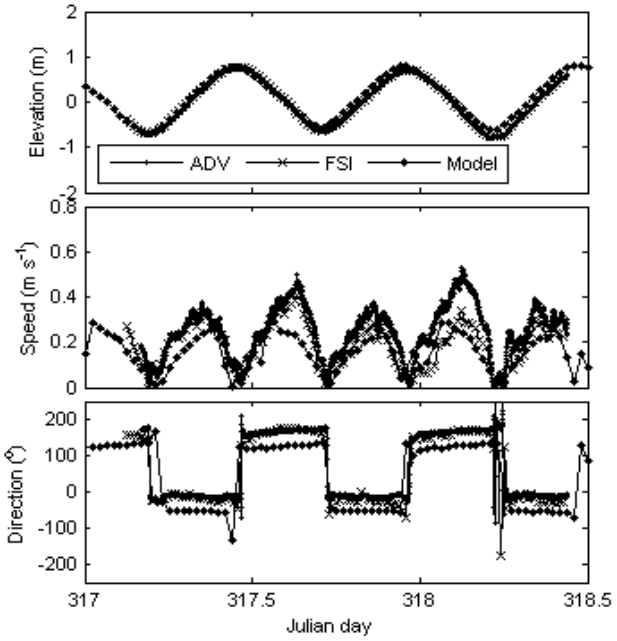

Figure 4.4 Modelled (ELCOM) water elevation, current speed and direction at Station A in Te Puna Estuary in comparison to measured data using ADV and FSI.

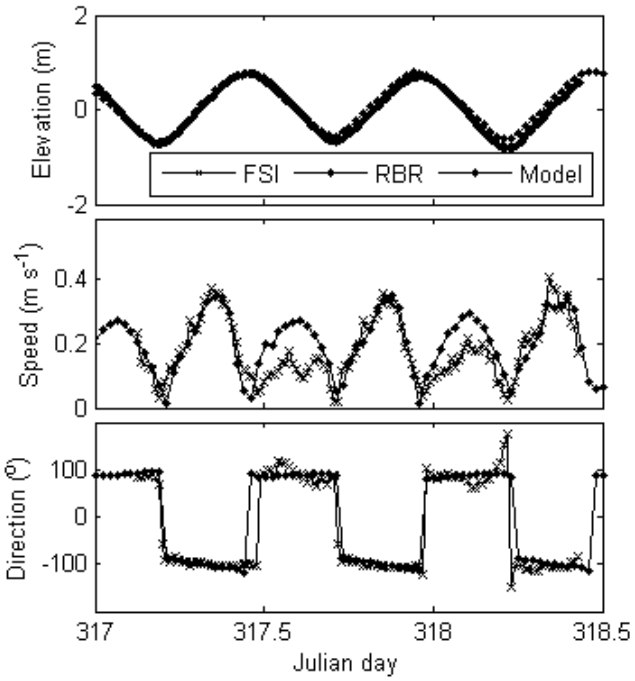

Figure 4.5 Modelled (ELCOM) water elevation, current speed and direction at Station B in Te Puna Estuary in comparison to measured data using FSI and RBR pressure sensor.

Table 4.4 Root mean square error (RMS) of speed for ADV and FSI current meters, and RBR pressure sensor using varying bottom drag coefficient for Te Puna Estuary. FSI (- ADV): FSI that was on the same frame as the ADV; FSI (-RBR): FSI that was on the same frame as the RBR pressure sensor; Vary: Varying bottom drag coefficient (0.01 at channel areas and 0.005 in tidal flat areas.

	RMS speed (m/s)		
BDC	ADV	FSI(-ADV)	FSI(-RBR)
0.001	0.127	0.083	0.090
0.002	0.124	0.078	0.092
0.003	0.119	0.073	0.094
0.004	0.114	0.070	0.097
0.005	0.110	0.067	0.099
0.006	0.107	0.066	0.101
0.007	0.105	0.065	0.103
0.01	0.104	0.067	0.107
0.02	0.115	0.076	0.115
Varying	0.112	0.067	0.100

Table 4.5 RMS error of elevation for ADV and FSI current meters, and RBR pressure sensor using varying bottom drag coefficient for Te Puna Estuary. FSI (- ADV): FSI that was on the same frame as the ADV; FSI (-RBR): FSI that was on the same frame as the RBR pressure sensor; Vary: Varying bottom drag coefficient (0.01 at channel areas and 0.005 in tidal flat areas).

	RMS height (m)			
BDC	ADV	FSI(-ADV)	FSI(-RBR)	RBR
0.001	0.088	0.107	0.081	0.107
0.002	0.085	0.105	0.079	0.107
0.003	0.082	0.103	0.078	0.106
0.004	0.079	0.101	0.077	0.106
0.005	0.077	0.099	0.076	0.106
0.006	0.075	0.098	0.075	0.107
0.007	0.073	0.097	0.075	0.107
0.01	0.071	0.095	0.074	0.109
0.02	0.083	0.103	0.083	0.124
Varying	0.072	0.096	0.074	0.106

4.3.1.2 Waikareao Estuary

Modelled (ELCOM) water elevations, current speed and direction from Stations A and B are shown in Figure 4.6 and 4.7. Due to fouling by sea lettuce of the ADV and FSI at Station A, on the second day of deployment, calibration was only done for the first tidal cycle for elevation, current speed and direction. Tidal elevation was modelled to within an RMS error of 0.1-0.15 m. Simulated current speed at Station A in comparison with FSI and ADV measured data did not compare well especially for the ADV. This may be caused by the sloping bathymetry at the sensor deployment location near the mouth of the estuary. In this area, the current speeds probably varied considerably making comparisons between model and data hard. The current speed was better represented for the FSI during outgoing tide with model speed only under-predicted by 0.06 ms^{-1}. At Station B, tidal elevation was generally consistent. The asymmetry in the current speed of the measured data was not predicted to the same extent by the model at Station B. However, the current speed was better represented during the outgoing tide with model speed under-predicted by 0.1 ms^{-1} at Station B.

As with the Te Puna modelling, the results of the calibration suggested that a varying BDC would be needed to best fit the model result with field data (Table 4.6 and 4.7). A varying bottom drag coefficient was applied across the model domain with areas with a higher (more bottom friction: 0.006) BDC value was set

in the channel areas and a lower (reduced bottom friction: 0.004) BDC for the tidal flat areas.

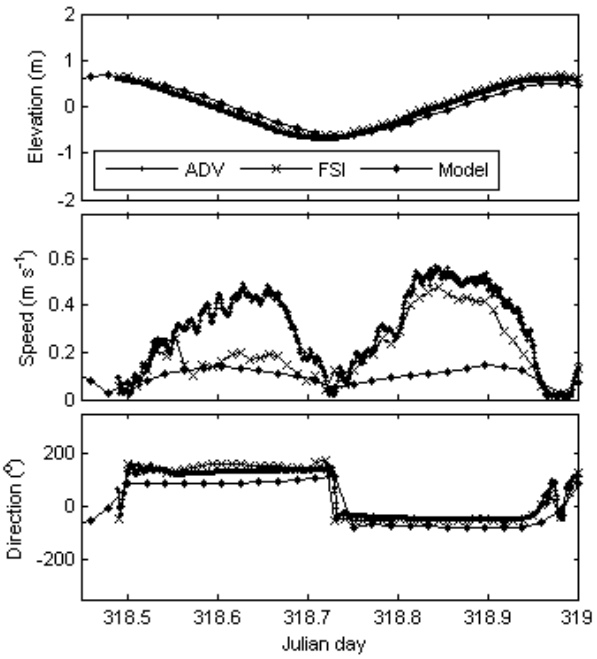

Figure 4.6 Modelled (ELCOM) water elevation, current speed and direction at Station A in Waikareao Estuary in comparison to measured data using ADV and FSI.

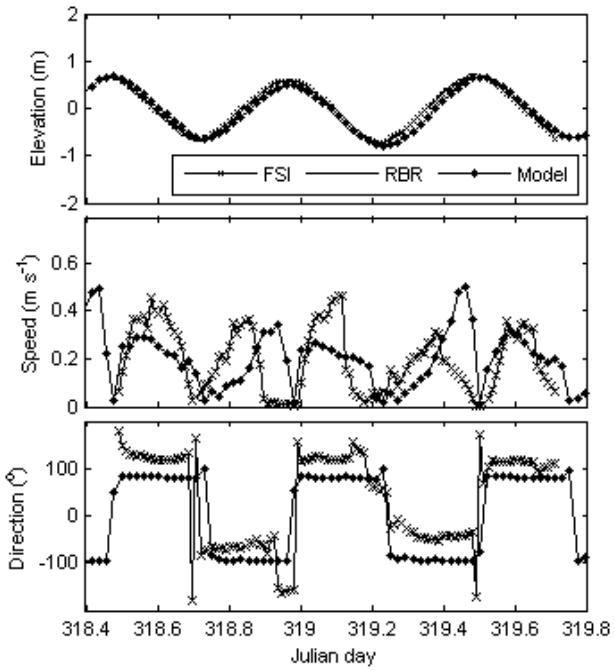

Figure 4.7 Modelled (ELCOM) water elevation, current speed and direction at Station B in Waikareao Estuary in comparison to data measured using FSI and RBR pressure sensor.

Table 4.6 Root mean square error of speed for ADV, FSI current meters and RBR pressure sensor using varying bottom drag coefficient for Waikareao Estuary. FSI (- ADV): FSI that was on the same frame as the ADV; FSI (-RBR): FSI that was on the same frame as the RBR pressure sensor; Vary: Varying bottom drag coefficient (0.006 at channel areas and 0.004 in tidal flat areas.

	RMS speed (m/s)		
BDC	ADV	FSI(-ADV)	FSI(-RBR)
0.001	0.246	0.162	0.159
0.002	0.254	0.171	0.157
0.003	0.249	0.165	0.157
0.004	0.247	0.161	0.157
0.005	0.245	0.159	0.156
0.006	0.244	0.157	0.154
0.007	0.243	0.157	0.153
0.01	0.244	0.157	0.149
0.02	0.253	0.165	0.145
Varying	0.242	0.154	0.156

Table 4.7 RMS error of elevation for ADV and FSI current meters, and RBR pressure sensor using varying bottom drag coefficient for Waikareao Estuary. FSI (- ADV): FSI that was on the same frame as the ADV; FSI (-RBR): FSI that was on the same frame as the RBR pressure sensor; Vary: Varying bottom drag coefficient (0.006 at channel areas and 0.004 in tidal flat areas).

	RMS height (m)			
BDC	ADV	FSI(-ADV)	FSI(-RBR)	RBR
0.001	0.125	0.137	0.092	0.093
0.002	0.131	0.139	0.094	0.095
0.003	0.137	0.142	0.097	0.098
0.004	0.144	0.146	0.101	0.101
0.005	0.150	0.151	0.104	0.104
0.006	0.157	0.155	0.108	0.107
0.007	0.164	0.160	0.111	0.111
0.010	0.184	0.173	0.122	0.121
0.020	0.239	0.215	0.155	0.154
Varying	0.154	0.154	0.106	0.118

4.3.2 Salinity

Vertical profiles of the salinity and temperature of the water were taken with a CTD. After examination of the data indicated insubstantial vertical variations (with minute difference of 0.01 between surface and bottom salinity), the CTD data were depth-averaged. Figure 4.8 and 4.9 shows hourly observed and modelled salinity at Te Puna and Waikareao jetties over two tidal cycles during the four sampling occasions modeled. The model-predicted salinities are in good agreement with the measured salinities with the difference between model and measured data that ranged from 1.5 to 3.1 over the 4 sampling periods for Te Puna

and 1.5-5 for Waikareao. However, the salinity at low tide in the start of spring in Te Puna was over-predicted by 8 while the salinity at high tide was in good agreement with measured salinity. In winter at Waikareao, the simulated low tide salinity was over-predicted by 5 compared to the measured CTD salinity. The modelled salinity distributions showed similar patterns generally in comparison to measured CTD.

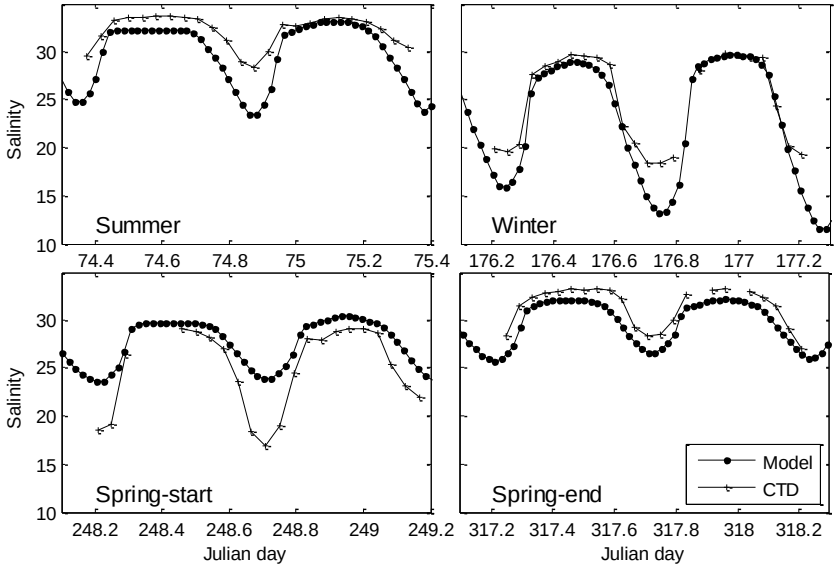

Figure 4.8 Modelled and depth-averaged measured (CTD) salinity profiles for summer, winter, start of spring and end of spring period with no wind condition simulated for Te Puna Estuary. Spring-start: start of spring; Spring-end: end of spring.

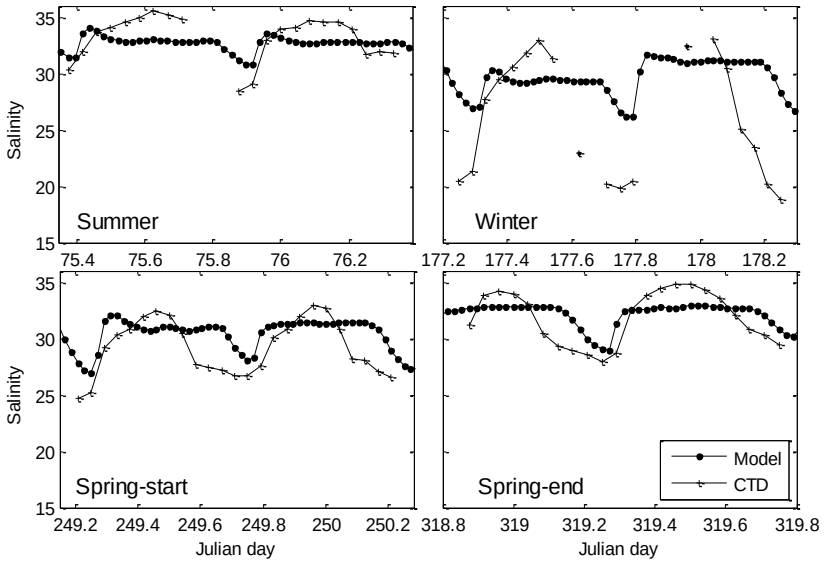

Figure 4.9 Modelled and depth-averaged measured (CTD) salinity profiles for summer, winter, start of spring and end of spring period with no wind condition simulated for Waikareao Estuary. Spring-start: start of spring; Spring-end: end of spring. Note that the salinity profiles started at nighttime in end of spring as sampling started at night cycle.

4.3.3 Temperature

Figure 4.10 and 4.11 showed the temperature profiles for Te Puna Estuary and Figure 4.12 and 4.13 for Waikareao Estuary simulated without wind (i.e. calm condition) and with wind. The model temperature was found to be sensitive to wind input, and in general, a better calibration was observed without wind input. Additional temperature measured by the ADV and RBR at the end of spring in both estuaries, also showed a better representation when modeled without the wind (Figure 4.14 and 4.16) compared to with the wind (Figure 4.15 and 4.17). Scatter plots highlight the improvement between ELCOM simulations conducted with and without wind simulations (Figure 4.18, 4.19). This is particularly evident for the Waikareao Estuary ADV and RBR temperature data, which show an improvement in the r^2 value from 0.1 to 0.8 and 0.2 to 0.7 respectively. The measured CTD showed that the water temperature tended to have a diurnal signal in summer and spring (start and end) and a tidal pattern in winter. ELCOM predicted the water temperature trend over the two tidal cycles at each estuary reasonably well. The temperature data collected showed a peak of temperature during low tide in the afternoon in summer and spring. ELCOM does not reproduce this feature. At Te Puna, this ebb-flow imbalance was observed in summer, start and end of spring, while at Waikareao, it was found in summer and start of spring. At Te Puna, the modelled temperature at the start of spring was under-predicted by 3-4 ^{o}C during this ebb-flow imbalance. While at the end of spring, the modelled temperature was under-predicted by ~5 ^{o}C during this ebb flow period. At Waikareao, the model under-predicted water temperature by 3 ^{o}C during this ebb tide period at the start of spring. In Waikareao, the measured ADV and RBR temperature showed a peaked in the late afternoon low tide in the end of spring. The simulated model including the effect of wind showed a drop in temperature during this period with a difference of 6 ^{o}C and 4 ^{o}C respectively with ADV and RBR measured temperature.

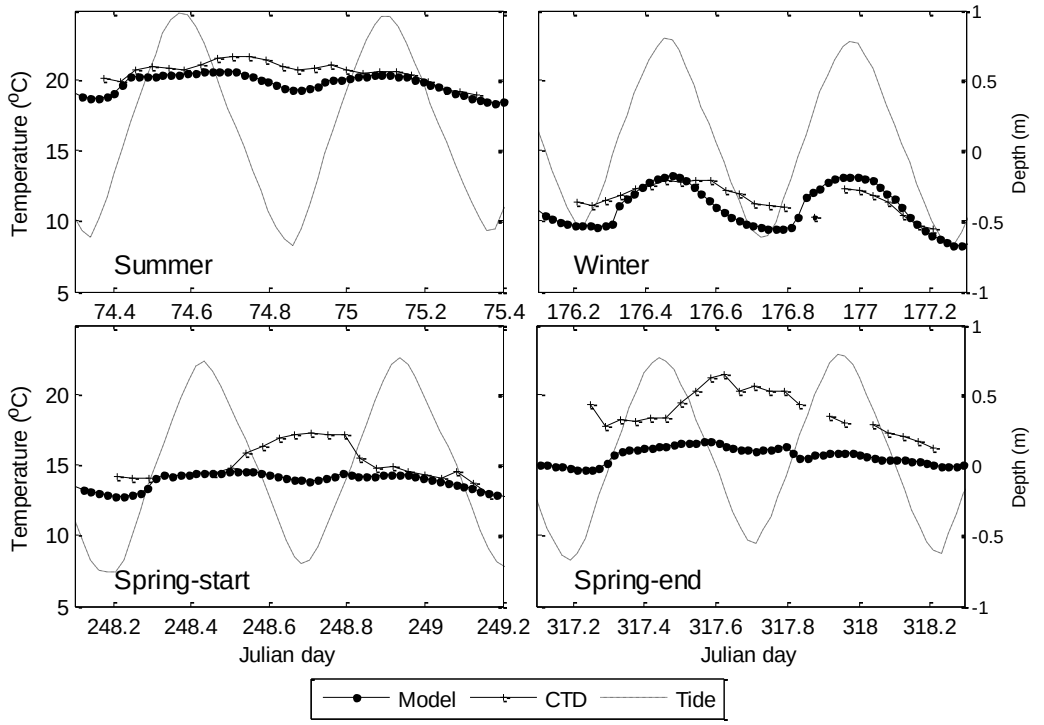

Figure 4.10 Modelled and depth-averaged measured (CTD) temperature profiles for summer, winter, start of spring and end of spring period under no wind condition in Te Puna Estuary. Spring-start: start of spring; Spring-end: end of spring.

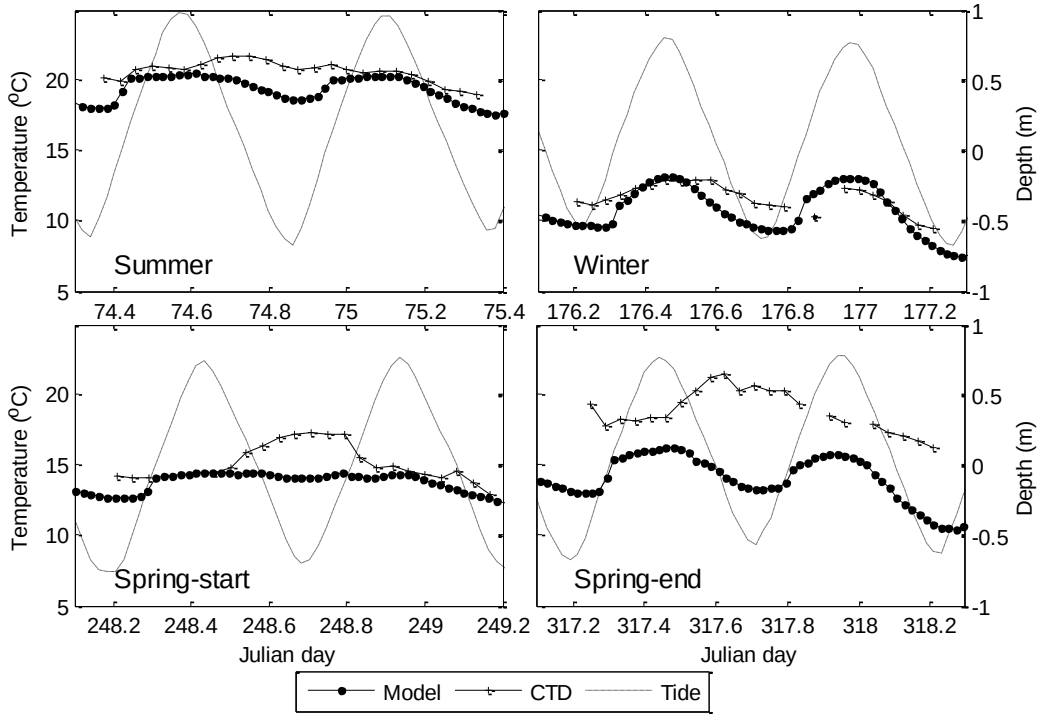

Figure 4.11 Modelled and depth-averaged measured (CTD) temperature profiles for summer, winter, start of spring and end of spring period under wind condition in Te Puna Estuary. Spring-start: start of spring; Spring-end: end of spring.

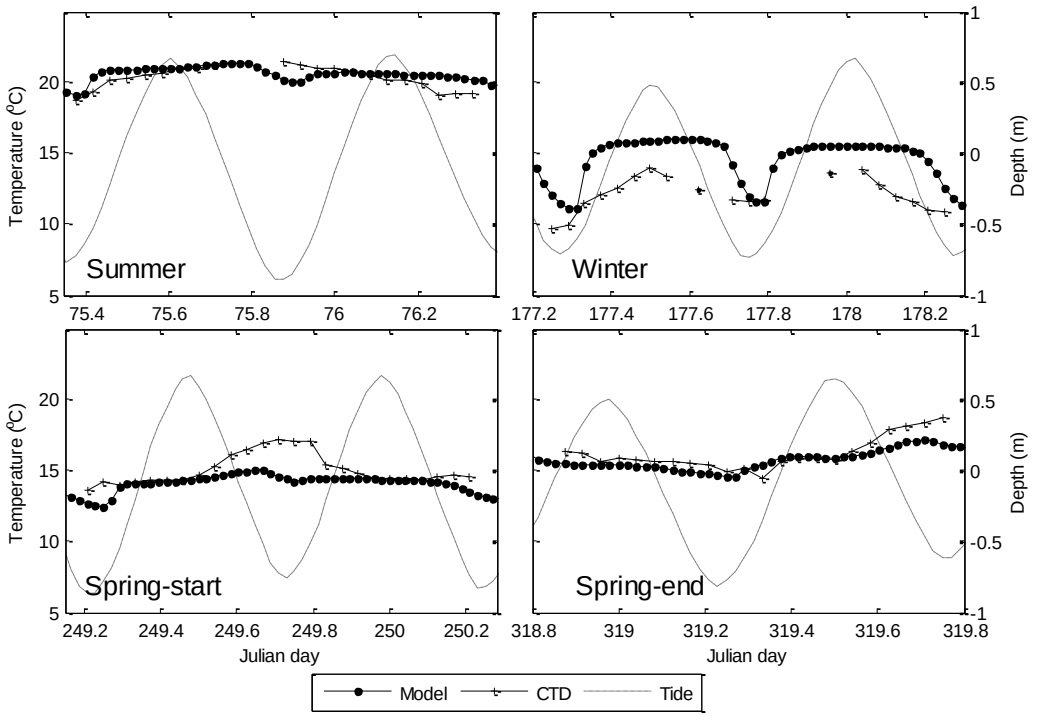

Figure 4.12 Modelled and depth-averaged measured (CTD) temperature profiles for summer, winter, start of spring and end of spring period under no wind condition for Waikareao Estuary. Spring-start: start of spring; Spring-end: end of spring. Note that the temperature profiles started at night time in end of spring as sampling started at night first.

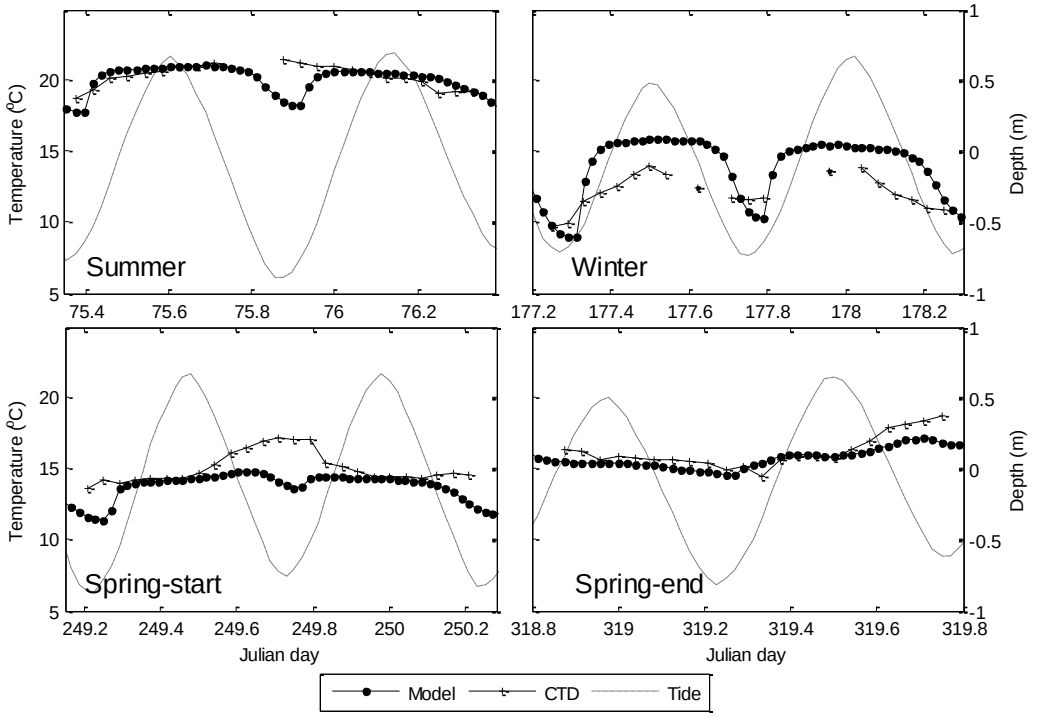

Figure 4.13 Modelled and depth-averaged measured (CTD) temperature profiles at the jetty during the four sampling occasions under wind conditions in Waikareao Estuary. Spring-start: start of spring; Spring-end: end of spring. Note that the temperature profiles started at night time in end of spring as sampling started at night cycle.

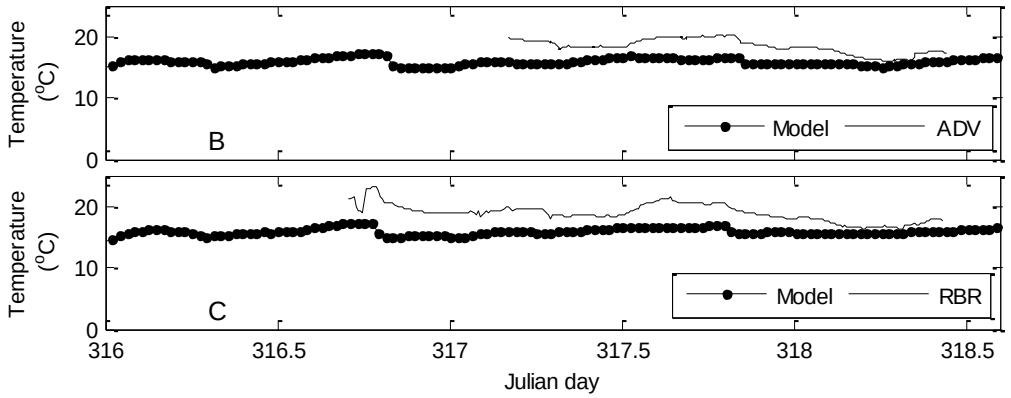

Figure 4.14 Measured (ADV, RBR) and modelled (ELCOM) temperature profiles at the end of spring with no wind condition in Te Puna Estuary.

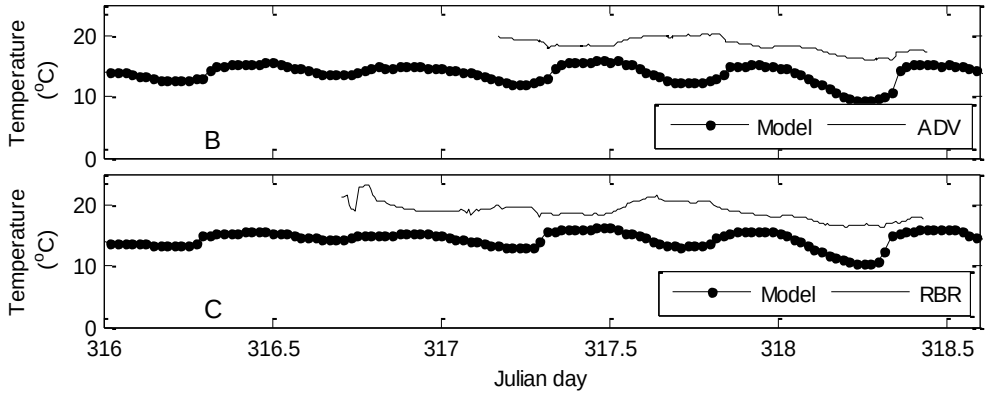

Figure 4.15 Measured (ADV, RBR) and modelled (ELCOM) temperature profiles at the end of spring with wind condition in Te Puna Estuary.

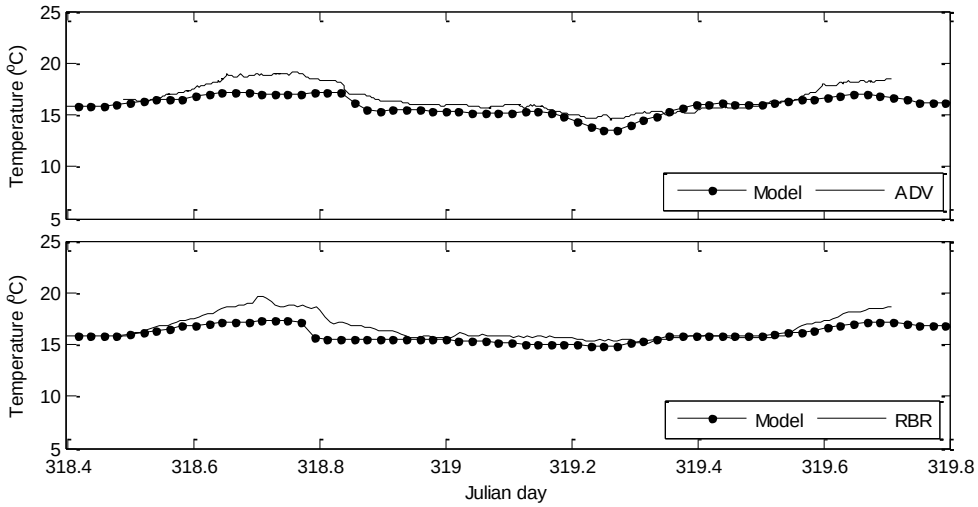

Figure 4.16 Modelled and measured (ADV and RBR) temperature profiles taken at the jetty in Waikareao Estuary during end of spring with no wind condition.

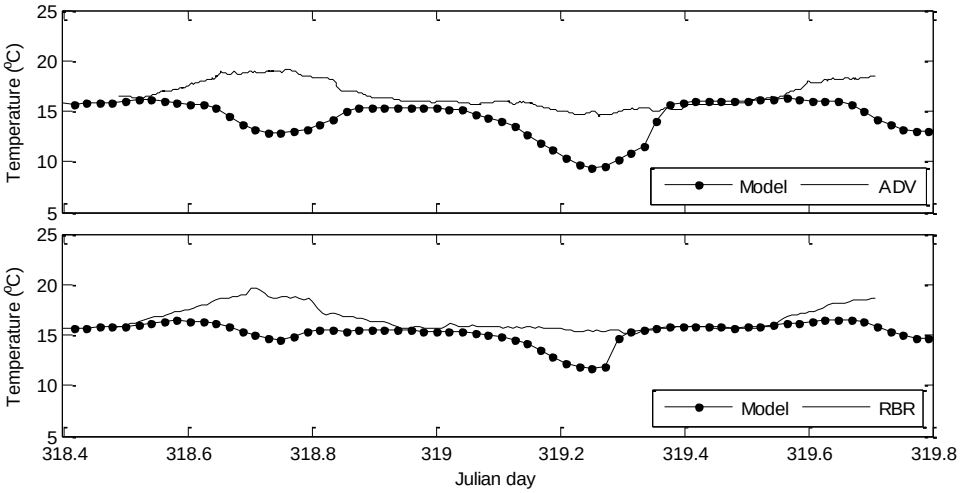

Figure 4.17 Modelled and measured (ADV and RBR) temperature profiles taken at the jetty in Waikareao Estuary during end of spring with wind condition.

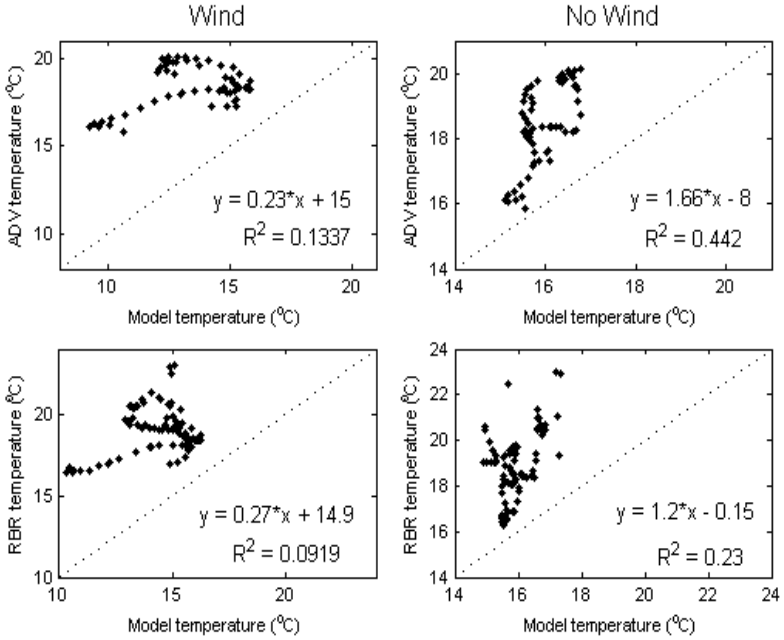

Figure 4.18 Scatter plots comparing ADV and RBR measured data with the equivalent ELCOM data for the end of spring Te Puna simulation.

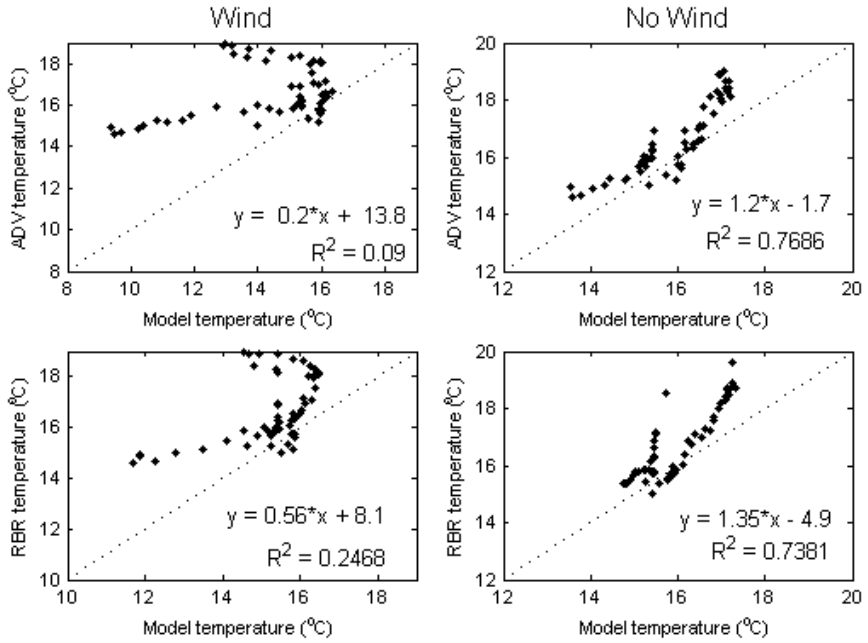

Figure 4.19 Scatter plots comparing ADV, and RBR measured data with the equivalent ELCOM data for the end of spring Waikareao simulation.

4.3.4 Residence times

Figure 4.20 and 4.21 show the time-averaged residence time of water in Te Puna Estuary and Waikareao Estuary respectively. The result indicated that both estuaries are relatively well flushed. The residence times showed decreasing gradients toward the upper estuary region. Note that the simulated residence times in this chapter are different from Chapter 3 as the model assumed that the water coming into the mouth of the estuary is new water, while in the harbour model, the outer boundary is further away. Lower residence times were observed in Waikareao compared to Te Puna largely due to freshwater inflows and tidal range. The presence of an island in the upper-west bank of Waikareao, leads to two distinct regions of residence times, with higher residence times in the upper-end and lower residence times in the lower-end of the west bank. In upper Waikareao, the residence time was higher in the end of spring and this could be related to lower freshwater input, as there were no rainfall events preceding the sampling event.

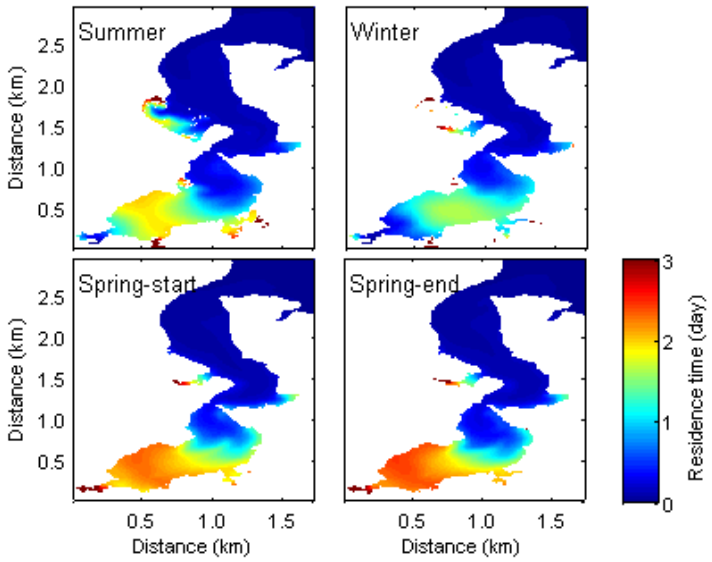

Figure 4.20 Depth-averaged residence time in summer, winter, start of spring and end of spring at high tide in Te Puna Estuary. White areas indicate dry land. Spring-start: start of spring; Spring-end: end of spring.

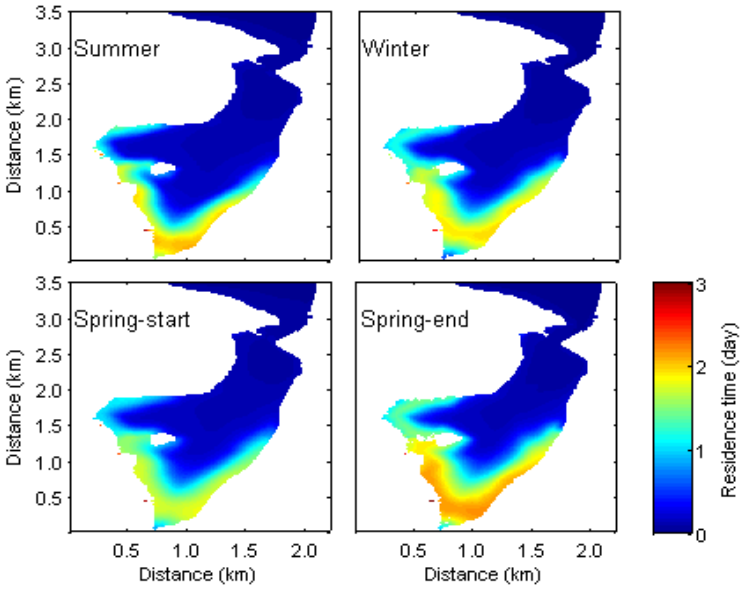

Figure 4.21 Depth-averaged residence time in summer, winter, start of spring and end of spring at high tide Waikareao Estuary. White areas indicate dry land. Spring-start: start of spring; Spring-end: end of spring.

4.3.5 Dissolved nutrients and oxygen

4.3.5.1 Te Puna

Figure 4.22 illustrates the nitrate and ammonium concentrations predicted by CAEDYM over a 24-hour period for summer, winter, start of spring and end of spring compared to measured water concentration at the jetty. The magnitude and timing observed in average concentrations of NO_3^- are reproduced well in the model simulations except at the start of spring where the simulated results under-

predicted observed measurements by 60% during the low tide period. This discrepancy observed in nitrate concentrations at the start of spring was also observed in the salinity profiles where the measured salinity was fresher than simulated results during ebb tide. This is attributed to not enough groundwater inflows and also Te Puna Stream discharge rate was estimated from a storm-hydrograph. Simulations of NH_4^+ (Figure 4.22) give good comparison with measured values at the jetty but show some divergence in winter during the flood tide period. Overall the simulated nitrate is similar to measurements except in the start of spring where the modelled results were lower than measured values (Figure 4.24). Simulated concentrations of ammonium were similar to measurements though the seasonal variability is not reproduced well especially for winter, (Figure 4.24) shown by modelled values remaining relatively low compared to measured value. DO concentrations measured were compared with simulated results (Figure 4.23) but did not compare well either in magnitude or the nature of the pattern. In particular, the simulated DO showing a tidal pattern, whereas measured DO showed a diurnal cycle.

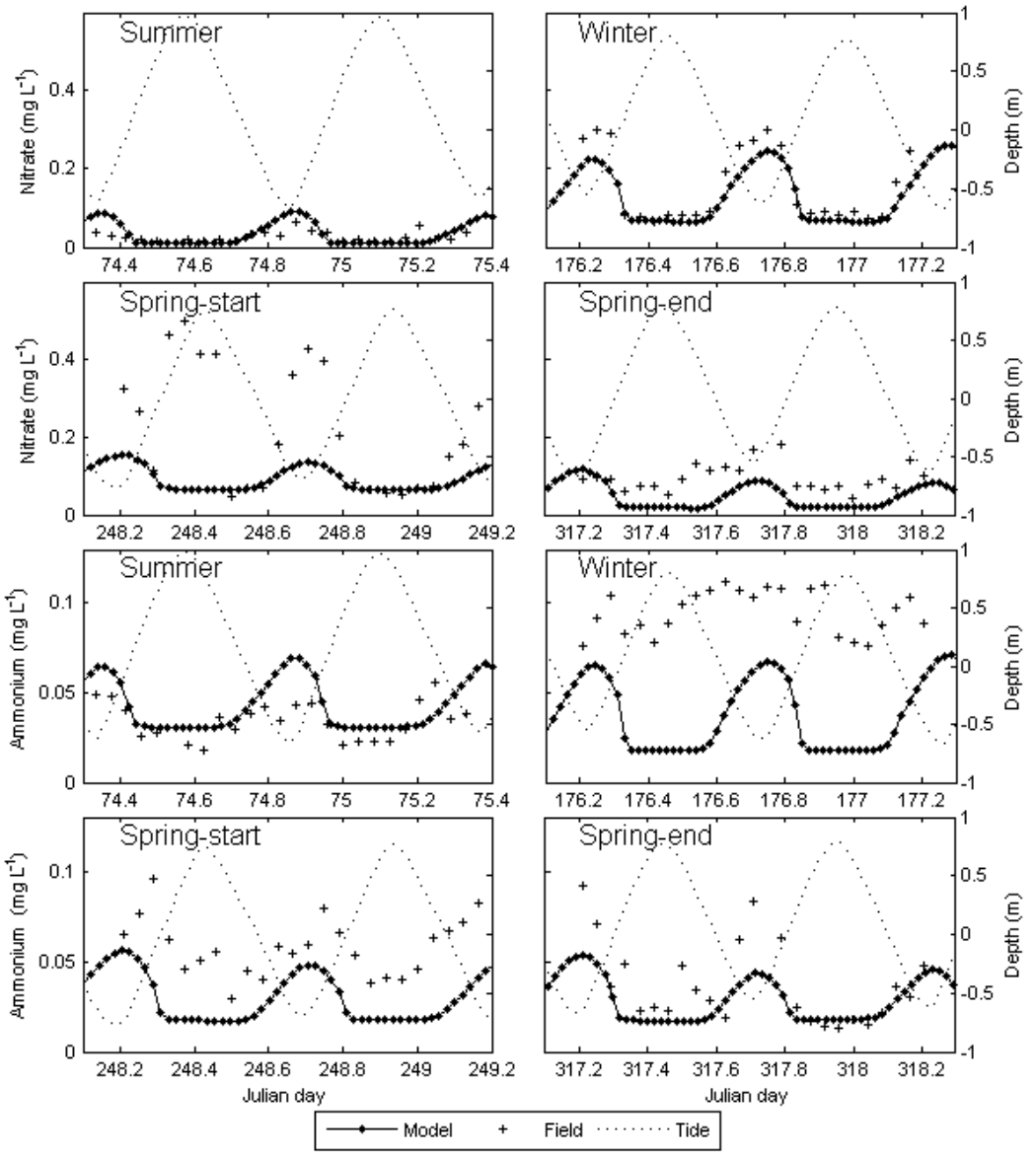

Figure 4.22 Modelled and measured (off the jetty at Te Puna Estuary) concentrations of nitrate and ammonium over two tidal cycles in summer, winter, start of spring and end of spring. Spring-start: start of spring; Spring-end: end of spring. Note the different scales on the y-axis and x-axis for nitrate and ammonium.

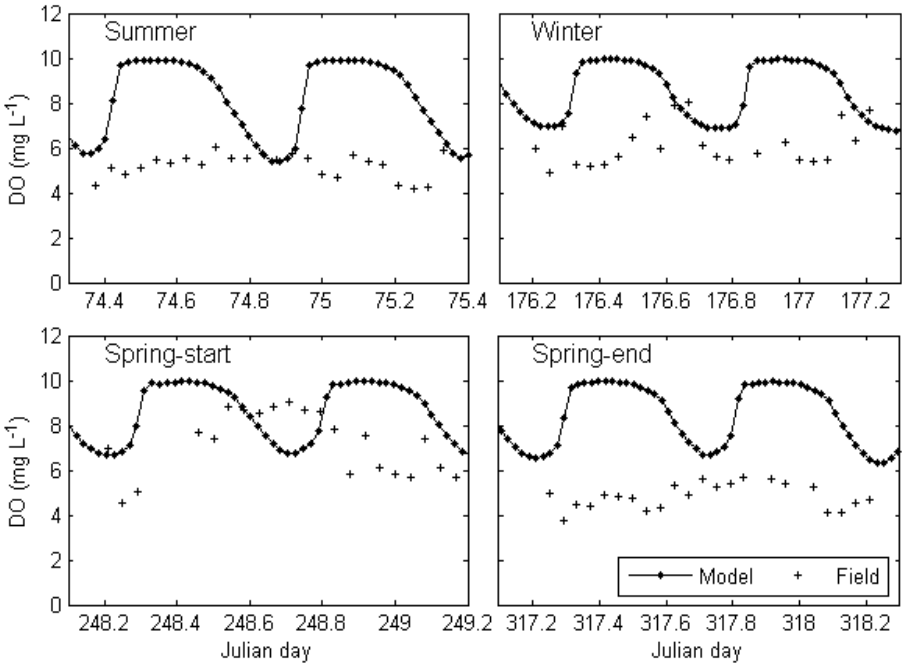

Figure 4.23 Modelled and measured concentrations of DO over two tidal cycles in summer, winter, start of spring and end of spring in Te Puna. Spring-start: start of spring; Spring-end: end of spring.

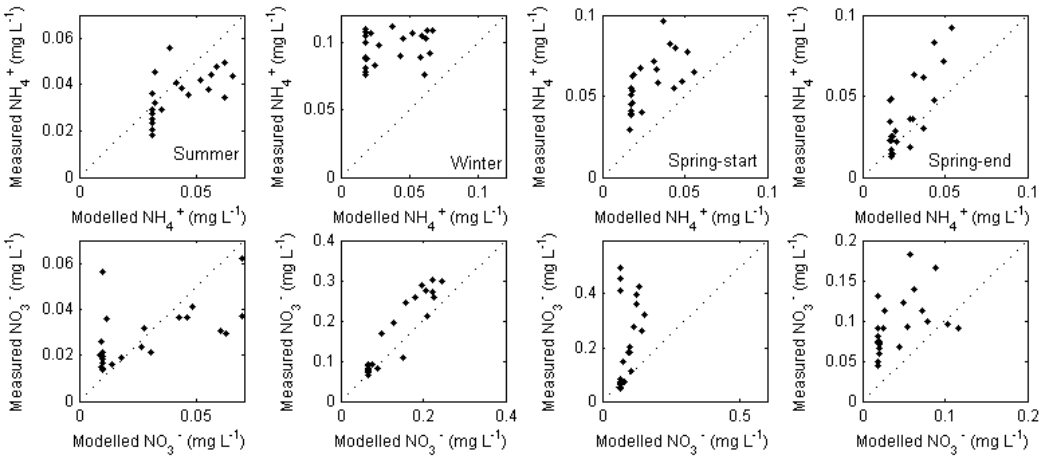

Figure 4.24 Comparison of modelled and measured ammonium (NH_4^+) and nitrate (NO_3^-) concentrations at Te Puna Estuary for summer, winter, start of spring and end of spring. Spring-start: start of spring; Spring-end: end of spring.

4.3.5.2 Waikareao Estuary

The magnitude and timing observed in the measured concentrations of NO_3^- and NH_4^+ reproduced well in the model except in winter (Figure 4.25). In winter, both the simulated nitrate and ammonium concentrations were lower than measured concentrations (Figure 4.25, 4.27). This discrepancy observed in both nitrate and ammonium concentrations was also observed in salinity in winter where the observed concentration was fresher than the simulated results especially during low tide. Overall the simulated concentrations of nitrate are similar to measurements though in winter and end of spring, the measured concentrations of

nitrate were higher (Figure 4.27). Simulated concentrations of ammonium are similar to measurements, though the observed seasonal variability is not reproduced well by the model especially in winter and start of spring, shown with modelled values remaining low compared to measured values in Figure 4.27. DO concentrations measured were compared with simulated results but did not compare well either in magnitude or the nature of the pattern especially during flood tide (Figure 4.26) except at the start of spring where simulated DO over-predicted measured DO by only 2 mg/L during this period.

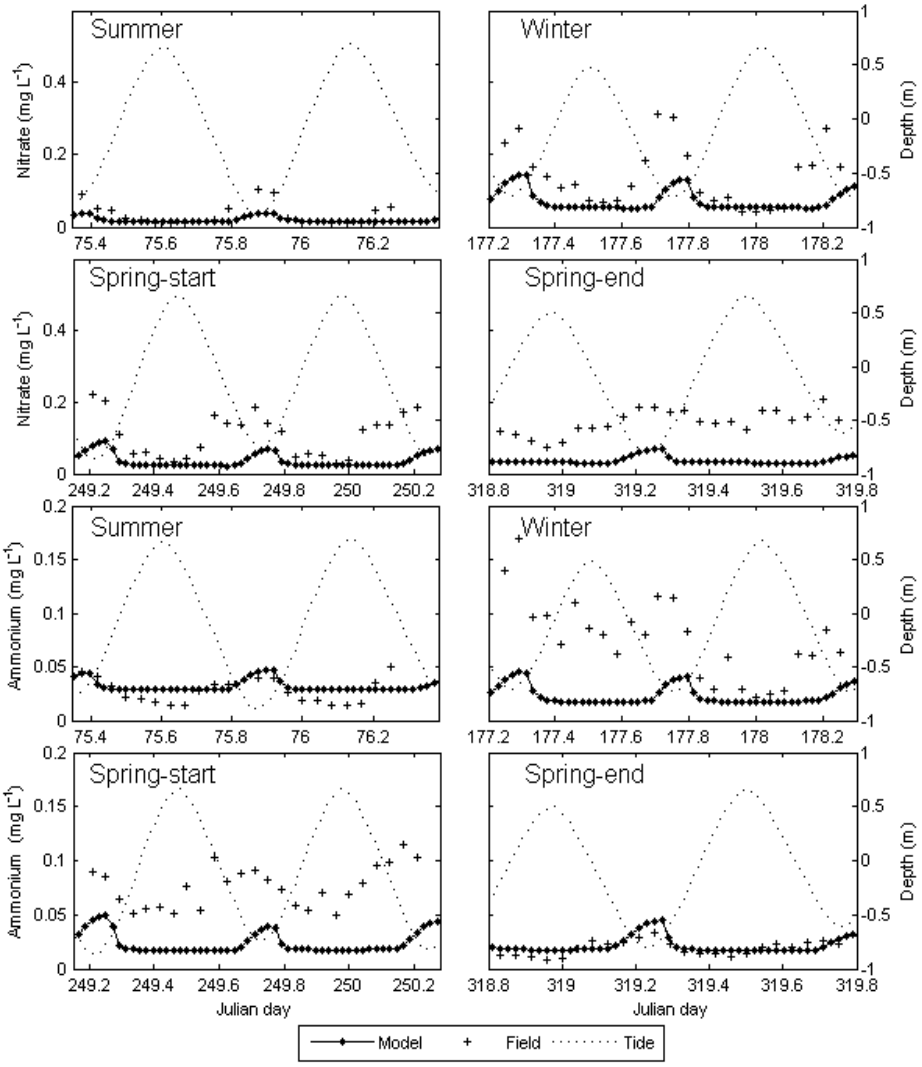

Figure 4.25 Modelled and measured off the jetty at Waikareao Estuary, concentrations of nitrate and ammonium over two tidal cycles in summer, winter, start of spring and end of spring. Spring-start: start of spring; Spring-end: end of spring. Note the different scales on the y-axis and x-axis for nitrate and ammonium. Also note that at the end of spring, the nutrient profiles started from the night cycle.

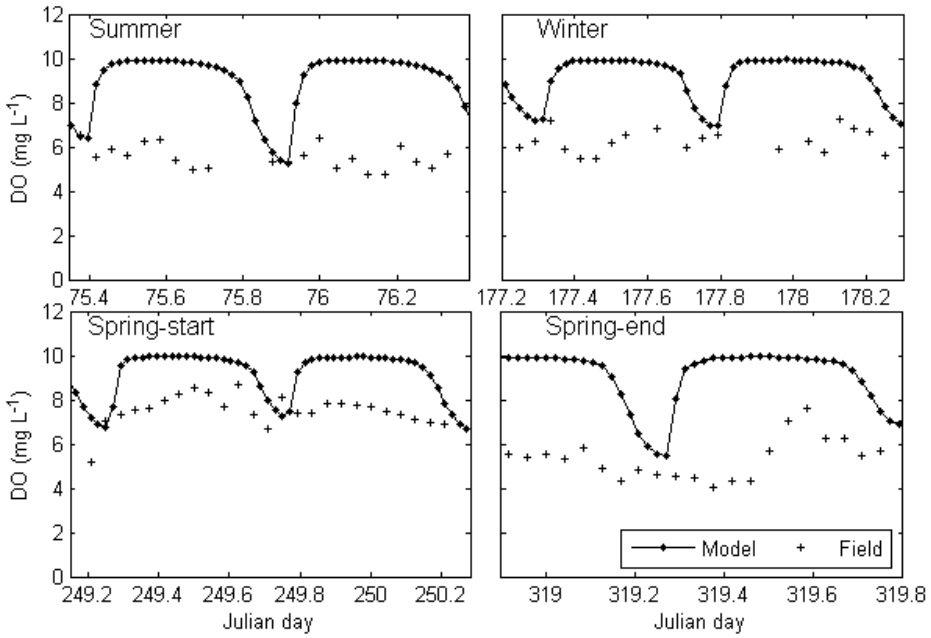

Figure 4.26 Modelled and measured concentrations of DO over two tidal cycles in summer, winter, start of spring and end of spring in Waikareao Estuary. Spring-start: start of spring; Spring-end: end of spring. Note that at the end of spring, the DO profiles started from the night cycle.

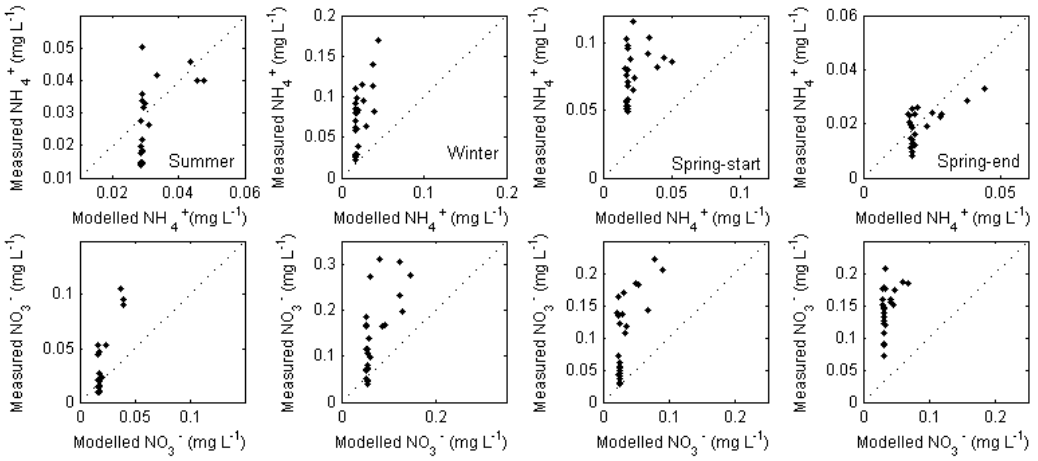

Figure 4.27 Comparison of modelled and measured ammonium (NH_4^+), and nitrate (NO_3^-), concentrations at Waikareao Estuary in summer, winter, start of spring and end of spring. Spring-start: start of spring; Spring-end: end of spring.

Comparison of summer (March), winter (June), start of spring (September) and end of spring (November) simulated nitrate and ammonium of Te Puna and Waikareao estuaries highlights the spatial and temporal variability in DIN concentrations (Figure 4.28-4.31). The overall agreement between simulated data and observations indicates that the model captures the important processes affecting nutrient concentrations. In general, nutrient concentrations show a seasonal trend characterized by high values in winter, a progressive decrease during the productive spring period to low levels in summer. In summer the

nutrient concentrations were the lowest compared to all other three sampling occasions in both estuaries. In the start of spring in Te Puna, the salinity was under-predicted at low tide with modelled salinity having higher concentration compared to measured salinity. In Waikareao, the simulated nitrate concentrations were under-predicted during the low tide period, which can be due to under-prediction of groundwater sources in the estuary. This potentially leads to an under-prediction of nitrate concentrations by 0.2 mg/L during low tide.

These seasonal trends in DIN concentrations are superimposed on the characteristic oscillatory tidal variability in the estuary. A pronounced decrease in DIN concentrations can also be observed along the estuary due to dilution and assimilation along the salinity gradient. In Te Puna Estuary, the constriction at 1.0-1.5 km from the estuary mouth lead to a distinct gradient in DIN concentration from the upper to lower estuary as also seen in the residence times in the estuary. At high tide, the DIN concentrations showed two distinct areas, with lower concentration in lower Te Puna, and higher concentration at upper Te Puna (Figure 4.28). However, at low tide with water being channelized, the high DIN concentration from upper Te Puna moved further downstream (Figure 4.29). The DIN concentrations in Waikareao also displayed the same pattern as Te Puna with decreasing concentration as the water moved downstream. During high tide, low nutrient water from the open water 'pushes' into the upper estuary (Figure 4.30). During low tide, the water from upper and shallow regions of Waikareao moved downstream carrying higher concentration DIN (Figure 4.31). The simulated phosphate concentrations were relatively low with no distinct seasonal patterns in both estuaries (Figure 4.32, 4.33). In winter, the simulated phosphate was higher in upper Te Puna Estuary suggesting freshwater source contribution.

DO concentrations in Te Puna and Waikareao estuaries are shown in Figure 4.34 and 4.35 for summer, winter, start of spring and end of spring. In summer, lower estuary waters are well-oxygenated till middle estuary with slightly lower DO on the west bank tidal flat region in Te Puna. In summer, at Waikareao, the estuary waters are well-oxygenated except on the west bank tidal flat margins and upper estuary area where DO concentrations were lower by 4 to 8 mg/L. This was observed in all four sampling periods. By winter, the water in Te Puna was super-saturated with DO whereas in Waikareao, the DO increased as water moved

downstream into the lower estuary. The DO concentration in the west bank area in Waikareao also increased during winter. In both estuaries the concentration gradient separating lower and upper estuaries regions weakens in winter enabling increased vertical mixing of harbour waters with upper estuary tidal flat waters.

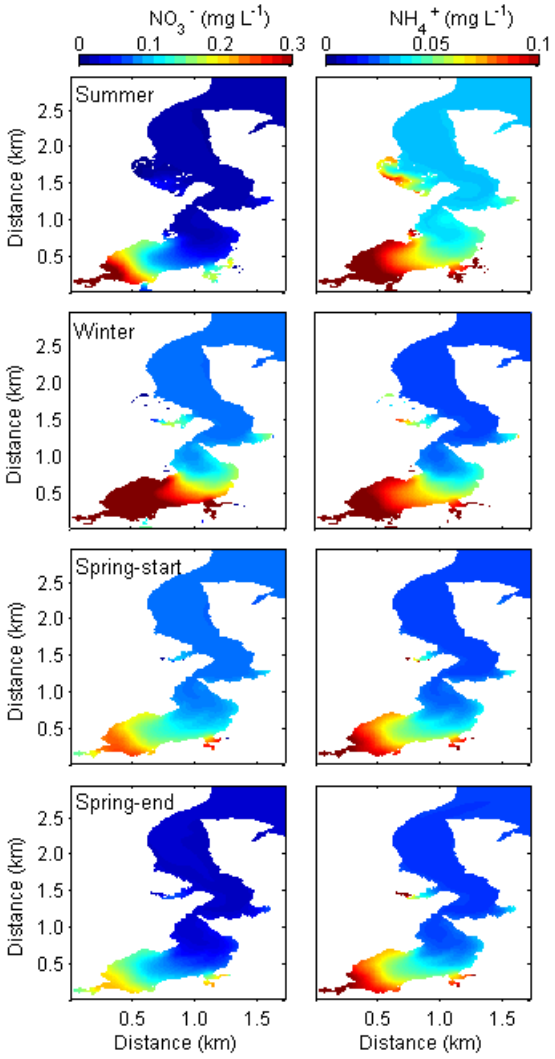

Figure 4.28 Depth-averaged modelled nitrate (NO_3^-) and ammonium (NH_4^+) concentrations in Te Puna Estuary at high tide days in summer, winter, start of spring and end of spring. White areas indicate dry land. Spring-start: start of spring; Spring-end: end of spring. Note different colourbar scales.

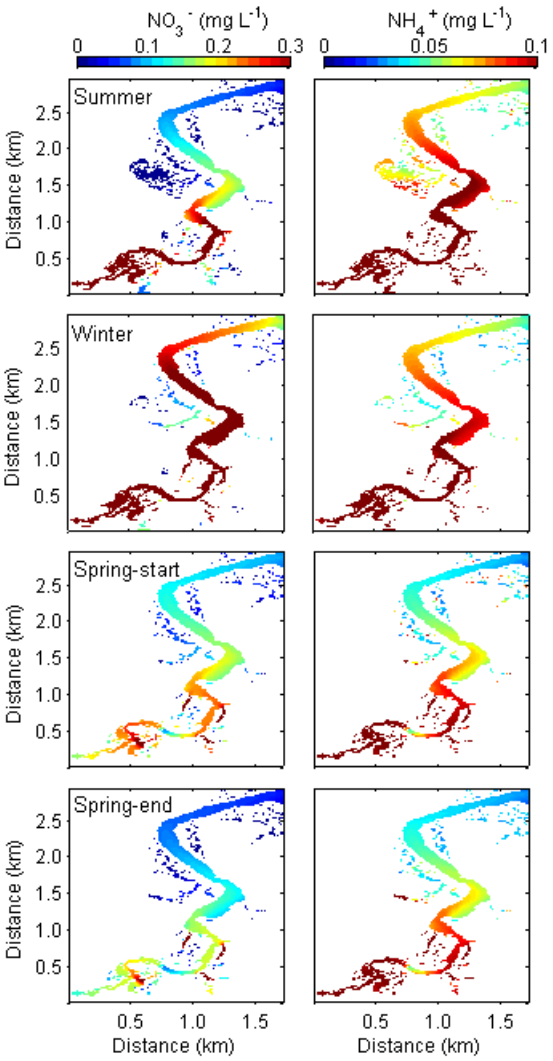

Figure 4.29 Depth-averaged modelled (NO_3^-) and ammonium (NH_4^+) concentrations in Te Puna Estuary at low tide in summer, winter, start of spring and end of spring. White areas indicate dry land. Spring-start: start of spring; Spring-end: end of spring. Note different colourbar scales.

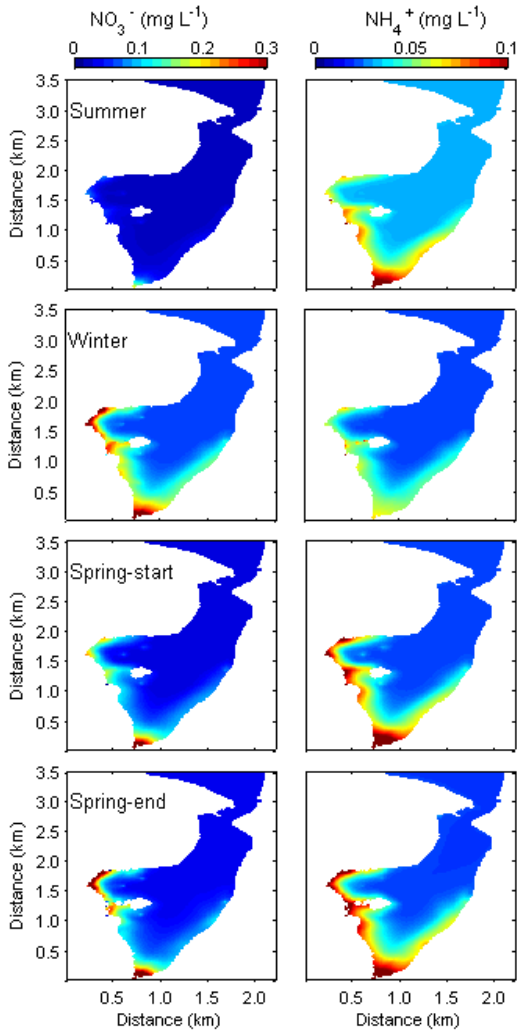

Figure 4.30 Depth-averaged modelled (NO_3^-) and ammonium (NH_4^+) concentrations in Waikareao Estuary during summer, winter, start of spring and end of spring at high tide. White areas indicate dry land. Spring-start: start of spring; Spring-end: end of spring. Note different colourbar scales.

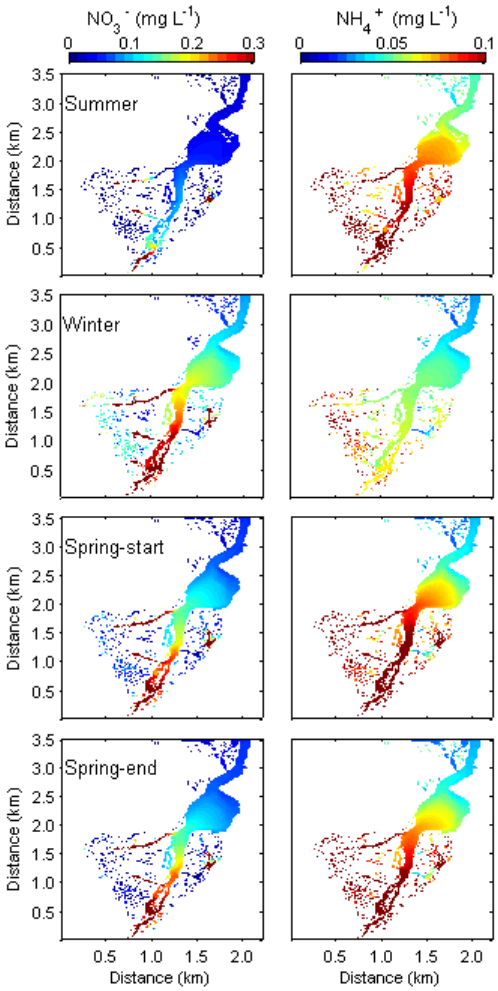

Figure 4.31 Depth-averaged modelled (NO_3^-) and ammonium (NH_4^+) concentrations in Waikareao Estuary during summer, winter, start of spring and end of spring at low tide. White areas indicate dry land. Spring-start: start of spring; Spring-end: end of spring. Note different colourbar scales.

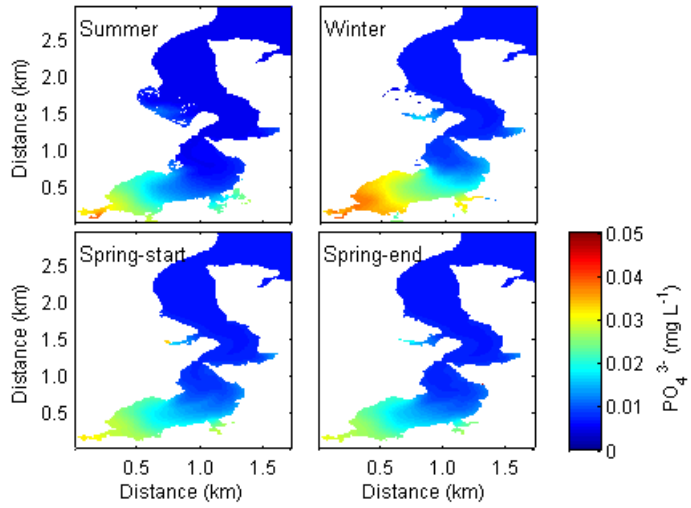

Figure 4.32 Depth-averaged modelled phosphate (PO_4^{3-}) concentrations in Te Puna Estuary at high tide during summer, winter, start of spring and end of spring. White areas indicated dry land. Spring-start: start of spring; Spring-end: end of spring.

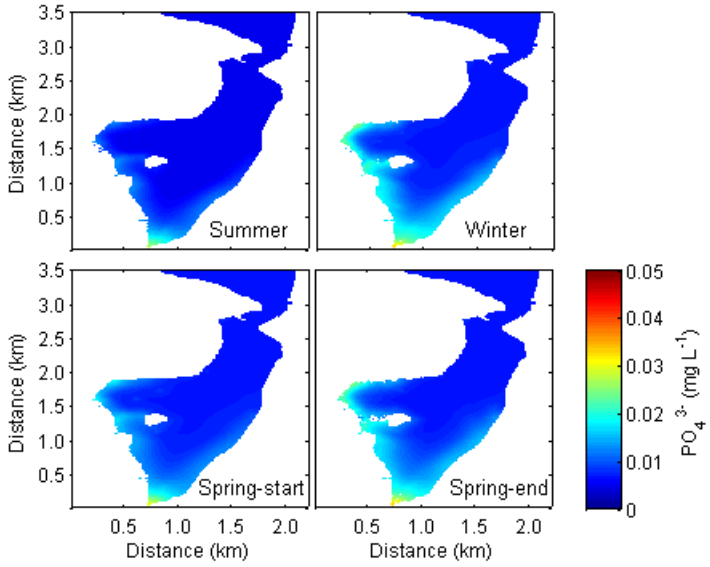

Figure 4.33 Depth-averaged modelled phosphate (PO_4^{3-}) concentrations in Waikareao Estuary at high tide during summer, winter, start of spring and end of spring. White areas indicated dry land. Spring-start: start of spring; Spring-end: end of spring.

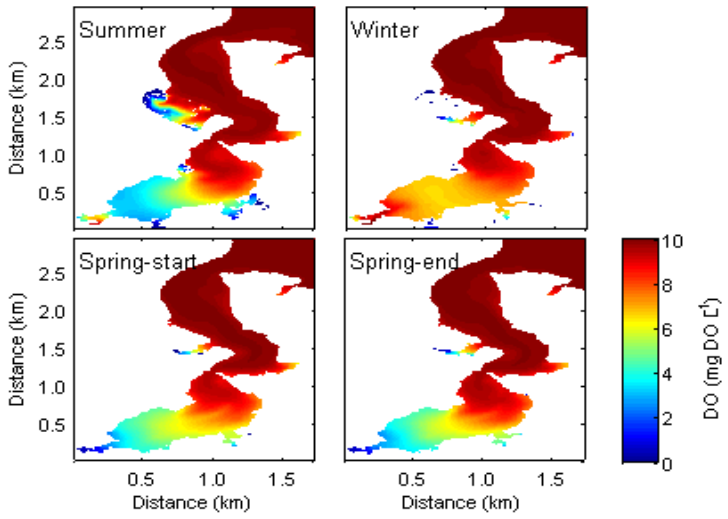

Figure 4.34 Depth-averaged DO concentrations for Te Puna Estuary at high tide in summer, winter, start of spring and end of spring. White areas indicate dry land. Spring-start: start of spring; Spring-end: end of spring.

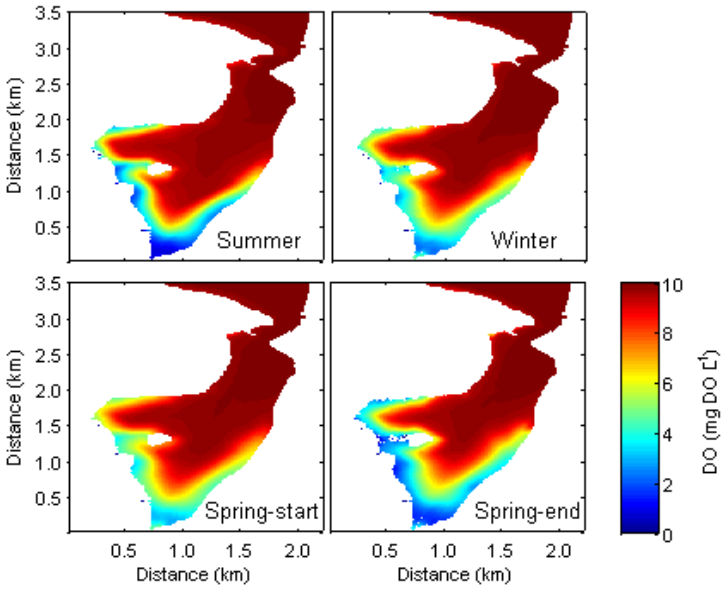

Figure 4.35 Depth-averaged DO concentrations for Waikareao Estuary at high tide in summer, winter, start of spring and end of spring. White areas indicate dry land. Spring-start: start of spring; Spring-end: end of spring.

4.4 Discussion

The influence of physical processes such as vertical mixing and circulation on water masses in both Te Puna and Waikareao estuaries is emphasized by the seasonality of salinity, temperature and nutrient concentrations in both estuaries. The close coupling of physical and biological processes ensures that fluctuations in nutrient inflows and climate forcing are reflected in the spatial and temporal variations in nutrient and DO distribution and consequently nutrient exchange

between tidal cycles. In shallow estuaries as Te Puna and Waikareao, the exchange of water with the main Harbour is relatively short, ~ hours to 1.5 days, leading to lower nutrient retention in both estuaries.

The hydrodynamic model calibration illustrates the model is capable of predicting the hydrodynamics of Te Puna and Waikareao estuaries, although outgoing currents were under-predicted in some cases. This is thought to be due to the difficulty in adequately representing the complex morphology in the model grid. The non-linear processes in a channel can contribute to significant asymmetry such that the flood tide and ebb tide may have different flow magnitudes. The model has been shown to predict well the relative current speeds and direction of tide reversal, which govern nutrient mixing and distribution.

The simulated salinity showed a seasonal pattern with higher salinity found in summer and lowest in winter in both estuaries. In Te Puna and Waikareao estuaries, the simulated salinity was lower than the observed salinity during low tide in start of spring and winter respectively, which could be due to under-estimation of groundwater discharge.

The modelled temperature at both Te Puna and Waikareao showed tidal patterns in summer and spring but as shown in the CTD measurements, the model has under-predicted the water temperatures notably during ebb tide. The ebb-flow imbalances observed in the water temperature during the late afternoon ebb tide at both estuaries could be due to the heating of the shallow tidal flat by solar radiation during ebb tide periods in the daytime. This peak in temperature was also observed at Omokoroa Channel stations (Chapter 3). As mentioned previously in Chapter 3, this heated water from the tidal flat is intermixed with the next flood tide water, and during the next ebb tide bring the intermixed heated water passing by the observation locations on the jetties at both estuaries. In shallow surface waters, the solar radiation can penetrate the entire water column with the remaining irradiance at the sediment bed-water interface being absorbed into the sediment (Ji 2008). By excluding wind inputs, the simulated temperature calibrated better with CTD measured temperature in both estuaries, as wind input exacerbates the badly modelled tidal flat heating issue.

The residence times in both estuaries showed a gradient of varying residence times from the estuary mouth to upper parts of the estuary. The residence time increases in the higher reaches of both estuaries and also laterally across both estuaries. The residence times in both estuaries are influenced mainly by tidal cycle and bathymetric changes in the upper estuary caused by a sharp gradient between the shallow tidal flat region and deeper channel areas. In Te Puna, the constriction at 1.5 km away from upper estuary limits the exchange of water resulting in a strong salinity gradient across the constriction. The residence time was lower at Waikareao Estuary compared to Te Puna Estuary due to the geomorphology of the estuary, as there is only a single constriction at the mouth of Waikareao Estuary. The short residence times are particularly important for exporting nutrients from the estuaries into the harbour especially in winter where influxes of freshwater nutrient input can be high. A similar situation was observed in the well-flushed Boston Harbour (2-10 days), where N-concentrations are relatively low despite a high loading (Kelly 1997; Nowicki et al. 1997). The distribution of the nutrients in the estuaries can influence the ecological conditions of the system along with physical factors by limiting the potential for phytoplankton bloom to occur as the short residence times do not provide enough time to allow for phytoplankton cell division to occur.

In general the direct source of anthropogenic freshwater input into both estuaries is from the Kopurereroa Stream and Te Puna Stream respectively. This nutrient source is typically modified by development in the upstream catchments including inputs from agricultural, industrial and urban areas (Correll et al. 1992; Saenger et al. 2008). Model simulations with CAEDYM show that the upper region of the Te Puna Estuary and upper and middle east-west bank of Waikareao Estuary has higher average nutrient concentrations due to input from Te Puna Stream and Kopurereroa Stream. This nutrient rich water is intermixed with marine water over a tidal cycle and is flushed from the system after remaining in the system for 1.5 days and 1.0 days at upper regions of Te Puna and Waikareao respectively. 54% and 83% of Waikareao and Te Puna catchment activities are dominated by agriculture (Park 2004). Using a sub-catchment to estuary nitrogen yield model in three South Island estuaries, Heggie and Savage (2009) discovered that nitrogen yield to coastal system increased directly with proportion of agricultural land area in the catchment, and nitrogen flux to coastal waters here is generally dominated

by non-point sources. Previous studies of fluxes of nutrients into aquatic systems have demonstrated a strong linkage between land use and nutrient levels of surface waters (e.g. Quinn and Stroud 2002; Bowen et al. 2007; Latimer and Charpentier 2010). With intensification of agricultural development in New Zealand, this leads to an increase in flux of nitrogen to coastal systems causing stress to ecological diversity.

The constricted headland at 1.5 km from Te Puna Estuary mouth and at the estuary mouth lead to two distinct patterns in the residence times and nutrient concentrations in the estuary. The constriction leads to higher residence times and consequently higher nutrient concentrations in the upper estuary whereas in the lower estuary, rapid tidal exchanges of water occurring over a tidal cycle lead to renewal of DO and lower nutrient. This constriction leads to spatial variability observed which can affect nutrient spatial distribution, and may limit phytoplankton growth due to the interacting factors of nutrient distribution, salinity variations, temperature variations and light availability. Local wind conditions and physical influences can modify this general pattern and result in differences in nutrient and DO concentrations.

The simulated results of both Te Puna and Waikareao showed lateral variation in nutrient concentration from the upper to lower estuary. On a system scale, tidal exchange is the key factor influencing nutrient and dissolved oxygen concentrations in both estuaries. During flood tide, marine water flows further inwards into the upper estuary regions. While at ebb tide, the opposite was observed, where water from the upper estuary with high nutrient concentrations and with shallow areas seepage, drained into the channel regions. This resulted in higher nutrient concentrations found during low tide.

In winter, the simulated nutrient concentrations were much higher, as illustrated by the increasing concentration in nutrient and lower salinity especially during low tide suggesting freshwater inputs and pore-water seepage was the primary source of nutrients. In contrast in summer where freshwater discharge was lower, the simulated ammonium concentration was still high, which suggests contribution from sediment flux as the main source as ammonium regeneration rates from sediment tends to increase with temperature (Nixon 1981). Previous

sediment work had also indicated that rates of ammonium release from sediment were higher in summer (Boynton and Kemp 1985; Kemp et al. 1990). The high ammonium concentration observed in the middle region of Te Puna and Waikareao estuaries during spring was likely due to remineralization of nitrogen within the estuaries and groundwater inputs. The ammonium concentration decreased as water moved from mid to lower estuary likely due to phytoplankton uptake. However the phytoplankton uptake rate in the model simulations may be over-estimated as the freshwater phytoplankton concentrations were derived from Lake Rotorua modelling. The underestimation of temperature in spring for both estuaries can lead to underestimation of DIN concentrations, as the N-cycle is temperature dependent. The underestimation of DIN concentrations lead to the estuaries being N-limited and can lead to lower phytoplankton biomass. With lower phytoplankton biomass, metabolic loss of N via mortality and excretion will be lower.

As noted above, the sediment nutrient fluxes were set to a constant flux rate. In shallow estuaries such as Te Puna and Waikareao, the sediment can contribute a significant amount of nutrients to the water column. The relative importance of this source of nutrients is further examined in Chapter 5 where the sediment parameters are switched off to estimate the contribution of the sediment fluxes towards the estuary nitrate and ammonium overall concentrations. In a benthic chamber study in Tauranga Harbour, Sandwell et al. (2009) found varying effluxes of nutrients that ranged from 0.003-0.03 $g/m^2/day$ for NO_3^-, 0.0078-0.078 $g/m^2/day$ for NH_4^+, and 0.0046 $g/m^2/day$ for PO_4^{3-}. The effluxes measured by Sandwell et al. (2009) were within the range of sediment fluxes set in these simulations.

This contribution of nutrient fluxes through sediment is an important process where nutrient regeneration in benthic sediments can supply a significant fraction of nutrient requirements for primary production to the overlying water (Callender and Hammond 1982). In a study in Pelorus Sound, Gibbs et al. (2002) demonstrated that benthic fluxes of dissolved nutrients varied substantially in different seasons. In summer, they found that the nutrient ranges from 0.0017-0.0023 $g/m^2/day$ for NO_3^-, 0.008-0.02 $g/m^2/day$ for NH_4^+ and 0.0046-0.0108 $g/m^2/day$ for PO_4^{3-}. While in winter, they found that the nutrient ranges from

0.0012-0.0021 g/m^2/day for NO_3^-, 0.0024-0.005 g/m^2/day for NH_4^+ and 0.0053-0.0035 g/m^2/day for PO_4^{3-}. The interannual variability in nutrient effluxes from sediment demonstrated by Gibbs et al. (2002) highlights the need for temporally varying sediment fluxes to reproduce concentration gradients and determine nutrient availability in different seasons. Sediment nutrient fluxes are closely coupled with the overall estuarine nutrient concentration, and in future models of shallow estuaries, the sediment fluxes should be set to temporally varying (e.g. seasonal varying) as the physical processes influencing the estuaries condition changes temporally and spatially as demonstrated in this chapter.

The freshwater discharges are reflected in nutrient distribution in both estuaries through both the freshwater influence on circulation and nutrient loadings. The simulated nitrate concentration showed pronounced seasonality with higher concentrations found during lower salinity periods, which suggest freshwater source. In addition to stream discharge, groundwater contribution is also an important source of nutrients in both estuaries. This can be seen in winter at the west bank region of Waikareao Estuary, where groundwater inflows are present, the nitrate concentration were higher compared to the east bank. As the nutrient from stream and groundwater moved through the estuary, biogeochemical nitrogen transformation occurs along with assimilation by phytoplankton. The high concentration of nutrients from freshwater sources would be attenuated within the estuaries before being exported out of the estuary during low tide (Seitzinger et al. 1984; Beck et al. 2007).

Simulated phosphate showed low concentrations and lack of seasonal patterns along both estuaries, which in part may be related to the highly reactive chemistry of this species and the adsorption-desorption process (Sundby et al. 1992; Spiteri et al. 2008). One explanation for this could be the flushing time for Waikareao and Te Puna are relatively short to permit desorption and sediment release to enhance water phosphate concentrations (Balls 1994). Previous studies have found phosphate released from remineralization processes (Jordan et al. 1991; Chambers et al. 1992) with release rates lower than ammonium (Chambers et al. 1992). However, the sediment release would vary along the estuary due to salinity gradients, oxygen and sediment resuspension (Page et al. 1995). This lead to variation in phosphate concentration along the estuary as observed in Te Puna.

From model simulations, the DO concentration was low in the upper estuary region in spring in Te Puna and summer in Waikareao. The low oxygen conditions also occur in parallel with rising temperature. This low DO environment with elevated temperature at the upper estuary may boost concentrations of ammonium in the water column through sediment flux (Cowan and Boynton 1996). The combination of high ammonium concentration, oxygen availability for nitrification (Berounsky and Nixon 1993), and higher residence times in upper estuary, can boost nitrification process. This can contribute to the high nitrate and further reducing DO concentration in upper estuary in spring at Te Puna.

4.5 Conclusions

This chapter outlined how the hydrodynamic-ecological model ELCOM-CAEDYM was initialized and applied to both Te Puna and Waikareao estuaries and where possible calibrated with field measurements. Calibrating the ELCOM model output against field data gave an overall reasonable fit. However, the main discrepancy occurred in the ebb tide currents and water temperature during late afternoon outgoing tide. The simulated model temperature including the effect of wind showed a drop in temperature during the ebb tide period with a lower temperature by 3 to 6 °C. The well-mixed nature of the estuary limits/prevents stratification, and the modelling and field data confirmed this assumption.

The model was able to capture the short durations in temporal variations in nitrate and ammonium concentrations. The governing influence in the distribution of chemical constituents of Waikareao and Te Puna estuaries is tidal flow with simulation results showing lateral variation in residence times, DO and nutrient concentrations from upper to lower estuary region. The constricted headland located in the middle of Te Puna further accentuates the lateral variations with higher simulated nutrients observed in the upper estuary as the water can reside in that region for >1 day. The constriction of the headland in Te Puna also influences the distribution of nutrients where lateral variations in residence time and nutrient were observed between upper and lower estuary. The modelling simulations predicted seasonal variations in nutrients in Te Puna and Waikareao estuaries with freshwater source being the main influence in winter, while sediment fluxes are the main contributor to nutrients in the estuaries in summer.

Chapter Five: Modelling scenarios

5.1 Introduction

Modifications to the boundary conditions and switching parameters on or off in the numerical model, ELCOM-CAEDYM, allows a range of hydrodynamic and biogeochemical processes to be studied in Te Puna and Waikareao estuaries. The objective of this chapter is to understand the interplay between hydrodynamic and biogeochemical processes and their influence on the spatial and temporal patterns of estuarine nutrient concentrations over short-term periods. Although Te Puna and Waikareao have no large rivers, the estuaries' ecological conditions can be affected by nutrient-enriched freshwater (i.e. streams and groundwater). However, water exchange with Tauranga Harbour is high and the two estuaries have residence times that are shorter than ~1.5 days. On the east and west bank of Te Puna Estuary, catchment activities are mainly agriculture. In Waikareao Estuary, the east bank site has road works and industrial areas, while on the west bank, it is dominated by urban households.

Scenarios were chosen to determine the role of wind in mixing, freshwater inflows and sediment fluxes in overall estuarine DIN concentrations. The analysis of field measurements in Chapter 2 showed that it was difficult to differentiate between these competing sources of DIN input into Te Puna and Waikareao estuaries. To determine the potential sources, scenarios were developed to test the hypothesis that nitrate concentration predominantly comes from freshwater inflows, and ammonium from sediment fluxes. This was examined in detail in separate scenarios by increasing and decreasing stream discharge, excluding groundwater inflows, and excluding sediment fluxes into the model. A toxic bloom of *Gymonodinium* cf. *breve* has been previously linked to toxic shellfish outbreaks in the Bay of Plenty region in early 1993. This toxic dinoflagellates bloom has been linked to the high concentrations of nutrient from upwelling events in the shelf (Chang et al. 1996; Longdill et al. 2008). A scenario was also developed to examine the effect of high nutrient concentration from open boundaries on the estuaries overall DIN concentrations.

5.2 Methods

As mentioned in Chapter 4, the model was simulated for five days over the sampling dates in (2007-2008) in summer, winter, start of spring and end of spring, unless stated otherwise in the text. Sampling was conducted during winter (24-26 June 2008), start of spring (4-6 September 2008), end of spring (13-15 November 2007) and late summer (14-16 March 2008) in both estuaries (Chapter 2). The simulations were run over five day periods to look at short-term changes in estuarine nutrient concentrations under different forcing conditions. Due to time constraints (the coupled model took 8 days to run), some scenarios were only run for one of the two estuaries. A brief description of these conditions is given in Table 5.1 below.

The effect of the dominant wind condition and natural temporal-varying wind condition was simulated to examine the effect of wind mixing on the DIN and oxygen concentrations in both Te Puna and Waikareao Estuaries. The influence of homogenous wind and varying wind conditions were compared with the case of no wind to elucidate the effect of wind on mixing within the estuaries. Dominant wind conditions for winter 2008 were simulated for both Te Puna (wind speed: 3.6 m/s; wind direction 220°, Case 1) and Waikareao (wind speed: 1.12 m/s; wind direction: 234°, Case 2) estuaries. A naturally varying wind scenario was simulated for Waikareao Estuary in winter and summer (Case 3, 4). The average wind condition in 2008 was mean wind speed of 2.3 m/s and wind direction of 188.2°.

In the hydrological scenarios, Te Puna Stream flow rates were increased by 10% and 30% for winter, decreased by 10% for summer and increased by 10% in start of spring to determine the influence of stream inputs in the estuary DIN concentrations. Simulations were run for winter 2008 with elevated Te Puna Stream (Case 5 and 6) discharges (by 10% and 30%) with other parameters the same as in the base case, and elevated stream with DIN discharge for Te Puna Stream (Case 7, 8). Elevated stream flow (10% and 30%) is within the average range of high flow in winter in gauged streams and rivers in Tauranga Harbour. A reduction in stream flow in summer by 10% was simulated for Te Puna Estuary (Case 9) and Waikareao Estuary (Case 10) but nutrients were set to present days

(base) levels. A 10% further reduction in stream flow rate is within the range of low flow in summer as the average flow rate in the gauged Kopurereroa Stream in summer was lower by 10-15 % compared to average flow rate. A scenario was also simulated for the start of spring with DIN concentrations elevated by 10% for both Te Puna (Case 11) and Kopurereroa (Case 12) streams but with stream flow set to present-day (base) levels.

The exchange of dissolved substances across the sediment-water interface is an important process affecting the chemical composition of shallow estuaries. The parameters (groundwater and sediment fluxes) were switched off for groundwater and sediment scenarios. Simulations were run to estimate the percentage of groundwater contributions towards the overall DIN concentrations in summer and winter in Te Puna Estuary (Case 13, 14) and Waikareao Estuary (Case 15, 16). As mentioned in Chapter 4, a constant flux rate of NH_4^+ (0.02 g/m^2/day (Robson and Hamilton 2004)), NO_3^- (-0.03 g/m^2/day (Hipsey et al. 2006; Missaghi and Hondzo 2010)) and PO_4^{3-} (0.004 g/m^2/day (Robson and Hamilton 2004)), between the sediment and overlying water was prescribed. Scenarios were simulated for summer and winter period to look at the influence of sediment input on the overall estuarine DIN concentrations for Waikareao Estuary (Case 17, 18). The sediment flux was set to a constant value as the model has a set value for each sediment flux.

A scenario was simulated to examine a pulse event consisting of 40mm rainfall entering the estuary as runoff. Most of the rainfall event occurring in Te Puna in 2008 was less than 20 mm. A 40 mm rainfall event was chosen as it will generate sufficiently large discharge to represent a storm event for summer and winter as rainfall event in winter of 2008 can be up to 15 mm. Simulations were carried out in winter and summer for Te Puna Estuary following a pulse event (Case 19, 20). A storm hydrograph was calculated for discharge following 40 mm rainfall event, and was released into the estuary through Te Puna Stream. All other parameters were the same as base case.

Summer of 1993 has been indicated as a strong upwelling event in the Western Bay of Plenty where nitrate rich water has been measured (Longdill et al. 2008). Upwelling events have been previously attributed to toxic dinoflagellates bloom

in the Bay of Plenty (Chang et al. 1996; Longdill et al. 2008). A scenario was simulated to highlight the subsequent impacts of upwelling-like conditions in Te Puna and Waikareao estuaries nutrient concentrations in summer (Case 21, 22). However summer 2008 was not an upwelling event. The open boundary nitrate was increased by 60% to be in the similar range as measured concentration in the Western Bay of Plenty during an upwelling event (Chang et al. 1996; Longdill et al. 2008). It was assumed there was no attenuation in the nitrate concentration as it moved into Tauranga Harbour. From Tauranga Harbour model simulation, it was found that a water parcel takes an hour to reach Te Puna Estuary from the harbor mouth; hence the nitrate attenuation should be minimal.

Note that all salinities reported here are given in the dimensionless practical salinity units (approximately equivalent to parts per thousand). DIN referred in this chapter is a combination of ammonium and nitrate.

Table 5.1 Description of different scenarios applied to Te Puna and Waikareao estuaries.

Scenario		Description
0	Base case	Current field conditions with base nutrient rates.
Wind scenarios		
1	Homogenous wind	Homogenous dominant wind condition for Te Puna.
2	Homogenous wind	Homogenous dominant wind condition for Waikareao.
3	Varying wind	Varying wind condition in winter for Waikareao.
4	Varying wind	Varying wind condition in summer for Waikareao.
Freshwater scenarios		
5	High Te Puna	10% increase in stream discharge/Winter.
6	High Te Puna	30% increase in stream discharge/Winter
7	High Te Puna & nutrient	10% increase in stream discharge and nutrient/Winter.
8	High Te Puna & nutrient	30% increase in stream discharge and nutrient/Winter.
9	Low Te Puna	10% decrease in stream discharge/Summer.
10	Low Kopurereroa	10% decrease in stream discharge/Summer.
11	High nutrient- Te Puna	10% increase in nutrient from stream/Start of spring.
12	High nutrient-Kopurereroa	10% increase in nutrient from stream/Start of spring.
No groundwater		
13	No groundwater	Summer in Te Puna
14	No groundwater	Winter in Te Puna
15	No groundwater	Summer in Waikareao.
16	No groundwater	Winter in Waikareao.
No sediment		
17	No sediment fluxes	Summer in Waikareao.
18	No sediment fluxes	Winter in Waikareao.
Pulse event		
19	Pulse event	Summer in Te Puna
20	Pulse event	Winter in Te Puna
Upwelling		
21	Upwelling event in summer	Summer in Te Puna.
22	Upwelling event in summer	Summer in Waikareao.

5.3 Results and discussion

Short-term episodic events (e.g. rain) and seasonal hydrological variations can trigger biogeochemical and trophic responses and change ecosystem functional properties. Nutrient concentrations and phytoplankton communities are particularly responsive to these perturbations (Paerl et al. 2006). In tidally dominated estuaries such as Waikareao and Te Puna estuaries, the water exchange with the harbour is high and the residence times shorter than 1.5 days (Chapter 4). This water exchange will influence nutrient dynamics although the influence of nutrient imports from the harbour and their interaction with freshwater sources, sediments, salinity and temperature is not well understood as these interactions depend on the spatial and temporal variability of physical parameters such as depth, cross section and flow velocity.

Rather than separating the results and discussion for all scenarios, in this section, results and discussion are presented separately for each scenario.

5.3.1 Wind

Model simulations using different wind forcing suggested that wind has a significant influence on the estuaries' circulation, which influences nutrient distribution and mixing in the water column. However, the extent of wind – influences depend on the wind sources and direction of the wind. As seen in Te Puna Estuary, the application of a dominant wind field resulted in lower nutrient concentration with a lateral decrease from the west to east bank in Te Puna (Figure 5.1). In the upper west bank of Waikareao, the nitrate concentration were relatively higher than the base case by 0.2 mg/L. DO concentrations in both estuaries increased by 2 mg/L with the application of dominant wind field. The application of hourly varying wind field resulted in an increase in nitrate concentration in Waikareao Estuary in summer and winter (Figure 5.2). While, the ammonium concentrations were relatively lower than the base case in winter for Waikareao. Varying wind speed and direction can result in different patterns of wind cooling and convective mixing when compared to a uniform case. The application of wind field resulted in intensification of mixing processes, which progressively improves water column oxygenation and ultimately results in oxygen concentrations close to saturation especially in winter. The strong

influence of wind on the DO concentration of these estuaries is due in part to their shallow depths, which accentuates the influence of winds stress on mixing the water column. The high DO concentration provides oxygen for nitrification processes to occur as observed with the higher nitrate concentrations and lower ammonium concentrations in Waikareao. This is especially important in summer where freshwater sources of nutrients are low, and sediment processes dominate. Rueda et al. (2005), using spatially homogenous and variable wind fields, investigated changes in nutrient residence times in Clear Lake, California, found that the magnitude of residence time change in sub-areas of the lake due to interaction of the topography with hydrodynamic and chemical behavior. However, the model simulations with two differing wind fields suggested that the variation in wind speed and direction over the model domain can have ramifications for circulation and consequently simulated nutrient concentrations.

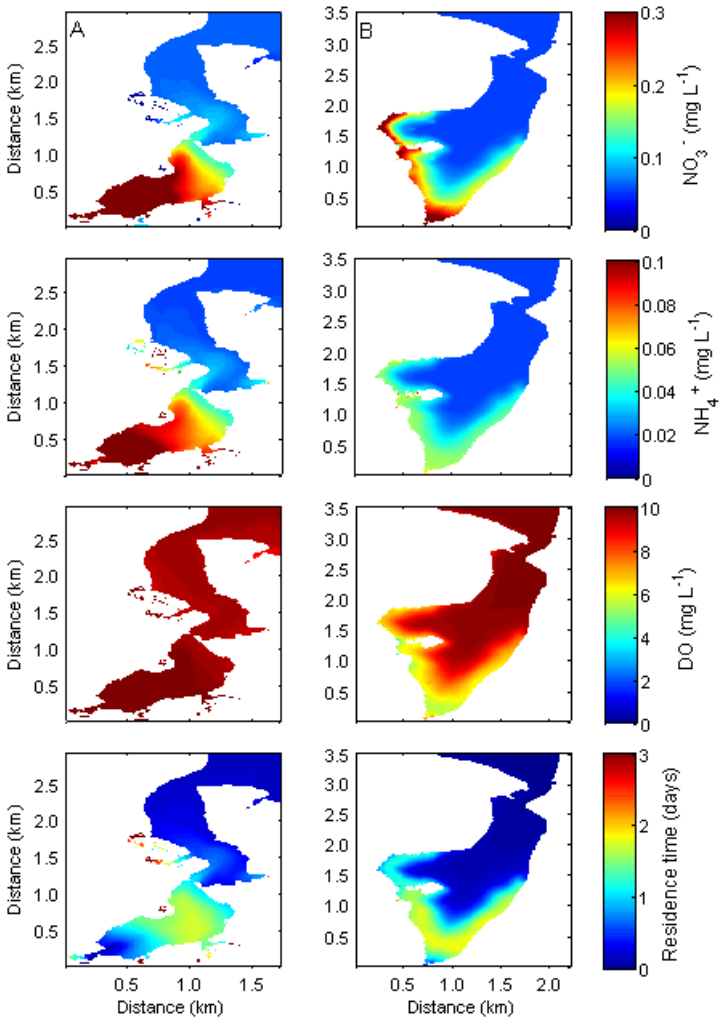

Figure 5.1 Depth-averaged nitrate (NO_3^-), ammonium (NH_4^+), and DO concentrations, and residence times in winter for Te Puna (A), and Waikareao (B) modeled using the dominant wind condition (Case 1, 2).

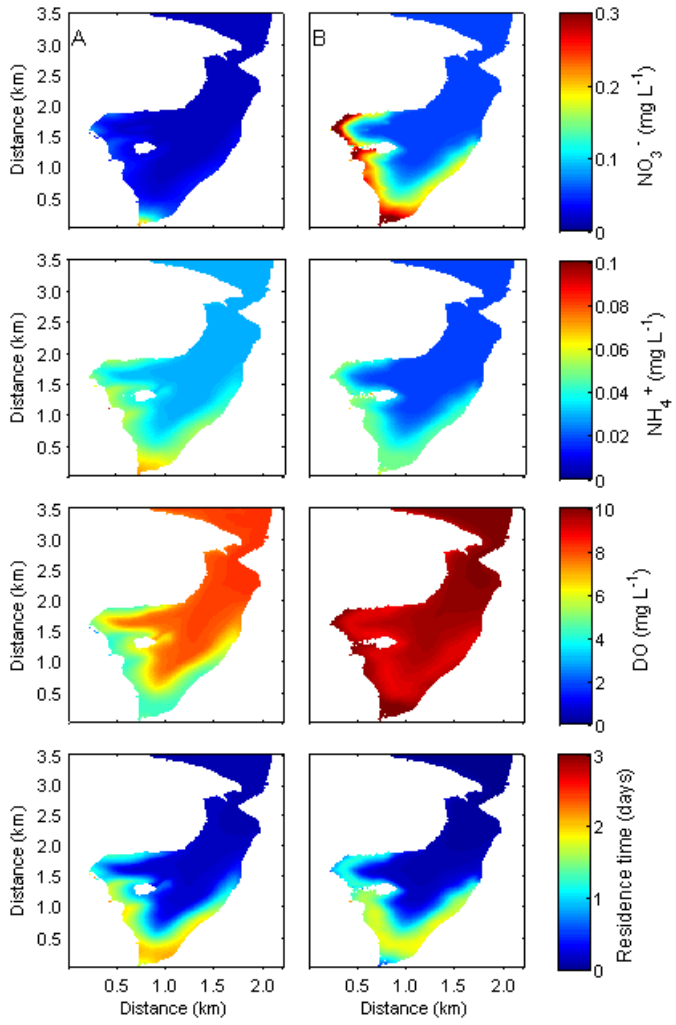

Figure 5.2 Depth-averaged nitrate (NO_3^-), ammonium (NH_4^+), and DO concentrations, and residence times for Waikareao modeled using a varying wind condition for summer (A) (Case 3), and winter (B) (Case 4).

5.3.2 Stream discharge

With an elevated Te Puna Stream discharge in winter, DIN concentrations decreased as the water moved from the upper to lower estuary (Figure 5.3, 5.4). With a 30% increase in Te Puna Stream discharge and DIN input, ammonium concentrations in the upper estuary increased by 28% and the average concentration decreased as water moved into the lower estuary with only a 15% increase relative to the base case. With a 30% increase in stream discharge and DIN (Case 8), the nitrate concentration in the upper estuary increased by 31% and lower estuary by 19%. The DO concentration remained unchanged in the lower estuary with increased stream discharge but in the upper estuary the DO was higher by 0.3 mg/L with the increase in stream and DIN discharge (Case 7, 8).

Despite an increase in stream loading in winter, the downstream DIN concentration was still low which is likely due to phytoplankton uptake and/or denitrification. Phytoplankton uptake in winter, by the fast-growing diatoms can utilize nutrients to reach their maximum growth rate. However, with an increase in stream flow rates and DIN loadings, the overall Te Puna estuarine DIN concentrations did not evoke major changes. This can be related to the low residence times in Te Puna Estuary (Chapter 4), which ranged from 0.5 days in the lower estuary to 1.5 days in the upper estuary. The rapidly flushed system lessens and prevents the accumulation of nutrients due to the high exchange of water between the estuaries and the open boundary.

It is not always the case that increased nutrient levels in freshwater inputs are so quickly flushed from the estuarine system. Although both Te Puna and Waikareao are sub-estuaries within a larger system, Tauranga Harbour, just like some other sub-system within larger estuaries such as the Baltic, the two estuaries are entirely different as in the other sub-system (e.g. the Baltic), the water is poorly flushed (Savchuk and Wulff 2009). For example, through nutrient tracking technique, Neumann (2007) found that nitrogen originating from River Oder remained in the Baltic Sea for a residence times of 30 years due to restricted exchange with the North Sea.

In summer, with reduced stream discharge (Case 9, 10), the overall estuaries' nutrient and DO concentrations showed a lateral decline from the upper to lower estuary (Figure 5.5). With reduced Te Puna Stream discharge, the ammonium average concentrations increased by 1% while nitrate and DO concentrations decreased by 3% and 1.7% respectively. The same pattern was observed in Waikareao, where the ammonium concentrations increased by 0.8% while the nitrate and DO concentrations decreased by 5% and 0.5% respectively. The higher concentrations of NH_4^+ observed in summer under reduced stream flow, indicate the sensitivity of regeneration to temperature. The reduction in simulated nitrate concentration and increased ammonium concentration in summer under reduced stream discharge suggested that freshwater discharges are the main source of nitrate, while estuarine processes such as sediment fluxes contributed towards ammonium. This source of nutrient is important especially in summer where freshwater discharges are low. With 10% increase in stream nutrient input in

spring (Case 11 and 12), the average ammonium concentrations increased slightly by 3% while the nitrate and DO concentration decreased by 0.2% and 2% respectively in Waikareao (Figure 5.6). However, in Te Puna, the average nitrate and DO concentration decreased by 8% and 7% respectively while ammonium increased by 2% in the upper estuary. The low DO in the upper estuary can enhance nutrient release, i.e. ammonium, from the sediment.

Spatial variability observed in Te Puna and Waikareao with different residence times along and across both estuaries in turn can influence the distribution of nutrients. The headland at 1.5 km away from Te Puna Estuary mouth caused increased residence times and consequently a rise in nutrient concentration and lower DO. However in the lower parts of both Te Puna and Waikareao estuaries, rapid tidal exchanges lead to renewal of DO concentrations which can be used for nutrient recycling processes within the estuaries. This spatial variability in residence times was also observed in Mildred Island at Sacramento-San Joaquin Delta where strong north-south gradients in residence times can influence the transport and accumulation of plankton and DO in the southeastern region due to slow tidal mixing but not in the northeastern region due to rapid tidal exchanges with outer channel systems (Lucas et al. 2002; Monsen et al. 2002).

The overall contributions of Te Puna Stream and Kopurereroa Stream towards estuarine DIN concentration are relatively small compared to some major rivers such as the Scheldt, Rhine and Seine which have been linked to nutrient enrichment and phytoplankton blooms in the Belgian Coastal Zone (Lacroix et al. 2007). However model scenarios revealed the sensitivity of such shallow systems with high water exchange with marine waters, to inputs from Te Puna and Kopurereroa streams in the overall estuarine nutrient distribution.

Simulated diatoms appear to be the dominant phytoplankton group, with marine diatoms in lower estuary and freshwater diatoms in upper estuary, in winter with increased stream discharge (Figure 5.7). This is likely due to reduced water residence times and salinity along with increased nutrient concentrations environment that favored fast-growing phytoplankton such as the diatom (Malone et al. 1988; Harding 1994; Pinckney et al 1999). By contrast in summer with reduced stream discharge, simulated cyanobacteria are the dominant group when

water temperature are warmer and nutrients are lower (Andersson et al. 1994; Piehler et al. 2002) with higher concentrations found in upper Te Puna till the constriction in middle estuary (Figure 5.8).

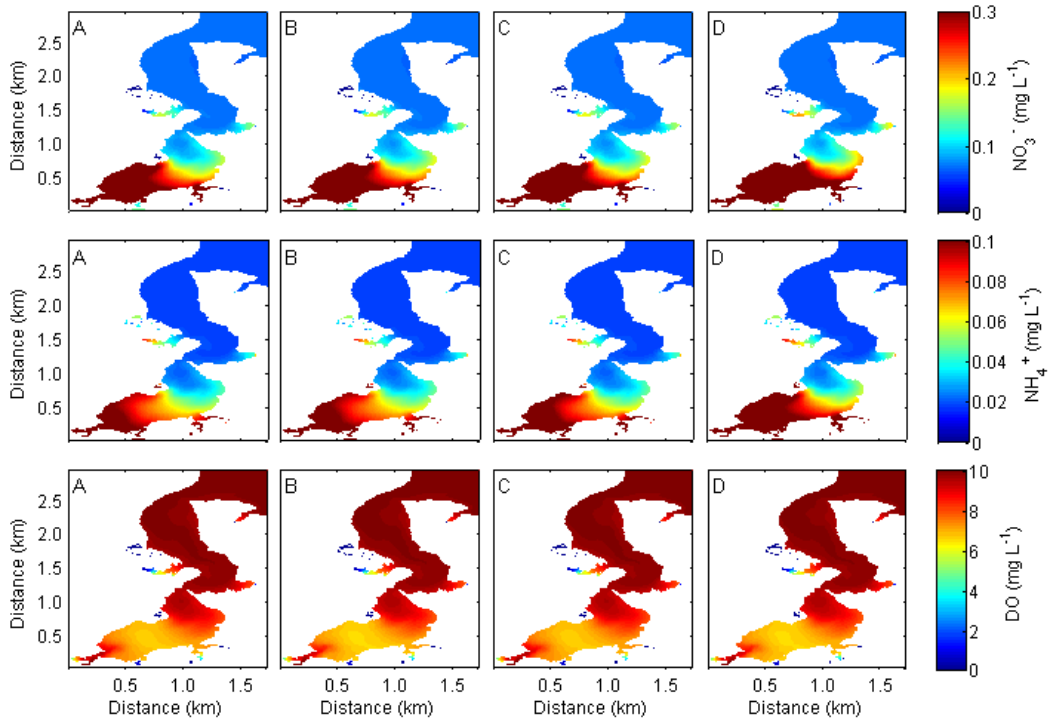

Figure 5.3 Depth-averaged nitrate (NO_3^-), ammonium (NH_4^+) and DO concentrations across Te Puna Estuary for 10% increase in Te Puna Stream flow (A) (Case 5), 30% increase in Te Puna Stream flow (B) (Case 6), 10% increase Te Puna Stream flow and nutrient (C) (Case 7), and 30% increase in Te Puna Stream flow and nutrient (D) (Case 8), in winter.

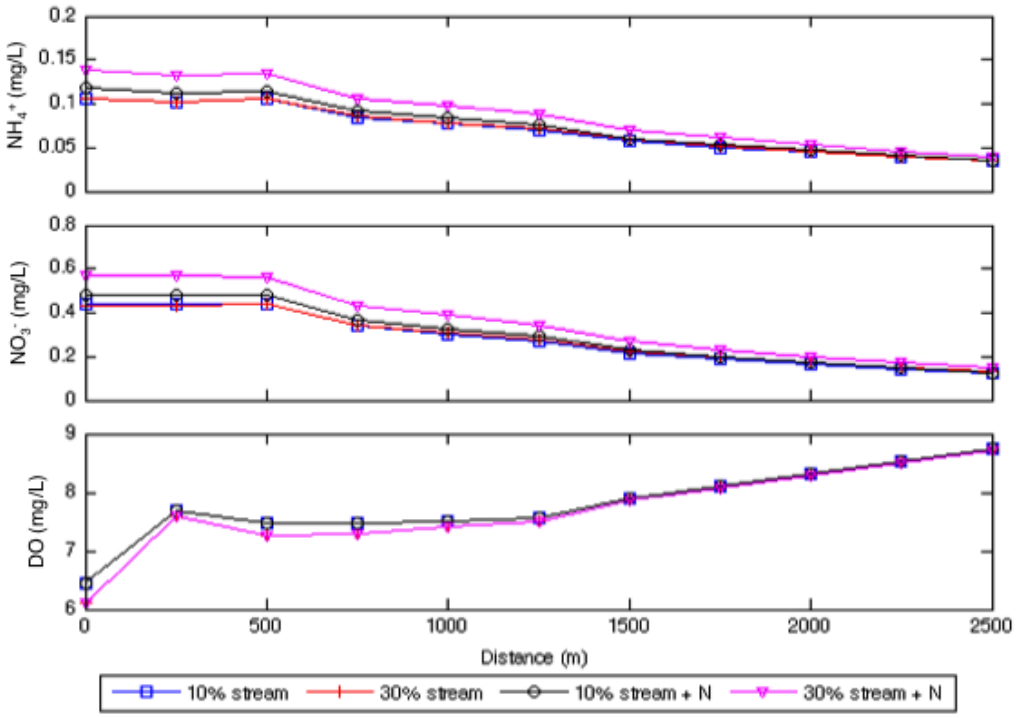

Figure 5.4 Along-channel average concentrations of ammonium (NH_4^+), nitrate (NO_3^-), and DO for Scenarios 7, 8, 9 and 10 for Te Puna Estuary in winter. The channel runs from the upper estuary (0 m) to estuary mouth (2500 m). Results are extracted at 250 m intervals along the main channel. 10% stream: 10% increase in stream discharge; 30%: 30% increase in stream discharge; 10% stream +N: 10% increase in stream discharge and DIN; 30% stream +N: 30% increase in stream discharge and DIN.

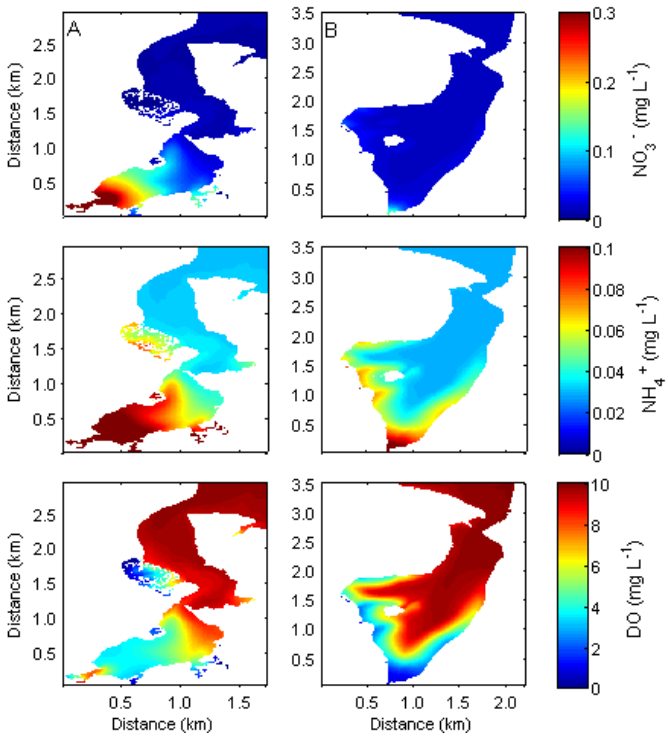

Figure 5.5 Depth-averaged nitrate (NO_3^-), ammonium (NH_4^+) and DO concentrations across Te Puna Estuary (A) and Waikareao Estuary (B) in summer with reduced stream discharge of 10% for Te Puna Stream (Case 9) and Kopurereroa Stream (Case 10).

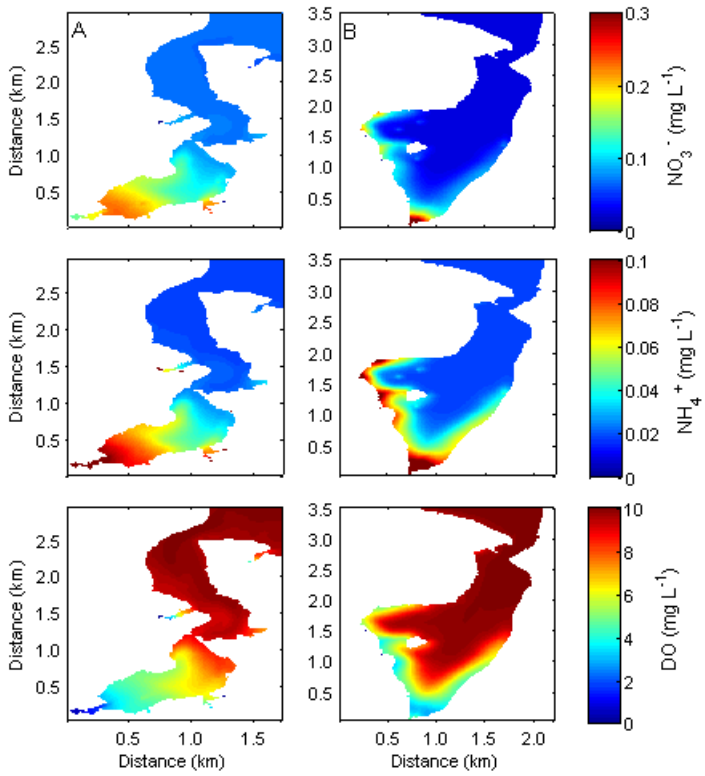

Figure 5.6 Depth-averaged nitrate (NO_3^-), ammonium (NH_4^+) and DO concentrations across Te Puna Estuary (A) and Waikareao Estuary (B) in start of spring with increased Te Puna Stream (Case 11) and Kopurereroa Stream (Case 12) nutrient by 10%.

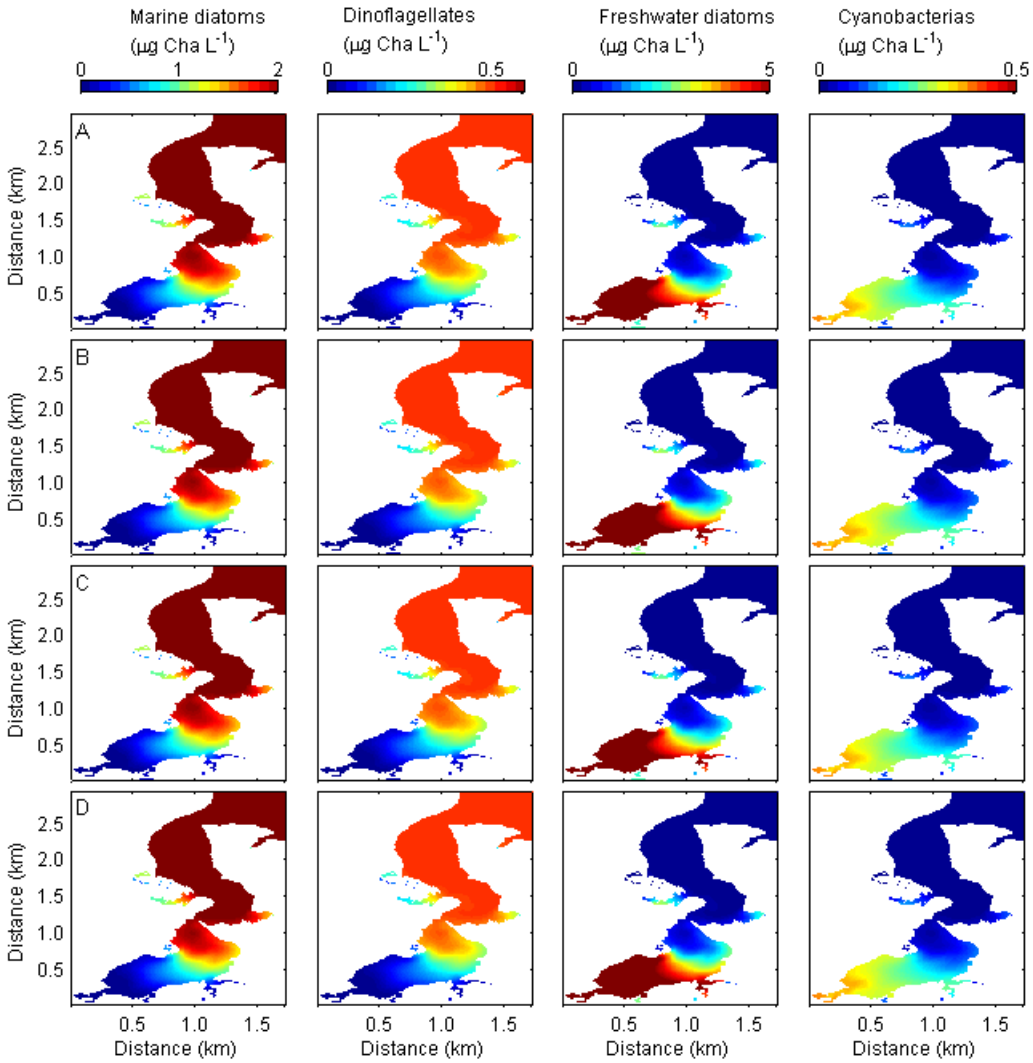

Figure 5.7 Depth-averaged of marine and freshwater phytoplankton concentrations across Te Puna Estuary for 10% increase in Te Puna Stream flow (A) (Case 5), 30% increase in Te Puna Stream flow (B) (Case 6), 10% increase Te Puna Stream flow and DIN (C) (Case 7), and 30% increase in Te Puna Stream flow and DIN (D) (Case 8), in winter. Note the different scales in phytoplankton concentrations.

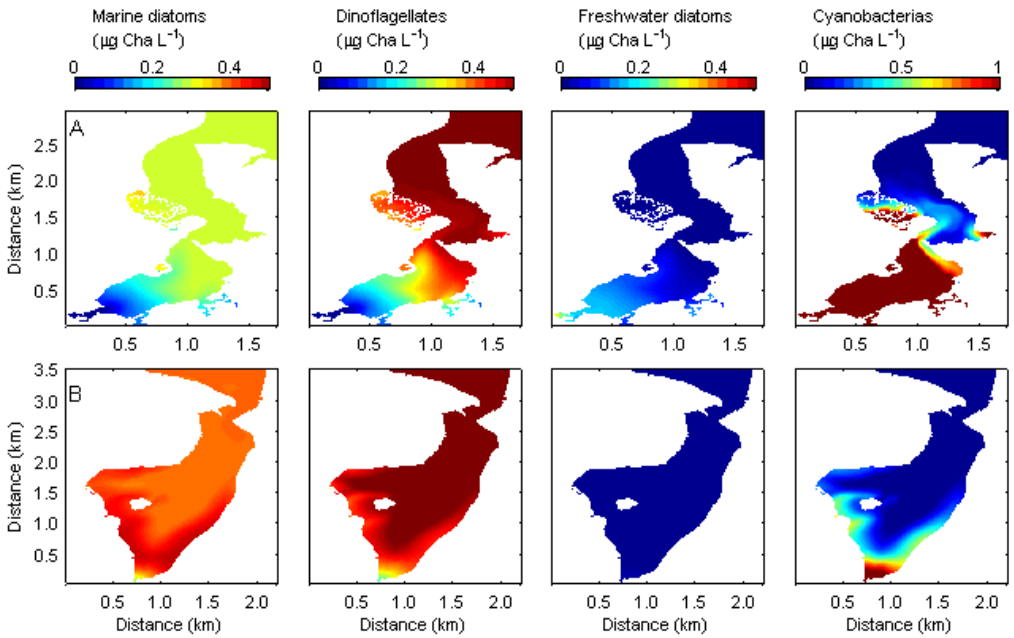

Figure 5.8 Depth-averaged phytoplankton concentrations for Te Puna Estuary (A) and Waikareao Estuary (B) in summer with reduced stream discharge for Te Puna Stream and Kopurereroa Stream (10%).

5.3.3 Groundwater discharge and sediment fluxes

For Te Puna Estuary, DIN and DO concentrations were extracted from four sites: two from the upper estuary and two from the lower estuary (Figure 5.9). For Waikareao Estuary, DIN and DO concentration from the east and west bank tidal flat regions were extracted (Figure 5.10) to look at the overall changes in concentrations in comparison with the base case with no groundwater inflows and sediment fluxes. By excluding groundwater discharges in Te Puna and Waikareao, the nitrate and ammonium concentrations remained unchanged in the lower estuary in summer (Figure 5.11, 12). In winter, with no groundwater inflow, nitrate concentration was lower compared to base case at upper to middle region of both estuaries. In Waikareao, the nitrate concentrations were lower by 0.3 mg/L in the upper estuary but the ammonium concentrations were higher by 0.05 mg/L in the upper estuary in winter over the base case with no groundwater input. Whereas with no sediment fluxes at Waikareao, the ammonium concentration decreased, along the estuary continuum in both summer and winter (Figure 5.13) while nitrate increased.

Groundwater contributes significantly towards the average nitrate concentrations in winter and summer. In terms of percentage with no groundwater inflows, Te

Puna, the nitrate concentrations were lower by 2-6% in summer and 10-37% in winter (Figure 5.14 and Table A6.1 in Appendix 6). The simulated DO in summer remained unchanged, while in winter the DO concentration was lower by 0.1% and 1.6% in upper Te Puna, with a minimal decrease in the lower estuary (0.03-0.15% decrease). In Waikareao, with no groundwater inflows, the nitrate concentrations were lower by 16-21% in summer and 14-24% in winter (Figure 5.15 and Table A6.2 in Appendix 6). In winter at Waikareao with no groundwater inflows, the DO concentration was lower by 3% on site West1 but showed an increase by 2-5% in the other three sites. In comparison with no sediment fluxes in Waikareao, the ammonium concentrations were lower by 19-40% in summer and 16-39% in winter (Figure 5.15; Table A6.3 in Appendix 6). With no sediment exchange, the nitrate concentrations were higher by 34-204% in summer and 9-26% in winter at Waikareao. The DO concentrations remained saturated in both winter and summer with no oxygen utilization at the sediment-water interface (Figure 5.15). On average in Waikareao, sites on the west bank (West1 and West2) contributed to higher sediment fluxes than the east bank (East1 and East2) which may be due to higher tidal flat regions on the west bank.

From the model scenarios (Case 13-16), groundwater contribution was higher for nitrate, while sediment fluxes contribution was higher for ammonium (Case 17, 18). The nitrate concentration showed pronounced seasonality with higher groundwater contribution in winter. In winter with no groundwater inflows, simulated nitrate fraction decreased, while ammonium fraction was higher. The higher ammonium fraction in winter was indicative of the contribution from sediment fluxes, remineralization and suppression of nitrification by low temperature (Berounsky and Nixon 1990). The sediment scenarios showed that sediment fluxes were higher in summer in Waikareao. The nitrate concentrations were relatively higher with no sediment fluxes in Waikareao. This suggests that recycling processes within the estuaries can attenuate the nitrate concentrations from freshwater sources, i.e. groundwater and streams, as it moved downstream. Generally in Waikareao, the groundwater contribution was higher on the west bank tidal flat region (West1 and West2). This could be due to larger tidal flat regions, which enable higher pore-water seepage activities. In Te Puna, groundwater contribution was higher on the upper east and west tidal flat bank.

In shallow estuaries such as Waikareao, sediment forms an important source for nutrients and the exchange of dissolved nutrients across the sediment-water interface. The relative importance of this source of nutrients from the sediment compared to external loadings (e.g. anthropogenic sources) has been found to vary substantially and could account for a large percentage of nitrogen demand in the water column as shown in previous studies in Chesapeake Bay (Boynton and Kemp 1985), and three North Carolina estuaries (Fisher et al. 1982). From model simulations, contribution of ammonium from sediment fluxes was higher than nitrate in Waikareao.

It must be remembered from Chapter 4 that the groundwater inflows into both estuaries have been estimated using very little in the way of measurements. Due to estimation of groundwater seepage, the groundwater inflows may have been underestimated. As mentioned above, the sediment fluxes of nutrients and DO were set to a standard value for all seasons, however the sediment fluxes may vary in different seasons. By setting the sediment fluxes to a standard value, the spatial differentiation of fluxes across the estuary also has not been taken into account. The sediment fluxes can differ considerably between the lower and upper estuary. In the upper estuary, organic matter contribution from mangroves for nutrient recycling can increase the sediment nutrient fluxes.

The relatively shallow environment of Te Puna and Waikareao results in mixing driven predominantly by tidal currents. Such systems differ from deeper estuaries such as Pelorus Sound and Beatrix Bay in the South Island, which is strongly stratified. This stratification often decoupled the exchange of nutrient between the upper and lower water column, hence the nutrient to the upper water column is most likely from external sources while the lower water column nutrient is supplied from the sediments (Sutton and Hadfield 1997; Gibbs et al. 2002). Whereas in Te Puna and Waikareao, which are relatively shallow, sediments and groundwater seepage play a role in supplying nutrient to the water column where the nutrients can be transported into the photic zone to fuel new primary production.

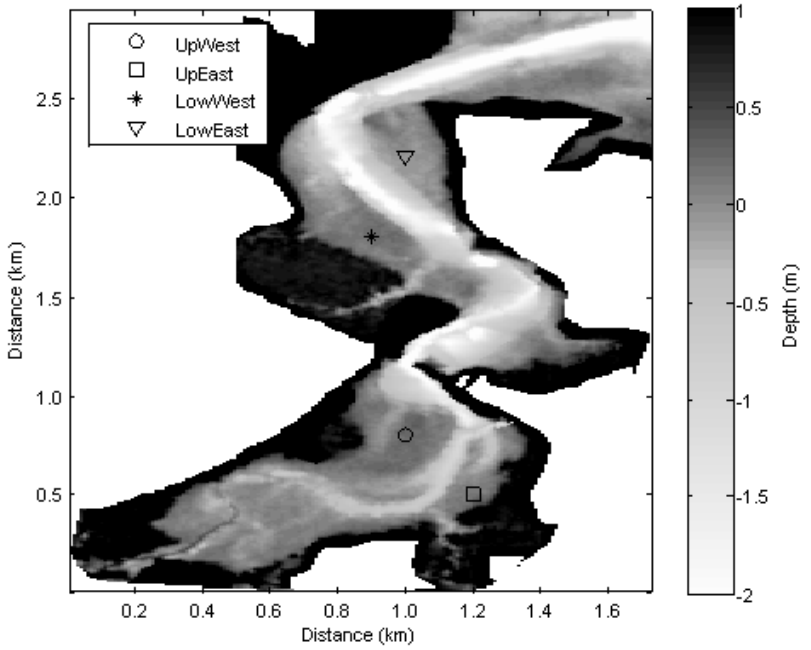

Figure 5.9 Sites of extraction of DIN (nitrate and ammonium) and DO concentrations in Te Puna Estuary for comparison of groundwater fluxes with base case. UpWest: Upper estuary tidal flat on the west side; UpEast: Upper estuary tidal flat on the east side; LowWest: Lower estuary tidal flat on the west side; LowEast: Upper estuary tidal flat on the east side.

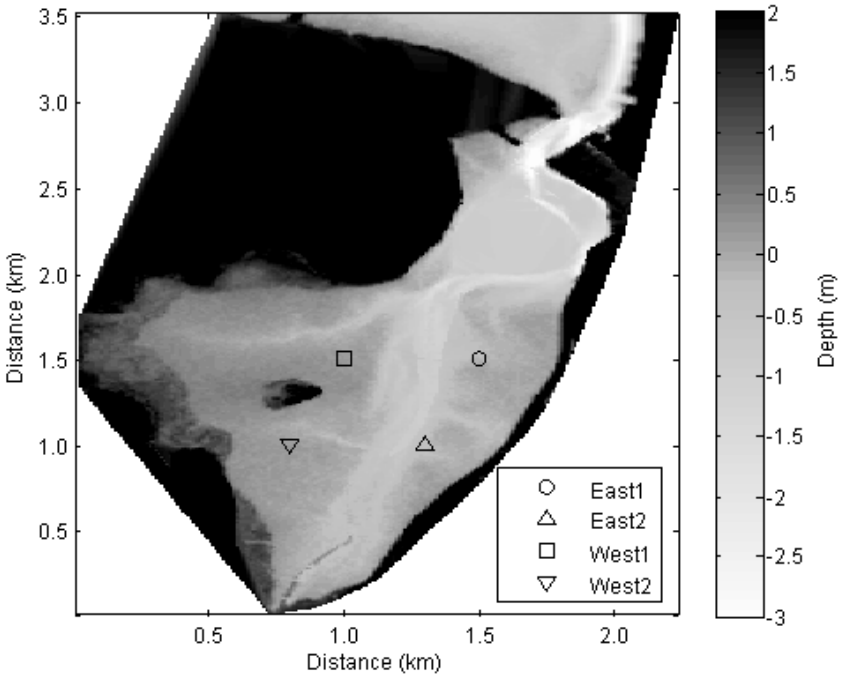

Figure 5.10 Sites of extraction of DIN (nitrate and ammonium) and DO concentrations in Waikareao Estuary for comparison of sediment and groundwater fluxes. East1: First site on the eastern tidal flat; East2: Second site on the eastern tidal flat; West1: First site on the western tidal flat; West2: Second site on the western tidal flat.

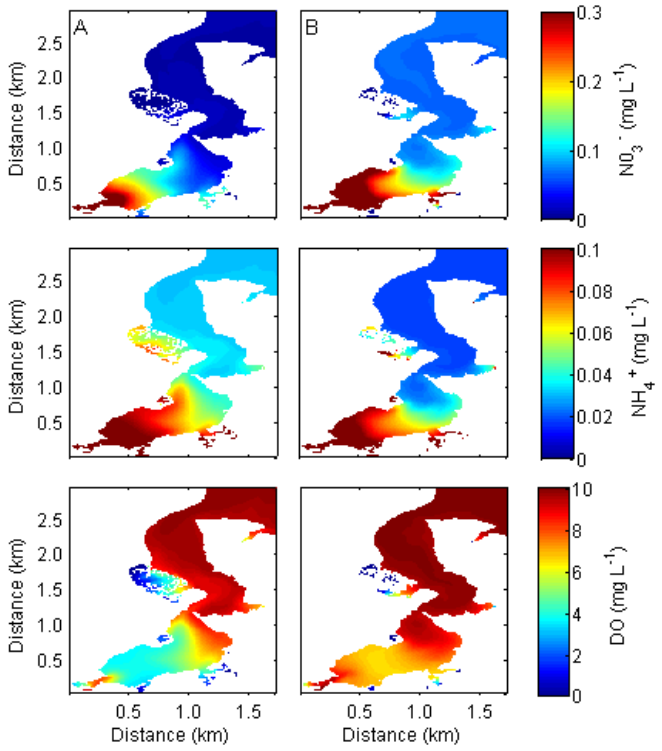

Figure 5.11 Depth-averaged nitrate (NO_3^-), ammonium (NH_4^+) and DO concentrations in Te Puna Estuary for (A) summer/no groundwater (Case 13), (B) winter/no groundwater (Case 14).

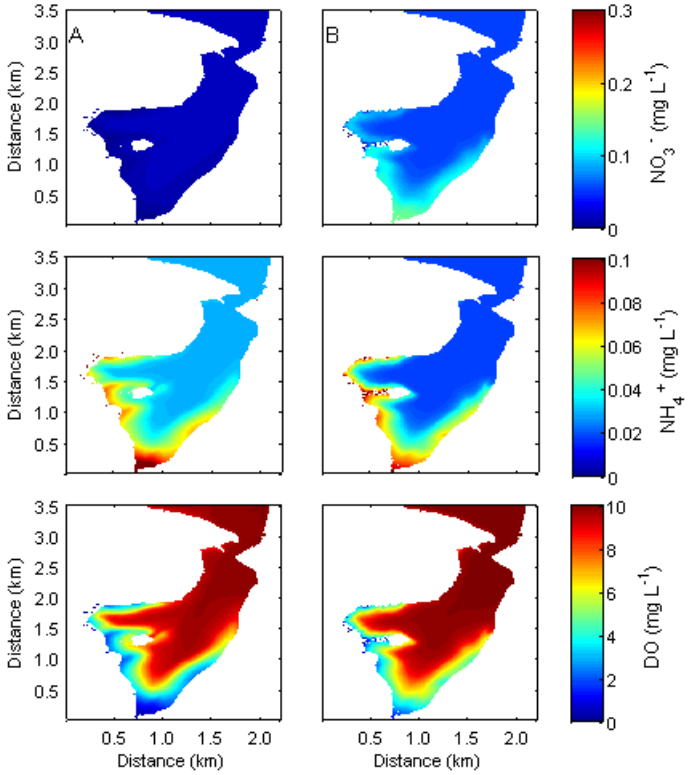

Figure 5.12 Depth-averaged nitrate (NO_3^-), ammonium (NH_4^+) and DO concentrations in Waikareao Estuary for (A) summer/no groundwater (Case 15), (B) winter/no groundwater (Case 16).

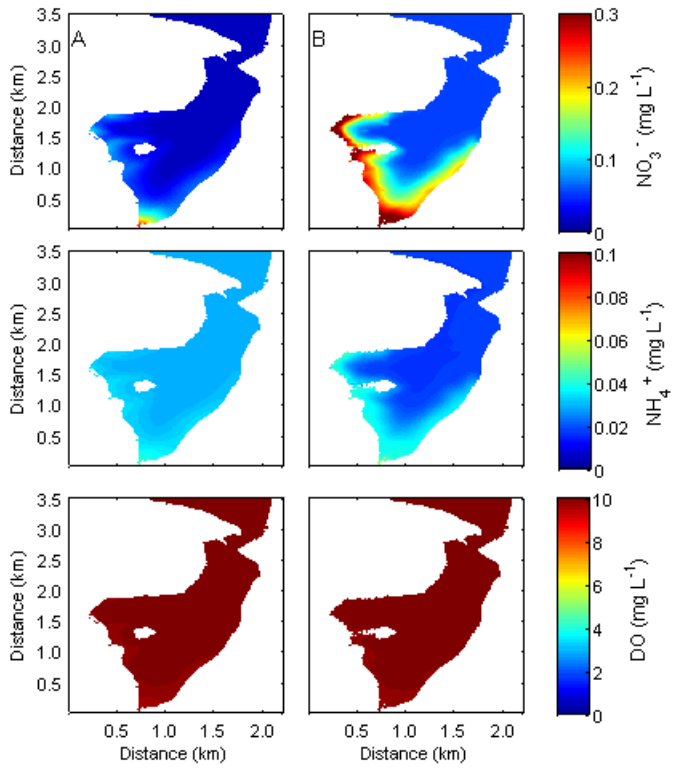

Figure 5.13 Depth-averaged nitrate (NO_3^-), ammonium (NH_4^+), and DO concentrations in Waikareao Estuary for (A) summer/no sediment (Case 17), (B) winter/no sediment (Case 18).

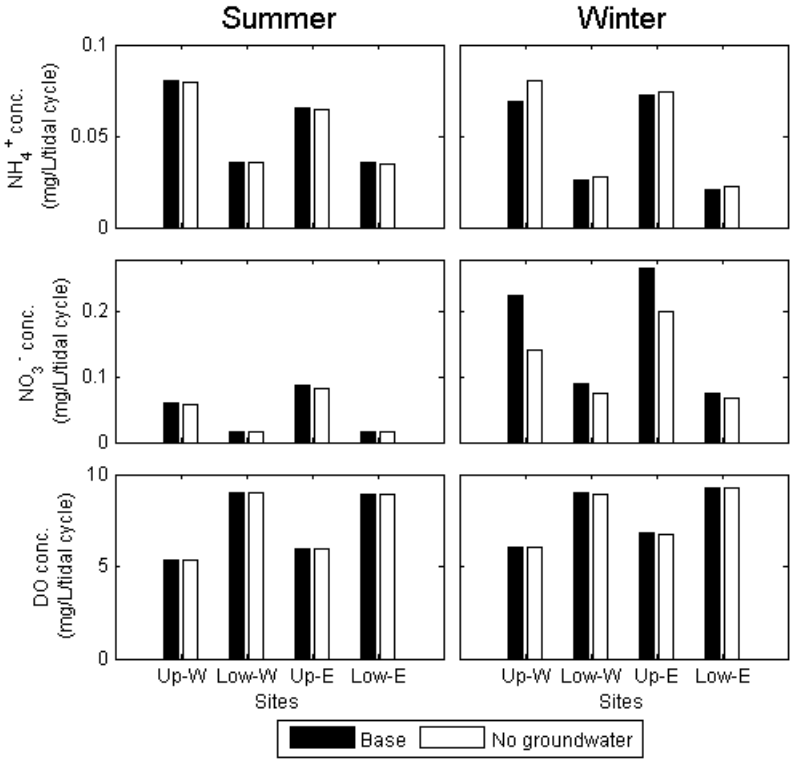

Figure 5.14 Ammonium (NH_4^+), nitrate (NO_3^-) and DO concentrations in summer and winter in Te Puna in comparison of base case with no groundwater input. Up-W: upper west tidal bank; Low-W: lower west tidal bank; Up-E: upper east tidal bank; Low-E: lower west tidal bank.

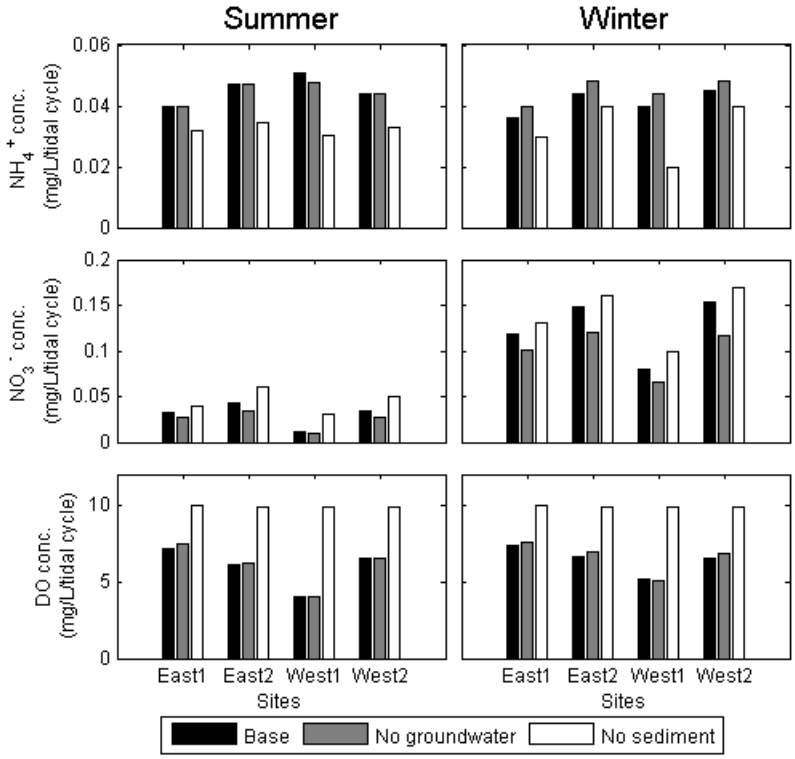

Figure 5.15 Ammonium (NH_4^+), nitrate (NO_3^-) and DO concentrations in summer and winter in Waikareao in comparison of base case with no groundwater input and no sediment fluxes. East1, East2, West1, West2 are tidal flat sites on the east and west bank.

5.3.4 Pulse event

Following a pulse event, higher concentrations of nitrate are found in the upper estuary where water velocities are greatly reduced (between 0-1.0 km from upper estuary). This is evident in the summer pulse scenario event where nitrate concentration increased by 27% in the upper estuary but ammonium concentration decreased by 27% in comparison to the base case (Figure 5.16). The high nitrate concentration observed in the upper estuary in summer can also be from nitrogen transformation such as nitrification, occurring within the estuary. As can be seen from the model simulation, following a high discharge, the ammonium concentration in middle to lower estuary increased. This resulting increase in ammonium concentration can enhance the nitrification processes, the effect which can be seen with the increase in nitrate with low DO concentration in middle estuary. However, in the lower estuary, a great proportion of the pulse-event nitrate loads are lost through remineralization and uptake from the water column, and through tidal exchange. In winter, the pulse event leads to dilution of DIN concentrations between 0-1.5 km from upper estuary, with 41% and 46% decreased in ammonium and nitrate concentration. As the water moved

downstream, the DIN concentration decreased likely due to phytoplankton uptake and sedimentation. In winter, the shorter residence times coupled with low temperatures usually found in times of high flows would limit the degree to which internal estuarine processes could retain nutrients. In comparison with the base case, the DO concentration in the upper estuary increased in summer, while in winter, the concentration decreased.

Results of the pulse event following a sudden high freshwater discharge indicate that Te Puna Estuary is sensitive to large pulse events especially in summer during low nutrient condition in the estuary. However from model simulations it is not known how long the effects of sudden pulse events last (i.e. how long it is before the nutrient concentration return to normal). Caffrey et al. (2007) found that pulses of nutrient from freshwater runoff can last from several hours with low concentrations returning on the following tidal cycles, or they can persist for weeks depending on whether the pulse event occurs early in the rainy season or later. Under storm runoff event, nutrient concentrations can increase suddenly reaching a maximum within a short period of time in summer. The freshwater pulse event leads to brief periods of lower salinity, however the duration and magnitude of pulse events in Te Puna is affected by the rapid flushing of the system. In catchments dominated by agricultural activity such as Te Puna, with 83% agricultural activity, sudden pulse events can lead to increase in nutrient and sediment loads to the estuary. Modifications of catchment for agricultural and urban activities can change the magnitude and timing of discharge of nutrient and sediment downstream.

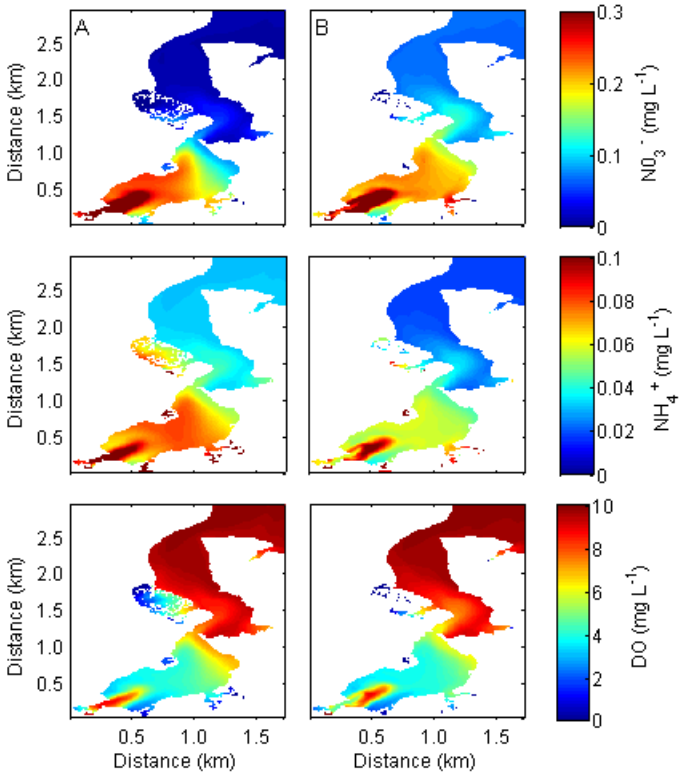

Figure 5.16 Depth-averaged nitrate (NO_3^-), ammonium (NH_4^+) and DO concentrations in Te Puna Estuary for (A) summer/pulse event (Case 19), (B) winter/pulse event (Case 20).

5.3.5 Upwelling event

From the model simulations, the nitrate concentrations across Te Puna and Waikareao were still low, <0.1 mg/L, despite an increase in open boundary concentrations (Figure 5.17). The ammonium concentration showed lateral gradient from upper to lower regions of both estuaries. The simulated DO concentration was high from upper to lower regions of both estuaries, with concentrations of >8 mg/L. This high DO concentration across the estuaries is likely due to the lower sediment oxygen utilization for nitrification and from algal productivity as higher nutrient concentrations from the open boundary provided more nutrient for primary production to occur. The lower residence times in both estuaries lead to little to no build-up of nutrient even with higher nutrient concentrations from the open ocean. It has to be noted that as Te Puna Estuary is situated further inwards of Tauranga Harbour, the effects of upwelling events might be different from Waikareao Estuary. Future work should simulate the upwelling events for more seasons as the physical and biogeochemical processes will differ in different seasons.

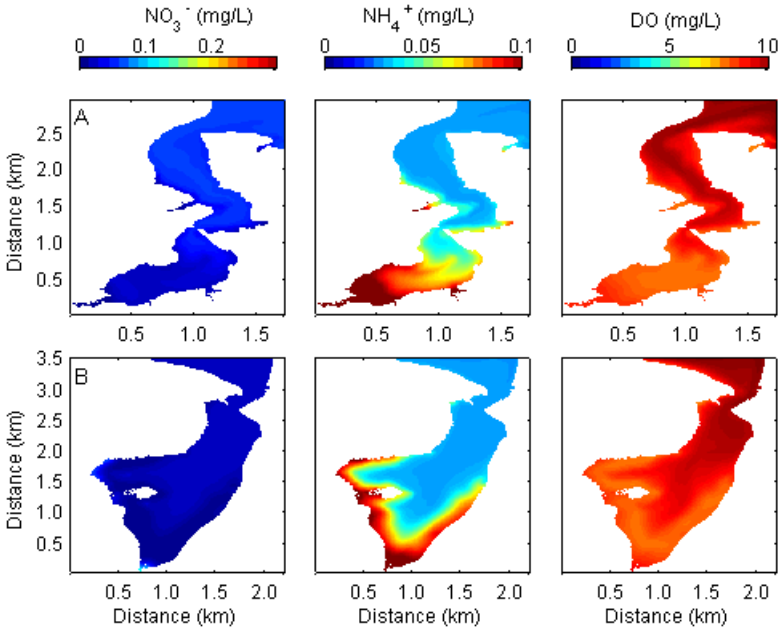

Figure 5.17 Depth-averaged nitrate (NO_3^-), ammonium (NH_4^+), and DO concentration in an upwelling event at Te Puna (Case 21) and Waikareao (Case 22) estuaries.

5.4 Conclusions

From the modelling scenarios, it has been shown that differences in DIN concentrations and distribution are a function of physical forcings such as wind, sediment, and salinity in both estuaries. Such differences need to be considered for future studies that investigate the ecosystem response of such shallow estuaries to extreme weather events (e.g. cyclones, storms) and development of area surrounding or within the estuaries. On a system scale, exchange with harbour water is the key factor influencing DIN supply and replenishing oxygen-depleted conditions. On a local scale, the distributions of DIN along the estuaries are tightly coupled with sediment input, groundwater inflows, and DO levels, with highly flushed regions.

From modelling scenarios, it was found that inter-annual variation in concentration of nitrate is influenced primarily by freshwater inputs, while ammonium is influenced primarily by sediment fluxes. Ammonium is sensitive to processes in the sediment and also to the seasonal variation in temperature. Interestingly, the effect of ammonium to temperature is more pronounced in summer in the shallow estuaries regions, with lower concentrations by 19-40% with no sediment fluxes scenario. In summer, with longer photic hours and higher temperature, lead to longer heating periods in the shallow regions. This can lead to rapid decomposition of organic matter and ammonium regeneration, thus

increasing ammonium concentrations. Although both Te Puna and Waikareao estuaries are heavily influenced by tidal exchange with open boundary water with regard to water exchange and salinity, model scenarios revealed the importance of freshwater discharges as dominant source of nitrate in the estuaries, hence it would be desirable to have long time series of flows and nutrient content of freshwater entering the estuaries both from groundwater and streams discharges to better constrain their fluxes and composition. The magnitude of sudden large freshwater discharge was also found to have an important influence on DIN concentration and distribution in the upper estuary in summer with an increase of nitrate by 27%. While in winter sudden large freshwater discharge, lead to decrease in DIN concentration by 41% for ammonium and 46% for nitrate. The short residence times in Te Puna would limit the degree to which internal estuarine processes could retain nutrients from the large freshwater pulses.

By altering the conditions within the model, it has been possible to compare the effect of a range of inflow, nutrient and meteorological events in both Te Puna and Waikareao estuaries. More recently, rapid development in both Te Puna and Waikareao catchments has led to the transformation to more agriculture and urban catchments from previously native forests and forestry area. Port activities and sub-catchment development in the southern end of the harbour, while not unduly influencing the hydraulic residence time of the estuary, may lead to localized variations in nutrient inputs. Both types of activities are likely to adversely affect water quality in parts of the estuaries, although on what scale remains uncertain.

This work also demonstrated the importance of considering both temporal and spatial measurements in order to describe the nutrient and ecological dynamics completely. The scenarios are manipulative experiments but in reality these processes have joint probability that could result in completely different outcomes. The next stage of this work is to model joint events in more detail such as climate events (e.g. El Niño and La Niña) which are often characterized by (1) changes in wind patterns, (2) shelf-upwelling, and (3) increase of pulse events. And so concentrating of on one of these aspects only will give short seasonal outcomes but by modelling joint events, the interannual variations in physical and biogeochemical processes can be captured.

Water management is usually based on a single monthly measurement at a fixed station. However, the heterogeneities observed here need to be taken into account. Other sites within the estuaries can be monitored such as sites with varying distance from the estuaries mouth and from drains would be informative. By basing water quality monitoring at a fixed station can lead to underestimation or overestimation of the measurements as from the scenarios shown above, the DIN concentration varied laterally from upper to lower estuary. Hence water management practice should increase monitoring at different sites within an estuary to allow for a more comprehensive outlook of the estuary.

Chapter Six: Dissolved inorganic nitrogen concentrations of an estuarine tidal flat

6.1 Introduction

Nutrients and organic matter from the catchment regions are transported to estuaries by surface waters, atmospheric deposition and direct groundwater discharges. Surface water discharges (e.g. effluents from wastewater treatment, sewage systems and chemical spills) can be monitored while atmospheric deposition is harder to quantify as each nutrient species has its own mode of emission, transport pathways and depositional cycle. Groundwater discharge is less visible and less easily quantified and previous studies in recent years have shown that direct groundwater discharge may be responsible for a substantial part of total freshwater input to estuaries and the ocean (Johannes and Hearn 1985; Slomp and Van Cappellen 2004; Kroeger et al. 2007). Previously, the primary concern associated with groundwater discharge into coastal areas is salt-water intrusion into coastal aquifers (Bond and Bredehoeft 1987; Melloul and Goldenberg 1997). However, in recent years there is concern that submarine and marginal marine discharges of nutrients and contaminants may have more significant impact in the coastal areas (Giblin and Gaines 1990; Valiela et al. 1990; Moore 1999). Groundwater discharge is difficult to gauge but due to enriched levels of nutrients, may contribute significantly to the nutrient balance in coastal and estuarine ecosystems (Valiela et al. 1990). Compared to stream and river discharges, which occur at relatively high rates, groundwater discharges are slower, patchy, diffuse and temporally variable with seepage occurring over an extensive area of the shoreline (Oberdorfer et al. 1990).

Geological material, changing recharge conditions, overlying sources of nutrients, groundwater residence time, inputs of oxygen and the consumption of oxygen and nutrients by bacterially-mediated decomposition are environmental processes that can influence N speciation (Drever 1982; Rivett et al. 2008). The discharge of sediment pore-water and associated nutrients and contaminants is a complex process. Fluid advection, mixing driven by tidal pumping and the chemical transformations that occur in the sediment contribute significantly to the impact on pore-water seepage ecosystems (Precht and Huettel 2003; Deborde et al. 2008; Billerbeck et al. 2006b). In particular the sediments of intertidal flats are sites of

intense biogeochemical processes (Rocha 1998), and have received much attention in recent years for the important role they play in attenuating high inorganic nitrogen loads from the land to the sea (Trimmer et al. 1998, 2000; Cabrita and Brotas 2000). However, estuarine sediments may also add fixed nitrogen primarily ammonium to the overlying water and are often a substantial source for primary production (Cowan and Boynton 1996).

High potential rates of nitrate reduction processes (denitirification and dissimilatory nitrate reduction to ammonium) have been demonstrated to occur at locations in which nitrate-bearing fresh groundwater contacts sediments within or just beneath fringing salt marsh (Tobias et al. 2001). However, in some cases flow paths carrying groundwater to surface waters bypass fringing wetlands and instead discharge occurs through permeable sediments and offshore of the wetlands. In some locations, where rapid discharge of fresh groundwater occurs through intertidal sediments, nitrogen transformations occur in the top meters of the sediments (Giblin and Gaines 1990; Nowicki et al. 1999). Land-derived nitrogen loads will be attenuated and transformed in the intertidal sediments depending on the biogeochemical setting.

In estuaries with extensive intertidal flat areas, pore-water exchanges take place between the sediment and the overlying water column during the flood tide. During low tide exposure of intertidal flats, pore-water pressure and hydraulic gradient transports pore water through the sediment towards the seepage face where these pore water discharges can constitute an important nutrient input to the coastal waters. While there is a considerable amount of research on interstitial hydrology of salt marshes (Tobias et al. 2001) and some on open beach environments (Miller and Ullman 2004; Dale and Miller 2007), there are limited studies concerning the behaviour of nutrients in tidal flat areas (e.g. Billerbeck et al. 2006a). Alternating exposure and inundation of sediment is a major factor resulting in the transport and transformation of nutrients in the intertidal flats (Rocha and Cabral 1998; Hou et al. 2007). Rocha and Cabral (1998) found that nitrate behaviour in Sado Estuary is strongly influenced by tidal action. The periodic submersion and exposure allows for the diversification of oxygen supply into deeper sediments for nitrification to occur. The alternating exposure and inundation of sediments has been linked to nitrification and denitrification rates in

sediments. During exposure, lower nitrification and denitrification rates were detected in intertidal sediment, while higher denitrification rates were observed in re-flooded sediments which was attributed to more available nitrate under inundated conditions (Hou et al. 2007).

The objective of this chapter is to determine the seasonal variation in ammonium and nitrate composition of the sediment pore-waters in a tidal flat margin in the shallow tidally dominated Waikareao Estuary. Vertical profiles of sediment porewater composition in a tidal flat in Waikareao Estuary were sampled to provide snapshots of nutrient concentrations (ammonium and nitrate) at different times of the year.

6.2 Methods

6.2.1 Site description

The pore-water nutrient study was undertaken in Waikareao Estuary, a sub-estuary located at the southern basin of Tauranga Harbour in the Bay of Plenty region, on the east coast of North Island, New Zealand (Figure 6.1). See Chapter 2 for further description on the study site. Waikareao Estuary was chosen over Te Puna Estuary due to site accessibility to the tidal sandflat regions. An experimental block (width of 80 m, length of 50 m) was established at the tidal flat margin on the east side of the estuary (Figure 6.2).

6.2.2 Groundwater sampling and analyses

Nine stations with wells were set-up in the experimental block (Figure 6.2). Research instrumentation consisted of three parallel transects of multilevel wells extending perpendicularly from the upland pipes. The nine stations were divided into three stations along three different transects (T1, T2 and T3), with 3 wells located at each of these nine stations. An additional station situated 10m into the mangroves from the upper tidal flat margin was also installed with 3 wells. At each station, the three wells were arranged at depths of 75, 50 and 25 cm deep into the sediment at each station with an additional 5 cm of the pipe extending above the sediment. Stations 1, 4 and 7 were 50 m away from the mangrove patch edge (upper tidal flat), while Stations 2, 5 and 8 (middle tidal flat) area 30 m from the mangrove patch edge, and Station 3, 6, and 9 (upper tidal flat) are 10 m away from the mangrove patch edge. The wells were constructed from PVC pipes with

holes drilled at the sampling depths in 5 cm bands. The drilled areas were covered with mesh to prevent blockage by sediment. The inside diameter of the pipes were 3.7 cm and the outside diameter was 4.1 cm. The location of the wells was surveyed using a Nikkon DTM-352 Total Station.

Field sampling was conducted monthly in winter-spring period (Jun 2009, July 2009, August 2009, September 2009, October 2009) and bi-monthly in summer (December 2009, February 2010). Sampling days were chosen when the low tide was between 7 and 8 in the morning for consistency in sampling time and tidal regime. Figure 6.3 shows the precipitation rate during the sampling period. The height of the water at each well was measured with a dipmeter before the water was pumped out with a hose connected to a syringe. Temperature and salinity in each well was measured with an YSI meter prior to water sampling. Water samples, 1 replicate each, were collected from the wells with a hose connected to a syringe for dissolved nutrient. Additional water samples at 5 cm and 10 cm depths were also collected during each sampling period.

The water samples were put on ice during transport to the laboratory. The water samples were centrifuged at 4000 rpm for 15 minutes to separate the sediment and the supernatant. The supernatant were then filtered to remove leftover sediments, before frozen until further analysis for ammonium, nitrate and nitrite using a Lachat Instruments flow injection analyser (FIA, Zellweger Analytics, 2000) (APHA 1992). DIN referred in this chapter is the combination of ammonium and nitrate.

Long-term monitoring data (nutrient and salinity) collected by Bay of Plenty Regional Council in Kopurereroa Stream, Kulim Avenue and Otumoetai, are presented as part of this chapter. Data were collected at intervals ranging from monthly to every two months.

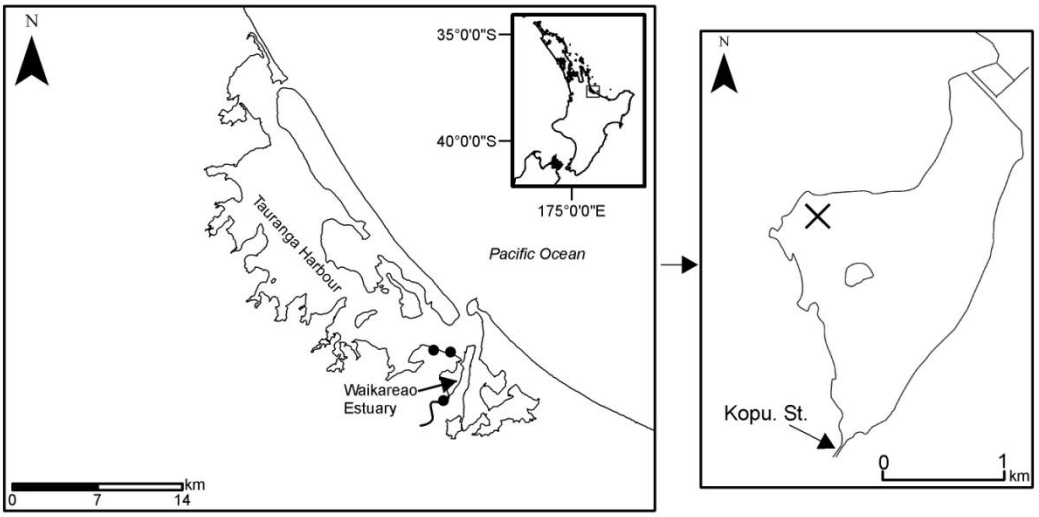

Figure 6.1 Location of the study area, Waikareao Estuary, in Tauranga Harbour located in the northeast coast of North Island, New Zealand. The 'X' mark the sampling location. Kopu. St.: Kopurereroa Stream. Black circles marked the locations monitored by the Bay of Plenty Regional Council.

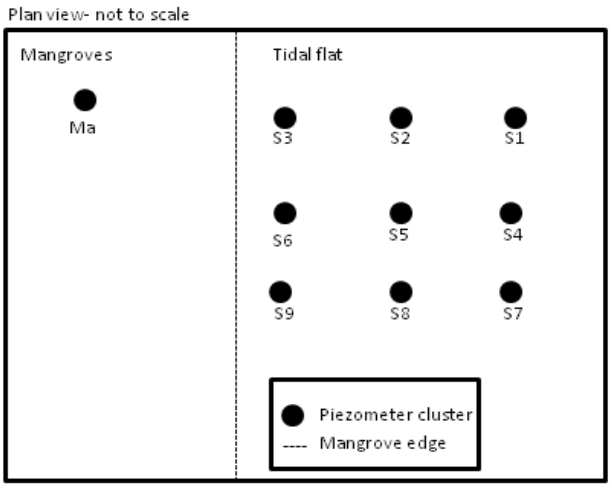

Figure 6.2 Schematic showing the well location. Each well cluster consisted of three sampling depths (25, 50 and 75-cm depth). S1-S9 represents the nine stations of three wells located on the tidal flat and Ma denotes the set of three wells located within the mangroves.

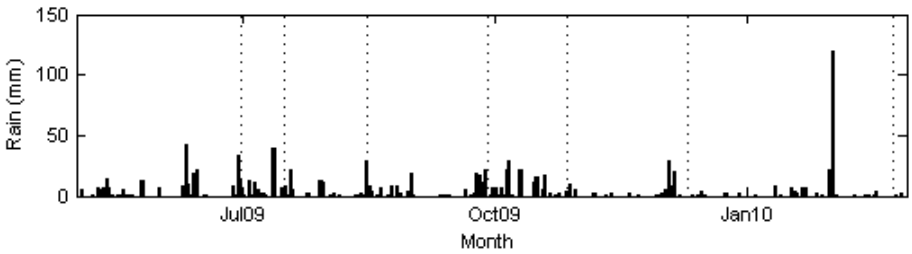

Figure 6.3 Monthly precipitation rates measured at Tauranga Airport. Dotted lines marked the sampling dates.

6.3 Results

The salinity gradually increased from winter to summer (Figure 6.4 and 6.5). The highest salinity in each well was observed at the end of summer, after a long dry period of little rain and the lowest salinity for each well was observed in early-and mid-winter. There were no consistent vertical variations in salinity (Figure 6.5). The temperature showed the same pattern as salinity with gradual increase from winter until summer. There is no vertical variation with depth in the salinity profiles in the wells in Station 1, 4 and 6 which is located furthest from the edge of the mangroves (Figure 6.5).

The ammonium and nitrate showed distinct seasonal patterns with higher concentrations measured in mid-winter and mid-summer (Figure 6.6, 6.7). The average concentration of ammonium varied with depth seasonally at 5 to 25 cm depth (Figure 6.6). For nitrate, the average concentration was lower at depth at 25 to 75 cm depth (Figure 6.7). Water samples from the wells demonstrated high DIN concentrations (between 0.002 to 6 mg L^{-1} DIN) and the majority was present in the form of ammonium (0.01 to 5.7 mg L^{-1} ammonium) (Figure 6.8 and 6.9). The nitrate and ammonium concentrations at the mangrove station were generally lower by 2 and 5 times respectively compared to the tidal flat stations 1 to 9 (Figure 6.10).

Generally, the nitrate and ammonium profiles demonstrated that the nitrate was the dominant form of dissolved N at the surface layers at most wells and ammonium dominated in the mid-region. There was no clear pattern in the nitrate concentration at depth in the tidal flat (Figure 6.9). The nitrate concentrations increased directly below the surface at Station 3, 4, 6, 7, 8 and 9. The ammonium concentrations also showed the same pattern with increased concentrations directly below the surface with maxima concentrations between the depths of 10-25 cm (Figure 6.8).

Ammonium concentrations at all nine stations showed a mid-depth decrease from around 3-5 mg L^{-1} at 25 cm depth to 0.001-2.5 mg L^{-1} from 50 to 75 cm depth (Figure 6.8). Variability in nutrient concentrations with depth was high at Stations 1 to 3 while Stations 4 to 9 showed a much more gradual change except for a few

spikes. There were four hotspots in the tidal flat wells where ammonium concentrations were much higher than in neighbouring wells, first in summer in stations 4, 5 and 6, and then during mid-winter in stations 4, 5 and 6 (Figure 6.8). At stations 1, 3 and 6, the nitrate concentrations were much higher than neighbouring wells in depths from 50 to 75 cm (Figure 6.9).

The nitrate concentrations measured by the council showed that the nitrate concentrations were high in Kopurereroa Stream ~1 mg/L in comparison to Kulim Avenue and Otumoetai concentrations which varied between 0.001-0.5 mg/L and 0.01-0.1 mg/L respectively (Figure 6.11). The ammonium concentrations in the stream were in the similar concentration range as Kulim Avenue and Otumoetai.

The pore-water surfaces elevations were generally located close to the surface of the tidal flat (Figure 6.12A). Magnitude of the water table level varied with distance, decreasing seaward, indicating a seaward-directed horizontal pressure gradient. The water level in the upper tidal flat, i.e. at the mangrove edge, was more varied through time for all three transects in comparison with the middle and lower tidal flat (Figure 6.12B), which suggests the upper tidal flat stations were driven more by local water table processes while the lower tidal flat, the water level was tidally driven. The root mean square error of the total station measurement was 0.2 cm. The average water levels in the wells (Figure 6.13) were higher during wetter periods, winter and spring, than in late summer when the precipitation rate was lower (Figure 6.3).

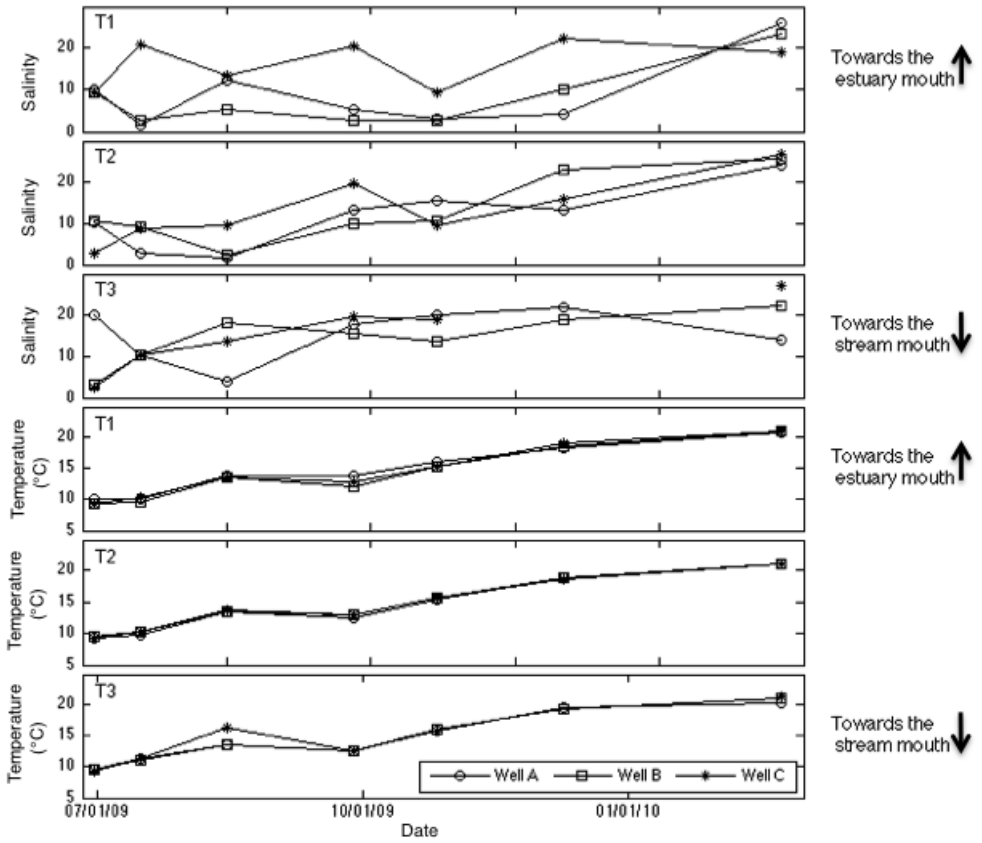

Figure 6.4 Surface sediment (10cm depth) salinity and temperature during the sampling occasions at the tidal flat in Waikareao Estuary.T1: Transect 1; T2: Transect 2; T3: Transect 3. Well A, Well B and Well C are stations located 50, 30 and 10 m away from the mangroves edge respectively. Transect 1 is for wells located towards estuary mouth; Transect 2 is for wells located between Transect 1 and 3; Transect 3 is for wells located towards the stream mouth.

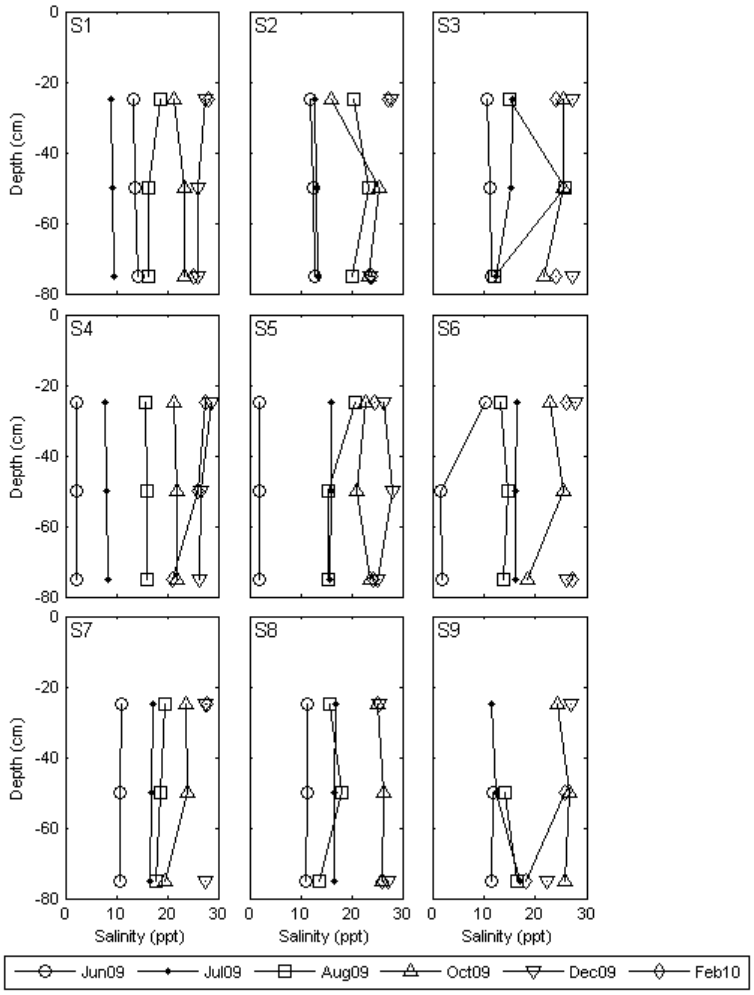

Figure 6.5 Vertical profiles of salinity measured in the wells at the tidal flat in June 2009, July 2009, August 2009, October 2009, December 2009 and February 2009. S1-S9: Station 1 to Station 9.

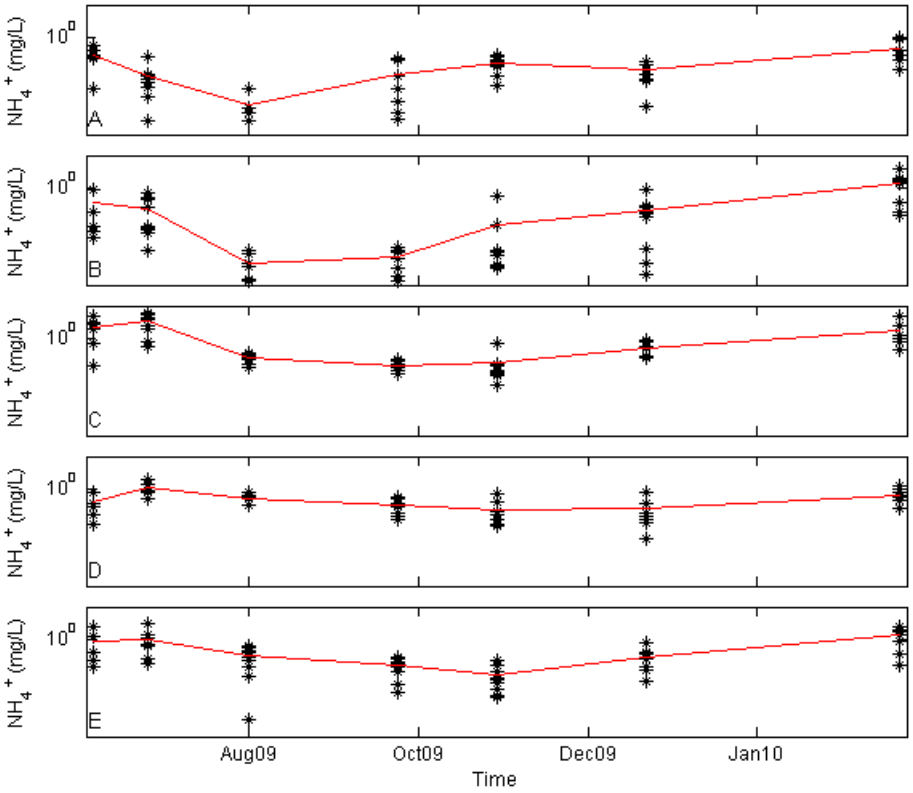

Figure 6.6 Relation between ammonium (NH_4^+) concentrations at 5cm depth (A), 10 cm depth (B), 25 cm depth (C), 50 cm (depth) and 75 cm depth (E) with time. The solid line represented the average concentration. Note the log scale used in y-axis.

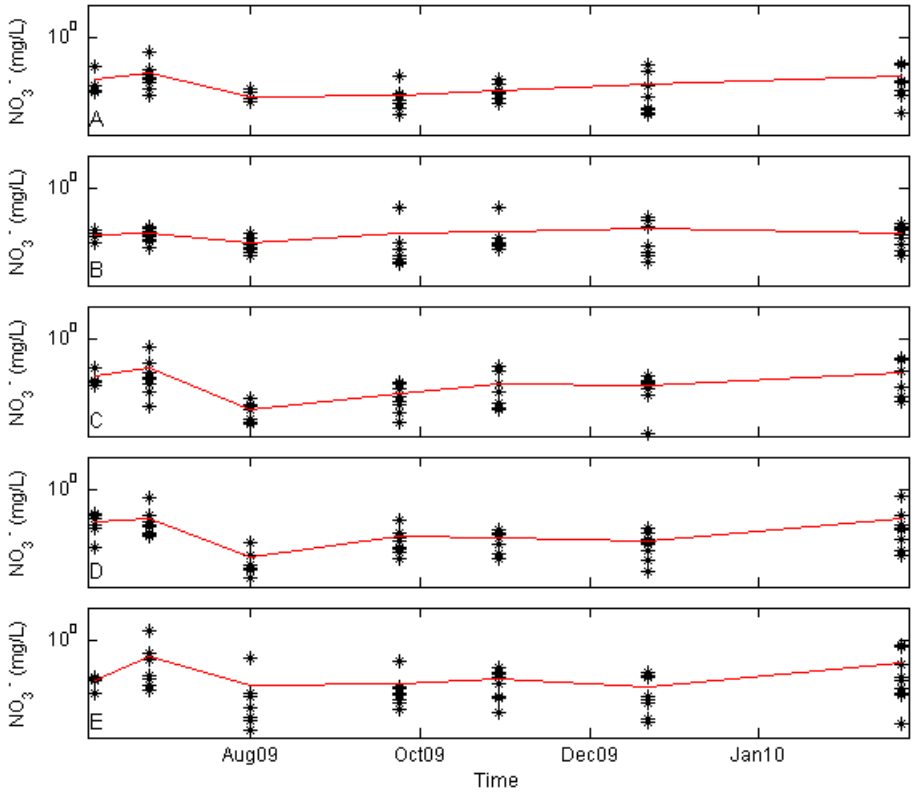

Figure 6.7 Relation between nitrate (NO_3^-) concentrations at 5 cm depth (A), 10 cm depth (B), 25 cm depth (C), 50 cm (depth) and 75 cm depth (E) with time. The solid line represented the average concentration. Note the log scale used in y-axis.

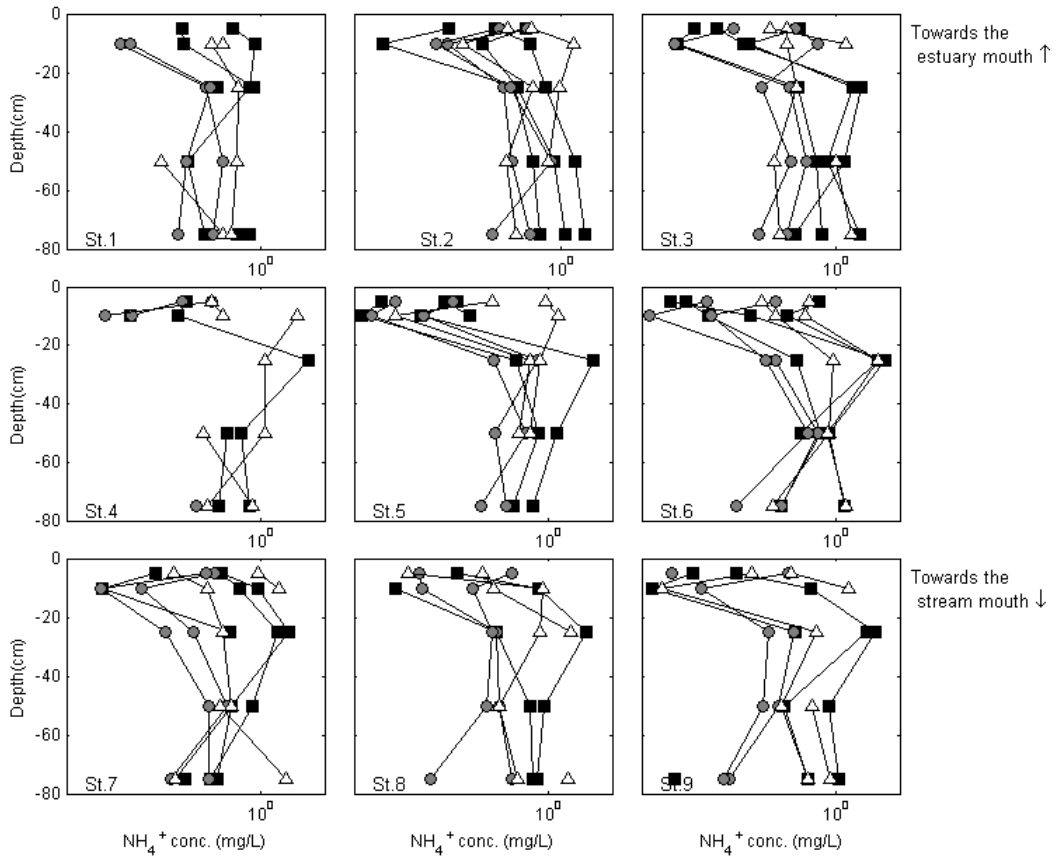

Figure 6.8 Ammonium (NH_4^+) concentrations from wells taken at the 9 stations over the sampling occasions. Note the log scale used for ammonium concentration. S1-S9: Station 1- Station 9. Black filled squares represented winter season, grey filled circles represented spring season and triangles represented summer season. Stations 1, 4, 7 at lower tidal flat; Stations 2, 5, 8 at middle tidal flat; and Stations 3, 6, 9 at upper tidal flat.

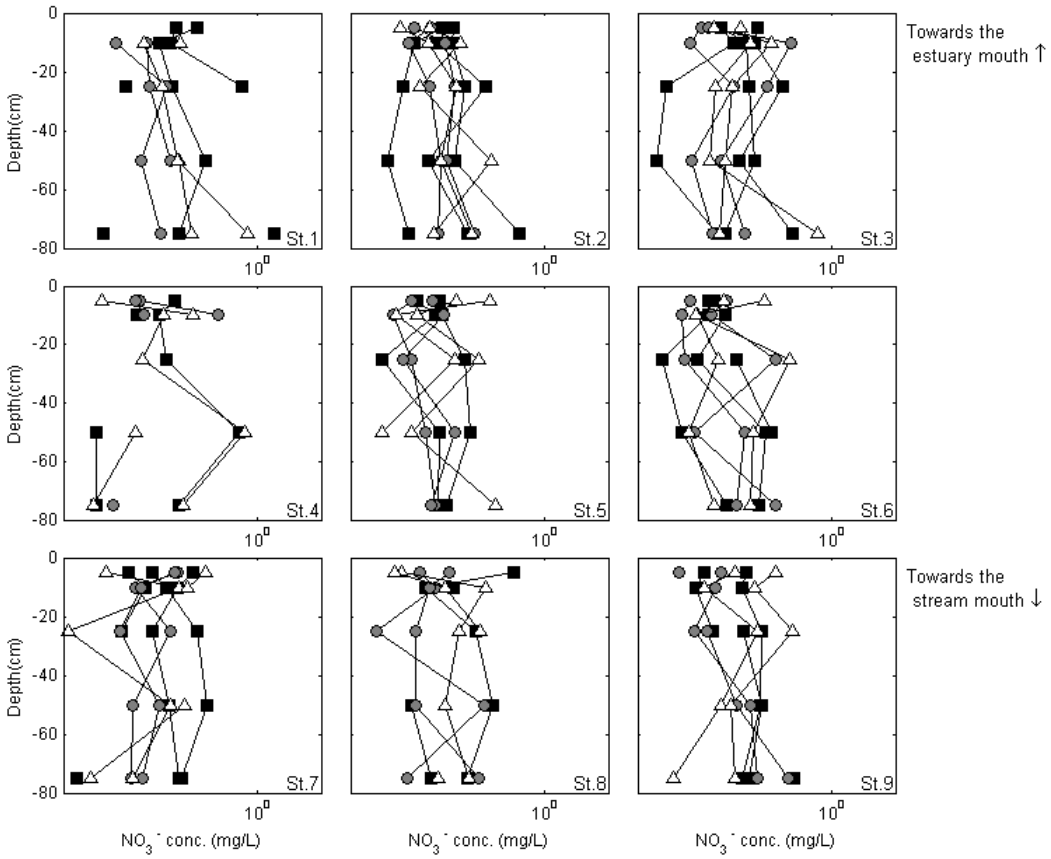

Figure 6.9 Nitrate (NO_3^-) concentrations from wells taken at the 9 stations over the sampling occasions. Note the log scale used for nitrate concentration. S1-S9: Station 1- Station 9. Black filled squares represented winter season, grey filled circles represented spring season and triangles represented summer season. Stations 1, 4, 7 at lower tidal flat; Stations 2, 5, 8 at middle tidal flat; and Stations 3, 6, 9 at upper tidal flat.

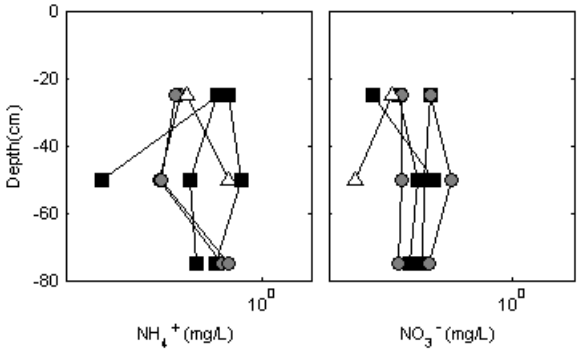

Figure 6.10 Ammonium (NH_4^+) and nitrate (NO_3^-) concentrations taken at the mangrove station over all the sampling occasions. Note the log scale used for nutrient concentrations. Black filled squares represented winter season, grey filled circles represented spring season and triangles represented summer season.

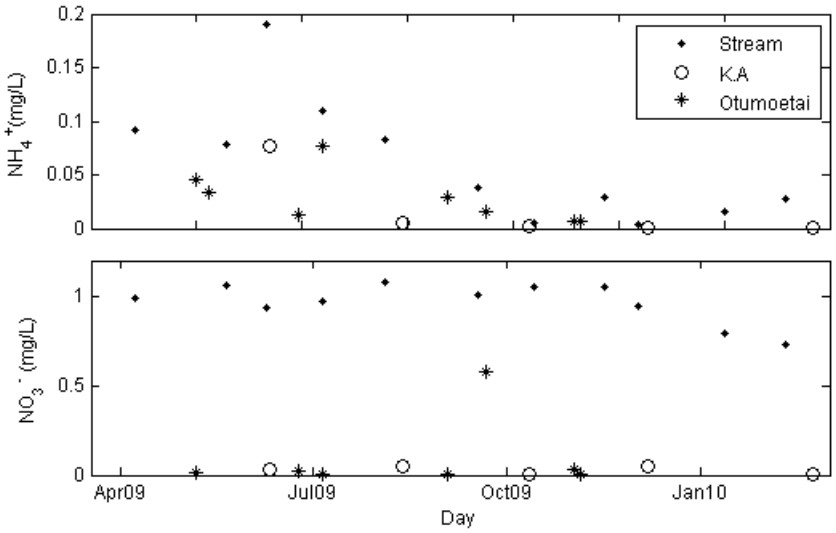

Figure 6.11 Ammonium (NH_4^+) and nitrate (NO_3^-) concentrations from Kopurereroa Stream (Stream), Kulim Avenue (K.A.) and Otumoetai.

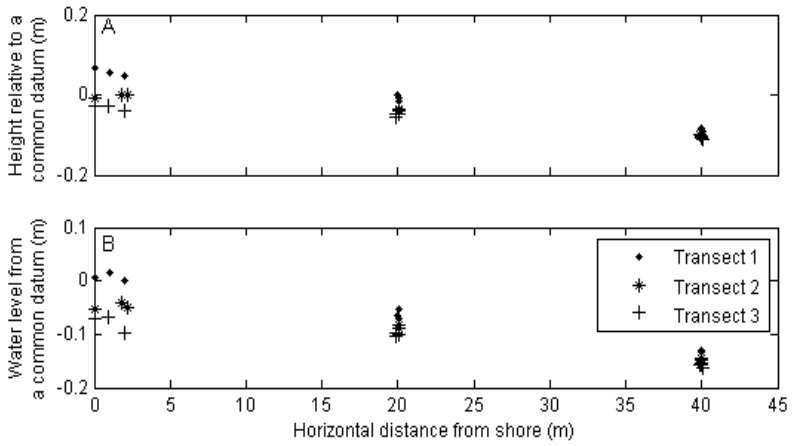

Figure 6.12 Distributions of morphological heights (A), and average water level of the wells of the 7 months relative to a common datum (B) across distance for each transects.

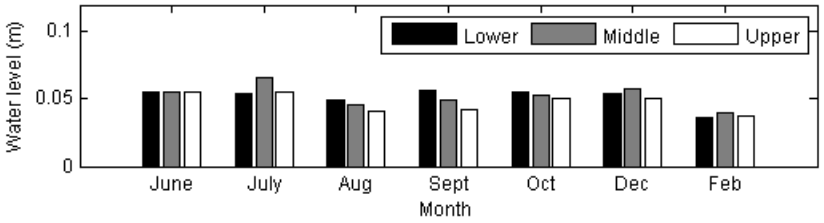

Figure 6.13 Water level relative to the common datum in the wells plotted against the sampling months at lower, middle and upper tidal flat. At the upper (or middle or lower) tidal flat station, the 9 wells (3 transects, with 3 wells each) were averaged.

6.4 Discussion

This study highlights a process unique to intertidal flats areas where pore-water is likely released by the process of seepage during low tide. This release is caused by the exposure of the tidal flats during ebb tide, which sets up a hydraulic pressure gradient between the pore water and seawater level (Nielsen 1990). The pressure gradient causes water flow through permeable sediment layers toward the seepage zone at the margin of the tidal flat where pore water is released into the tidal gullies (Billerbeck et al. 2006a).

Coastal groundwater seepage is driven by groundwater table elevation, mean sea level and tidal amplitude (Turner et al. 1997; Robinson et al. 2007a, b). Water samples were collected during low tide to capture maximum outflow from the tidal flats, which includes saline and fresh groundwater. Salinity was higher in summer (February) indicating the weakening of the freshwater hydraulic gradient and landward progression of the marine interface in the groundwater but also in summer estuarine water has higher salinity. Refreshening was observed in winter, as the water samples were less saline. The salinity was also higher in summer (start and end) compared to winter (start and mid) with lower freshwater input.

Higher concentrations of ammonium were observed in the pore-water samples compared to nitrate. Low nitrate concentrations in the wells could occur because of generally reducing conditions, which is a prerequisite for denitrification (Simon 1988). The presence of nitrate in the sediments with decreasing oxygen with depth will be influenced by bacterial population composition and abundance as well as redox conditions and ammonium concentrations (Murray et al. 2006). Elevated nitrate concentration observed at Stations 1, 2 and 3 with depth could be caused by diffusion from pore water in surface sediment and from pooled water (Murray et al. 2006). Long-term monitoring of Kopurereroa Stream showed that nitrate concentration was higher than those measured at Otumoetai, Kulim Avenue and tidal flat stations. This suggests that the primary source of nitrate into Waikareao Estuary was through freshwater discharge and ammonium concentration is dominated by sediment recycling processes. Thus the tidal flat acts as a recycled nutrient source to the estuary system through pore-water seeping and tidal flat draining. This source of nutrient recycling through sediment is important

especially in summer when freshwater flow rates are low. From the Chapter 5 modelling scenarios, it was also found that sediment contributed towards the overall estuarine ammonium concentration, as by turning the sediment parameter off, the ammonium concentrations were lower by 19-40% in summer and 16-39% in winter. As the DIN from freshwater source (stream and groundwater) moved through the estuary, biogeochemical nitrogen transformation occurs along with assimilation by phytoplankton. The high concentration of nitrate from the stream would be attenuated within the intertidal flat sediments before being exported out of the estuary. However the rates of attenuation differ between estuaries. In some estuaries, denitrification may remove up to 45-50% of the nitrogen entering as DIN (Seitzinger et al. 1984; 1987), while in others the degree of attenuation of nitrogen flux appears to be small (Nielsen et al. 1995). The rate of attenuation depends on the interaction between organic matter in the sediment (Nixon 1981), chemical status of the surface sediments and the water column (Koop et al. 1990), both benthic fauna and flora activity (Sundbäck et al. 1991; Pelegrí et al. 1994) and flushing time (Balls 1994). The relatively short residence time in Waikareao Estuary, ~0.5-1.5 days (Chapter 4), implies that water column DIN will be in contact with the sediments in the tidal flat for only a limited time, provided limit opportunity for the sediment to play a role in denitrifying process (Nielsen et al. 1995; Ogilvie et al. 1997). This effect will be greatest in winter when the residence time is lower. Lower rates of denitrification would also occur in winter due to lower temperature.

As mentioned above, nitrate was the dominant form of dissolved N at the surface sediment in most wells and ammonium dominated in the mid-depth regions. This suggested that oxic conditions were overlying reducing conditions in the tidal flats (Corbett et al. 2000; Slomp and Van Cappellen 2004; Kroeger and Charette 2008). The vertical stratification of nitrate and ammonium in the wells was the result of nitrogen oxidation at the top where oxygen is available for nitrification producing higher nitrate concentrations. At intermediate depths (10-25 cm) the nitrate concentrations were generally higher than ammonium, so potentially there is nitrification coupled with denitrification. At deeper depths (25-50 cm), ammonification and dissimilatory nitrate reduction to ammonium (DNRA) can produce higher ammonium concentrations. A study by Ullman et al. (2003) on a beach-face, found that nitrification occurs at the top of beach groundwater where

there is aeration from tidal pumping and wave swash while ammonification and DNRA are dominant processes in the deeper groundwater and these processes sustain elevation ammonium concentrations in the deeper zone. These nitrogen processes may switch on and off as oxygen conditions change in the sediment layer. This may happen as the water table drops or as oxygen diffuses from the surface sediment (Korom 1992). The presence of bioturbators in high densities in the sediment, will also lead to oxygen being prevalent for nitrogen cycling (Marinelli and Williams 2003). As shown in Figure 6.6, the average ammonium concentrations showed a time lag with depth, i.e. minimum concentration at surface layer (5-10 cm depth) was measured in end of winter and the concentration increased in spring, however with deeper depths the time lag gets slower with minimum concentration measured at 75 cm depth in winter, which may be due to the decrease in oxygen layers with depth in winter whereas in spring the higher oxygen content from phytoplankton release was able to re-oxygenate the deeper layers as the water table drops during low tide. This can also be seen in nitrate where it showed declining concentrations with depth from the surface sediment. However the DNRA production in deeper sediments was probably only a minor contributor to the total ammonium production due to low nitrate concentration especially at 50-75 cm depth (Figure 6.9). The mid-depth decreased in ammonium concentrations from 50 to 75 cm depth at all nine stations may be derived predominantly from organic matter and rates of decomposition.

Sedimentology of the intertidal flat influences water fluxes across the sediment-water interface and hence the transport of recycled DIN from deeper depths of the sediment to the surface. From previous sediment cores taken between 0-10 cm depth, on the east bank tidal flat in Waikareao Estuary, the sediment type varied from coarse sand to silt (mean grain size between 0.0625-0.5 mm) with 48% of the fraction comprising of fine sand (Burgraff et al. 1994). While two sediment cores collected on the west bank tidal flat to 1.8 and 1.4 m depths respectively, the sediment type varied from medium fine sand to medium silt (mean grain size between 0.024 to 0.3 mm). From the two cores collected, between the depths of 0 to 50 cm, the sediment type comprised of medium to fine sand, while from 50 to 75 cm deep, the sediment type is medium silt (Stokes 2010). Permeability of sand facilitates advective pore-water processes transporting solutes from biogeochemical transformations to surface sediments as seen in the ammonium

profiles in winter and summer where the ammonium concentration peaked at 25-50 cm depth. With large percentages of the surface sediment comprised of sandy sediments, advective pore-water transport occurs as pressure gradient changes leading to water discharging through drainage channels/seepage face (Nielsen 1990). The advection process also allowed for inorganic nutrients to be removed from the sediment to be used in the water column for primary production (Fisher et al. 1982; Huettel et al. 1998).

As mentioned above, Waikareao Estuary tidal flat sediment is predominantly sand material which permeability facilitates advective transport through the upper sediment layers (Huettel and Gust 1992; Huettel et al. 1996). The depth of the advection process is dependent on the permeability of the sediment and is usually restricted to the surface layers (de Beer et al. 2005) where recycling and feedback processes of metabolic products occurred in a matter of hours to days (Billerbeck et al. 2006b). Billerbeck et al. (2006a) did tracer injections study and revealed that pore water drainage in an exposed tidal flat during low tide affects sediment down to 50cm depth. As a consequence of this discharge, highly concentrated water is found in the upper surface layer of the sediment. For deeper depths below the regularly flushed upper layer, the sloping water table causes horizontal gradient, which drives flow over scales of tens to hundreds of metres (Jahnke et al. 2003; Billerbeck et al. 2006a). The sloping water table at the study site can lead to horizontal transport of rich DIN water from upper tidal flat to lower tidal flat. In the deeper layer, the residence time and pore-water flows are longer, and the feedback of mineralization to the ecosystem is delayed (Billerbeck et al. 2006b). Such slow flows coupled with recycling processes within the sediments may additionally contribute to the high pore-water solute concentrations at the lower flat sampling stations (Stations 1, 4, 7). The longer residence times in deeper depths are also supported by intermediate levels of ammonium concentrations at that depth (75 cm) where the longer residence time allow for remineralization to take place.

The pore-water DIN collected were mostly influenced by pore-water sediment recycling processes instead of groundwater discharge as the average salinity was >15 and did not showed freshwater increases with increasing depth. During immersion, permeable sediments at the surface at the mangrove station become

saturated with seawater by infiltration. At low tide, pore-water table in the upper sediment decreases and the sediment becomes less saturated with water in the upper centimetres. In the tidal flat zone, bioturbation activity driven by numerous burrows of bivalves, gastropods and benthic organisms were noticed during sampling occasions. Bioturbating activity of benthic fauna reworked sediment and also reoxygenating surface sediment thereby enhancing nitrification.

There were hotspots observed in the stations where nutrient concentrations were much higher than in neighbouring wells in summer and winter. Hotspots were observed in stations 4, 5 and 6 for ammonium and in stations 1, 3 and 6 for nitrate where the nutrient concentrations were higher than neighbouring wells. The hotspots may have been the result of a localised injection of nutrients, however, the sampling resolution was not sufficient to identify a point source of nitrate within the flow field. This could also be a surplus of organic matter and changing oxygen conditions at these stations, which could drive a coupled nitrification-denitrification.

Intertidal flats generally have the cross-shore morphological profiles that gently incline in the offshore direction. The sloping morphology is a consequence of long-term morphological evolution closely linked with sediment transport caused by water and tidal currents processs (Le Hir et al. 2000). From the measurements taken at the tidal flat in Waikareao, the pore-water surfaces were generally located close to the level of the tidal flat. However, the difference between the water level and the morphological height varied depending on the location of the flat, with more variation in upper tidal flat compared to lower flat. This is because the water level in upper tidal flat is driven by the local upland water table and geology, while in the bottom tidal flat, the water level is mainly driven by tidal action. The sloping morphology of the tidal flat can lead to horizontal drainage of pore-water from deeper depths in upper flat to lower flat, and may additionally contribute to higher pore-water solute concentrations in the lower flat (Billerbeck et al. 2006a).

6.5 Conclusions

This chapter suggested that recycling processes instead of groundwater discharge mostly influences the pore-water nutrients, as the average salinity profiles did not

show strong freshwater changes with increasing depth, which suggest groundwater input is minimal. Billerbeck et al. (2006a, b) showed that the underground drainage mechanism through permeable sediment tidal flat was an important nutrient sources to coastal waters during ebb tide. The authors demonstrated that the sand flat acted as a buffer system for nutrient according to filtration cycle due to the long residence time of pore water. From the sampling occasions, the greatest concentrations of DIN occurred in mid-winter and summer. During low tide, pore-water release from tidal flat sediments lead to these areas as sites of efficient nutrient turnover. However, more detailed studies are necessary to evaluate the tidal flat and terrestrial nutrient input, and the residence time of pore-water within the tidal flat in order to estimate the mineralization feedback loop. The ammonium concentration measured at the tidal flat in this chapter, was higher by an average of 70% than the estimated groundwater inputs in the model for Chapter 4 and 5. Hence, the groundwater contribution of ammonium into both Te Puna and Waikareao model scenarios was underestimated. Hence the extent of groundwater inputs need to be better assessed as biogeochemical processes in the sediment can have a significant influence on the discharge of DIN into the water column, and also in nutrient transformation and removal within a system.

This chapter highlights the importance of pore-water seepage contribution during low tide. However during high tide, there is also groundwater seepage. During inundation of the intertidal flats, the percolation of water through the sediment is driven by pressure gradients generated by the interaction of bottom currents with sediment topography and by waves passing over the permeable bed. This hydrodynamic forcing can lead to groundwater percolation into the water column.

Chapter Seven: Conclusions

7.1 Summary

The objective of this thesis was to understand the magnitude, fate and transport of nutrients (DIN) in a spatially and temporally complex setting. This study is the first comprehensive attempt to investigate the coupling of hydrodynamic and biological/chemical processes in Te Puna and Waikareao estuaries located in Tauranga Harbour and subsequent exchanges that occurred between the sub-estuaries within the harbour waters. Numerical models have been previously used to study harbours and estuaries in New Zealand (e.g. Bell et al. 1998; Proctor and Hadfield 1998; Spiers et al. 2009). However, these studies have largely concentrated on the circulation patterns of the estuaries and harbours.

Nutrient regimes of estuaries in New Zealand differ from many previously described estuaries in other parts of the world (e.g. Chesapeake Bay; Seine Estuary) (Boynton et al. 1995; Garnier et al. 2010). A primary difference is due to the much lower population densities found in New Zealand catchments than those of heavily studied estuarine systems in the Northern Hemisphere. Additional features such as low rates of atmospheric nitrogen deposition (Parfitt et al. 2006; Heggie and Savage 2009) and more variation in inter-annual flow regimes also impact on nutrient region and differentiate them from estuaries in Northern Hemisphere.

The first component of this thesis investigated inter-annual/seasonal, tidal and diurnal variations in dissolved inorganic nutrient concentration and the flux to and from surrounding coastal regions. Tidal changes in nutrient concentrations were compared to seasonal measurements made during a 20-year monitoring program in the same system to see whether the range of tidal variability outweighs the seasonal/inter-annual range. Sub-seasonal timescales constitute the largest source of variability and is likely balanced between episodic and tidally driven processes. Freshwater inflows from catchments were largely attributed to the variations in nitrate concentrations while ammonium and phosphate concentrations were attributed more to estuarine recycling processes. The DIN concentrations were relatively lower than some overseas examples (e.g. Dähnke et al. 2008; Falco et al.

2010) but the large differences between ebb tide and flood tide resulted in higher fluxes of DIN.

Water exchange within the harbour and its sub-estuaries was shown to have an impact on the hydrodynamics, temperature, salinity and residence times at various parts of Tauranga Harbour. Physical processes such as freshwater inputs from river inflow, wind mixing and tidal flushing strongly influenced circulation patterns and residence times of water in the system, which in turn can influence other biological/chemical processes in the system. A detailed hydrodynamic modelling exercise of the southern basin of Tauranga Harbour was undertaken as the transport and mixing of water quality parameters are heavily dependent on accurate hydrodynamic predictions. Hydrodynamic modelling was conducted using the three-dimensional (3D) Estuary Lake and Coastal Ocean Model (ELCOM), which is based on the hydrostatic Reynold's Averaged Navier-Stokes equations. Initial assessment of the model found temperature to be sensitive to wind forcing. It was found that the water temperature generally increased by 4°C when there was no wind in the harbour. Measured temperature in various parts of the harbour especially further north of the harbour showed diurnal signals with the heating up of water temperature in late afternoon low tide. This temperature difference could potentially affect ecological (Guarini et al. 1997) and chemical processes (Berounsky and Nixon 1990) in the harbour along with other interacting factors such as light. From model simulations of the harbour, it was also found that the residence times varied across the harbour with increasing residence times as the water moved further inwards into the harbour and also in sub-estuaries with constricted mouths.

Water exchange between the harbour and Te Puna and Waikareao estuaries was shown to have a large impact on the hydrodynamics and nutrient fluxes of these relatively small and shallow sub-estuaries located at varying distances from the harbour mouth. The aim of the model is to understand the interplay between hydrodynamic and biogeochemical processes and their influence on the timing and magnitude of estuarine nutrient dynamics. It was also found that the temperature in the two estuaries were sensitive to wind in summer and spring where the temperature showed a better correlation under no wind condition model simulation. Hydrodynamic simulations showed the two estuaries to be relatively

well flushed with maximum of ~1.5 days in upper estuaries. The second component of the model, the water quality model, investigated the interactions of meteorological forcing, freshwater inflows, sediment fluxes and nutrient distributions in both Waikareao and Te Puna estuaries. The governing influence on the distribution of nutrients in the estuaries is tidal flow and is influenced episodically by variations in circulations and freshwater inflows. The model was able to capture the short durations in temporal variations in nitrate and ammonium concentrations. The constriction in the middle of Te Puna Estuary leads to distinct lateral variation in DIN and DO distribution between the upper and lower estuary. The modelling simulations predicted seasonal variations in nutrient distributions with freshwater inflows as the main contributor in winter while in summer sediment fluxes were the dominant source.

From the modelling scenarios presented in Chapter 5, it was found that different combinations of nutrient loadings, meteorological forcing and freshwater input evoked varied system responses, reflected in changes in the nutrients concentrations and distribution. A temporally varying wind field was found to be important addition to mixing and it resulted in improving water column dissolved oxygen concentration. The high DO in turn can be used for nutrient recycling within the estuaries. Increasing freshwater inputs and nutrients resulted in a slight increase in overall nutrient concentration but as the residence times were low, between 0.5-1.5 days from lower to upper regions of both estuaries, it prevented the accumulation of nutrients. Previous modelling study conducted by Timmerman et al. (2010) of Horsens Estuary found that in a heavily tidally-exchange estuary, the reduction of N loadings resulted in a substantial decrease in nitrate concentrations (20-25%) in the entire estuary. This showed that even in highly flushed estuaries, local nutrient discharges from freshwater source could dominate nutrient concentrations in the estuary. It was also found that exchange of DIN between the sediment and the overlying water influenced the overall nitrate and ammonium concentration in these shallow estuaries. Ammonium has been found to be rather sensitive to sediment fluxes with the effect more pronounced in summer. The ammonium concentration was lower by 19-40% in various parts of Waikareao Estuary during summer. Model scenarios also demonstrated the sensitivity of such shallow estuaries to a sudden pulse of freshwater event in summer. The nutrient loads from such pulse events differ from freshwater

discharge rate due to sudden increase in discharge rate and lead to substantial increase in nutrient concentration in the water. While the model scenarios have been mainly simulated in winter and summer conditions, it must also be taken into account that climatological and inter-annual variability may induce changes in nutrient delivery into the estuaries. Tidal exchanges are the main influence on DIN concentrations in both Te Puna and Waikareao estuary, but from model scenarios, it was found that nitrate variation is primarily influenced by freshwater source, i.e. groundwater, stream, while ammonium variation can be attributed to sediment fluxes. In the Scheldt Estuary, model simulation indicated that a pronounced seasonal variability in nutrient recycling is resulted from the combined effect of biogeochemical transformations and nutrient flux imbalances, which arise from hydrological perturbations (Arndt et al. 2009). From Te Puna and Waikareao model simulations, hydrological perturbations have also been found to influence the nutrient concentration from upper to lower estuary's region.

In comparison to some shallow estuaries overseas (e.g. Lillebø et al. 2005; Neto et al. 2008; Timmermann et al. 2010) both Waikareao and Te Puna estuaries are not eutrophic. From both the 24-hour field experiments and modelling scenarios in Te Puna and Waikareao, it was found that tidal exchange exert a dominant control on nutrient concentrations. As mentioned above, even with increase stream DIN loadings scenarios, the overall estuary DIN concentration did not evoke major changes as the residence times of both Te Puna and Waikareao estuaries are very low (hours to 1.5 days). This lessens and prevents the accumulation of nutrients within the estuaries.

The last component of this thesis investigates the temporal variations in porewater discharge in the tidal flat embayment in Waikareao Estuary. The temporal scale examined in this component has revealed that the nutrient concentrations showed seasonal patterns with higher variability observed in winter and summer. The higher seasonal variability of ammonium in summer at Waikareao's tidal flat is also observed at Chesapeake Bay (Kemp et al. 1990). The relatively higher rates of ammonium recycling at higher temperature at Chesapeake Bay were attributable to the decline in nitrification and denitrification in summer. The porewater nutrient profiles also change with depth with nitrate being the dominant form of dissolved N at the surface sediment and ammonium dominated the mid-

regions. The porewater DIN collected was mostly influenced by sediment recycling processes instead of groundwater discharge as the average salinity was >15 and did not show freshwater pulses with increasing depth. Ammonium concentrations were influenced primarily by estuarine sediment processes while the main sources of nitrate were likely to be from freshwater discharge as shown with higher concentrations measured at Kopurereroa Stream. The importance of tidal flat areas as sites of efficient nutrient turnover has been examined by several studies overseas (Rocha 1998; D'Andrea et al. 2002; Beck et al. 2008). However, there are limited studies (e.g. Sandwell et al. 2009) concerning the behaviour of nutrients in tidal flats in New Zealand. Chapter 6 and sediment modelling scenarios demonstrated the contribution of pore-water nutrients and sediment fluxes into Waikareao Estuary, it also higlighted the importance of sediment as an ammonium source. These results reinforce the importance of nutrient recycling from intertidal sediments.

This thesis highlighted the likely causes of dissolved inorganic nutrient variations in Tauranga Harbour. Figure 7.1 summarizes the main biogeochemical and hydrodynamic processes influencing the DIN variations in both Te Puna and Waikareao estuaries. DIN concentrations are subjected to physical forcings (tidal exchange, stream input, pore-water seepage, groundwater seepage, and wind-induced mixing) that can influence the rate of mixing, transport and recycling rate. From field measurements and numerical modelling, it was found that sediment processes predominantly influence ammonium, while nitrate main source is from freshwater input.

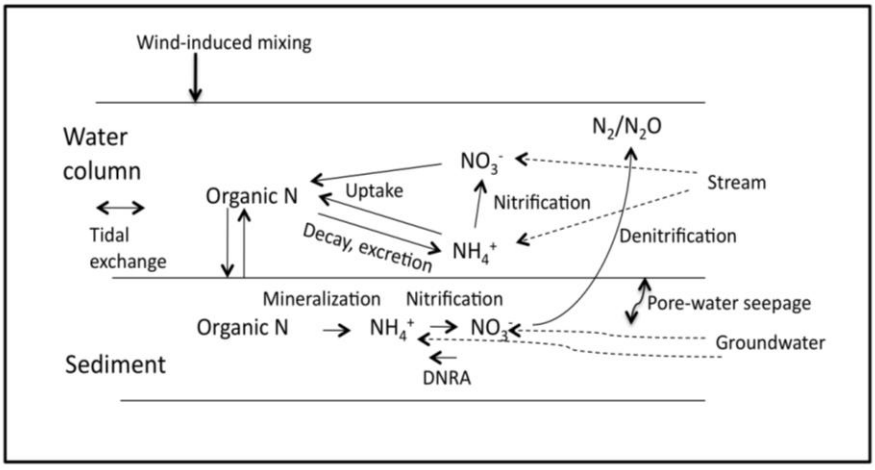

Figure 7.1 Schematic of the key hydrodynamic and biogeochemical processes in Te Puna and Waikareao estuaries (nitrogen cycle adapted from Herbert 1999).

7.2 Future work and recommendations

This study demonstrates the need for further research on the processes controlling the rates and distribution of DIN fluxes and discharge in shallow estuaries. Future research should couple studies of hydrodynamics, hydrochemistry and biogeochemistry to better predict the effects of nutrient fluxes on the ecology of the shallow estuaries and the adjacent harbour communities. The first objective of this study has shown that nutrient fluxes changed over short-time scales and inter-annually. The temporal pattern observed in this study is not yet fully understood and thus further research in Te Puna and Waikareao sites, as well as in similar locations would be very beneficial. Such a study should be expanded to include more frequent measurements of physical properties and nutrient concentrations to provide an enhanced understanding of the inter-annual pattern and the influence of harbour activities on estuarine nutrient concentrations.

The computational requirements of a fully coupled 3D hydrodynamic-ecological model place major constraints on the ability to carry out multiple model runs and extensive parameters calibrations. In this study, temporally varying results of the southern basin of Tauranga Harbour simulations were used to force open boundaries of Te Puna and Waikareao Estuaries, a step forward in investigation of the influence of a large basin on smaller coastal systems. This approach is based on assumption that the estuaries have no impact on the adjacent sea, however, in reality outgoing water from the estuaries would mix with marine waters and be reintroduced into the estuaries on the incoming time. The next step in this work would be to employ a fully coupled model in which the estuaries and the harbour could be simulated concurrently and exchange between the two systems looked at in detail. This however involves a substantial investment in resources and detailed surveys of the harbour bathymetry to adapt the model and would require a significant increase in the computing capacity used in this study. Multi-year simulations would also be valuable for investigation of inter-annual variations in N cycling the harbour, in addition to the assessment of the impact of changes in harbour dredging, opening of bypass at Ruahihi Power Station, management practices and water quality of the harbour on estuaries nutrient cycle. Again, this would also require a significant increase in computing capacity required and is currently not practical for this study.

The nutrient data from the high frequency sampling and groundwater study have suggested the importance of nitrogen cycling processes occurring within the estuaries. The nitrogen cycling cannot be fully understood by only examining the concentrations of nutrient species and their fluxes alone. If nitrogen isotopes were examined simultaneously, a better understanding of the cycling mechanism would be gained. A study to determine if nitrogen discharging from the tidal flat and estuary is primarily derived from fresh groundwater or from other sources would be particularly useful. Nitrogen isotopic methods may not alone fully address this question, as there are multiple sources, reactions and transport. There is also a potential for isotopic enrichment experiments. If the fate of nitrate was well understood, conclusions could be drawn regarding the remainder of the nitrogen cycle and thus the relationship between the estuary water column and groundwater processes.

This study also demonstrated that porewater discharges and the associated nutrient discharges occurred in the tidal flat area of Waikareao Estuary. The relationship between groundwater processes and shallow estuary processes is not yet fully understood and thus further research at Waikareao Estuary site, as well as in similar locations in the harbour would be beneficial. Such a study should be expanded to include additional parameters and more frequent measurements of discharge and nutrient concentrations to provide an enhanced understanding of the inter-annual cycles and a more precise determination of discharge rate. Ideally, such a study should examine the tidal level on discharge rates, perhaps taking advantage of the temporal resolution provided by modern automated seepage meters and radon measurements.

All of the ideas mentioned above for future research have one specific aim, which is to have a better understanding of the harbour/estuarine boundaries and within the estuaries. The hydrodynamics, chemical, biological and hydrological aspects of these relationships should all be examined. It is doubtful that any one study will be able to fully address all of these aspects, however a better understanding of any of these four aspects would be beneficial. The knowledge that could be gained from further research at Tauranga Harbour and its sub-estuaries would be extremely important to the understanding of coastal nutrient cycling and the response of ecological assemblages that inhabit the shallow intertidal areas.

Tauranga Harbour provides a model system for experimental and numerical studies of estuarine processes. The harbour has a single entrance at the southern basin of the harbour, which makes it ideal to track the pathways of a water parcel as it enter and leave the harbour. The tidally dominated nature of the harbour, also allow for determination of possible sources of nutrients in the harbour.

References

Abrahim G, Parker R 2002. Heavy-metal contaminants in Tamaki Estuary: impact of city development and growth, Auckland, New Zealand. Environmental Geology 42: 883–890.

American Public Health Association, American Water Works Association, and Water Environment Federation 1992. Standard Methods for the Examination of Water and Wastewater. 18th Edition. American Public Health Office, Washington DC.

Andersson A, Haecky P, Hagström A 1994. Effect of temperature and light on the growth of micro-nano-and pico-plankton: impact on algal succession. Marine Biology 120: 511–520.

Arar EJ, Collins GB 1997. *In vitro* determination of chlorophyll *a* and pheophytin *a* in marine and freshwater algae by fluorescence. National Exposure Research Laboratory, Office of Research and Development, U.S. Environmental Protection Agency.

Arndt S, Regnier P, Vanderborght J-P 2009. Seasonally-resolved nutrient export fluxes and filtering capacities in a macrotidal estuary. Journal of Marine Systems 78: 42-58.

Balls PW 1994. Nutrient inputs to estuaries from nine Scottish east coast rivers; influence of estuarine processes on inputs to the North Sea. Estuarine, Coastal and Shelf Science 39: 329–352.

Barnett A 1985. Tauranga Harbour study: a report for the Bay of Plenty Board. Part I: Overview, Part III: Hydrodynamics. New Zealand Ministry of Works and Development.

Beca Carter Hollings and Ferner Ltd 1999. Guidelines for stormwater runoff modelling in the Auckland Region. Technical Report 108. 26 p.

Beck AJ, Tsukamoto Y, Tovar-Sanchez A, Huerta-Diaz M, Bokuniewicz HJ, Sañudo-Wilhelmy SA 2007. Importance of geochemical transformations in determining submarine groundwater discharge-derived trace metal and nutrient fluxes. Applied Geochemistry 22: 477–490.

Beck M, Dellwig O, Liebezeit G, Schnetger B, Brumsack HJ 2008. Spatial and seasonal variations of sulphate, dissolved organic carbon, and nutrients in deep pore waters of intertidal flat sediments. Estuarine, Coastal and Shelf Science 79: 307–316.

Becker ML, Luettich RA, Seim H 2009. Effects of intratidal and tidal range variability on circulation and salinity structure in the Cape Fear River Estuary, North Carolina. Journal of Geophysical Research 114, C04006, doi: 10.1029/2008JC004972.

Bell RG, Dumnov S, Williams BL, Greig MJN 1998. Hydrodynamics of Manukau Harbour, New Zealand. New Zealand Journal of Marine and Freshwater Research 32: 81-100.

Berounsky VM, Nixon SW 1990. Temperature and the annual cycle of nitrification in waters of Narraganset Bay. Limnology and Oceanography 35: 1610–1617.

Berounsky VM, Nixon SW 1993. Rates of nitrification along an estuarine gradient in Narragansett Bay. Estuaries 16: 718–730.

Billen G 1978. A budget of nitrogen recycling in North Sea sediments off the Belgian Coast. Estuarine and Coastal Marine Science 7: 127–146.

Billerbeck M, Werner U, Bosselmann K, Walpersdorf E, Huettel M 2006a. Nutrient release from an exposed intertidal sand flat. Marine Ecology Progress Series 316: 35–51.

Billerbeck M, Werner U, Polerecky L, Walpersdorf E, deBeer D, Huettel M 2006b. Surficial and deep pore water circulation governs spatial and temporal scales of nutrient recycling in intertidal sand flat sediment. Marine Ecology Progress Series 326: 61–76.

Black K 1984. Tauranga Harbour study: a report for the Bay of Plenty Board. Part IV: Sediment Transport. New Zealand Ministry of Works and Development.

Bond LD, Bredehoeft JD 1987. Origins of seawater intrusion in a coastal aquifer-a case study of the Pajaro Valley, California. Journal of Hydrology 92: 363–388.

Bowen JL, Kroeger KD, Tomasky G, Pabich WJ, Cole ML, Carmichael RH, Valiela I 2007. A review of land-sea coupling by groundwater discharge of nitrogen to New England estuaries: mechanisms and effects. Applied Geochemistry 22: 175–191.

Boynton WR, Kemp WM 1985. Nutrient regeneration and oxygen consumption by sediments along an estuarine salinity gradient. Marine Ecology Progress Series 23: 45–55.

Boynton WR, Garber JH, Summers R, Kemp WM 1995. Inputs, transformations and transport of nitrogen and phosphorus in Chesapeake Bay and selected tributaries. Estuaries 18: 285–314.

Brock DA 2001. Nitrogen budget for low and high freshwater inflows, Nueces Estuary, Texas. Estuaries 24: 509–521.

Burger DF 2006. Dynamics of internal nutrient loading in a eutrophic polymictic lake (Lake Rotorua, New Zealand). PhD Thesis, Department of Biological Sciences, University of Waikato, NZ. 139 p.

Burger DF, Hamilton DP, Pilditch CA 2008. Modelling the relative importance of internal and external nutrient loads on water column nutrient concentration and

phytoplankton biomass in a shallow polymictic lake. Ecological Modelling 211: 411–423.

Burkholder JM, Dickey DA, Kinder CA, Reed RE, Mallin MA, McIver MR, Cahoon LB, Melia, G, Brownie C, Smith J, Deamer N, Springer J, Glasgow HB, Toms D 2006. Comprehensive trend analysis of nutrients and related variables in a large eutrophic estuary: a decadal study of anthropogenic and climatic influences. Limnology and Oceanography 51: 463–487.

Burggraaf S, Langdon AG, Wilkins AL 1994. Organochlorine contaminants in sediments of the Tauranga Harbour, New Zealand. New Zealand Journal of Marine and Freshwater Research 28: 291–298.

Cabrita MT, Brotas V 2000. Seasonal variation in denitrification and dissolved nitrogen fluxes in intertidal sediments of the Tagus estuary, Portugal. Marine Ecology Progress Series 202: 51–65.

Caccia VG, Boyer JN 2005. Spatial patterning of water quality in Biscayne Bay, Florida as a function of land use and water management. Marine Pollution Bulletin 50: 1416–1429.

Caffrey JM, Cloern JE, Grenz C 1998. Changes in production and respiration during a spring phytoplankton bloom in San Francisco Bay, California, USA: implications for net ecosystem metabolism. Marine Ecology Progress Series 172: 1–12.

Caffrey JM, Harrington N, Solem I, Ward BB 2003. Biogeochemical processes in a small California estuary. 2. Nitrification activity, community structure and role in nitrogen budgets. Marine Ecology Progress Series 248: 27–40.

Caffrey JM 2004. Factors controlling net ecosystem metabolism in U.S. estuaries. Estuaries 27: 90–101.

Caffrey JM, Chapin, TP, Jannasch HW, Haskins JC 2007. High nutrient pulses, tidal mixing and biological response in a small California estuary: variability in nutrient concentrations from decadal to hourly time scale. Estuarine, Coastal and Shelf Science 71: 368–380.

Callender E, Hammond DE 1982. Nutrient exchange across the sediment water interface in the Potomoc River Estuary. Estuarine, Coastal and Shelf Science, 15: 395–413.

Cederwall H, Elmgren R 1990. Biological effects of eutrophication in the Baltic Sea, particularly the coastal zone. Ambio 19: 109–112.

Chagué-Goff C, Nichol SL, Jenkinson AV, Heijnis H 2000. Signatures of natural catastrophic events and anthropogenic impact in an estuarine environment, New Zealand. Marine Geology 167: 285–301.

Chambers RM, Harvey JW, Odum WE 1992. Ammonium and phosphate dynamics in a Virginia salt marsh. Estuaries 15: 349–359.

Chan TU, Hamilton DP, Robson BJ, Hodges BR, Dallimore C 2002. Impacts of hydrological changes on phytoplankton succession in the Swan River, Western Australia. Estuaries 25: 1406–1415.

Chang FH, Sharples J, Grieve JM 1996. Temporal and spatial distribution of toxic dinoflagellates in Bay of Plenty, New Zealand, during the early 1993 toxic shellfish outbreaks. In: Yasumoto T, Ohisma Y, Fukuyo Y eds. Harmful and toxic algal blooms. Proceedings of the seventh international conference on toxic phytoplankton, 12-16 July 1995, Sendai, Japan. Intergovernmental Oceanographic Commission of UNESCO 1996. Pp. 235–238.

Christian RR, Boyer JN, Stanley DW 1991. Multi-year distribution patterns of nutrients within the Neuse River Estuary, North Carolina. Marine Ecology Progress Series 71: 259–274.

Cole RG, Hull PJ, Healy TR 2000. Assemblage structure, spatial patterns, recruitment, and post-settlement mortality of subtidal bivalve mollusks in a large harbour in north-eastern New Zealand. New Zealand Journal of Marine and Freshwater Research 34: 317–329.

Corbett DR, Chanton J, Burnett W, Dillon K, Rutkowski C, Fourqurean JW 1999. Patterns of groundwater discharge into Florida Bay. Limnology and Oceanography 44: 1045–1055.

Corbett DR, Kump L, Dillon K, Burnett W, Chanton J 2000. Fate of wastewater-borne nutrients under low discharge conditions in the subsurface of the Florida Keys, USA. Marine Chemistry 69: 99–115.

Correll DL, Jordan TE, Weller DE 1992. Nutrient flux in a landscape effects of coastal land use and terrestrial community mosaic of nutrient transport to coastal waters. Estuaries 15: 431–442.

Cowan JL, Boynton WR 1996. Sediment-water oxygen and nutrient exchanges along the longitudinal axis of Chesapeake Bay: seasonal patterns, controlling factors and ecological significance. Estuaries 19: 562–580.

D'Andrea AF, Aller, RC, Lopez GR 2002. Organic matter flux and reactivity on a South Carolina sandflat: the impacts of porewater advection and macrobiological structures. Limnology and Oceanography 47: 1056–1070.

D'Avanzo CD, Kremer JN, Wainright S 1996. Ecosystem production and respiration in response to eutrophication in shallow temperate estuaries. Marine Ecology Progress Series 141: 263–274.

Dähnke K, Bahlmann E, Emeis K 2008. A nitrate sink in estuaries? An assessment by means of stable nitrate isotopes in the Elbe estuary. Limnology and Oceanography 53: 1504–1511.

Dale RK, Miller DC 2007. Spatial and temporal patterns of salinity and temperature an intertidal groundwater seep. Estuarine, Coastal and Shelf Science 72: 283–298.

Dalsgaard T 2003. Benthic primary production and nutrient cycling in sediments with benthic microalgae and transient accumulation of macroalgae. Limnology and Oceanography 48: 2138–2150.

Davies-Colley RJ, Healy TR 1978. Sediment and hydrodynamics of the Tauranga entrance to Tauranga Harbour. New Zealand Journal of Marine and Freshwater Research 12: 225–236.

Dauer DM, Weinsberg, SB, Ranasinghe JA 2000. Relationship between benthic community condition, water quality, sediment quality, nutrient loads and land use patterns in Chesapeake Bay. Estuaries 23: 80–96.

de Beer D, Wenzhöfer F, Ferdelman TG, Boehme SE, Huettel M, van Beusekom JEE, Böttcher ME, Musat N, Dubilier N 2005. Transport and mineralization rates in North Sea sandy intertidal sediments, Sylt- Rømø Basin, Wadden Sea. Limnology and Oceanography 50: 113–127.

Deborde J, Anschutz P, Auby I, Glé C, Commarieu M-V, Maurer D, Lecroart P, Abril G 2008. Role of tidal pumping on nutrient cycling in a temperate lagoon (Arcachon Bay, France). Marine Chemistry 109: 98–114.

DiLorenzo JL, Filadelfo RJ, Surak CR, Litwack HS, Gunawardana VK, Najarian TO 2004. Tidal variability in the water quality of an urbanized estuary. Estuaries 27: 851–860.

Doney SC, Glover DM, Najjar RG 1996. A new coupled, one-dimensional biological-physical model for the upper ocean: applications to the JGOFS Bermuda Atlantic Time-series Study (BATS) site. Deep Sea Research II 43: 591–624.

Dong LF, Nedwell DB, Stott A 2006. Sources of nitrogen used for denitrification and nitrous oxide formation in sediments of the hypernutrified Colne, the nitrified Humber, and the oligotrophic Conwy estuaries, United Kingdom. Limnology and Oceanography 51: 545–557.

Drever J 1982. The geochemistry of natural waters: surface and groundwater environments. Prentice-Hall, New Jersey. 388 p.

Environment Bay of Plenty Regional Council. Tauranga Moana (The Tauranga Harbour). Resource Planning Publication 97/2. 35 p.

Evans EC, McGregor GR, Petts GE 1998. River energy budgets with special reference to river bed processes. Hydrological Processes 12: 575–595.

Eyre BD 1993. Nutrients in the sediments of a tropical north-eastern Australian Estuary, catchment and nearshore coastal zone. Australian Journal of Marine and Freshwater Research 44: 845–866.

Eyre BD, Ferguson AJP 2005. Benthic metabolism and nitrogen cycling in a subtropical East Australian estuary (Brunswick): temporal variability and controlling factors. Limnology and Oceanography 50: 81–96.

Falco S, Niencheski LF, Rodilla M, Romero I, del Río J, Sierra J, Mösso C 2010. Nutrient flux and budget in Ebro estuary. Estuarine, Coastal and Shelf Science 87: 92–102.

Falkowski PG 1997. Evolution of the nitrogen cycle and its influence on the biological sequestration of CO_2 in the ocean. Nature 387: 272–275

Fisher TR, Carlson PR, Barber RT 1982. Sediment nutrient regeneration in three North Carolina Estuaries, Estuarine, Coastal and Shelf Science 14: 101–116.

Francis CA, Beman JM, Kuypers MMM 2007. New processes and players in the nitrogen cycle: the microbial ecology of anaerobic and archaeal ammonia oxidation. International Society of Microbial Ecology 1: 19–27.

Galloway JN, Dentener FJ, Capone DG, Boyer EW, Howarth RW, Seitzinger SP, Asner GP, Clevelad CC, Green PA, Holland EA, Karl DM, Michaels AF, Porter JH, Townsend AR, Vörösmarty CJ 2004. Nitrogen cycles: past, present and future. Biogeochemistry 70: 153–226.

Gameiro C, Cartaxana P, Brotas V 2007. Environmental drivers of phytoplankton distribution and composition in Tagus Estuary, Portugal. Estuarine, Coastal and Shelf Science 75: 21–34.

Gardner WS, McCarthy MJ, Soonmo A, Sobolev D, Sell KS, Brock D 2006. Nitrogen fixation and dissimilatory nitrate reduction to ammonium (DNRA) support nitrogen dynamics in Texas estuaries. Limnology and Oceanography 51: 558–568.

Gardner LR, Kjerfve B 2006. Tidal fluxes of nutrients and suspended sediments at the North Inlet-Winyah Bay National Estuarine Research Reserve 70: 682–692.

Garnier J, Billen G, Némery J, Sebilo M 2010. Transformations of nutrients (N, P, Si) in the turbidity maximum zone of the Seine Estuary and export to the sea. Estuarine, Coastal and Shelf Science 90: 129–141.

Geyer WR 1997. Influence of wind on dynamics and flushing of shallow estuaries. Estuarine, Coastal and Shelf Sciences 44: 713–722.

Gibbs M, Ross A, Downes M 2002. Nutrient cycling and fluxes in Beatrix Bay, Pelorus Sound, New Zealand. New Zealand Journal of Marine and Freshwater Research 36: 675–697.

Giblin AE, Gaines AG 1990. Nitrogen inputs to a marine embayment: the importance of groundwater. Biogeochemistry 10: 309–328.

Gordon DC, Boudreau PR, Mann KH, Ong JE, Silvert WL, Smith SV, Wattayakorn G, Wulff F, Yanagi T 1996. LOICZ biogeochemical modelling guidelines. LOICZ Report and Studies No. 5, Texel, Netherlands. 96p. http://nest.su.se/mnode/ [accessed October 2007].

Grall J, Chauvaud, L 2002. Marine eutrophication and benthos: the need for new approaches and concepts. Global Change Biology 8: 813–830.

Grelowski A, Pastuszak M, Sitek S, Witek Z 2000. Budget calculations of nitrogen, phosphorus and BOD5 passing through the Oder estuary. Journal of Marine Systems 25: 221–237.

Guarini JM, Blanchard GF, Gros P, Harrison SJ 1997. Modelling the mud surface temperature on intertidal flats to investigate the spatio-temporal dynamics of the benthic microalgal photosynthetic capacity. Marine Ecology Progress Series 153: 25-36.

Hamilton DP, Schladow SG 1997. Prediction of water quality in lakes and reservoirs. Part I- model description. Ecological Modelling 96: 91–110.

Hamilton D, McBride C, Uraoka T 2005. Lake Rotoiti fieldwork and modelling to support considerations of Ohau channel diversion from Lake Rotoiti. Centre of Biodiversity and Ecology Research Report. 110 p.

Hamilton DP, Douglas GB, Adeney JA, Radke LC 2006. Seasonal changes in major ions, nutrients and chlorophyll a at two sites in the Swan River estuary, Western Australia. Marine and Freshwater Research 57:803–815.

Harding L 1994. Long-term trends in the distribution of phytoplankton in Chesapeake Bay: roles of light, nutrients and streamflow. Marine Ecology Progress Series 104: 267–291.

Harrison SJ, Phizacklea AP 1987a. Temperature fluctuation in muddy intertidal sediments, Forth Estuary, Scotland. Estuarine, Coastal and Shelf Science 24: 279–288.

Harrison SJ, Phizacklea AP 1987b. Vertical temperature gradients in muddy intertidal sediments in the Forth Estuary, Scotland. Limnology and Oceanography 32: 954–963.

Harvey JW, Nuttle WK 1995. Fluxes of water and solute in a coastal wetland sediment. 2. Effects of macropores on solute exchange with surface water. Journal of Hydrology 164: 109-125.

Healy TR 1985. Tauranga Harbour study: a report for the Bay of Plenty Board. Part II: Field data collection programme, Part V: Morphological Study.

Healy TR, Kirk RM 1992. Coasts. In: Soons JM, Selby MJ eds. Landforms of New Zealand. 2nd Edition. Auckland, New Zealand, Longman Paul Ltd. Pp. 81–104.

Heath RA 1976. Broad classification of New Zealand inlets with emphasis on residence times. New Zealand Journal of Marine and Freshwater Research 10: 429–444.

Heath RA 1977. Heat balance in a small coastal inlet Pauatahanui Inlet, North Island, New Zealand. Estuarine and Coastal Marine Science 5: 783–792.

Heath RA 1985. A review of the physical oceanography of the seas around New Zealand-1982. New Zealand Journal of Marine and Freshwater Research 19: 79–124.

Heggie K, Savage C 2009. Nitrogen yields from New Zealand coastal catchments to receiving estuaries. New Zealand Journal of Marine and Freshwater Research 43: 1039–1052.

Herbert RA 1999. Nitrogen cycling in coastal marine ecosystems. FEMS Microbiology Reviews 23: 563–590.

Hewitt A 1993. New Zealand Soil Classification. Landcare Research Science Series 1. Landcare Research New Zealand Ltd, Lincoln. 133 p.

Hipsey M, Romero J, Antenucci J, Hamilton D 2006a. Computational Aquatic Ecosystem Dynamics Model: CAEDYM v2.3 Science Manual. Centre for Water Research, University of Western Australia, Nedlands, WA 6907, Australia.

Hipsey M, Gal G, Antenucci J, Zohary T, Makler V, Imberger J 2006b. Lake Kinneret water quality modelling system. In: The 7th International Conference on Hydroscience and Engineering (ICHE-2006), 10-13 September 2006, Philadelphia, USA.

Hodges BR, Imberger J, Saggio A, Winters KB 2000. Modelling basin scale waves in a stratified lake. Limnology and Oceanography 45: 1603–1620.

Hodges BR, Dallimore C 2001. Estuary and Lake Computer Model: ELCOM Science Manual Version 2.2. Centre for Water Research, University of Western Australia, Perth.

Holm NP, Armstrong DE 1981. Role of nutrient limitation and competition in controlling the populations of Asterionella Formosa and Microcystis aeruginosa in semicontinuous culture. Limnology and Oceanography 26: 622–634.

Hou LJ, Liu M, Xu SY, Ou DN, Yu J, Cheng SB, Ling X, Yang Y 2007. The effects of semi-lunar spring and neap tidal change on nitrification, denitrification and N_2O vertical distribution in the intertidal sediments of the Yangtze estuary, China. Estuarine, Coastal and Shelf Science 73: 607–616.

Howarth RW 1988. Nutrient limitation of net primary production in marine ecosystems. Annual Review of Ecological System 19: 89-110.

Howarth RW, Schneider R, Swaney D 1996. Metabolism and organic carbon fluxes in the tidal freshwater Hudson River. Estuaries 19: 848–865.

Howarth RW, Swaney DP, Butler TJ, Marino R 2000. Climatic control on eutrophication of the Hudson River Estuary. Ecosystems 3: 210–215.

Howarth RW, Sharpley A, Walker D 2002. Sources of nutrient pollution to coastal waters in the United States: implications for achieving coastal water quality goals. Estuaries 25: 656–676.

Howarth RW, Marino R 2006. Nitrogen as the limiting nutrient for eutrophication in coastal marine ecosystems: evolving views over three decades. Limnology and Oceanography 51: 364-376.

Hubertz ED, Cahoon LB 1999. Short-term variability of water quality parameters in two shallow estuaries of North Carolina. Estuaries 22: 814–823.

Huettel M, Gust G 1992. Impact of bioroughness on interfacial solute exchange in permeable sediments. Marine Ecology Progress Series 89: 253–267.

Huettel M, Ziebis W, Forster S 1996. Flow-induced uptake of particulate matter in permeable sediments. Limnology and Oceanography 41: 309–322.

Huettel M, Ziebis W, Forster S, Luther GW 1998. Advective transport affecting metal and nutrient distributions and interfacial fluxes in permeable sediments. Geochmica et Cosmochimica Acta 62: 613–631.

Hume TM, Snelder T, Weatherhead M, Liefting R 2007. A controlling factor approach to estuary classification. Ocean and Coastal Management 50: 905–929.

Hume TM, Green MO, Elliott S 2009. Tauranga Harbour sediment study: assessment of predictions for management. NIWA Client Report HAM2009-139 December 2009 for Environment Bay of Plenty.

Jahnke RA, Alexander CR, Kostka JE 2003. Advective pore water input of nutrients to the Satilla River Estuary, Georgia, USA. Estuarine, Coastal and Shelf Science 56: 641–653.

Ji Z 2008. Hydrodynamics and water quality: modelling rivers, lakes, and estuaries. John Wiley & Sons Inc., New Jersey. 676 p.

Johannes RE, Hearn CJ 1985. The effect of submarine groundwater discharge of nutrient and salinity regimes in a coastal lagoon off Perth, Western Australia. Estuarine, Coastal and Shelf Science 21: 789–800.

Jordan TE, Correll DL 1985. Nutrient chemistry and hydrology of interstitial water in brackish tidal marshes of Chesapeake Bay. Estuarine, Coastal and Shelf Science 21: 45-55.

Jordan TE, Correll DL, Miklas J, Weller DE 1991. Nutrients and chlorophyll at the interface of a watershed and an estuary. Limnology and Oceanography 36: 251–267.

Kelly JR 1997. Nitrogen flow and the interaction of Boston Harbour with Massachusetts Bay. Estuaries 20: 365–380.

Kemp WM, Sampou P, Caffrey J, Mayer M, Henriksen K, Boynton WR 1990. Ammonium recycling versus denitrification in Chesapeake Bay sediments. Limnology and Oceanography 35: 1545–1563.

Kim T-W, Cho Y-K, Dever EP 2007. An evaluation of the thermal properties and albedo of a macrotidal flat. Journal of Geophysical Research 112, C12009, doi:10.1029/2006JC004015.

Koop K, Boynton WR, Wulff F, Carman R 1990. Sediment-water oxygen and nutrient exchanges along a depth gradient in the Baltic Sea. Marine Ecology Progress Series 63: 65–77.

Korom SF 1992. Natural denitrification in the saturated zone: a review. Water Resources Research 28: 1657–1668.

Kroeger KD, Swarzenski PW, Greenwood WJ, Reich C 2007. Submarine groundwater discharge to Tampa Bay: nutrient fluxes and biogeochemistry of the coastal aquifer. Marine Chemistry 104: 85–97.

Kroeger KD, Charette MA 2008. Nitrogen biogeochemistry of submarine groundwater discharge. Limnology and Oceanography 53: 1025–1039.

Krüger JC, Healy TR 2006. Mapping the morphology of a dredged ebb tidal delta, Tauranga Harbour, New Zealand. Journal of Coastal Research 22: 720–727.

Lacroix G, Ruddick K, Gypen N, Lancelot C 2007. Modelling the relative impact of rivers (Scheldt/Rhine/Seine) and Western Channel waters on the nutrient and diatoms/ *Phaeocystis* distributions in Belgian waters (Southern North Sea). Continental Shelf Research 27: 1422–1446.

Lampman GG, Caraco NF, Cole JJ 1999. Spatial and temporal patterns of nutrient concentration and export in the tidal Hudson River. Estuaries 22: 285–296.

Latimer JS, Charpentier MA 2010. Nitrogen inputs to seventy-four southern New England estuaries: application of a watershed nitrogen loading model. Estuarine, Coastal and Shelf Science 89: 125–136.

Le Hir P, Roberts W, Cazaillet O, Christie M, Bassoullet P, Bacher C 2000. Characterization of intertidal flat hydrodynamics. Continental Shelf Research 20: 1433–1459.

Li M, Gargett A, Denman K 2000. What determines seasonal and interannual variability of phytoplankton and zooplankton in strongly estuarine systems? Application to the semi-enclosed estuary of Strait of Georgia and Juan de Fuca Strait. Estuarine, Coastal and Shelf Science 50: 467–488.

Lillebø AI, Neto JM, Martins I, Verdelhos T, Leston S, Cardoso PG, Ferreira SM, Marques JC, Pardal MA 2005. Management of a shallow temperate estuary to control eutrophication: the effect of hydrodynamics on the system's nutrient loading. Estuarine, Coastal and Shelf Science 65: 697–707.

Lima ID, Doney SC 2004. A three-dimensional, multinutrient, and size-structured ecosystem model for the North Atlantic. Global Biogeochemical Cycles 18, GB3019, doi:10.1029/2003GB002146.

Liu G, Chai F 2009. Seasonal and interannual variation of physical and biological processes during 1994-2001 in the Sea of Japan/East Sea: a three-dimensional physical-biogeochemical modelling study. Journal of Marine Systems 78: 265–277.

Longdill PC, Healy TR, Black KP 2008. Transient wind-driven coastal upwelling on a shelf with varying width and orientation. New Zealand Journal of Marine and Freshwater Research 42: 181–196.

Lucas LV, Cloern JE, Thompson JK, Monsen NE 2002. Functional variability of habitats within the Sacramento-San Joaquin Delta: restoration implications. Ecological Applications 12: 1528–1547.

MacCready P 1999. Estuarine adjustment to changes in river flow and tidal mixing. Journal of Physical Oceanography 29: 708–726.

Magnien RE, Summers RM, Sellner KG 1992. External nutrient sources, internal nutrient pools, and phytoplankton production in Chesapeake Bay. Estuaries 15: 497–516.

Malone TC, Crocker LH, Pike SE, Wendler BW 1988. Influences of river flow on the dynamics of phytoplankton production in a partially stratified estuary. Marine Ecology Progress Series 48: 235–249.

Marra J, Ho C 1993. Initiation of the spring bloom in the northeast Atlantic (47^{o}N, 20^{o}W): a numerical simulation. Deep Sea Research II 40: 55–73.

Marinelli RL, Williams TJ 2003. Evidence for density-dependent effects on infauna on sediment biogeochemistry and benthic-pelagic coupling in the nearshore systems. Estuarine, Coastal and Shelf Science 57: 179-192.

McLeod RJ, Wing SR 2008. Influence of an altered salinity regime on the population structure of two infaunal bivalve species. Estuarine Coastal and Shelf Science 78: 529–540.

Melloul AJ, Goldenberg LC 1997. Monitoring of seawater intrusion in coastal aquifers: basics and local concerns. Journal of Environmental Management 51: 73–86.

Michel P, Boutier B, Chiffoleau, JF 2000. Net fluxes of dissolved arsenic, cadmium, copper, zinc, nitrogen and phosphorus from the Gironde Estuary (France): Seasonal variations and trends. Estuarine, Coastal and Shelf Science 51: 451–462.

Miller DC, Ullman WJ 2004. Ecological consequences of groundwater discharge to Delaware Bay, United States. Groundwater 72: 959–970.

Missaghi S, Hondzo M 2010. Evaluation and application of a three-dimensional water quality model in a shallow lake with complex morphometry. Ecological Modelling 221: 1512–1525.

Møhlenberg F, Petersen S, Petersen AH, Gameiro C 2007. Long-term trends and short-term variability of water quality in Skive Fjord, Denmark- nutrient load and mussels are the primary pressures and drivers that influence water quality. Environmental Monitoring and Assessments 127: 503–521.

Monsen NE, Cloern JE, Lucas LV, Monismith SG 2002. A comment on the use of flushing time, residence time, and age as transport time scales. Limnology and Oceanography 47: 1545–1553.

Moore JK, Doney SC, Klypas JA, Glover DM, Fung IY 2002. An intermediate complexity marine ecosystem model for the global domain. Deep Sea Research II 49: 403–462.

Moore W 1999. The subterranean estuary: a reaction zone of groundwater and seawater. Marine Chemistry 65: 111–125.

Murray L, Mudge S, Newton A, Icely J 2006. The effect of benthic sediments on dissolved nutrient concentrations and fluxes. Biogeochemistry 81: 159–178.

Neto JM, Flindt MR, Marques JC, Pardal MA 2008. Modelling nutrient mass balance in a temperate meso-tidal estuary: implications for management. Estuarine, Coastal and Shelf Science 76: 175-185.

Neumann T 2007. The fate of river-borne nitrogen in the Baltic Sea- an example for the River Oder. Estuarine, Coastal and Shelf Science 73: 1–7.

Newsome P, Wilde R, Willoughby E 2000. Land resource information system spatial data layers, Volume 1. Landcare Research New Zealand Ltd. 81 p.

Nielsen P 1990. Tidal dynamics of the water table in beaches. Water Resources Research 26: 2127–2134.

Nielsen K, Nielsen LP, Rasmussen P 1995. Estuarine nitrogen retention independently estimated by the denitrification rate and mass balance methods: a study of Norminde Fjord, Denmark. Marine Ecology Progress Series 119: 275–283.

Nixon SW, Oviat CA, Hale SS 1976. Nitrogen regeneration and the metabolism of coastal marine bottom communities. In: Anderson JM, Macfayden A eds., The role of terrestrial and aquatic organisms in decomposition processes, Blackwell Scientific Publications, Oxford. 269–283.

Nixon SW 1981. Remineralization and nutrient cycling in coastal marine ecosystems. In: Neilson BJ, Cronin LE eds. Estuaries and nutrients. Clifton, New Jersey, Havana Press. Pp 111–138

Nowicki BL, Kelly JR, Requintina E, van Keuren D 1997. Nitrogen losses through sediment denitrification in Boston Harbour and Massachusetts Bay. Estuaries 20: 626–639.

Nowicki BL, Requintina E, van Keuren D, Portnoy, J 1999. The role of sediment denitrification in reducing groundwater-derived nitrate inputs to Nauset Marsh Estuary, Cape Cod, Massachusetts. Estuaries 22: 245–259.

Oberdorfer JA, Valentino MA Smith SV 1990. Groundwater contribution to the nutrient budget of Tomales Bay, California. Biogeochemistry 10: 199–216.

Ogilvie B, Nedwell DB, Harrison RM, Robinson A, Sage A 1997. High nitrate, muddy estuaries as nitrogen sinks: the nitrogen budget of the River Colne estuary (United Kingdom). Marine Ecology Progress Series 150: 217–228.

Oldman JW, Black KP, Swales A, Stroud MJ 2009. Prediction of annual average sedimentation rates in an estuary using numerical models with verification against core data-Mahurangi Estuary, New Zealand. Estuarine, Coastal and Shelf Science 84: 483–492.

Paerl HW 1997. Coastal eutrophication and harmful algal blooms: importance of atmospheric deposition and groundwater as "new" nitrogen and other nutrient sources. Limnology and Oceanography 42: 1154–1165.

Paerl HW, Valdes LM, Peierls BL, Adolf JE, Harding LW 2006. Anthropogenic and climatic influences on the eutrophication of large estuarine ecosystems. Limnology and Oceanography 51: 448–462.

Page HM, Petty RL, Meade DE 1995. Influence of watershed runoff on nutrient dynamics in a Southern California salt marsh. Estuarine, Coastal and Shelf Science 41: 163–180.

Parfitt RL, Schipper LA, Baisden WT, Elliott AH 2006. Nitrogen inputs and outputs for New Zealand in 2001 at national and regional scales. Biogeochemistry 80: 71–88.

Parfitt RL, Baisden WT, Elliot AH 2008. Phosphorus inputs and outputs for New Zealand at national and regional scales. Journal of the Royal Society of New Zealand 38: 37–50.

Park S 2004. Aspects of mangrove distribution and abundance in Tauranga Harbour. Environment Bay of Plenty Environmental Publication 2004/16. 40 p.

Park S 2005. Bay of Plenty coastal water quality 2003–2004. Report No. 2005/13. Environment Bay of Plenty, Whakatane, NZ. 86 p.

Pelegrí SP, Nielsen LP, Blackburn TH 1994. Denitrification in estuarine sediment stimulated by the irrigation activity of the amphipod *Corophium volutator*. Marine Ecology Progress Series 105: 285–290.

Pereira-Filho J, Schettini CAF, Rörig L, Siegle E 2001. Intratidal variation and net transport of dissolved inorganic nutrients, POC and chlorophyll a in the Camboriú River Estuary, Brazil. Estuarine, Coastal and Shelf Science 53: 249–257.

Piehler MF, Dyble J, Moissander PH, Pinckney JL, Paerl HW 2002. Effects of modified nutrient concentrations and ratios on the structure and function of the

native phytoplankton community in the Neuse River Estuary, North Carolina, USA. Aquatic Ecology 36: 371–385.

Pinckney JL, Paerl HW, Harrington MB 1999. Responses of the phytoplankton community growth rate to nutrient pulses in variable estuarine environments. Journal of Phycology 35: 1455–1463.

Precht E, Huettel M 2003. Advective pore-water exchange driven by surface gravity waves and its ecological implications. Limnology and Oceanography 48: 1674–1684.

Proctor R, Hadfiled M 1998. Numerical investigation into the effect of freshwater inputs on the circulation in Pelorus Sound, New Zealand. New Zealand Journal of Marine and Freshwater Research 32: 467-482.

Quinn JM, Stroud MJ 2002. Water quality and sediment and nutrient export from New Zealand hill-land catchments of contrasting land use. New Zealand Journal of Marine and Freshwater Research 36: 409–429.

Rabouille C, Mackenzie FT, Ver LM 2001. Influence of the human perturbation on carbon, nitrogen, and oxygen biogeochemical cycles in the global coastal ocean. Biogeochemistry 65: 3615–3641.

Ram ASP, Nair S, Chandramohan D 2003. Seasonal shift in net ecosystem production in a tropical estuary. Limnology and Oceanography 48: 1601–1607.

Rao YR, Marvin CH, Zhao J 2009. Application of a numerical model for circulation, temperature and pollutant distribution in Hamilton Harbour. Journal of Great Lakes Research 35: 61–73.

Raymond PA, Bauer JE, Cole JJ 2000. Atmospheric CO_2 evasion, dissolved inorganic carbon production, and net heterotrophy in the York River Estuary. Limnology and Oceanography 45: 1707–1717.

Reeve GMD 2008. Sedimentation and hydrodynamics *of Whitianga Estuary*. MSc Thesis (Earth and Ocean Sciences), University of Waikato, 176 p.

Rivett MO, Buss SR, Morgan P, Smith JWN, Bemment CD 2008. Nitrate attenuation in groundwater: a review of biogeochemical controlling processes. Water Research 42: 4215–4232.

Robson BJ, Hamilton DP 2003. Summer flow even induces a cyanobacterial bloom in a seasonal Western Australia estuary. Marine and Freshwater Research 54: 139–151.

Robson BJ, Hamilton DP 2004. Three dimensional modelling of *Microcystis* bloom event in the Swan River Estuary, Western Australia. Ecological Modelling 174: 203–222.

Robinson C, Gibbes B, Carey H, Li L 2007a. Salt-freshwater dynamics in a subterranean estuary over a spring-neap tidal cycle. Journal of Geophysical Research 112, C09007,doi10.1029/2006JC003888.

Robinson C, Li L, Prommer H 2007b. Tide-induced recirculation across the aquifer-ocean interface. Water Resources Research 43, W07428, doi:10.1029/2006WR005679.

Rocha C 1998. Rhythmic ammonium regeneration and flushing of intertidal sediments of the Sado Estuary. Limnology and Oceanography 43: 823–831.

Rocha C, Cabral AP 1998. The influence of tidal action on porewater nitrate concentration and dynamics in intertidal sediments of the Sado Estuary. Estuaries 21: 635–645.

Romero J, Antenucci J, Imberger J 2004. One-and three-dimensional biogeochemical simulations of two differing reservoirs. Ecological Modelling 174: 143–160.

Roper D 1990. Benthos associated with an estuarine outfall, Tauranga Harbour, New Zealand. New Zealand Journal of Marine and Freshwater Research 24: 487–498.

Rosenberg R, Elmgren R, Fleischer S, Jonsson P, Persson G, Dahlin H 1990. Marine eutrophication case studies in Sweden. Ambio 19: 102–108.

Rueda FJ, Schladow SG, Monismith SG, Stacey MT 2005. On the effects of topography on wind and the generation of currents in a large multi-basin lake. Hydrobiologia 532: 139–151.

Russell MJ, Montagna PA, Kalke RD 2006. The effect of freshwater inflow on net ecosystem metabolism in Lavaca Bay, Texas. Estuarine, Coastal and Shelf Science 68: 231–244.

Russell MJ, Montagna PA 2007. Spatial and temporal variability and drivers of net ecosystem metabolism in Western Gulf of Mexico estuaries. Estuaries and Coasts 30: 137–153.

Saenger C, Cronin TM, Willard D, Halka J, Kerhin R 2008. Increased terrestrial to ocean sediment and carbon fluxes in the northern Chesapeake Bay associated with twentieth century land alteration. Estuaries and Coasts 31: 492–500.

Sandwell DR, Pilditch CA, Lohrer AM 2009. Density dependent effects of an infaunal suspension-feeding bivalve (*Austrovenus stutchburyi*) on sandflat nutrient fluxes and microphytobenthic productivity. Journal of Experimental Marine Biology and Ecology 373: 16–25.

Santoro AE 2010. Microbial nitrogen cycling at the saltwater-freshwater interface. Hydrogeology Journal 18: 187-202.

Savchuk OP, Wulff F 2009. Long-term modelling of large-scale nutrient cycles in the entire Baltic Sea. Hydrobiologia 629: 209–224.

Seitzinger SP, Nixon SW, Pilson MEQ 1984. Denitrification and nitrous oxide production in coastal marine ecosystem. Limnology and Oceanography 29: 73–83.

Seitzinger SP 1987. Nitrogen biogeochemistry in an unpolluted estuary: the importance of benthic denitrification. Marine Ecology Progress Series 41: 177–186.

Shiah F-W, Ducklow H. W 1994. Temperature and substrate regulation of bacterial abundance, production and specific growth rate in Chesapeake Bay, USA. Marine Ecology Progress Series 103: 297-308.

Sigleo AC, Mordy CW, Stabeno P, Frick WE 2005. Nitrate variability along the Oregon coast: estuarine-coastal exchange. Estuarine, Coastal and Shelf Science 64: 211-222.

Sigleo AC, Frick WE 2007. Seasonal variations in river discharge and nutrient export to a Northeastern Pacific estuary. Estuarine Coastal and Shelf Science 73: 368–378.

Simon NS 1988. Nitrogen cycling between sediment and shallow-water column in the transition zone of the Potomac River Estuary. I. Nitrate and ammonium fluxes. Estuarine, Coastal and Shelf Science 26: 483–497.

Sin Y, Wetzel RL, Anderson IC 1999. Spatial and temporal characteristics of nutrient and phytoplankton dynamics in the York River Estuary, Virginia: analyses of long-term data. Estuaries 22: 260–275.

Slomp CP, Van Cappellen P 2004. Nutrient inputs to the coastal ocean through submarine groundwater discharge: controls and potential impact. Journal of Hydrology 295: 64–86.

Soetaert K, Middelburg JJ, Heip C, Meire P, van Damme S, Maris T 2006. Long-term change in dissolved inorganic nutrients in the heterotrophic Scheldt estuary (Belgium, the Netherlands). Limnology and Oceanography 51: 409–423.

Soil Conservation Service (SCS) 1972. SCS national engineering handbook: hydrology. U.S. Government Printing Office. Washington.

Soil Conservation Service (SCS) 1975. United States Department of Agriculture, Soil Conservation Service Technical Release No. 55: Urban hydrology for small watersheds. U.S Department of Agriculture, Soil Conservation Service, Engineering Division. Washington.

Spiers KC, Healy TR, Winter C 2009. Ebb-jet dynamics and transient eddy formation at Tauranga Harbour: implications for entrance channel shoaling. Journal of Coastal Research 25: 234–247.

Spillman CM, Imberger J, Hamilton DP, Hipsey MR, Romero JR 2007. Modelling the effects of Po River discharge, internal nutrient cycling and

hydrodynamics on biogeochemistry of the Northern Adriatic Sea. Journal of Marine Systems 68: 167–200.

Spiteri C, van Cappellen P, Regnier P 2008. Surface complexation effects on phosphate adsorption to ferric iron oxyhydroxides along pH and salinity gradients in estuaries and coastal aquifers. Geochimica et Cosmochimica Acta 72: 3431–3445.

Stokes DJ 2010. The physical and ecological impacts of mangrove expansion and mangrove removal: Tauranga Harbour, New Zealand. PhD Thesis. Department of Earth and Ocean Sciences, University of Waikato, NZ. 214 p.

Stokes DJ, Healy TR, Cooke PJ 2010. Expansion dynamics of mono-specific, temperate mangroves and sedimentation in two embayment of a barrier-enclosed lagoon, Tauranga Harbour, New Zealand. Journal of Coastal Research 26: 113-122.

Sundbäck K, Enoksson V, Granéli W, Pettersson K 1991. Influence of sublittoral microphytobenthos on the oxygen and nutrient flux between sediment and water: a laboratory continuous-flow study. Marine Ecology Progress Series 74: 263–279.

Sundby B, Gobeil C, Silverberg N, Mucci A 1992. The phosphorus cycle in coastal marine sediments. Limnology and Oceanography 37: 1129–1145.

Sutton PJH, Hadfield MG 1997. Aspects of the hydrodynamics of Beatrix Bay and Pelorus Sound, New Zealand. New Zealand Journal of Marine and Freshwater Research 31: 271–279.

Timmermann K, Markager S, Gustafsson KE 2010. Streams or open sea? Tracing sources and effects of nutrient loads in a shallow estuary with a 3D hydrodynamic-ecological model. Journal of Marine Systems 82: 111-121.

Tobias CR, Macko SA, Anderson IC, Canuel EA, Harvey JD 2001. Tracking the fate of a high concentration groundwater nitrate plume through a fringing marsh: a combined groundwater tracer and in situ isotope enrichment study. Limnology and Oceanography 46: 1977–1989.

Trimmer M, Nedwell DB, Sivyer DB, Malcolm SJ 1998. Nitrogen fluxes through the lower estuary of the river Great Ouse, England: the role of the bottom sediments. Marine Ecology Progress Series 163: 109–124.

Trimmer M, Nedwell DB, Sivyer DB, Malcolm DJ 2000. Seasonal organic mineralisation and denitrification in intertidal sediments and their relationship to the abundance of Enteromorpha sp. and Ulva sp. Marine Ecology Progress Series 203: 67–80.

Tuerk KJS, Aelion CM 2005. Microbial nitrogen removal in developing suburban estuary along the South Carolina coast. Estuaries 28: 364–372.

Turner IL, Coates BP, Acworth RI 1997. Tides, waves and the super-elevation of groundwater at the coast. Journal of Coastal Research 13: 46–60.

Ullman WJ, Chang B, Miller DC, Madsen JA 2003. Groundwater mixing, nutrient diagenesis, discharges across a sandy beachface, Cape Henlopen, Delaware (USA). Estuarine, Coastal and Shelf Science 57: 539–552.

Valiela I, Teal J.M, Volkmann S, Shafer D, Carpenter EJ 1978. Nutrient and particulate fluxes in a salt marsh ecosystem: tidal exchanges and inputs by precipitation and groundwater. Limnology and Oceanography 23: 798–812.

Valiela I, Costa J, Foreman K, Teal J, Howes B, Aubrey D 1990. Transport of groundwater-borne nutrients from watersheds and their effects on coastal waters. Biogeochemistry 10: 177–197.

Valiela I, Foreman K, LaMontagne M, Hersh D, Costa J, Peckol P, DeMeo-Anderson B, D'Avanzo C, Babione M, Sham C, Brawley J, Lajtha K 1992. Couplings of watersheds and coastal waters: sources and consequences of nutrient enrichment in Waquoit Bay, Massachusetts. Estuaries 15: 443–457.

Valiela I, McClelland J, Hauxwell J, Behr PJ, Hersh D, Foreman K 1997. Macroalgal blooms in shallow estuaries: controls and ecophysiology and ecosystem consequences. Limnology and Oceanography 42: 1105–1118.

Valiela I, Bowen JL, Kroger KD 2002. Assessment of models for estimation of land-derived nitrogen loads to shallow estuaries. Applied Geochemistry 17: 935–953.

van der Struijk LF, Kroeze C 2010. Future trends in nutrient export to coastal waters of South America: implications for occurrence of eutrophication. Global Biogeochemical Cycles 24:GB0A09, doi: 10. 1029/2009GB003572.

Vennell R 2006. ADCP measurements of momentum balance and dynamic topography in a constricted tidal channel. Journal of Physical Oceanography 36: 177–188.

Wang F, Juniper SK, Pelegrí SP, Macko SA 2003. Denitrification in sediments of the Laurentian Trough, St. Lawrence Estuary, Québec, Canada. Estuarine, Coastal and Shelf Science 57: 515–522.

Werner U, Billerbeck M, Polerecky L, Franke U, Huettel M, van Beusekom JEE, de Beer D 2006. Spatial and temporal patterns of mineralization rates and oxygen distribution in a permeable intertidal sand flat (Sylt, Germany). Limnology and Oceanography 51: 2549–2563.

Whiting GJ, Mckellar HN, Kjerfve B, Spurrier JD 1987. Nitrogen exchange between a southeastern USA salt marsh ecosystem and the coastal ocean. Marine Biology 95: 173–182.

Wiegner TN, Seitzinger SP, Breitburg DL, Sanders JG 2003. The effects of multiple stressors on the balance between autotrophic and heterotrophic processes in an estuarine system. Estuaries 26: 352–364.

Xu J, Hood RR 2006. Modelling biogeochemical cycles in Chesapeake Bay with a coupled physical-biological model. Estuarine, Coastal and Shelf Science 69: 19–46.

Zhang J 1996. Nutrient elements in large Chinese estuaries. Continental Shelf Research 16: 1023–1045.

Appendix 1: Long-term data statistics

Table A1.1 Mean and coefficient of variation (C.O.V) values derived from the long-term dataset (LT), Te Puna and Waikareao Estuaries during winter, start of spring (SS), end of spring (SE) and summer.

Season	Station	Ammonium (mg L^{-1})		Nitrate (mg L^{-1})		Phosphate (mg L^{-1})	
		Mean	C.O.V	Mean	C.O.V	Mean	C.O.V
Winter	LT	0.031	1.046	0.072	1.040	0.008	0.654
	Te Puna	0.095	0.128	0.158	0.569	0.016	0.087
	Waikareao	0.076	1.046	0.143	1.040	0.014	0.654
SS	LT	0.021	0.650	0.067	1.632	0.006	0.508
	Te Puna	0.058	0.281	0.219	0.713	0.015	0.512
	Waikareao	0.076	0.650	0.108	1.632	0.011	0.508
SE	LT	0.024	1.295	0.029	1.372	0.007	0.694
	Te Puna	0.037	0.608	0.094	0.366	0.021	0.229
	Waikareao	0.019	1.295	0.145	1.372	0.025	0.694
Summer	LT	0.019	0.838	0.043	1.018	0.006	0.773
	Te Puna	0.034	0.304	0.027	0.472	0.020	0.248
	Waikareao	0.027	0.838	0.035	1.018	0.015	0.773

Appendix 2: Net ecosystem metabolism

Overview

Diel changes in dissolved oxygen were used to examine gross primary production, respiration and net ecosystem metabolism within Te Puna and Waikareao estuaries. For each of the four sampling periods, gross primary production exceeded respiration demonstrating that both sites were net autotrophic.

Introduction

Estuaries are transition zones between land and sea through which land-derived nutrients reach the coastal areas. Increased nutrient loads to estuaries have resulted in increased nuisance and toxic algal blooms and degradation of water quality (Howarth et al. 2002; Paerl et al. 2006). One way to assess how a coastal ecosystem will respond to increased loads of nutrients is to make an integrative measure of its ecological properties. The condition can be determined by estimating the net ecosystem metabolism (NEM), which represents the overall metabolic balance of an ecosystem (Howarth et al. 1996). Once the nutrients and organic matter are in the estuary, transformations occur as a result of biogeochemical cycling, e.g. primary production and respiration processes. These transformations are important because the combination of net fluxes of water, dissolved nutrients and organic matter will determine the role of the system as autotrophic (production exceeds respiration) or heterotrophic (respiration exceeds production).

Freshwater inflows into estuaries are changing in most estuaries because of changes in land use and cover, water diversion for human uses and climate effects. These changes generally result in changes in timing of pulse events, increase and in some cases decrease in freshwater inflows. Freshwater inflow transports sediment, nutrients and organic matter from a catchment to an estuary. Thus the inherent variability in freshwater inflow affects nutrient and organic loading which in turn can be linked to estuarine metabolic rates (D'Avanzo et al. 1996; Caffrey 2004). Spatial and temporal variability in other environmental conditions may also modify estuarine ecosystem metabolic rates. Estuarine metabolic rate can be affected by the interaction of nutrient and organic matter loading with light availability, temperature, dissolved oxygen and salinity within the water column

of an estuary (Russell and Montagna 2007). Increased loading of nutrients leads to increased NEM by stimulation of production over respiration. Changes in NEM may be driven by environmental conditions that vary temporally on daily scales such as rain and inflows to seasonal scales such as temperature.

Within an aquatic system, metabolic rates vary temporally and spatially. For example in San Francisco Bay, seasonal phytoplankton blooms shifted the system from heterotrophy to autotrophy (Caffrey et al. 1998). In some estuaries, variation along salinity and depth gradients has also been observed, where NEM changes from heterotrophy to autotrophy along the estuarine gradient (Howarth et al. 1996; Raymond et al. 2000). Most NEM studies have focused on large estuarine systems, whereas both Te Puna and Waikareao estuaries are shallow tidally dominated estuaries. The objective of this appendix is to present the results of net ecosystem metabolism (NEM) from diel changes in dissolved oxygen measurements over four sampling periods (summer, winter, start of spring and end of spring) in both Te Puna and Waikareao estuaries.

Methods

Consecutive hourly dawn-dusk-dawn measurements of dissolved oxygen taken by CTD were used to estimate each estuary's rates of gross primary production (*GPP*), respiration (*RESP*), and net ecosystem metabolism (*NEM*) in mg O_2 L^{-1} d^{-1} based on methods of Wiegner et al. (2003). For location of the sampling sites, refer to Chapter 2, Figure 2.1. Rates of the whole system net primary production (*NPP*) were first calculated from the dissolved oxygen concentration for the first dawn of the 24 h sampling period (dawn1) to dusk:

$$NPP = (O_{2dusk} - O_{2dawn1})/t + AS$$

where O_2 = dissolved oxygen concentration measured (mg L^{-1}), t = the number of h between the measurements and, AS = the diffusive flux (g m^{-2} h^{-1}) across the air-water interface. *RESP* was calculated from the decrease in the dissolved oxygen concentration from dusk to dawn2 (the second dawn of the 24 hour sampling):

$$RESP = (O_{2dusk} - O_{2dawn2})/t + AS$$

GPP was estimated from the sum of *NPP* and *RESP,* and *NEM* as the difference between *GPP* and *RESP*. For this calculation, the *RESP* was assumed constant

over a diurnal cycle (i.e. $RESP_{day}$ = $RESP_{night}$; Wiegner et al. 2003). Oxygen diffusion across the air-water interface was calculated as:

$$AS = S \times k_s \times d$$

$$= [1 - (DO/20)] \times k_s \times dt$$

where S is the mean fractional saturation deficit (%), DO is the percent oxygen saturation over the time interval dt (in this case an hour). The coefficient, k_s, was assumed to be 0.5 g O_2 m^{-2} hr^{-1} at zero DO concentration (Caffrey 2004).

Results and discussion

NEM was positive indicating that both Waikareao and Te Puna were autotrophic (Figure A2.1). The *GPP* and *GRP* rates at the start of spring were 1.2-1.4 times higher than rates in other seasons. The *NEM* rates at both Waikareao and Te Puna were remarkably consistent through the four sampling periods. Apart from the higher values in early spring, *NEM* showed little seasonal variation in both estuaries.

Large seasonal variations in estuarine metabolic rate were not evident in this study, unlike patterns in other estuaries examples as reported by Caffrey (2004) and Russell and Montagna (2007). A direct consequence of the net export of nutrients from these two estuaries is that there may be ample supplies of nutrients to allow photoautotrophic behaviour regardless of season and may support production in other parts of the harbour. The *NEM* showed that both estuaries were net autotrophic during the four sampling periods while, previous studies in other estuarine environments have shown that the *NEM* switches between net autotrophic and net heterotrophic seasonally (Howarth et al. 1996; Caffrey 2004; Russell and Montagna 2007). The net autotrophy in Waikareao and Te Puna could be due to the shallow environment where benthic production likely plays a greater role than in deeper estuaries where many previous studies on estuaries were focused (Caffrey et al. 1998; Ram et al. 2003). Changes in catchment activities, hydrology and organic or nutrient enrichment along with influences of environmental factors such as temperature and light can be influential on estuarine metabolic activities as once in the estuaries, biogeochemical cycling takes place

which can lead to a balance between autotrophy and heterotrophy in estuaries (Caffrey 2004; Russell et al. 2006; Russell and Montagna 2007).

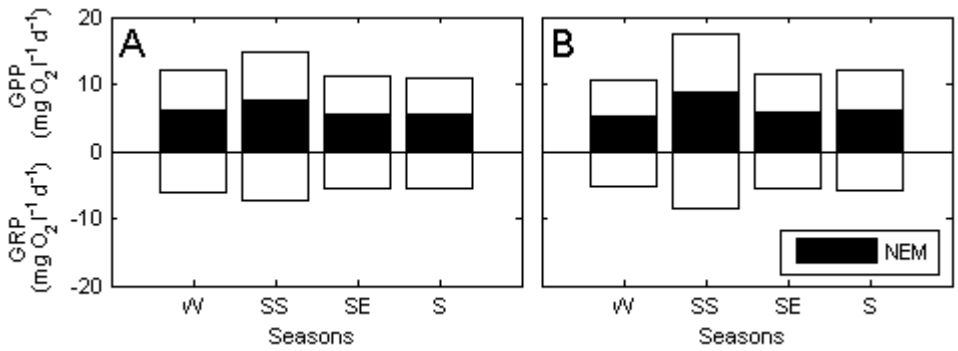

Figure A2.1 Seasonal variations in gross production (*GPP*), gross respiration (*GRP*) and net ecosystem metabolism (*NEM*) in Waikareao (A) and Te Puna (B) estuaries. W: winter; SS: start of spring; SE: end of spring; S: summer.

Appendix 3: Design hydrograph for freshwater input

Overview

Some streams and rivers in the Tauranga Harbour region are either not gauged or have sparse records. Hence in order to estimate the amount of stream or river discharge into the estuary, inflow rate is required at a high resolution timescale. Factors such as the timing of peak discharge and runoff volume are of interest. Therefore a storm hydrograph was created to estimate the flow rate. Storm hydrographs were created based on the empirical model in the U.S. Soil Conservation Service handbook (SCS 1972; SCS 1975) for Te Puna Stream (ungauged), Wainui River (sparse records) and Aongatete River (sparse records). The stream and rivers flow through catchments dominated by forestry and agricultural activities. An example of a storm hydrograph calculation for Te Puna Stream is shown in this Appendix.

Design hydrograph

Runoff was estimated from rainfall data using the empirical model outlined in the U.S. Soil Conservation Service Handbook (SCS 1972) which has been previously adapted to specific catchments in the Auckland Region (Beca 1999). Daily rainfall data measured by the Tauranga Aero Aws climate station were acquired for the area for a period of one year. All rainfall data are available from the National Climate Database (Cliflo). A histogram of rainfall events in 2007 measured by Tauranga Aero Aws was shown in Figure A3.1. The probability of rainfall occurrence, which is determined from the percentage of occurrence of rainfall in one year is shown in Table A3.1. Based on the SCS rainfall-runoff model, to generate any discernible stream flow, a minimal rainfall event of 10 mm was required. Hence a minimal rainfall event of 20 mm was used as a sufficient discharge would be required to flush catchment's nutrient into the estuary. Calculation of storm hydrograph for freshwater discharge was also conducted for rainfall events of 20, 40, 60 and 100 mm.

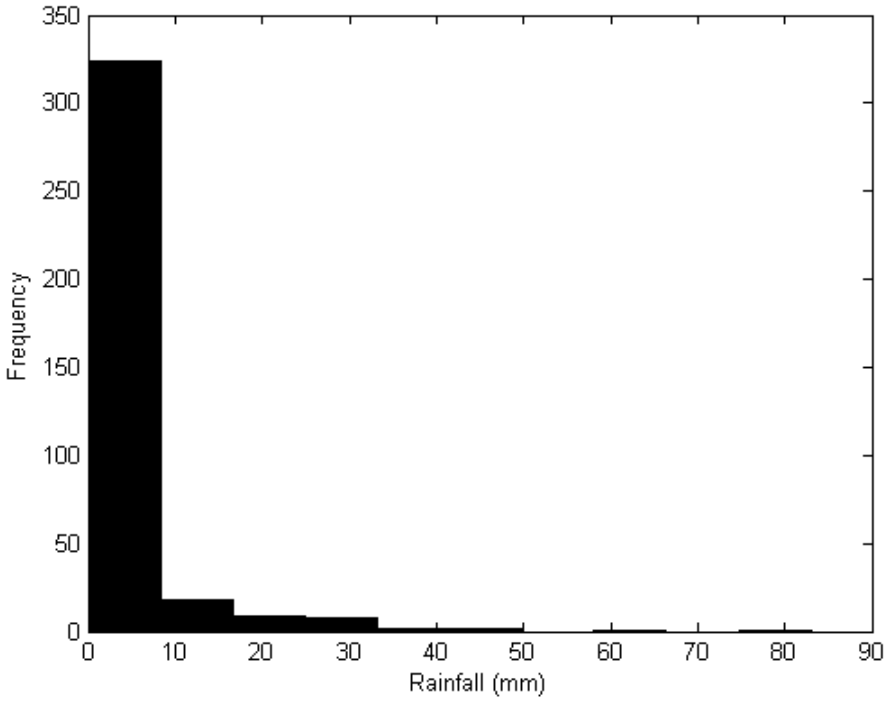

Figure A3.1 Histogram of the frequency of rainfall events (mm) measured by the Tauranga Aero Aws site in 2007 downloaded from the NIWA Cliflo database.

Table A3.1 Rainfall bands, probability of rainfall event and the recurrence interval with rainfall data measured by the Tauranga Aero Aws.

Rainfall (mm)	Occurrence	Percentage of rainfall events	Probability, p	Recurrence Interval, T(years)
>10mm	329	90.1	0.9	1
10-20	19	5.2	0.05	19
20-40	12	3.3	0.03	30
40-60	3	0.8	0.008	121
60-100	2	0.5	0.005	183

To determine discharge from the catchment, soil type and land-use properties were determined (Figure A3.2, A3.3). The soil properties of the catchment were classified according to the New Zealand Soil Classification (NZCS) (Figure A3.2) and was assigned a SCS hydrologic soils group class based on drainage and soils properties (SCS 1972; Hewitt 1993; Newsome et al. 2000). Table A3.2 soil classification based on drainage and soil properties for Te Puna Estuary. The same type of classifications was also conducted for Wainui and Aongatete catchments. The area size of each of the soil units and land-use classes were calculated. Then a curve number for each unit was determined based on the land-use classification and hydrologic soil group (Table A3.3). The curve numbers for each unit for the three catchments were derived from the SCS National Engineering Handbook

(1972, 1975) (see Table A3.3 for Curve Number examples). The U.S SCS empirically derived rainfall-runoff curves to define relationship between the landuse and hydrologic soil group. The curve number range between 0 (i.e. no runoff), to 100 (i.e. total runoff) and are based upon the properties of the catchment (SCS 1972).

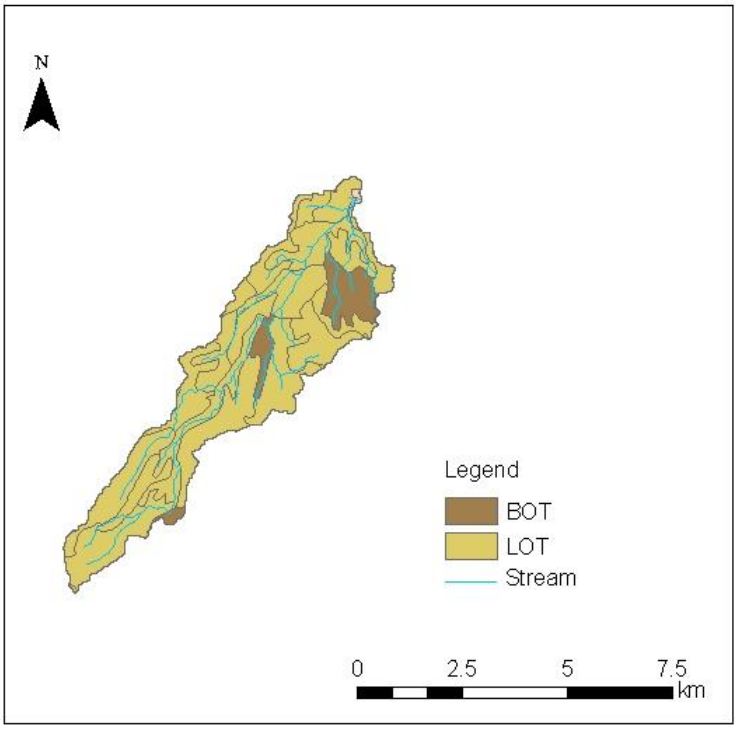

Figure A3.2 Te Puna catchment soils classification based on New Zealand Soil Classification.

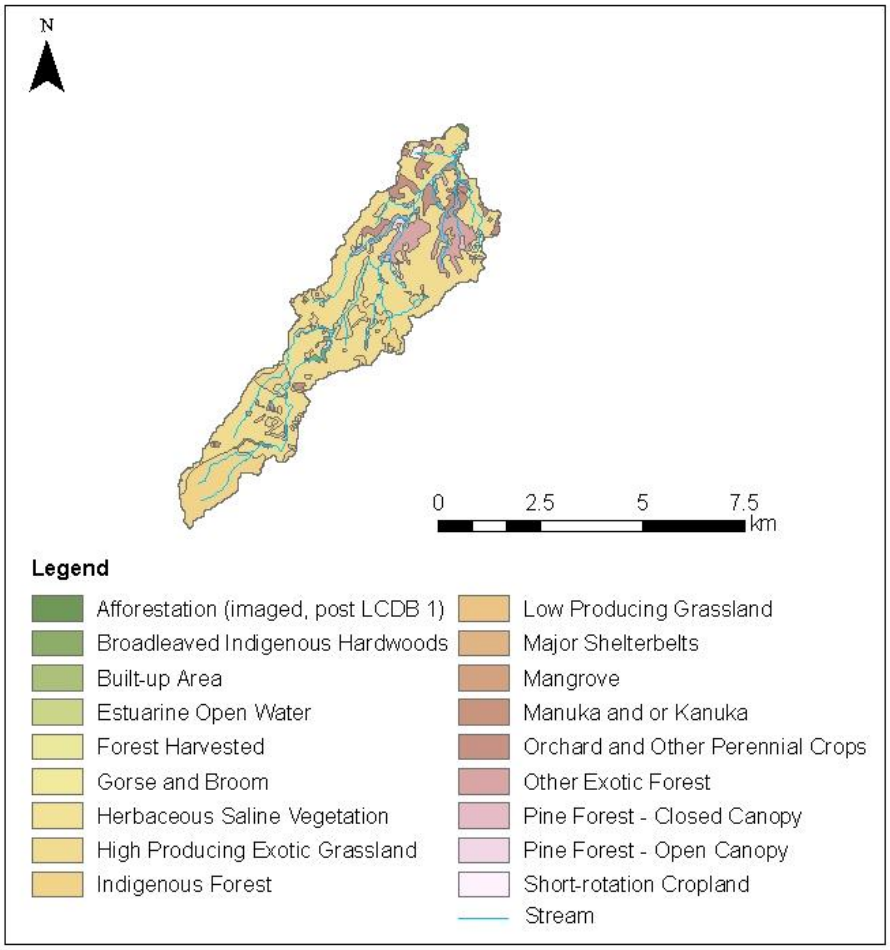

Figure A3.3 Te Puna catchment land-use classifications and the areal extent of each unit based on New Zealand Land Cover Database 2 (2004).

Table A3.2 Te Puna catchment soil classification based on New Zealand Soil Classification (NZSC), predominant soil characteristics and the assigned SCS hydrological class based on SCS handbook.

Soil type	NZCS	Characteristics	SCS hydrological soil group
Typic orthic brown soils	BOT	Weak soil strength depth Commonly occur on hilly or steep slopes	B
Sandy loam	LOT	Orthic allophanic soils	B

Table A3.3 Land-use type at Te Puna catchment and the associated curve numbers. Curve numbers are from SCS handbook (1972).

Type of land-use	Hydrological soil group	Curve number
Indigenous Forest	B	55
High Producing Exotic Grassland	B	58
Major Shelterbelts	B	79
Orchard and Other Perennial Crops	B,C	71, 66
Pine Forest - Open Canopy	B	55
Estuarine Open Water	-	-
Afforestation (imaged, post LCDB 1)	B	55
Mangrove	-	-
Broadleaved Indigenous Hardwoods	B,C	55, 70
Built-up Area	B	51
Manuka and or Kanuka	B	55
Herbaceous Saline Vegetation	B	66
Other Exotic Forest	B	55
Short-rotation Cropland	B	71
Low Producing Grassland	B	79
Gorse and Broom	B	56
Forest Harvested	B	66

As the three catchments were heterogenous in catchment soil and land-use characteristics, a weighted curve number (Equation A3.1) was required:

$$CN = \frac{\sum CN_i A_i}{A_{tot}}$$

(Equation A3.1)

where CN is the weighted curve number, CN_i is the curve number for the particular classification, A_i is the area with the particular CN_i classification and A_{tot} is the total area. The curve numbers were then combined into a weighted curve number for the whole catchment. This weighted curve number which represents the soil and landuse properties for the whole catchment was used in the calculation of storage (Equation A3.2) for the catchment:

$$S = \left(\frac{1000}{CN}\right) 25.4$$

(Equation A3.2)

Then the time of concentration, T_c, i.e. the time taken for rainfall to concentrate into the stream/rivers to produce a measurable discharge, is then calculated using

catchment storage. The time of concentration is then used to calculate the peak discharge flow rate which is then applied to a set of ordinates which predetermine the percentage of flow per unit time to give an idealised hydrograph shown in Figure A3.4. T_c is calculated using the following parameters outlined in Table A3.4 for Te Puna Estuary.

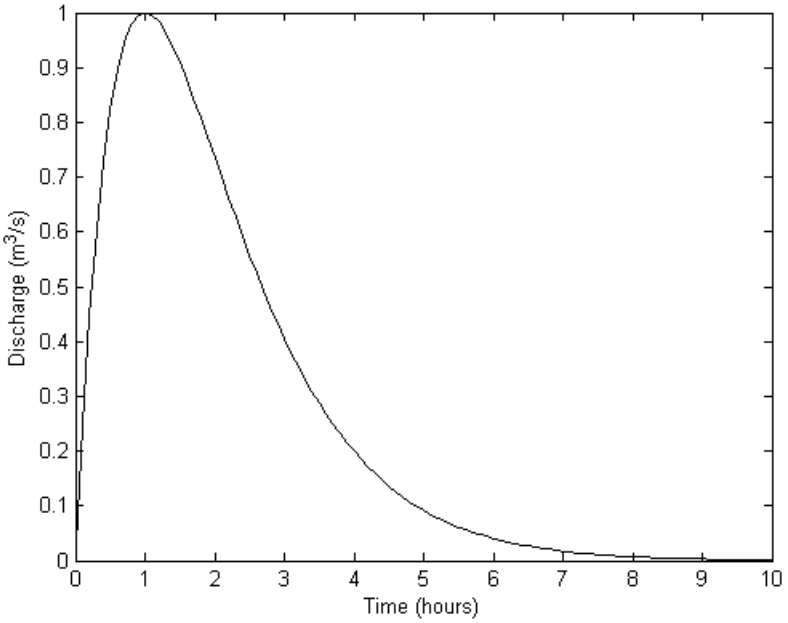

Figure A3.4 Schematic of an idealised hydrograph. The values of peak discharge and time of concentration are applied to a given set of ordinates (from SCS 1972) which predetermine percentage of flow per unit time to give the idealised hydrograph curve.

Table A3.4 Parameters used in the calculation of the time of concentration for Te Puna Estuary.

Parameter	Value
Channelisation factor, C	0.6 (BCHF 1999)
Catchment length, L (km)	11.86 (derived using ArcGIS)
Catchment slope, Sc (m.m)	0.017 (derived using ArcGIS)

BCHF: Beca Carter Hollings & Ferner Ltd

The effect of urbanization on runoff velocities is allowed through channelisation factor and T_c is then calculated using the following equation (Equation A3.3):

$$T_c = 0.14\ C\ L^{0.66}\left(\frac{CN}{200-CN}\right)^{-0.55} S_c^{-0.30}$$

(Equation A3.3)

The time of peak concentration, T_p, (Equation A3.4) is calculated as:

$$T_p = \frac{2}{3} T_c$$

(Equation A3.4)

The peak flow rate, q_p, is then calculated using catchment properties summarized in Table A3.5 below.

Table A3.5 Catchment properties used in the calculation of peak flow rate for Te Puna Estuary.

Parameter	Value
Catchment area, A (km^2)	22.2
Runoff curve number (CN)	58
Initial abstraction, Ia (mm)	5
Time of concentration, Tc (hours)	2.4

The initial abstraction is the loss of rainfall before runoff occurs and is attributable to land storage, evaporation, infiltration and vegetation. The initial abstraction value was derived by Beca Carter Hollings & Ferner Ltd (1999) based on empirical data as:

$$Pervious\ areas\ = 5$$
$$Impervious\ areas\ = 0$$

To calculate the specific peak flow rate, the runoff index, c*, has to be calculated using the following equation (Equation A3.5):

$$c* = \frac{p - 2Ia}{p - 2Ia + 2S}$$

(Equation A3.5)

where p is the rainfall depth, Ia is the initial abstraction and S is storage. The calculated c* was then used to determine specific peak flow rate, q* based on Figure 5.1 in the report of Beca Carter Hollings & Ferner Ltd 1999.

The peak flow rate, q_p, is then able to be calculated using the following equation (Equation A3.6):

$$q_p = q^* A\, p$$

(Equation A3.6)

where p is the rainfall depth, A is the catchment area and q is specific peak flow rate. The peak flow rate, $q_{p,}$ and time of concentration, $T_{c,}$ can then be multiplied with the SCS design hydrograph ordinates (Table A3.6).

Table A3.6 Time and discharge ordinates for which time of concentration and peak flow rate is multiplied (From SCS 1972).

Time ratios	Discharge ratios
0	0
0.1	0.03
0.2	0.1
0.3	0.19
0.4	0.31
0.5	0.47
0.6	0.66
0.7	0.82
0.8	0.93
0.9	0.99
1	1
1.1	0.99
1.2	0.93
1.3	0.86
1.4	0.78
1.5	0.68
1.6	0.56
1.7	0.46
1.8	0.39
1.9	0.33
2	0.28
2.2	0.207
2.4	0.147
2.6	0.107
2.8	0.077
3	0.055
3.2	0.04
3.4	0.029
3.6	0.021
3.8	0.015
4	0.011
4.5	0.005
5	0

The runoff depth, *Q*, can be calculated using Equation A3.7:

$$Q = \frac{(p - Ia)^2}{(p - Ia) + S}$$

(Equation A3.7)

where *p* is the rainfall depth, *Ia* is the initial abstraction and *S* is storage.

Appendix 4: Individual profile results of current speeds, direction, salinity and temperature for Omokoroa, Motuhou and Western stations

This appendix contains figures of model fits of tidal elevation, current speed and direction for Omokoroa, Motuhou and Western stations as mentioned in Section 3.3.1 in Chapter 3.

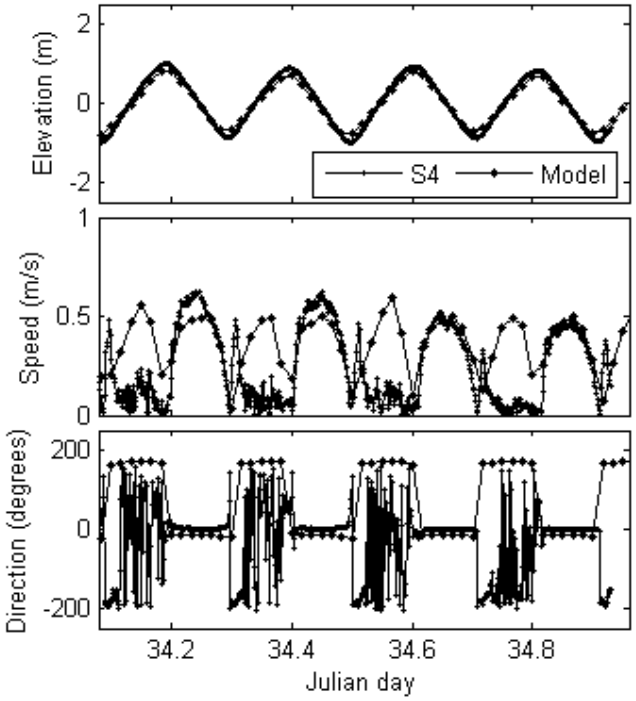

Figure A4.1 Modelled (ELCOM) against measured (S4) water elevation, current speed and direction at Omokoroa Station 1.

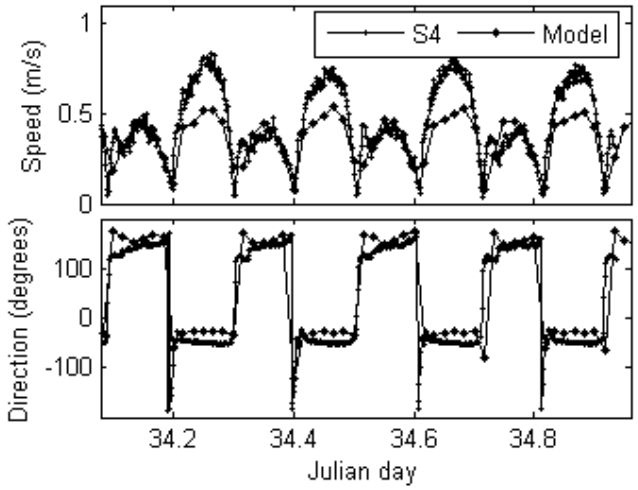

Figure A4.2 Modelled (ELCOM) against measured (S4) water elevation, current speed and direction at Omokoroa Station 2.

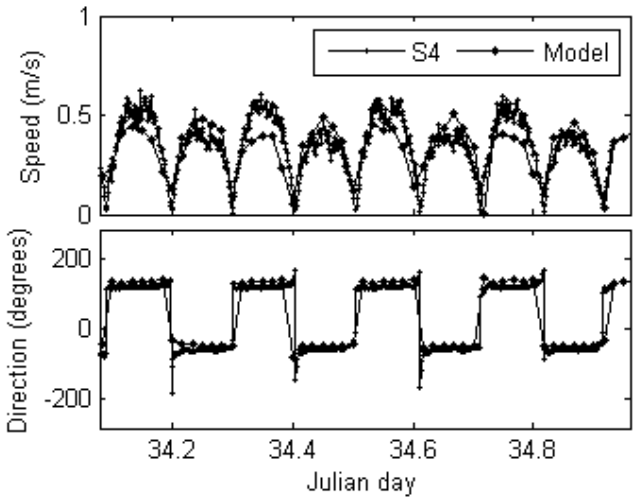

Figure A4.3 Modelled (ELCOM) against measured (S4) water elevation, current speed and direction at Omokoroa Station 3.

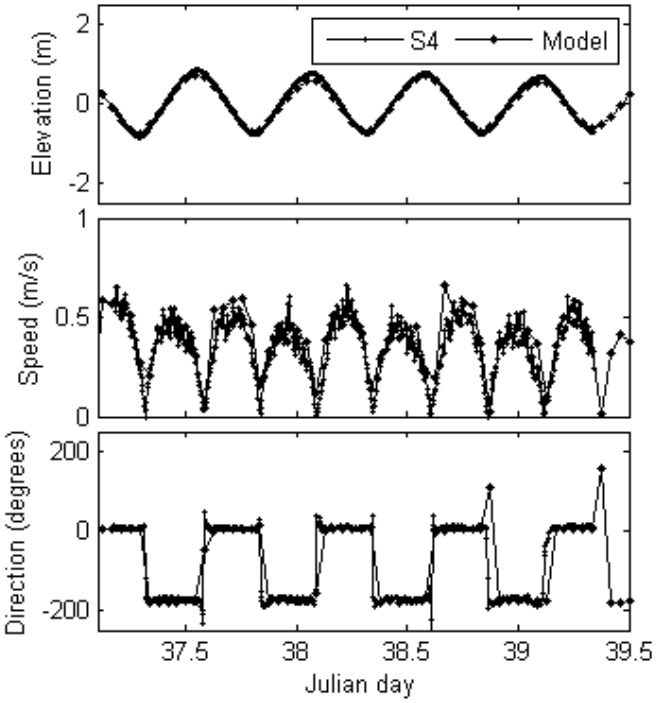

Figure A4.4 Modelled (ELCOM) against measured (S4) water elevation, current speed and direction at Motuhou Station 1.

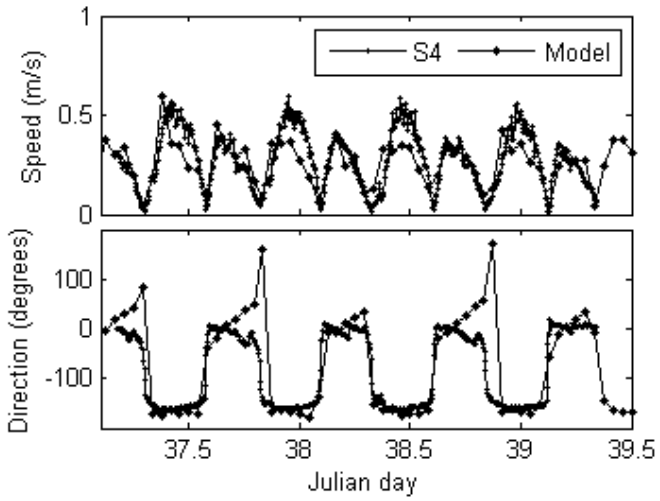

Figure A4.5 Modelled (ELCOM) against measured (S4) water elevation, current speed and direction at Motuhou Station 2.

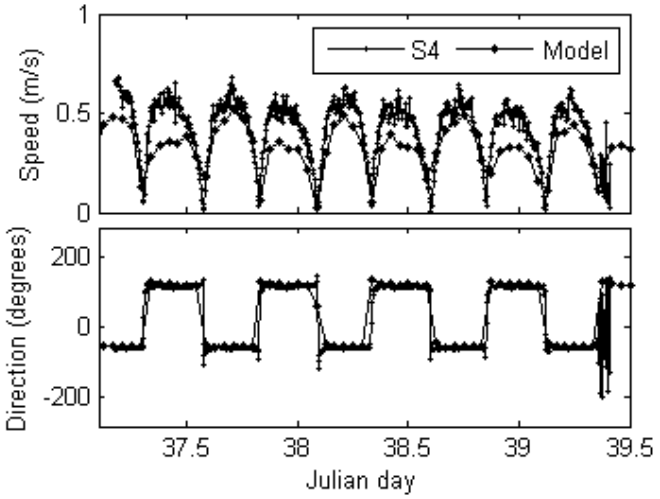

Figure A4.6 Modelled (ELCOM) against measured (S4) water elevation, current speed and direction at Motuhou Station 3.

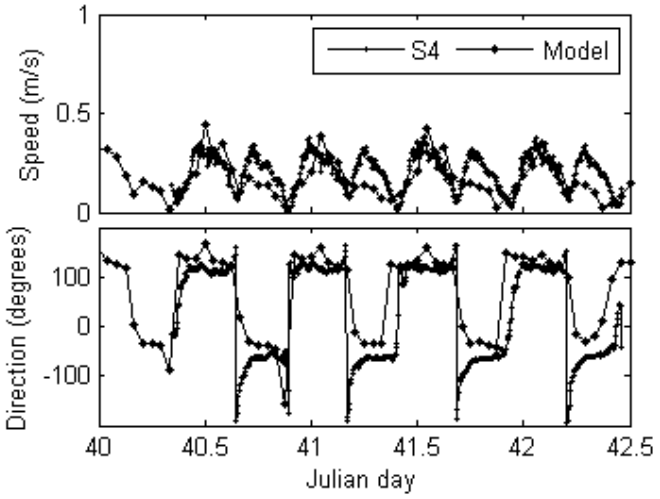

Figure A4.7 Modelled (ELCOM) against measured (S4) water elevation, current speed and direction at Western Station 2.

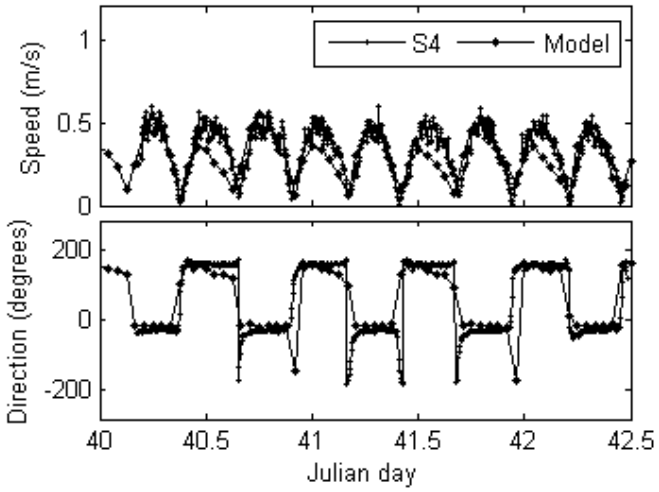

Figure A4.8 Modelled (ELCOM) against measured (S4) water elevation, current speed and direction at Western Station 3.

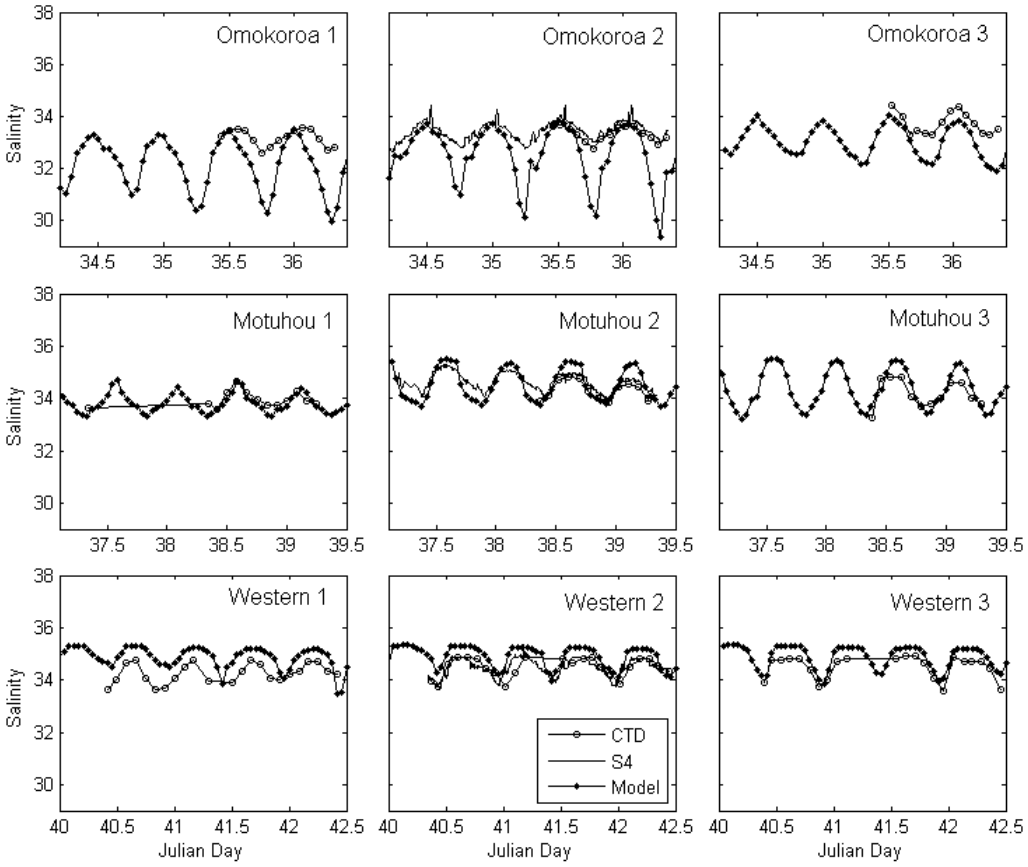

Figure A4.9 Depth-averaged measured (CTD and S4) and modelled (ELCOM) salinity at Omokoroa, Motuhou and Western stations. Omokoroa 1: Omokoroa station 1; Omokoroa 2: Omokoroa station 2; Omokoroa 3: Omokoroa station3; Motuhou 1: Motuhou station 1; Motuhou 2: Motuhou station 2; Motuhou 3: Motuhou station3; Western 1: Western station 1; Western 2: Western station 2; Western 3: Western station 3.

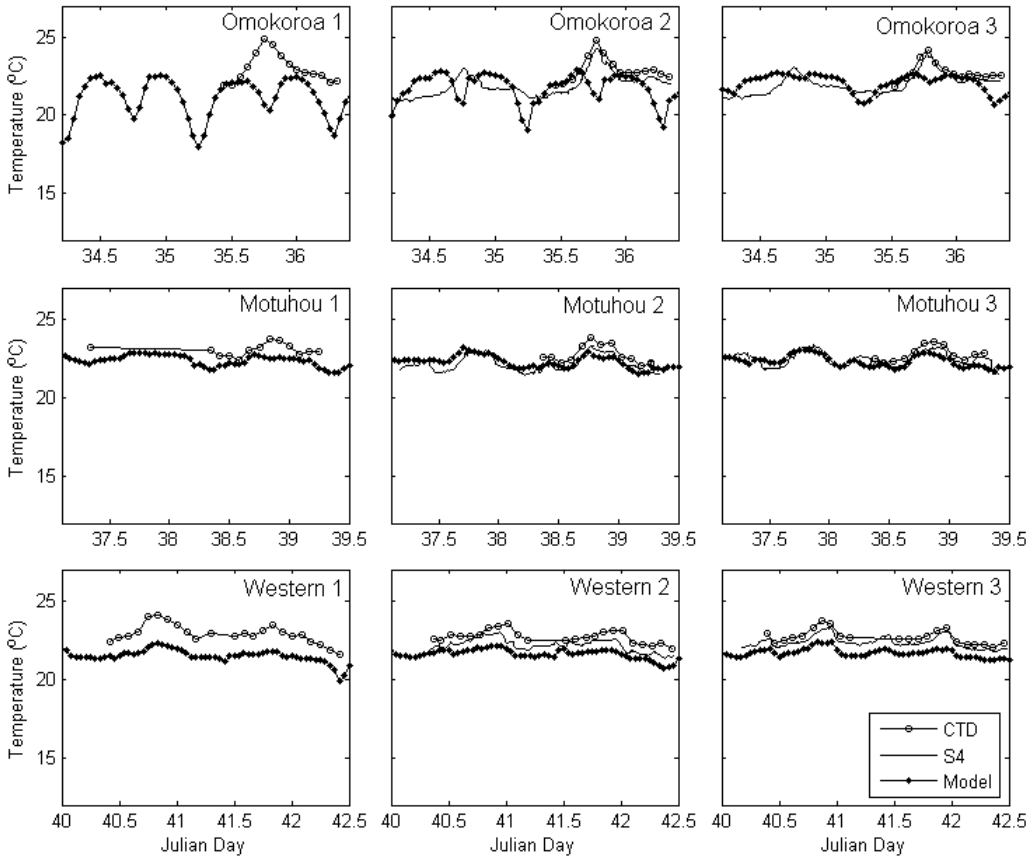

Figure A4.10 Depth-averaged measured (CTD and S4) and modelled (ELCOM) temperature at Omokoroa, Motuhou and Western stations. Omokoroa 1: Omokoroa station 1; Omokoroa 2: Omokoroa station 2; Omokoroa 3: Omokoroa station3; Motuhou 1: Motuhou station 1; Motuhou 2: Motuhou station 2; Motuhou 3: Motuhou station3; Western 1: Western station 1; Western 2: Western station 2; Western 3: Western station 3.

Appendix 5: Summary of parameter values for CAEDYM

This appendix contains the listing of the parameters and their description used in the CAEDYM model for Chapter 4 and 5.

Table A5.1 Parameter value used in CAEDYM.

Parameter	Unit	Value	References/Remarks
Dissolved oxygen parameter			
Temperature multiplier for sediment oxygen demand	Dimensionless	1.08	Robson and Hamilton (2004)
Half-saturation constant for sediment oxygen demand	mg L^{-1}	0.5	Robson and Hamilton (2004); Romero et al. (2004)
Nitrogen parameters			
Denitrification rate coefficient	d^{-1}	0.5	Burger et al. (2008)
Temperature multiplier for denitritication	Dimensionless	1.08	Robson and Hamilton (2004)
Nitrification rate coefficient	d^{-1}	0.01	Burger et al. (2008)
Temperature multiplier for nitrification	Dimensionless	1.08	Robson and Hamilton (2004)
Maximum potential sediment ammonium release rate	gm^{-2} d^{-1}	0.02	Robson and Hamilton (2004)
Maximum potential sediment nitrate release rate	gm^{-2} d^{-1}	-0.03	Hipsey et al. (2006); Missaghi and Hondzo (2010)
Phosphorus parameters			
Maximum sediment phosphate release rate	gm^{-2} d^{-1}	0.004	Robson and Hamilton (2004)
Phytoplankton parameters		Cyano, other	
Maximum potential growth rate at 20°C	d^{-1}	1.2, 1.4	Robson and Hamilton (2004)
Half saturation constant for phosphorus uptake	mg L^{-1}	0.006, 0.010	Holm and Armstrong (1981)
Half saturation constant for nitrogen uptake	mgL^{-1}	0.052, 0.04	Hamilton and Schladow (1997); Robson and Hamilton (2004)
Minimum internal nitrogen concentrations	mg N (mg chl-a)$^{-1}$	2.5, 5	Robson and Hamilton (2004)
Maximum internal nitrogen concentration	mg N (mg chl-a)$^{-1}$	5.0, 12	Robson and Hamilton (2004)
Maximum rate of nitrogen uptake	mg N (mg chl-a)$^{-1}$ d^{-1}	1.5, 12	Robson and Hamilton (2004)
Minimum internal phosphorus	mg P (mg chl-a)$^{-1}$	0.27, 0.25	Robson and Hamilton

concentration			(2004)
Maximum internal phosphorus concentration	mg P (mg chl-a)$^{-1}$	0.4, 0.6	Robson and Hamilton (2004)
Maximum rate of phosphorus uptake	mg P (mg chl-a)$^{-1}$ d^{-1}	0.2, 0.4	Robson and Hamilton (2004)
Temperature multiplier for growth multiplication	Dimensionless	1.08, 1.06	Robson and Hamilton (2004)
Respiration rate coefficient	d^{-1}	0.05, 0.12	Robson and Hamilton (2004)
Temperature multiplier for respiration	Dimensionless	1.08, 1.07	Robson and Hamilton (2004)

Appendix 6: Tables for groundwater and sediment modelling scenarios

This appendix contains Tables A6.1 and A6.2 for model-derived averages for ammonium, nitrate and DO concentrations over summer and winter. This is for both Te Puna and Waikareao estuaries with no groundwater contribution in comparison to base case. Table A6.3 shows model-derived averages for ammonium, nitrate and DO concentrations over summer and winter in Waikareao Estuary with no sediment fluxes in comparison to base case. For further discussion on groundwater and sediment fluxes, referred to Section 5.3.3 in Chapter 5.

Table A6.1 Model derived averaged nutrient (NH_4^+ and NO_3^-) and DO concentrations in summer 2008 and winter 2008, comparing with groundwater input (Case 0) and without groundwater input (Case 13, 14) from sites: UpWest, LowWest, UpEast, and LowEast in Te Puna Estuary.

Variable	Base (mg/L/tidal cycle)				No groundwater (mg/L/tidal cycle)				% change			
	UpWest	LowWest	UpEast	LowEast	UpWest	LowWest	UpEast	LowEast	UpWest	LowWest	UpEast	LowEast
Summer												
NH_4^+	0.081	0.035	0.066	0.035	0.079	0.035	0.065	0.035	-1.7	-0.3	-1.7	-0.3
$N0_3^-$	0.06	0.016	0.088	0.016	0.057	0.016	0.083	0.016	-5.6	-2.3	-5.6	-2.3
DO	5.31	8.97	5.94	8.93	5.31	8.97	5.92	8.93	0.01	-0.01	-0.3	0.0
Winter												
NH_4^+	0.069	0.026	0.072	0.021	0.080	0.028	0.074	0.022	16.2	7.4	2.1	3.1
$N0_3^-$	0.22	0.090	0.27	0.075	0.141	0.075	0.200	0.068	-37.1	-16.9	-25.0	-10.3
DO	6.08	8.97	6.87	9.24	6.08	8.96	6.75	9.24	-0.09	-0.2	-1.6	-0.03

Table A6.2 Model derived averaged nutrient (NH_4^+ and NO_3^-) and DO concentrations in summer 2008 and winter 2008, comparing with groundwater input (Case 0) and without groundwater input (Case 15, 16) from sites: East1, East2, West1, and West2 in Waikareao Estuary.

Variable	Base (mg/L/tidal cycle)				No groundwater (mg/L/tidal cycle)				% change			
	East1	East2	West1	West2	East1	East2	West1	West2	East1	East2	West1	West2
Summer												
NH_4^+	0.04	0.047	0.051	0.044	0.040	0.047	0.046	0.044	0.1	-0.03	-6.2	-0.2
$N0_3^-$	0.032	0.043	0.011	0.034	0.027	0.035	0.009	0.028	-16.3	-18.6	-21.4	-18.4
DO	7.16	6.11	4.01	6.50	7.489	6.160	4.002	6.569	4.7	0.8	-0.3	1.1
Winter												
NH_4^+	0.036	0.044	0.040	0.045	0.040	0.048	0.044	0.048	11.1	10.2	8.1	7.7
$N0_3^-$	0.118	0.149	0.079	0.154	0.101	0.120	0.066	0.117	-14.0	-19.5	-17.1	-24.1
DO	7.403	6.648	5.191	6.477	7.578	6.986	5.060	6.790	2.4	5.1	-2.5	4.8

Table A6.3 Model derived averaged nutrient (NH_4^+ and NO_3^-) and DO concentrations in summer 2008 and winter 2008, comparing with sediment input (Case 0) and without sediment input (Case 17, 18) from sites: East1, East2, West1, and West2.

Variable	Base (mg/L/tidal cycle)				No sediment (mg/L/tidal cycle)				% change			
	East1	East2	West1	West2	East1	East2	West1	West2	East1	East2	West1	West2
Summer												
NH_4^+	0.04	0.05	0.05	0.04	0.03	0.03	0.03	0.03	-19.3	-27.0	-39.9	-25.2
$N0_3^-$	0.03	0.04	0.01	0.03	0.04	0.06	0.03	0.05	33.7	45.1	204.3	47.3
DO	7.16	6.11	4.01	6.50	9.92	9.87	9.85	9.89	38.6	61.5	145.5	52.3
Winter												
NH_4^+	0.04	0.04	0.04	0.04	0.03	0.04	0.02	0.04	-15.8	-17.6	-38.5	-18.8
$N0_3^-$	0.12	0.15	0.08	0.15	0.13	0.16	0.10	0.17	9.4	10.0	25.9	10.1
DO	7.40	6.65	5.19	6.48	9.92	9.91	9.88	9.91	34.0	49.1	90.4	53.0